UNIVERSITÀ DEGLI STUDI DI MILANO BICOCCA
Dipartimento di Scienze dell'Ambiente e del Territorio e di Scienze della Terra

Dottorato in Scienze
della Terra

XXVIII ciclo

NUTRIENTS INFLUENCE ON MIOCENE CARBONATE FACTORIES

Relatore: Professoressa Daniela Basso

Candidato: Giovanni Coletti

Milano – 2016

Foreword

The PhD thesis is conceived as a systematic research using logical argument and incorporating empirical evidence in support of a hypothesis. Back when PhD programs were introduced in Italy, the traditional language of a PhD thesis was of course Italian. Nowadays, albeit not compulsive, the use of English is highly recommended. This happened because English is presently main language of scientific literature, and since the PhD program is, or at least was conceived as the training step for an academic career, the scientific results of PhD research need to be written in English.

Just has Italian has been the traditional language the traditional form of a thesis has been for long a treatise. However, through the decades as the role of journals expanded in science, directly constructing the dissertation as a set of essays has been considered more convenient. Not surprisingly the essay format is now widely diffused in the USA and in Europe. This format trains PhD students to do what they hope to do throughout their careers, namely, write articles. Furthermore the essay format allows to address more than one question or to combine different methodological approaches to a single objective.

This PhD thesis, like probably every other existing PhD thesis, deal with a complex problem: the effect of nutrients in the Miocene carbonate factories. Nutrification, namely an increase in nutrient input to an environment resulting in a detectable change in community structure (Hallock et al. 1993), can be easily mistaken, in the paleontological record, for shift toward cooler climate. Furthermore there are almost no recognized bio-proxy of high nutrient level among fossil benthic species. For these reasons, an in-depth paleontological and sedimentological study was needed before I could start comparing different carbonate sequences on the basis of their paleo-nutrient levels. I performed

different analyses and followed various approaches to accomplish this task.
Within this context, for the sake of clarity, the essay-format was the best choice to present my findings. This thesis is therefore divided in to six chapter. The importance of nutrients in the biogeochemical cycle of Earth and geological history of the Miocene are covered in first introductory chapter. The second, third and fourth chapter are in the form of research papers. The second chapter deals with the paleoecology and the sedimentology of the Pietra da Cantoni Group and the third analyzes in detail the paleoenvironment of the Sommières Basin. In the fourth chapter the two sequences are directly compared and the paleontological results are integrated with geochemical analyses to prove and support the hypotheses. The fifth chapter is a brief summary of all the results of this study and the sixth chapter is a taxonomic appendix.

Index

1-Introduction

The aim of this work is to improve our knowledge of nutrients influence in the fossil record of the Miocene. The studied succession were analyzed trough a multidisciplinary approach encompassing paleontology, sedimentology and geochemistry in order to extract information and disclose the existing relation between fossil skeletal assemblages and nutrient abundance.

The Miocene has been a turning point for our Planet evolution. During the Miocene the ocean circulation finally become comparable to the present-day situation and a decrease in temperature brought climatic conditions very close to those of the present. Land and marine life were fairly modern and many present-day ecosystems arose in the Miocene. Lower Miocene is also the oldest period in which the principle of taxonomic uniformity can be safely applied. Miocene is the first Epoch of modern Earth and therefore is the perfect setting to study, on a geological time frame, ecological processes and draw conclusions useful in the comprehension of present-day ecosystems.

While many other works have tried to analyzed productivity and nutrient fluctuation in deep water sediments, this is one of the first attempt to approach the problem in shallow water setting. Shallow water biota is deeply influenced by variations in nutrients supply and may record these differences. Even thought chemical analyses may be sizeably biased by diagenesis in coarse-grained shallow-water sediment, with certain techniques and accurate combination of different groups of data it is possible to unveil precious information.

The studied successions of the Pietra da Cantoni Limestone Group of the Tertiary Piedmont Basin and of the Sandy Molasse Unit of the Sommières Basin are both of Burdigalian age and they were close-by during the Miocene. They were also characterized by similar skeletal assemblages and by the abundance of coralline algae and of heterotroph suspension-feeders. They were chosen to minimize climatic and geographical variability and to concentrate over productivity.

Nutrient-rich waters have left a clear imprint on the fossil record by influencing the marine biota. These traces can be brought to light and used to improve our knowledge of the nutrients cycle of the Earth.

1.1 - Essential Nutrients

Essential nutrients are components that an organism uses to survive and grow. In marine ecology this term is generally used to define those elements and compounds that are needed for the development of photosynthetic organisms. Since plankton and benthic algae are the base of the food chain, their health is of paramount importance for the whole ecosystem.

To develop and grow plants needs water, oxygen, carbon dioxide, phosphorous, nitrogen, potassium, calcium, magnesium, sulfur, iron, silica and other minor elements. Oxygen and carbon dioxide are used for respiration and photosynthesis respectively, while the others are involved in various and different metabolic processes. Phosphorous is used as a structural component of the nucleic acid (both DNA and RNA) and in the phospholipids of the cell membrane. Phosphorus is also a key component of the Adenosine triphosphate (ATP) which is the coenzime used in the process of intracellular energy transfer. Nitrogen is a fundamental constituent of amino acid, the building block of proteins, and it is also essential to synthesize chlorophyll. Potassium is involved in the production of carbohydrates and protein but also act as a contributor to photosynthesis, especially under low-light conditions. Calcium regulates the transport of other nutrients within the tissues and is involved in the activation of different enzymes. Magnesium is a constituent of chlorophyll molecule and is also involved in various enzyme reactions. Sulfur is a structural component of amino acids and vitamins and is essential in the production of chloroplasts. Iron is another important element in the photosynthesis reaction and other microbial processes. Silica while not directly involved in metabolic processes, is used by diatoms, radiolarians, silicoflagellates, and other less common planktonic organisms, to produce their skeleton.

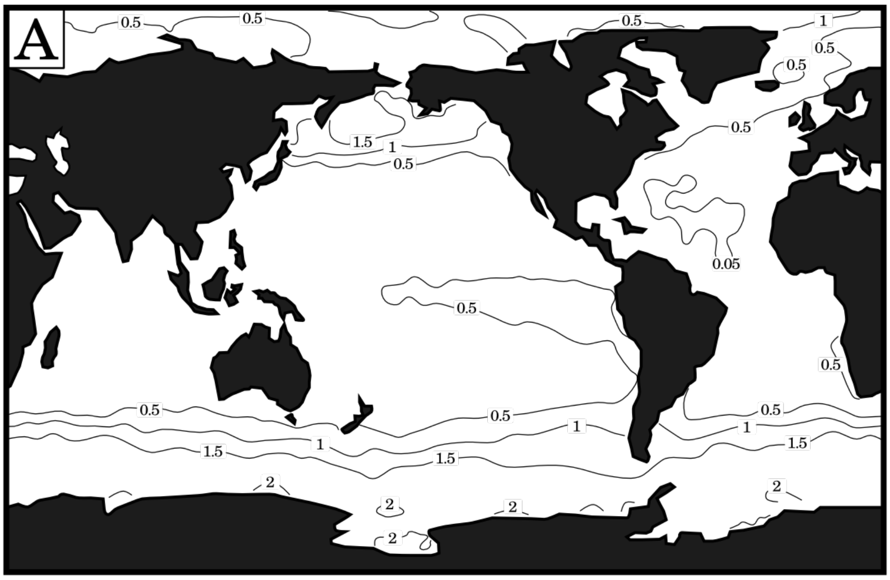

Figure 1.1.1A : Mean annual phosphate [µmol/l] at the surface (Garcia et al., 2010)

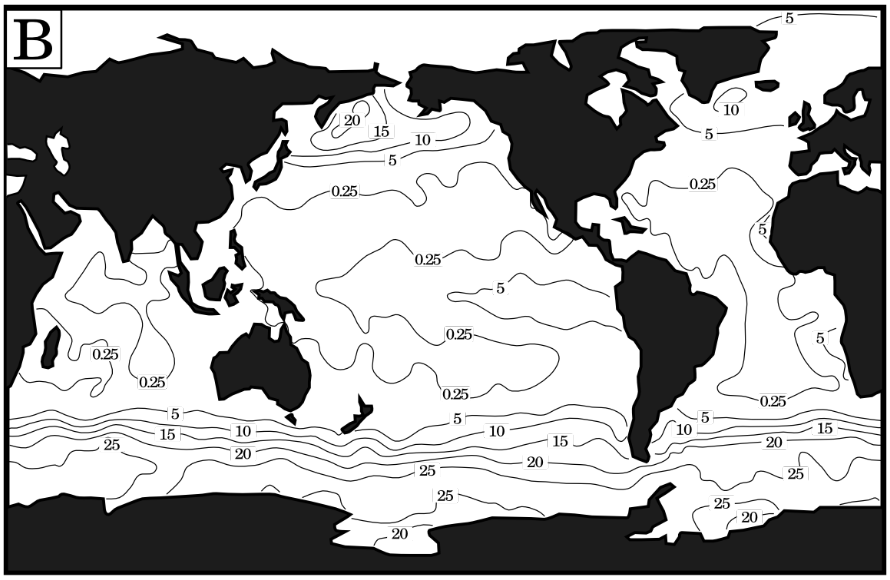

Figure 1.1.1B : Mean annual nitrate [µmol/l] at the surface (Garcia et al., 2010)

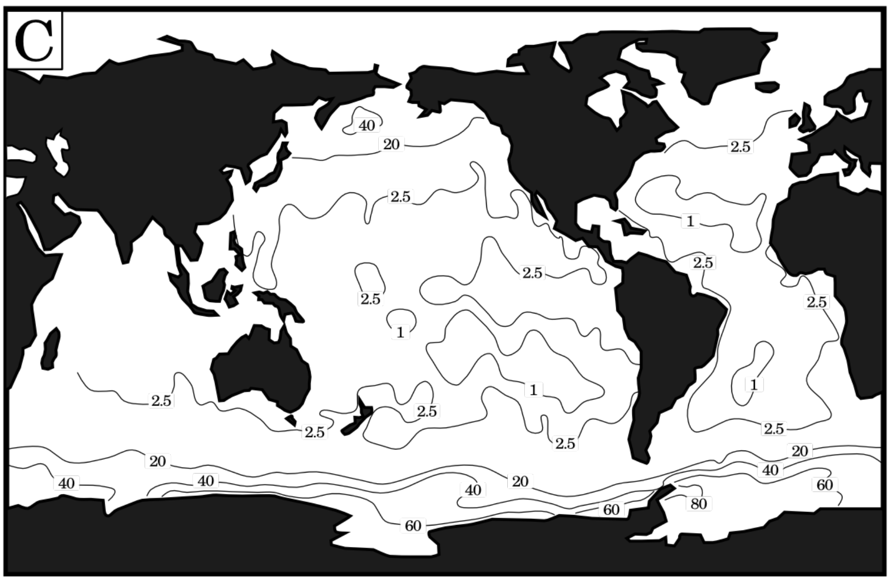

Figure 1.1.1C : Mean annual silicate [µmol/l] at the surface (Garcia et al., 2010)

Most of these nutrients are plentiful in the oceans, but P, N, Fe and Si can be limited. Thus the abundance of these nutrients constrain the formation of phytoplankton biomass by fixing its upper threshold level (Fig 1.1.1; Fig. 1.1.2).

Alan Redfield in 1958 assumed that most of marine environments are limited by P abundance. This assumption was based on chemical analyses of the elemental composition of marine organism and some fundamental concepts. The elemental ratio of marine particles is 106C/16N/1P. N and C are supplied to ocean from the whole atmosphere (*via* N_2 and CO_2), while P is mainly supplied by river outflow. N fixation (*i.e* the microbial process that reduces the inert N_2 into biologically available forms) and N loss (the denitrification of organic matter, *i.e* the microbial process that oxidate the N of organic matter to release N_2) allow for a concentration of biologically available nitrogen that keeps pace with the demands of photoautotrophs. Therefore, P availability is the ultimate limiting factor. However, biological oceanographers have demonstrated, through experiments and observations, that primary production is also very often limited by the availability of fixed organic nitrogen.

Fe is not only necessary for photosynthesis but is also directly involved in nitrogen fixation process (Falkowsky et al. 1998). Actually the vast majority of N fixation in the oceans appears to be accomplished by a handful of species of cyanobacteria notably *Trichodesmium* spp. (Capone et al. 1997). In this group of species photochemical and N fixation processes require Fe (Postgate, 1971). Therefore, Fe abundance limits primary production in environments otherwise limited by N availability. Since one of the major source of Fe in the oceans is wind-blown dust, vast areas of world oceans are Fe limited, notably the South Pacific (Falkowsky et al. 1998).

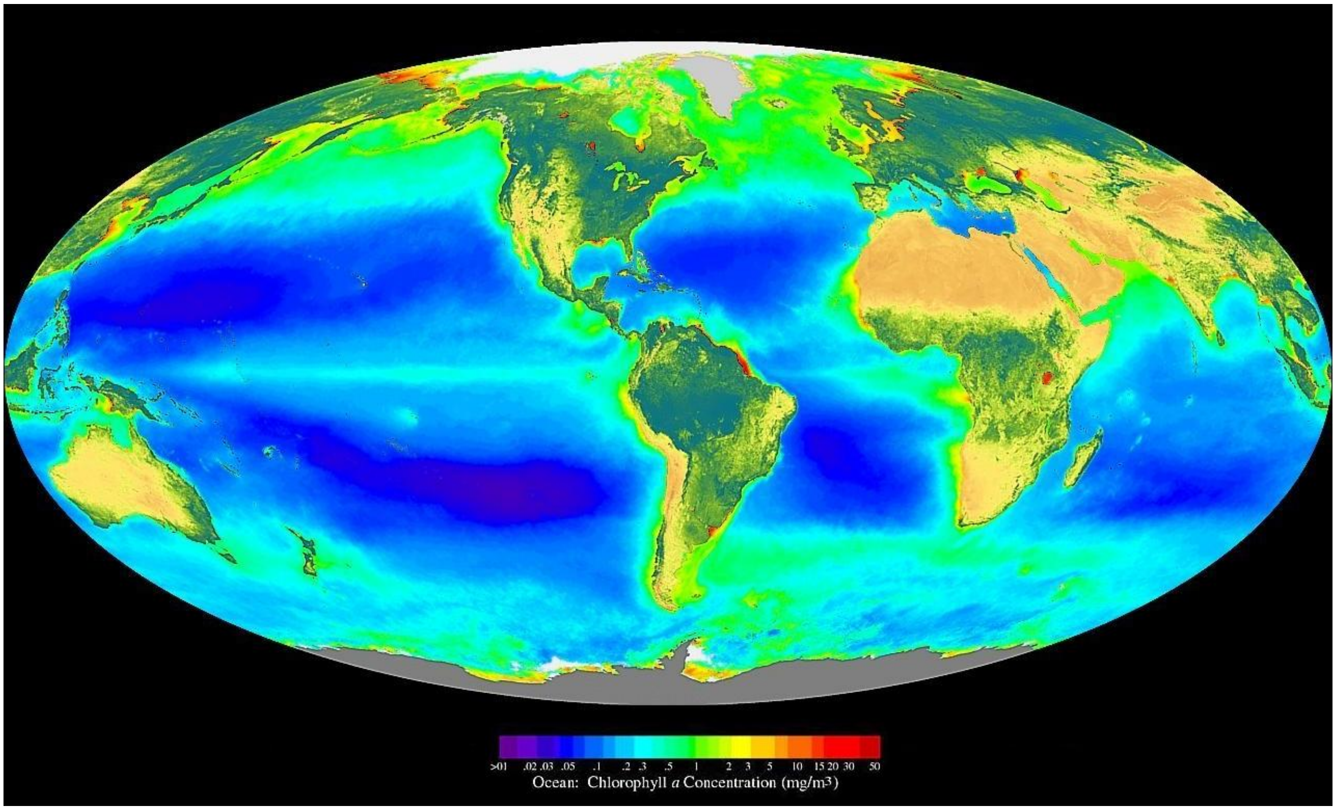

Figure 1.1.2 : Mean annual chlorophyll α concentration, a proxy of primary production, at ocean surface (Data source: NOAA)

Silica, unlike the other nutrients which are needed by almost all marine plankton, is an essential requirement just for siliceous-shelled biota. However, since diatom are one of the dominant phytoplankton group responsible for world primary production (Dugdale et al. 1995), silica availability is an important limiting factor for phytoplankton biomass formation. Silica is supplied to the oceans primary from the rivers, but also from basalt weathering, eolian dust and hydrothermal emanations and is immediately used by siliceous phytoplankton (DeMaster, 2002).

These essential nutrients are fixed in the organic matter by the primary producers, in the upper layer of the water column, the euphotic zone. After their death, marine organisms start to sink down to oceans depth where photosyntesis is prevented by the lack of light and destructive processes (either decomposition and dissolution) prevail. Here nutrients are lost by particulate and dissolved organic matter (POM and DOM) and enrich bottom waters.

Since almost no primary production occurs in the ocean depth, bottom waters become rich of the essential nutrients which are conversely consumed in the primary production of the photic zone. Wherever these bottom waters rise toward the surface, due to oceanographic reasons, they fertilize the photic zone. This process of internal recycle of nutrients, through upwelling currents and mixing of the water column, actually is one of the main supplier of these essential molecules into the photic zone.

In paleoecological reconstruction is fundamental to understand which one of the above mentioned nutrients is responsible for controlling primary production in the long run. P and N are indeed the key players, the former is the ultimate limiting nutrient (*i.e*. the nutrient whose supply rate forces total system productivity on the long time scale) while the latter is the world wide most common proximate limiting nutrient (*i.e.* the nutrient whose increases result in an enhancement of primary production within hours or days) (Tyrrel, 1999). This statement resolve the divergence between the geochemical view of the oceans (which predict that the production should be limited by the biologically-available P abundance due to it limited supply by the river) and the biological view (which observe that primary production is mainly limited by the biologically-available N supply). Actually phytoplankton may be separated into two broad categories: those who can fix nitrogen from the atmosphere and those who cannot. In a situation where biologically-available P is present, the N-fixers (like *Trichodesmium* spp.) have an obvious advantage if biologically-available N is scarce. The latter have an advantage instead when biologically available N is abundant since N fixation requires a lot of energy. In a normal environment, where both N-fixers and N-users phytoplankton groups occur, an increase in biologically available nitrogen increases N-user abundance but at the same time diminishes the niches for N-fixers thus reducing their ability to

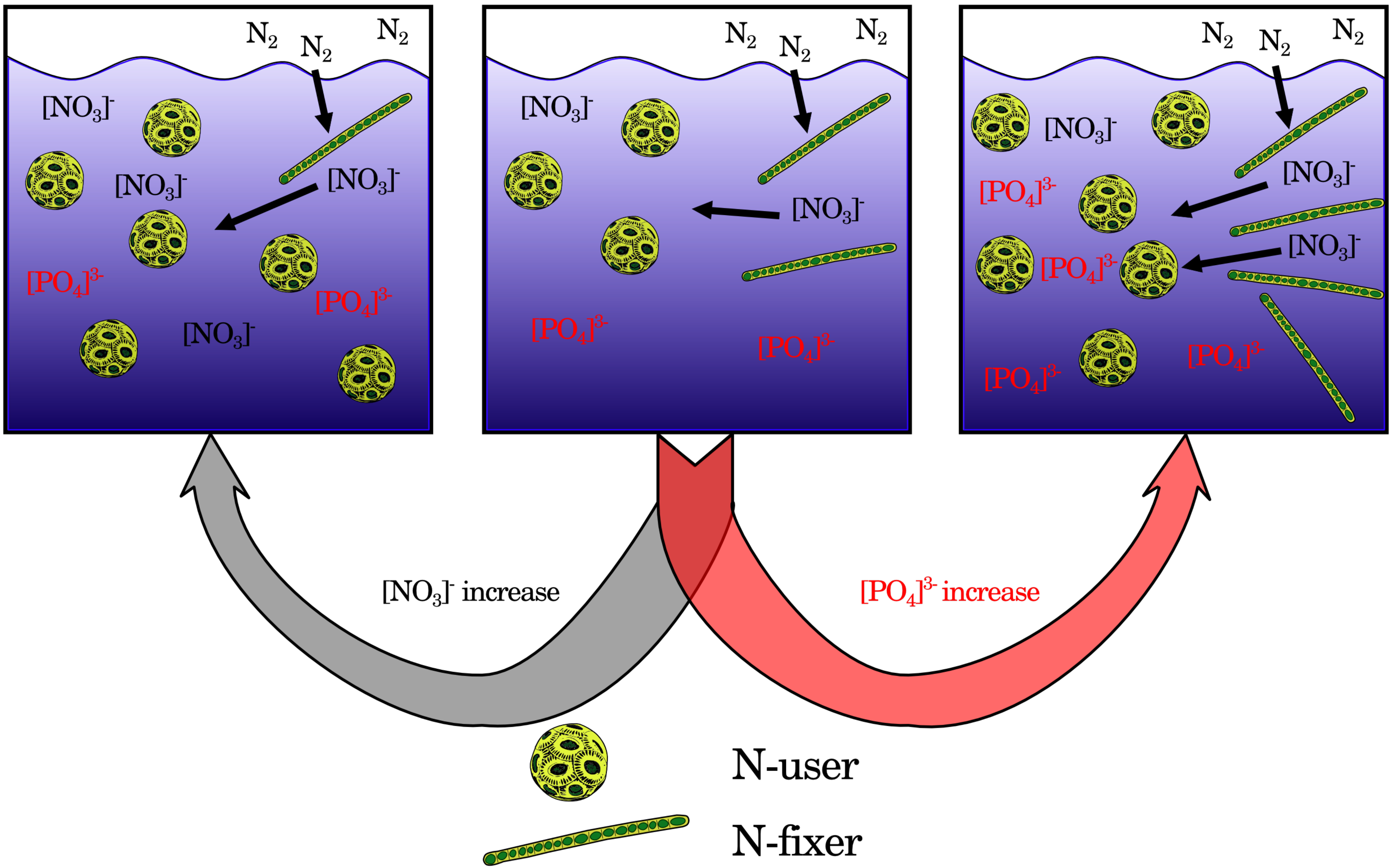

Figure 1.1.3 : simplified environmental reaction to the increase of biologically-avialable N and biologically-available P

supply further biologically-available N to the environment. An increase of biologically-available P instead boost N-users, creating a deficit of biologically-available N which in turn open new possibilities for N-fixer to thrive (Fig. 1.1.3). Therefore a steady increase in biologically-available P lead also to a steady increase of biologically available N. This model (Tyrrell, 1999) explain why the scatter plot of the concentrations of biologically available P and biologically available N in the oceans intersect near the origin of the axis (Fig. 1.1.4). The model also proves that P is the ultimate limiting nutrient on the geological time scale (Tyrrel, 1999).

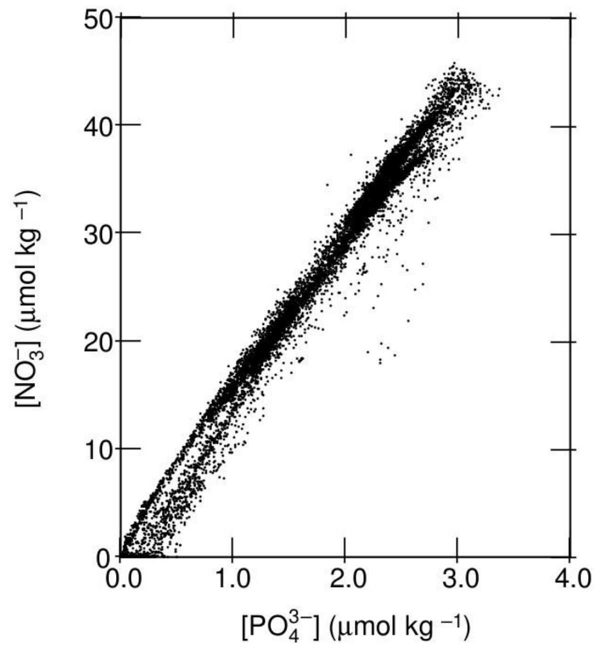

Figure 1.1.4: Nitrate concentrations vs phosphate concentrations in modern oceans (from Tyrrel, 1999)

1.2 - Biogeochemical cycle of Phosphorous

Phosphorous is the ultimate limiting element of ocean environment and thus hold a remarkable importance in the regulation over the geological time scale of primary production, organic carbon burial and even diversity of the marine biosphere (Hallock, 1987; Sarnthein et al. 1988; Brasier, 1992; Raymo, 1994; Martin, 1996; Delaney, 1998). Therefore, paleontologists focus on the fluxes of P into and out of the oceans, on the oceanic P inventory and its internal distribution.

P is not found free in nature, due to its high reactivity, its most common occurrence is the phosphate ion $[PO_4]^{3-}$. P is widely distributed in many minerals, mainly phosphate and continental crust has an average of 0.1% of P in weight (Delaney, 1998). The continental weathering of phosphate-bearing igneous and sedimentary rocks is the most important (and the largest pre-anthropogenic one) source of P (Froelich et al. 1982; Föllmi, 1996; Fig 1.2.1 A). The direct contribution of continental volcanism is poorly quantified and although it may be important on a local to regional scale, it may represent a negligible source of P when integrated over the geological time.

Hydrotermal activity and wheathering of basalts at mid-oceans spreading centers provide neglible amount of P (Froelich et al. 1982; Delaney, 1998). These processes may also act as additional sinks for P, due to removal of dissolved P onto suspend iron oxyhydroxides derived from hydrothermal activity and direct uptake of P through reaction with basalt (Froelich et al. 1982; Föllmi, 1996; Fig. 1.2.1 B).

Weathering of P-containg rock is therefore the main source of all biologically-available in natural systems. Apatite ($Ca_{10}[PO_4]_6(OH,F,Cl)_2$) is the most abundant P-bearing mineral, its dissolution is largely driven by exposure to acid, especially organic acids generated by soil microorganism like fungi (Slomp, 2011).

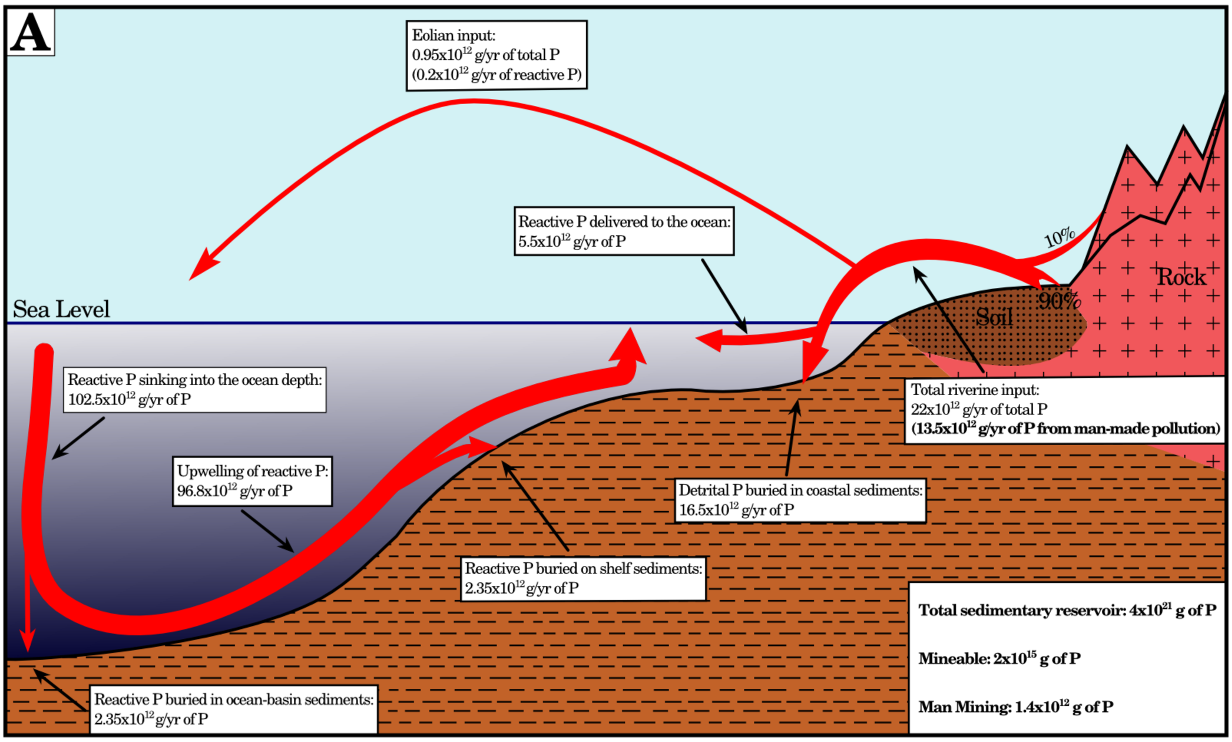

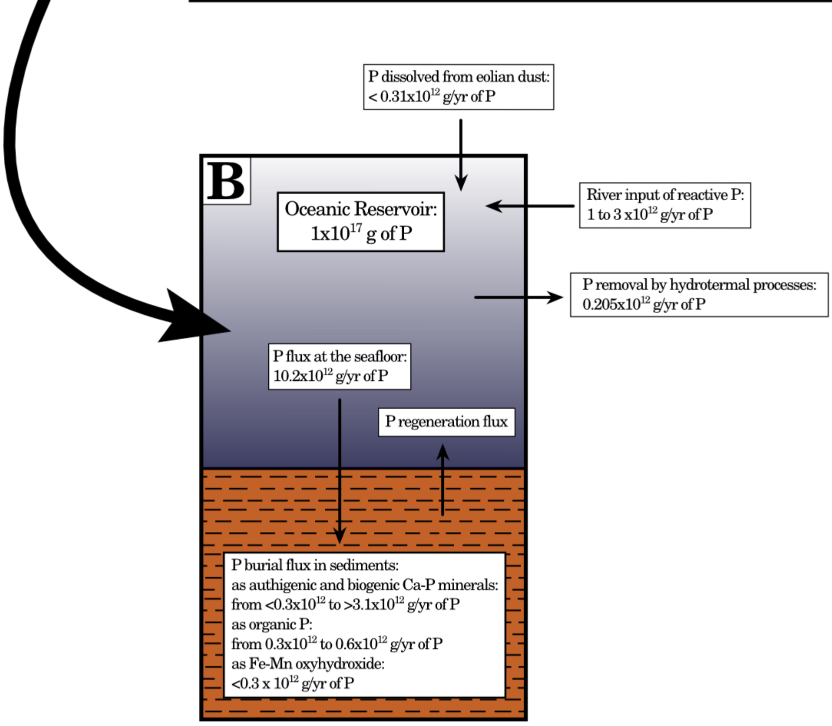

C Estimates of natural (pre-antropogenic) and modern (present-day) river fluxes

Type of fluxes (g/yr)	Dissolved P	Particulated P	Total P
Natural			
Meybeck et al. (1982)	$1x10^{12}$	$20x10^{12}$	$21x10^{12}$
Froelich et al. (1982)	n.a	n.a	$10x10^{12}$
Howarth et al. (1995)	$1x10^{12}$	$7x10^{12}$	$8x10^{12}$
Ruttenberg (2004)	$1\text{-}2x10^{12}$	$18\text{-}20x10^{12}$	$19\text{-}22x10^{12}$
Modern			
Froelich et al. (1982)	n.a	n.a	$22\text{-}30x10^{12}$
Howarth et al. (1995)	$2x10^{12}$	$20x10^{12}$	$22x10^{12}$
Smith et al. (2003)	$2x10^{12}$	n.a	n.a
Harrison et al. (2010)	$2x10^{12}$	$13x10^{12}$	$15x10^{12}$

Figure 1.2.1 : the cycle of Phosphorous

A: Exogenous P cycle (modified from Föllmi et al., 1996)

B: Ocean P inventory and fluxes (modified from Delaney, 1998)

C: pre-antropogenic and modern river fluxes of P (modifed from Slomp, 2011)

Human activities and pollution represent an other large source to the environment. Man's acceleration of the denudation processes (through deforestation, agriculture and urbanization) may have doubled the natural P-flux toward the oceans (Froelich et al. 1982; Howart et al. 1995; Fig. 1.2.1 C). In addition to increased continental erosion, the runoff of water from agricultural land and the discharge of sewage from highly populated areas are a major and man-made source of P to the environment (Slomp, 2011).

P moves from continent toward the oceans through water and eolian transport; soils constitute important temporary reservoirs and have high phosphate content, therefore denudation rate has a significant effect on P supply rate (Froelich et al. 1982; Föllmi, 1996). P occurs in river runoff as solution and suspended particulate, in both mineral and organic forms (Föllmi, 1996; Baturin, 2003). Dissolved organic and inorganic P appear usually in low quantities (Föllmi, 1996). The portion of suspended P incorporated in volcanic apatite is almost geochemically inert, whereas the portion associated with organic matter and iron oxyhydroxides is instead reactive (Baturin, 2003). Submarine groundwater discharge is an additional source of dissolved P especially in areas where groundwater flow rate is high (Slomp, 2011). While rivers are the main carrier, a non negligible (approximately 4-5%, Duce et al. 1991; Fig 1.2.1A-B) fraction of particulate P is transported through the air in the form of mineral particles and small organic remains (Föllmi, 1996); eolian transport become significant especially in those oceanic regions far away from terrestrial input.

Just a fraction of the P eroded from the continents enters the oceans in a form that is available for the marine organisms (Föllmi, 1996). Froelich (1988) estimated that approximately 25% of the P that is delivered to the oceans is in a bioavailable form. Almost all this reactive and bioavailable P is used in the surface zone of primary productivity and incorporated into organic matter, while the fraction of P that is not biologically available is directly buried within the sediments (Föllmi, 1996).

Eventually P is transferred to the deep ocean in the form of organic matter and, upon oxidation, of dissolved inorganic phosphate. Most of P is taken up by intermediate and deep water circulation and reintroduced to the photic zone by upwelling processes (Föllmi, 1996; Fig. 1.2.1 A). A small fraction of the sinking P reaches the sea floor and is incorporated into the sediment either as organic P (in organic matter and fish debris) or as inorganic P, through adsorption on iron and manganese oxyhydroxides or incorporation in phosphate-bearing minerals (Föllmi, 1996). Once P has reached marine sediments it can either be incorporated again into the lithosphere or being recycled back in to the biosphere (Fig. 1.2.1 B). Whether it follows one or another path is up to its form and the sedimentological and chemical conditions at the water-sediment interface. The key forms of P in sediments are exchangeable (or loosely-bound) P, Fe-oxyhydroxides-bound P, authigenic and biogenic Ca-P minerals, detrital apatite and organic P (Ruttenberg, 2004). Authigenic and biogenic Ca-P minerals and even more detrital apatite are mostly refractory, whereas exchangeable P, organic P and Fe-oxyhydroxides-bound P and may show considerable postdepositional mobility. The latter group is particularly sensible to changes in redox potential and can easily release P back in to the water. The abundance of “weak” sinks of P, like exchangeable P and Fe-oxyhydroxides-bound P, is also related to the grain-size and the chemical and mineralogical characteristic of sediments (Andrieux-Loyer and Aminot, 2001).
P that is finally buried within the sediment may be eventually lost in the mantle through subduction, this loss is balanced, over the geological time scale, by the formation of new rocks through igneous activity.
Since the major input of P in the exogenous cycle is from the weathering of continental rocks, the P supply rate to the oceans represent a powerful link between geological activity and biological activity, allowing the reconstruction of long-term feedback mechanisms between climate, environment and ecology (Froelich, 1988; Garzanti, 1993; Föllmi, 1996; Delaney, 1998; Guidry et al. 2000; Baturin, 2003) .

Furthermore understanding the effects of the variations in P supply rate in the geological past may allow present-day researchers to gaze in the long-term effects of human P-based pollution on the environment, the consequences of which can not yet be clearly seen (Hallock, 1988).

1.3 – Fossil Record of Nutrients

Limiting nutrients and P in particular affect global primary production this in turn has various major consequences on world climate. Since the ocean store much more CO_2 than the atmosphere, relatively small changes in the dissolved oceanic CO_2 can bring about large changes in the atmospheric CO_2, which in turn has a major control over the green-house effect. The most likely means of achieving this is by changing the rate of carbon fixation by marine primary productivity. Increased delivery of reactive P from the land and/or faster recycling of P through upwelling currents can actually boost CO_2 uptake and therefore it may start a global cooling (Sarnthein et al. 1988). Conversely low nutrient supply and limited CO_2 uptake may led to global warming. Variations in primary production also influence water chemistry, both its chemical composition and isotopic signature. Of course nutrient supply doesn't simply and only controls primary production: the whole food web is influenced. Different supply of essential nutrients may lead to completely different environment. These changes are on such a large scale that are indeed recorded, directly or indirectly, in the geological history of the Earth and therefore they may be investigate by paleontology (Hallock and Schalger, 1986; Hallock, 1988; Brasier, 1992; Brasier, 1995a; Brasier, 1995b; Martin, 1996).

Since several process of organic synthesis result in a disequilibrium fractionation of carbon stable isotope, primary production may be recorded by the isotopic signature of C (Brasier, 1992). Actually marine autotroph during the photosynthesis shows a preference toward the light isotope of C, ^{12}C, leaving surface water enriched in the heavier isotope ^{13}C. Where light and temperature are optima, availability of dissolved nutrients controls primary production and hence the carbon isotope fractionation. Heterotrophic organisms consume this light carbon, releasing light CO^2 back into the ocean.

This light CO2 is favored for the photosynthesis by autotroph. Where light and temperature are optimal, availability of limiting nutrients, and above all P, controls the limits of primary production and hence of carbon isotope fractionation. Thus a trend towards heavier carbon isotopes cannot take place in sea-water unless there is an adequate supply of P to fuel primary production and fractionation. Therefore positive $\partial^{13}C$ indicates an higher P content, while negative $\partial^{13}C$ indicates an oligotrophic environment (Brasier, 1992). The inverse correlation between biologically-available P and $\partial^{13}C$ is so strong that the latter can be regarded as a proxy for reconstruction of changes in P supply (Brasier, 1992). However $\partial^{13}C$ is also controlled by other factors. Studies on modern skeletons show that vital effects (i.e. biological processes that involve the utilization of metabolic C in the secretion of the skeleton) may overprint the environmental signal producing $\partial^{13}C$ values which are not in equilibrium with the environment. Furthermore organic decomposition in mid waters and upwelling currents may bring light C into the water column (Brasier, 1995a). For these reasons $\partial^{13}C$ are often contradictory and their interpretation is difficult (Brasier, 1995a).
Paleoproductivity may also be estimated by comparing the difference between $\partial^{13}C$ values of a pair of benthic foraminifers (e.g. *Cibicioides wuellerstorfi*) which can record bottom waters at the water-sediment interface and below, in the interstitial pore-waters (e.g. *Uvigerina peregrina*; Corliss, 1985). The decomposition of organic matter within the sediment release ^{12}C into the interstitial water, this ^{12}C become incorporated in *Uvigerina* tests. *Cibicides* lives above the sediment surface and therefore has a lower $^{13}C/^{12}C$ ratio. This gradient exist and can be measured at any given site. The difference between the two species increase when surface waters are more fertile, since large amount of organic matter reaches the bottom and are decomposed in the sediment, releasing ^{12}C (Brasier, 1995a).

An other geochemical proxy of paleoproductivity is Barium. Ba is strongly associated with organic matter and more than 90% of barium in oceanic sediments (far away from mid-ocean ridge since hydrothermal inputs are significant close to the spreading center) is a residue of biogenic material (Dymond et al. 1992). Ba in suspended organic particles is dominantly in the form of barite and the mineral forms in the upper water column by decomposition of organic matter (Dymond et al. 1992). The Ba content of sediment is then related to the primary production, however, in strongly-reducing environment, barite is dissolved and Ba mobilized again (Dymond et al. 1992). Ba/Ca ratio in biogenic skeletons is also a good tracer for high productivity and upwelling zones (Von Breymann et al. 1992; Brasier, 1995a).

Cadmium has a similar distribution to Ba and P in the water column, being depleted in surface waters and concentrated in the oxygen minimum zone or at depth. Due to this strong correlation between Cd and P concentration in sea water, the former (as Cd/Ca ratio) has been exploited to reconstruct past nutrient distribution (Delaney and Boyle 1987; Boyle, 1992; Brasier 1995a). This distribution is characteristic of an algal nutrient and actually the element is used by some group of marine phytoplankton, generally but not always in place of Zinc, to develop en enzyme involved in the inorganic carbon acquisition (Cullen et al. 1999). It has been proved that Cd uptake is also largely regulated by CO_2 concentration in the water mass. A modulation of Cd uptake by CO2 suggests that indeed the biogeochemical cycle of this element should respond to major changes in global climate (Cullen et al. 1999). However since the relationship between Cd and P in moder ocean is mediated by CO_2 and Zn concentration, past changes in these two may have altered Cd-P relationship, either regionally or globally (Cullen et al. 1999).

The rare earth element Cerium is also used in studying paleoproductivity. Normal marine biogenic apatite is markedly deficient in Ce when compared with other rare earth like Lanthanum and Neodymium. However in anoxic regions of the sea floor, such as the Black Sea, the Ce deficiency is reduced.

SEDEX extraction line

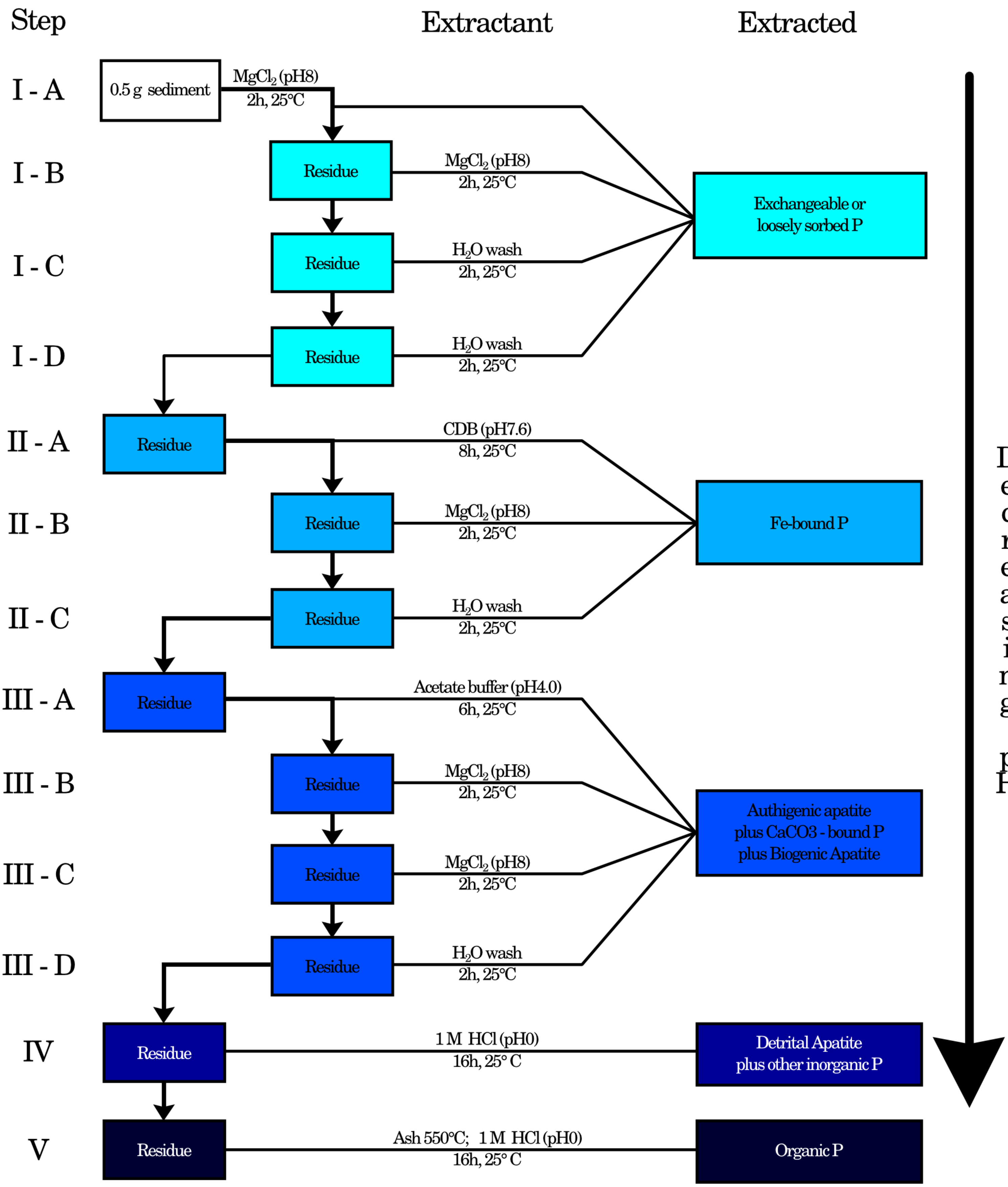

Figure 1.3.1 : SEDEX extraction line; modified after Ruttenberg 1992

Actually marine authigenic phosphates and carbonates incorporate rare element distribution pattern of the sea-water in which they precipitated. In normal oxic condition Ce exists as insoluble Ce^{4+} and therefore is scarce into seawater. Under suboxic/anoxic environment, Ce undergoes reduction to soluble Ce^{3+} and become available to be incorporated in authigenic minerals.

The magnitude of Ce anomaly, compared to the other rare earths, can be therefore used as a proxy of anoxic conditions, which is generally associated to high primary production on the surface (Brasier, 1995a). However post-depositional alteration, diagenesis and weathering may considerably affect the original rare earth elements pattern and thus destroy the original paleoenvironmental signal (Shields and Stille, 2001; Pattan et al. 2005).

A different and possible approach is to directly measure the P content of the sediment or of the rock with colorimetric (molybdenum blue with stannous chloride) and X-ray fluorescence analyses (Föllmi, 1995). However to produce more complete results it is necessary to separate biologically-available P from non-reactive P, it is necessary to separate and quantify the various solid-phase reservoirs of sedimentary P. This is difficult because P is present in low concentration and therefore direct identification of mineral phases with techniques, such as X-ray diffraction, is almost impossible. The most viable method to achieve this results are sequential extraction techniques. Sequential extraction methods consist in a series of chemical reaction, or step, based on the reactivity of a particular mineral phase in a given extractant. The extractant is a chemical compound specifically devised and tested to remove efficiently just a given phase from the bulk of the sample. Such techniques for P, where initially developed of continental setting (Williams et al. 1976) and become routinely applied in marine settings after the seminal work of Ruttenberg, 1992 (Fig. 1.3.1). The SEDEX scheme presented by Ruttenberg (1992; Fig. 1.3.1), consists of five step which separate the major reservoir of sedimentary P into five pools: loosely sorbed or exchangeable P; ferric Fe-bound P;

authigenic carbonate fluorapatite + biogenic apatite + $CaCO_3$-bound P; detrital apatite of igneous or metamorphic origin; organic P (Fig. 1.3.1). This method can detect P concentration as low as 0.005% in weight with a 4% error (Ruttenberg, 1992). The strength of SEDEX is that this method is able to perfectly separate authigenic/biogenic apatite from metamorphic/igneous apatite, while the first is actually related to biologically-available P the latter is not. Furthermore the extraction is devised to avoid analytical artifacts resulting from redistribution and adsorption, during the extraction, of P onto the surface of the residue. These sediment-matrix effect is successfully reversed by washing the sediment with $MgCl_2$ between the steps (Ruttenberg, 1992; Fig. 1.3.1). In the various years the technique has been modified and improved (e.g. Slomp et al. 1996; Ruttenber et al. 2009) and is commonly applied for the study of recent and fossil sediments (e.g. Slomp et al. 2002; Bodin et al. 2006; Kraal et al. 2012).

Paleobiological proxies can also be good indicators for the nutrients status in the fossil record since the nutrient supply rate has large consequences on the ecological structure of the environment and on its species assemblage (Hallock and Schalger, 1986; Hallock, 1987; Brasier, 1995a; Brasier, 1995b).

Major biogenic silica deposits have long been thought to accumulate during past episodes of high ocean productivity (e.g. Calvert, 1966). Studies on sediment traps confirm that under area of high productivity the flux of siliceous skeletons is indeed more abundant, on the other hand calcareous plankton dominates in the oligotrophic mid-ocean gyre (Takahashi, 1986). The accumulation rate of siliceous skeletons may also be derived from ancient sediments and then used to estimate past ocean productivity (e.g Tiedemann et al. 1989). Among siliceous skeletons the relative ratio of diatom and radiolarian skeletons can be used to map upwelling intensity since the former dominate in the highly fertile core of the most upwelling areas, while the latter dominate in the surrounding areas (e.g. Molina-Curz, 1977). However the diatoms are more vulnerable than radiolarians to solution in the water column and in the sediment, therefore their ratio is greatly altered through time (e.g. Abrantes, 1992). The abundance of eutrophic-adapted diatom may also be used to track paleoproductivity of the environment (Brasier, 1995a).

Large deposits of phosphatic skeletons are also typical of upwelling areas of present-day oceans (e.g. Thiede and Junger, 1992). Assemblages dominated by phosphatic skeletons, associated with phosphorites are known since the early Paleozoic (Brasier, 1992) and grainstone-phosphorite sediments are often related to nutrient enrichment, although they can also be produced by very slow sedimentation rate (Brasier, 1995a). The fossil accumulation of phosphatic remains therefore can be used, with caution, to identify past areas of high primary production (Brasier, 1995a).

Areas of high primary production are characterized by organic-matter rich sediments. The combined effect of a remarkably high production in surface waters and reduced mixing and oxygenation at the sea floor may lead to the preservation of the organic matter produced and then at the formation of a sapropel layer. The presence of these layers may be used to identify period of enhanced nutrient supply and high primary production (e.g. Slomp et al., 2002)

Since also Ba is also a good tracer for area of high primary production, the accumulation of biogenically secreted baryte may also be used as a productivity indicator (Brasier, 1995a).

Upwelling areas are also characterized by peculiar assemblages of planktonic foraminifers and coccolithophorids. These assemblages are composed by species well adapted to the high nutrient supply of these areas. Planktonic foraminiferal taxa best adapted to upwelling conditions prefers cool water and a diet of phytoplankton, they lack spines and supplementary apertures and seldom have endosymbionts (e.g. *Neogloboquadrina pachyderma*; Brasier, 1995a). Among modern coccolithophorids small placoliths are abundant in upwelling areas and display an opportunistic behavior, quickly increasing their numbers whenever favorable conditions occur, a suitable strategy to take advantage of the high nutrient supply present (Okada and Honjo, 1973).

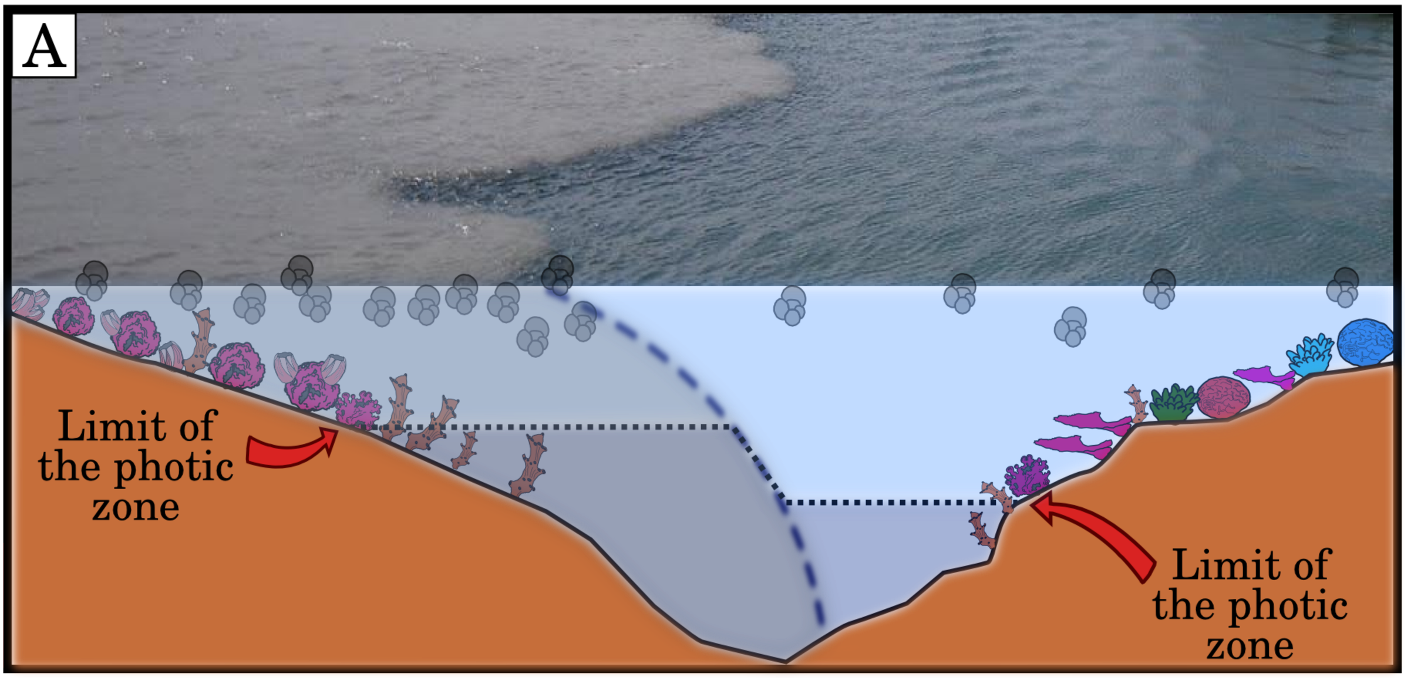

B	Non-oligotrophic carbonates (Mesotrophic) Vs Oligotrophic carbonates	
	Mesotrophic	Oligotrophic
Limit of the photic zone	50m	130m
Reefs	Bindstones, bafflestones, mudmounds	Framestone
Larger foraminifera	Archaids, soritids	Rotaliids
Coralline algae	May flourish	Less important
Fleshy algae	Abundant	Incospicuos
Seagrasses	May flourish	Present
Microbes and bacteria	Fourish and mats may develop	Incospicuos
Micritized grains	Common	Incospicuos
Bioeroders	Abundant	Incospicuos
Carbonate sediments	Detrital sands	Skeletal sands

C	Non-oligotrophic (Eutrophic) environment Vs Oligotrophic environment	
	Eutrophic	Oligotrophic
New nutrient supply	High, unstable	Lower, more stable
Net productivity	High, especially plankton	Lower, especially benthos
Water clarity	Low	High
Diversity	Low	High
Trophic strategy	Generalist/Opportunist	Specialist
Population stability	Unstable	Stable
Benthic feeding method	Suspension feeders	Grazers, Symbiosis
C and P loss to sediment	High	Low
Bioerosion level	High	Low
Associated sediments	Concentraed pelagic limestone, phospohorite, black shale, diatomite	Shelly-benthic limestone, framework reefs

Figure 1.3.2 : Oligotrophic Vs Non-oligotrophic environment. A) Sketch model of water clarity and benthic communties under oligotrophic and non-oligotrophic conditions. B) Characteristics of carbonates developed under oligtrophic and non-oligotrophic conditions; modified from Brasier (1995b). C) Characteristics of an oligotrophic environment and of a non-oligotrophic environment; modified from Brasier (1995a).

The same behavior was displayed by small reticulofenestrids (e.g. *Reticulofenestra minuta*), these forms, beside their biostratigraphic significance, could be important paeloecological indicators (Negri and Villa, 2000; Kramer et al., 2006).
Nutrient supply rate do not only have effect on planktonic organism (and the accumulation rate of their remains) but they affect the whole marine ecosystem, including also the benthic communities of the shelf. Actually optimal conditions for primary production are very often confined to coastal areas, which can benefit from the abundant nutrient supplied by rivers and continental run-off. This where the highest levels of mean primary productivity may be achieved and highest benthic biomass is present. Furthermore this area may as important as the vastness of the ocean in carbon burial processes. The oceanic systems, although more extensive, is less effective in permanently remove carbon from the coupled atmosphere-ocean system, because the organic carbon exported to the deep oceans is largely oxidized in the water column and the CO_2 released back in to the environment (Brasier, 1995a). The neritic system, on the other hand, may permanently store organic carbon on the shelf ad upper-slope sediments since both high primary production and large benthic communities contribute toward oxygen-depletion of the bottom sediments and therefore higher burial rate of organic matter (Tyson and Pearson, 1991; Brasier, 1995a). Therefore benthic indicators of nutrient abundance are essential to study the nutrient cycle of the oceans through time. One the major physical mechanism by which increased nutrient availability affects benthic communities, aside of course its direct influence on the food availability, is through the reduction of water transparency (Hallock and Schlager, 1986; Fig. 1.3.2). Nutrients control the biomass of plankton and, consequently, the amount of particulate organic carbon in the ecosystem. As nutrients increase, plankton biomass increases, reducing water transparency (Hallock and Schlager, 1986; Fig. 1.3.2). Reduced water transparency is a major detrimental factor for hermatypic corals, it decreases the depth ranges of other benthic autotrophs and mixotrophs including calcareous algae and large

benthic foraminifers, and generally move shoreward the whole benthic zonation (Hallock and Schlager, 1986; Vannucci et al. 2003; Hallock, 2005; Fig. 1.3.2).

Nutrient supply also influences the distribution of skeletal assemblages. Grain association dominated by debris of benthic foraminifera, mollusks, barnacles, bryozoans, echinoderms and calcareous red algae (heterozoan, sensu James, 1997) are generally typical of temperate and cold water, while assemblages where the contribution from zooxanthellate hermatypic corals and calcareous green algae are important (photozoan, sensu James, 1997) are more common in warm water settings. However significant shifts from this ideal model exist in the oceans and these differences are tied to nutrients supply rate (Hallock and Schlager, 1986). Wherever nutrients are plentiful, and consequently water transparency is scarce, photozoan assemblages are at disadvantage to heterozoan assemblages. The former thrive due to their bond with zooxanthellae, which provide to the host the products of photosynthesis, but in eutrophic condition this mutual symbiosis is not beneficial anymore. When food supply is plentiful active feeding is more efficient and therefore the heterozoan assemblage, where heterotroph suspension feeders (like bryozoans and barnacles) are abundant, has an advantage. Furthermore photozoan assemblage also require high water transparency, therefore hermatypic corals and green calcareous algae are even more at disadvantage when nutrients are abundant. On the other hand, coralline red algae (which are present in both assemblages but are more important and abundant in the heterozoan association) can thrive also in low light. Consequently heterozoan grain association in warm water setting, where photozoan association would be expected, may be related to high nutrient supply (Hallock and Schlager, 1986; Hallock, 2005; Halfar et al. 2006).

The species assemblage of benthic foraminifers is also influenced by nutrient supply and certain species can be used to draw information on the organic matter abundance and oxygen concentration at the sea floor (Brasier, 1995a). Infaunal species of the genera *Uvigerina*, *Bolivina*, *Bulimina* and *Nonionella* can tolerate low oxygen concentrations.

They are smaller, when compared to their relative that live in normal conditions, and they reproduce fast. These assemblage have been used to track changes in upwelling intensity and map eutrophication-induced anoxia (Brasier, 1995a).

Invertebrates with autotrophic protistan endosymbionts may provide an other useful index to nutrient levels (Brasier, 1995b). In the case of large benthic foraminifers, that have a long stratigraphic range and therefore are a perfect potential tool to study nutrients through time, the presence of photosymbionts is associated with a particularly complex endoskeletal architecture (Brasier, 1995b). The test actually become larger, develop multiple apertures and a large number of chamberlets that works as miniature green-houses for the photosymbionts (Hottinger, 1982). Once symbiosis is established in a group, diversity appears to be favored by prolonged, stable, oligotrophic conditions (Hallock and Schalger, 1986). An increase in nutrient levels instead could bring about a decline and maybe the extinction of the group (Hallock and Schalger, 1986; Hallock, 1988b).

Trace fossil and bioturbation are also related to nutrient supply rate. Increased availability of nutrients and organic carbon stimulates bioerosion, because many bioeroders feed on plankton which is abundant when nutrients are plentiful (Hallock and Schlager, 1986). Whenever primary production become really intense, the large flux of sinking organic matter may cause widespread anoxia at the sea floor. Anoxic sediments are consequently generally well-laminated, barren of burrow structures and bioturbation in general (Brasier, 1995a).

Tracking down nutrient variations in the distant past of Earth History may be an exceedingly difficult task, but a wealth of useful research instruments exists. Since different possibilities are available an integrated approach should be preferred. The single results obtained from a single line of analysis may be equivocal but the combined use of both geochemical and paleobiological indicators can provide consistent results and allow meaningful reconstructions of the past.

1.4 – The Miocene Geological Setting

The Miocene is the first geological epoch of the Neogene period. During the Miocene the definitive transition between the old, “greenhouse”, Earth and modern, “icehouse” Earth took place. The beginning of this fundamental transition date back to the Eocene, when the Drake Passage opened, starting the isolation of Antarctica from the other land masses (Lagabrielle et al. 2009). The isolation became complete near the Oligocene/Eocene boundary when also the Tasman gateway was sufficiently open (Stickley et al. 2004). As a consequence of this, in the stretch of sea along Antarctica, which was now clear of any landmass, the Antarctic Circumpolar Current began forming. This current is still active nowadays and prevents the warm surface water from subtropical gyres from reaching Antarctica, thermally isolating the continent in a ring of cool water, resulting in substantial cooling of the South Pole (Nong et al., 2000). After the development of the current an ice sheet began to form. The ice cover expanded rapidly during the earliest part of the Oligocene, reaching a mass as great as 50% that of the present-day ice sheet, this glacial event is clearly recorded in $\partial^{18}O$ record and is the first major glaciation of the Cenozoic (Zachos et al. 2001). This ice sheet persisted until the latter part of the Oligocene, when it was greatly reduced by warm period. From this point until the middle Miocene global ice volume remained low and albeit a remarkable glacial event (the Mi-1 Glaciation of 21 Ma ago) and other minors occurred (recorded in the $\partial^{18}O$ record and in antarctic sediments of Ross Bay; De Santis et al. 1995), ice sheets in Antarctica where ephemeral and partial (Zachos et al. 2001). After the Mi-1 Glaciation Miocene climate become again warmer, this warm phase peaked in the late middle Miocene climatic optimum (17 to 15 Ma; Zachos et al. 2001). During this warm period thermophilic fauna and flora are present even in Northern Europe, Northern Japan and New Zealand (Flower and Kennet, 1994; Böhme, 2003; Böhme et al. 2007; Harzhauser and Piller, 2007).

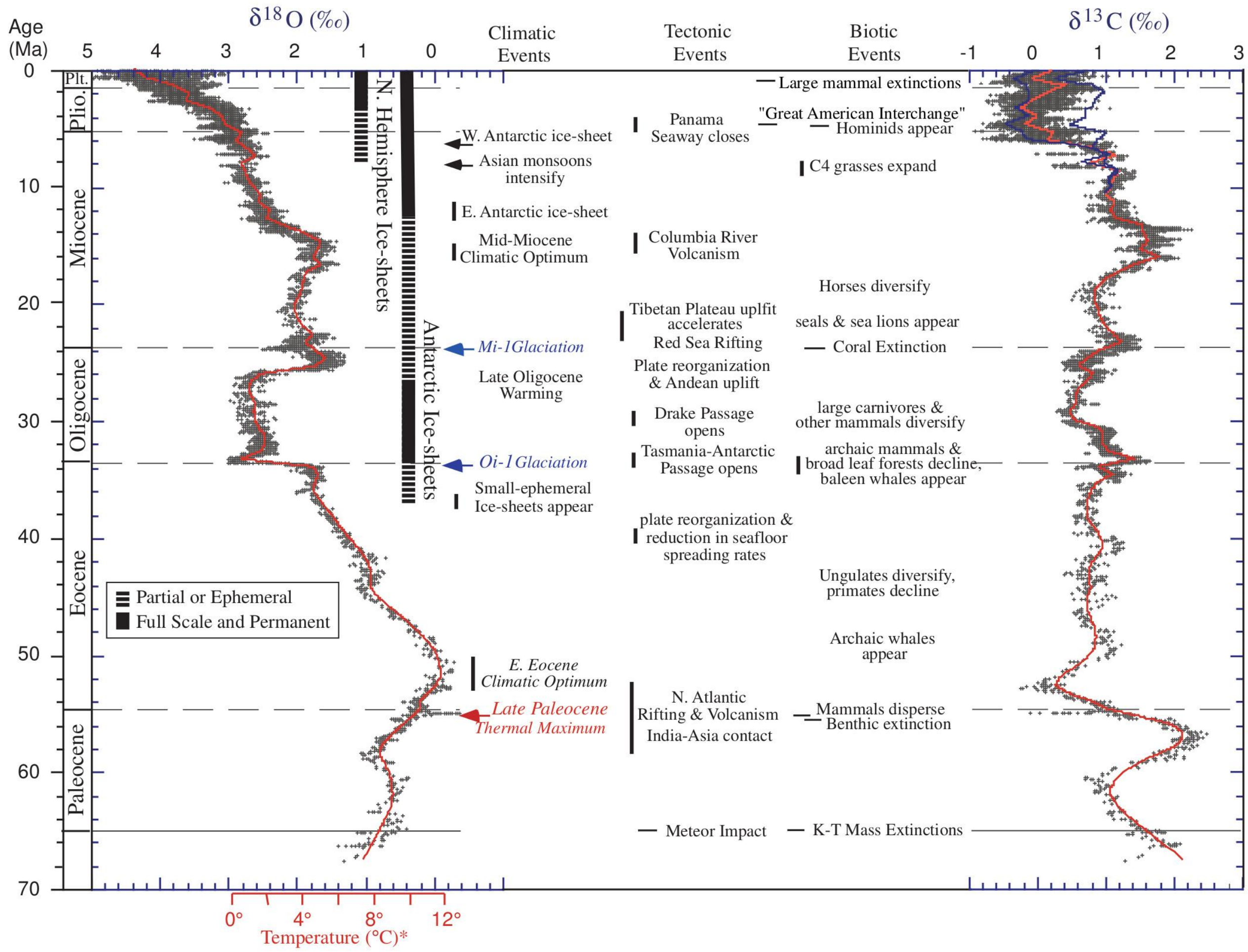

Figure 1.4.1 : Principal global events of the Cenozoic and global, deep-sea, oxygen and carbon isotope records for the Era (Zachos et al., 2001)

In the warm Early Miocene red calcareous algae replaced corals as the most abundant carbonate producers in platform environment. In the circum-Mediterranean region, rhodalgal carbonates (i.e a bioclastic-grain association dominated by coralline algae; Carannante et al. 1988) were volumetrically more abundant than coral reef facies and thick accumulation of rhodolith-dominated facies were widespread in the Pacific and Atlantic Ocean (Esteban, 1996; Halfar and Mutti, 2005). Coralline algae are common carbonate producers since the Cretaceous, but became most widespread and exhibited their greatest species richness during the Miocene (Aguirre et al., 2000). The prevalence of rhodalgal carbonates was probably initially triggered by a global enhancement of trophic resources started in the Burdigalian (Halfar and Mutti, 2005). In the Middle Miocene nutrient availability was further augmented and this increase, together with declining temperatures, led to a further expansion of the rhodalgal facies (Halfar and Mutti, 2005).

During the warm lower part of the Miocene a world-wide important geodynamic occurred: the uplift of the Tibetan Plateau. A major phase of deformation and reorganisation of the orogenic wedge occurred between 21 and 17 Ma with fast exhumation rate and relief increase (Raymo, 1994; White et al. 2002). The elevation of the Plateau, with its large mass, probably had a profound effect on the atmospheric circulation pattern, but certainly in connection with the uplift event an associated increase in chemical weathering and river suspended load is recorded by the strontium isotopic curve (Raymo and Ruddiman, 1992; Raymo, 1994). Tibetan Plateau position and elevation promoted an accelerated and massive weathering of an enormous amount of rocks, this released huge amount of nutrients to the sea through rivers suspended load and the chemical weathering processes sequestered large amount of CO_2 from the atmosphere (Raymo and Ruddiman, 1992; Raymo, 1994).

Immediately after the increase in global weathering rate (principally caused by the erosion of the Himalaya mountain range) the Monterey Excursion event began (De Paolo and Finger, 1991; Raymo, 1994). This long-lasting positive excursion in $\partial^{13}C$ started in the warm Lower Miocene (17 Ma) and ended at 13.5 Ma (Holburn et al. 2007). The event got his name from the Monterey formation in California, the formation is composed by a calcareous and organic-rich facies, a phosphatic facies and a siliceous and diatom-rich facies and its clearly connected to a period of very high primary production (Raymo, 1994). Diatomaceous rocks and phosporite of the same age of the Monterey Formation deposited around the rim of the Pacific Ocean and in the Atlantic (Raymo, 1994). The Monterey event is also recored in the Western Tethys, in the Oligo-Miocene carbonate platform and shelf sediments of the Maltese Islands, here the deposition of phosphatic facies occurred between 25 and 16 Ma and the $\partial^{13}C$ excursion between 18 and 12.5 Ma (Jacobs et al. 1996). The timing of the Monterey event suggests that the uplift and erosion of Tibetan Plateau had a main role in the $\partial^{13}C$ excursion, but periodic orbital variations were also forcing factors (Holburn et al. 2007).

Just slightly before the end of the Monterey event, the warm period that characterized the Miocene thus far, came to an end. The Middle Miocene Climate Transition occurred between 14.2 and 13.8 Ma and is one of the major steps in Earth's Cenozoic climate evolution (Zachos et al. 2001; Shevenell et al. 2004). Large-scale growth of Antartica ice sheet occurred (Flower and Kennet, 1994 ; De Santis et al. 1995). Actually the antarctic cryosphere prior to the Middle Miocene Climatic Transition was substantially different from that of today: the volume of the ice Sheet varied significantly over time scales as short as 100 k.y. (Pekar and DeCanto, 2006; Lewis et al. 2007), and the glaciers were wet based (i.e glacier with temperatures at the ice-ground interface above the freezing point). After the transition Antartic climate become much colder, the ice sheet largely more stable and the glacier cold based (i.e glacier with temperatures at the ice-ground interface below the freezing point), like those of present-day Antartica (Lewis et al. 2007).

After the Middle Miocene Climatic Transition Earth climate become definitively colder and as a matter of fact, the Middle Miocene Climatic Optimum, that preceded the transition, is the last warm period of Earth Geological History.

In the second, cold, half of the Miocene, Earth experienced a number of important ecological events. Modern savannas, temperate grasslands and arid shrublands are dominated by C_4 plants (i.e plants characterized by a Hatch-Slack cycle photosynthetic pathways). C_4 plants appeared during the Oligocene but did not become ecologically important till the Late Miocene. Actually paleontological and geochemical studies indicate a world-wide rapid expansion of C_4 biomass starting between 7-5 Ma. Since C_4 plants have a competitive advantage over C_3 plants, under conditions of drought, high temperatures and CO_2 limitation, they were able to thrive in the post climatic-transition, “icehouse”, world, characterized by low CO_2 concentration in the atmosphere and widespread aridity (Cerling et al. 1993; Pagani et al. 1999). An other important group of organism arose in the Late Miocene: the hominids. Molecular studies suggest that the lineages leading to humans and chimpanzees diverged approximately at 6.5- 5.5 Ma, in the cold Late Miocene (Haile-Selassie, 2001).

During the end of the Miocene an other geodynamic event further cooled Earth climate: the closure of Panama isthmus (Haug and Tiedemann, 1998; Zachos et al. 2001; Bartoli et al. 2005; Schneider and Schmittner, 2006). The gradual closing of the Isthmus of Panama lasted from 14 Ma to 2.75 Ma (Lunt et al. 2008; Schneider and Schmittner, 2006), and its effect become more and more obvious starting from about 6 to 5 Ma (Haug and Tiedemann, 1998). The event caused a large reorganization of the oceanic circulation that became very similar to the modern one, with with strong climatic impact. The closure of the seaway actually led to decreased mixing of Atlantic and Pacific water masses intensifying the Gulf Stream, strengthening the Atlantic thermohaline circulation and increasing global primary productivity (Haug and Tiedemann, 1998; Bartoli et al. 2005; Schneider and Schmittner, 2006). Due to the strengthening of thermohaline circulation the high latitude of the Northern hemisphere, received an intensified moisture supply resulting in the build-up of a larger ice-sheet and culminating in the intensification of Northern hemisphere glaciation (Haug and Tiedemann, 1998; Bartoli et al. 2005).

The end of the Miocene in the Mediterranean region is characterized by spectacular and massive event: the Messinian salinity crisis. In the Mediterranean basin nowadays evaporation exceeds precipitation and river run off. The basin, to keep its balance is continuously refilled by Atlantic waters. In the Late Miocene the Mediterranean become isolated from the Atlantic Ocean (the eastern connection with the Indo-pacific has been severed at the end of the Early Miocene; Adams et al. 1977) and underwent a salinity crisis during which vast evaporites deposits were laid down in the dried up basin (Hsü et al. 1973). The massive extraction of the dissolved salts in the world oceans, brought about by Mediterranean dessication, could also have an influence on the global climate by lowering the average salinity of the water of the oceans (Adams et al. 1977). At the end of the Messinian age, the Gibraltar Strait opened and the waters of Atlantic Ocean flooded the Mediterranean basin. The flood was an extremely fast event, consistent with the exceptionally rapid restoration of deep marine conditions at the Miocene-Pliocene boundary (Hsü et al. 1973; Garcia-Castellanos et al. 2009). Although the whole process may have lasted for up to several thousand years most of the water was transferred in short period (some years or even just few months), with maximum rate of sea level rise of over 10 m per day: an outburst flood larger than any other similar events in Earth History (Garcia-Castellanos et al. 2009).
The Miocene was a time of climatic changes, from the warm Early Miocene, to the Middle Miocene Climatic Optimum, to the cold Late Miocene. In the oceans modern termohaline circulation established. Nutrients supply changed as well due to the increased weathering rate and the strengthened oceanic circulation. This Epoch of changes give us the opportunity to follow the evolution of marine ecosystems during one of the turning point in our Planet Evolution.
The area where the study presented hereafter has been performed, the Mediterranean region, during the Miocene was directly involved in the major geodynamic and oceanographic events of the Epoch. Plate tectonic activity caused the shrinking of the

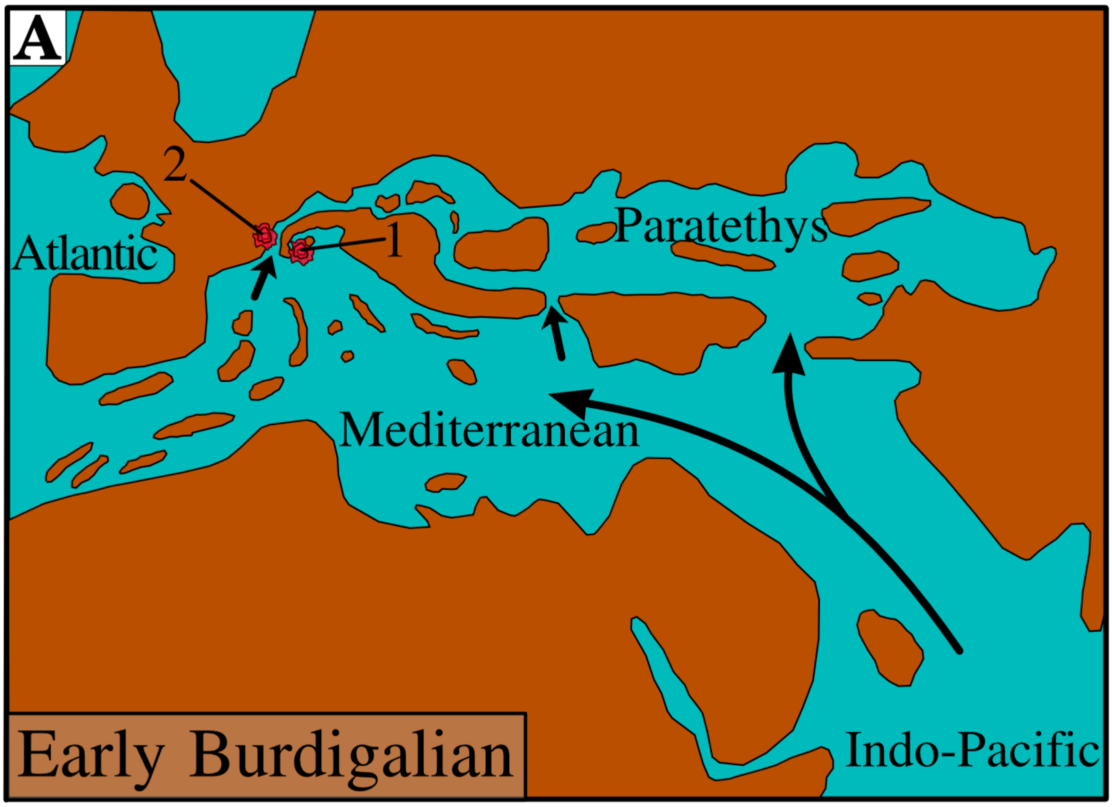
A
2
1
Atlantic
Paratethys
Mediterranean
Indo-Pacific
Early Burdigalian

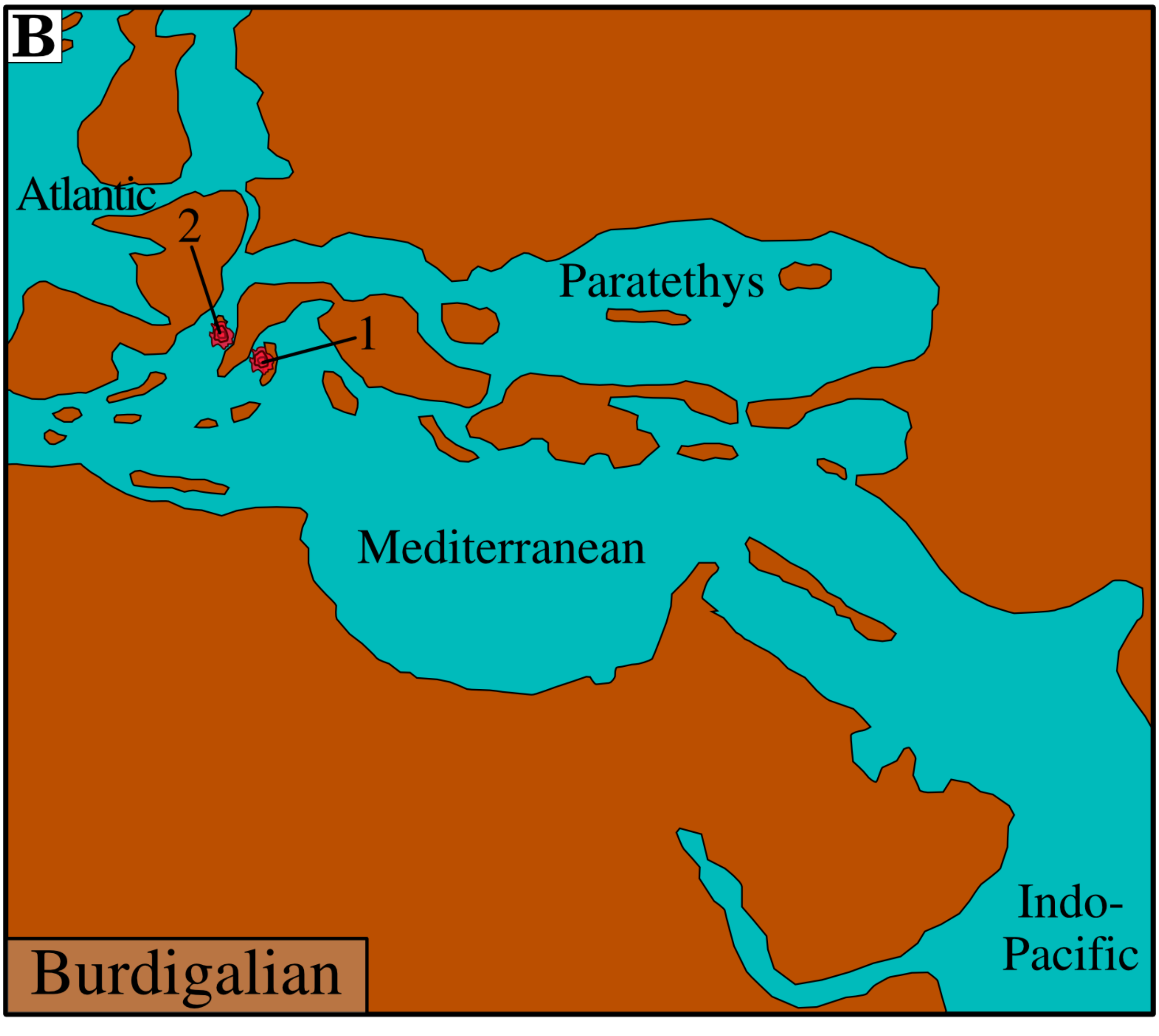
B
Atlantic
2
1
Paratethys
Mediterranean
Indo-
Pacific
Burdigalian

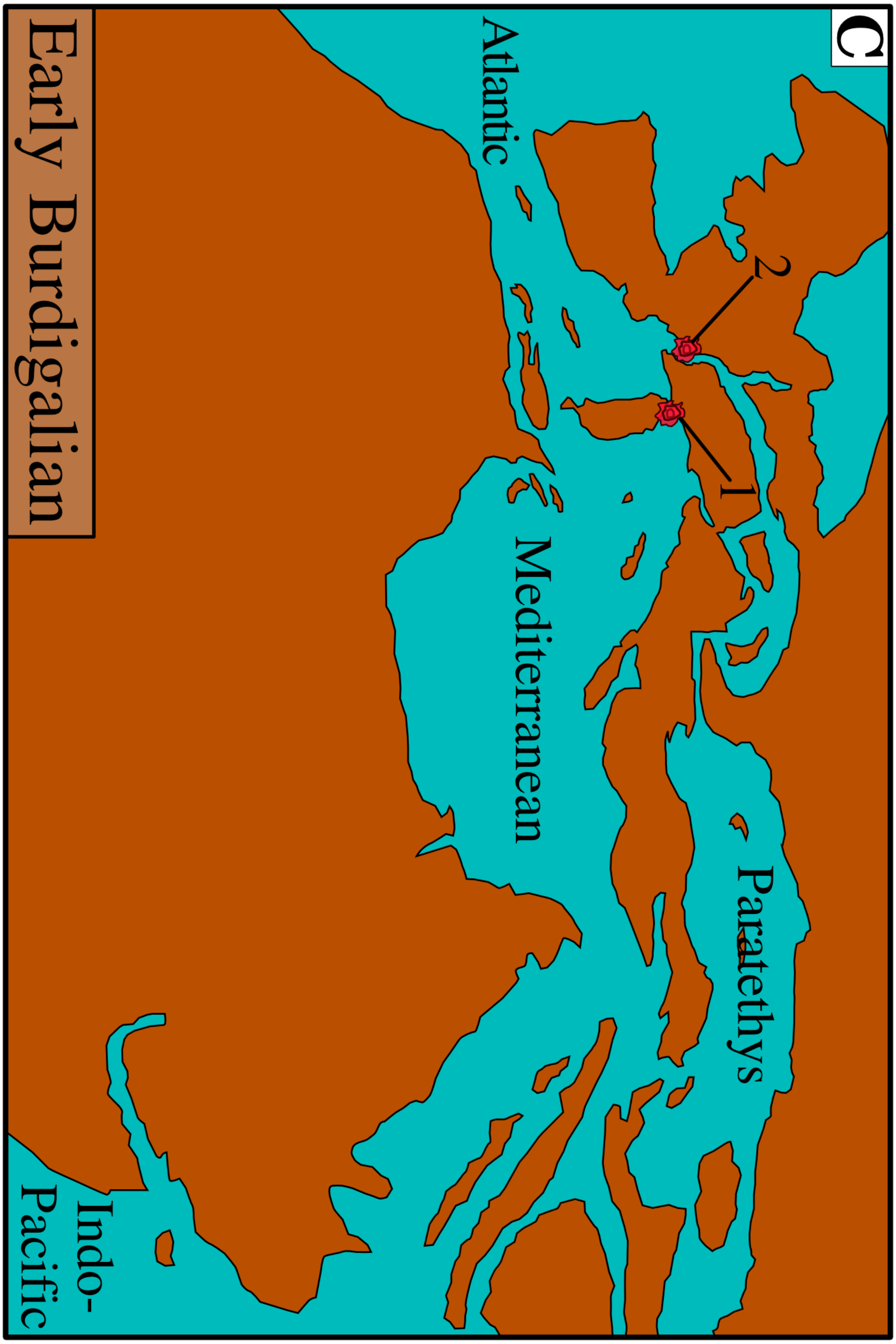

Figure 1.4.2 : Paleogeographic reconstructions of the Mediterranean area during the Burdigalian; 1= Pietra da Cantoni Basin; 2= Sommières Basin. A) Paleogeograhic reconstruction of the basin during the Early Burdigalian; black arrow= main current direction; modified from Rögl (1999). B) Paleogeograhic reconstruction of the basin during the Burdigalian; modified from Harzhauser & Piller (2007). C) Paleogeograhic reconstruction of the basin during the Early Burdigalian; modified from Meulenkamp (2000)

Mesozoic Tethys Ocean and by the end of the Eocene the Tethys basin was reduced to a sea almost completely enclosed by land: the Proto-Mediterranean (Rögl, 1999; Harzhauser and Piller, 2007). The basin was divided in two major water masses by the rising Alpine island chains, which acted as geographic barriers: the Paratethys Sea in the North and the Proto-Mediterranean s.s. in the South (Rögl, 1998; Rögl, 1999; Harzhauser and Piller, 2007). During the Late Oligocene/Early Miocene the basin had extensive connection with both the Atlantic and Indo-Pacific Ocean, and multiple open seaways connected the Paratethys and the Proto-Mediterranean s.s. (Rögl, 1998; Rögl, 1999). During this period also a small connection could have existed between the Paratethys and the North Sea Basin (Rögl, 1998; Rögl, 1999; Harzhauser and Piller, 2007).

In the Early Burdigalian, the period analyzed in this thesis project, one of the main connection between the Proto-Mediterranean s.s. and the Paratethys was the Alpine Foreland Basin (Fig. 1.4.2; Rögl, 1998; Rögl, 1999; Harzhauser and Piller, 2007). This narrow seaway (about 100 Km wide and about 1000 Km long; Allen et al. 1985) was dominated by tidal currents (Allen et al. 1985; Harzhauser and Piller, 2007). Atlantic tide entered the basin from a southwesterly direction, becoming progressively amplified by the narrow and shallow passage, promoting vigorous currents reflected in the tidally controlled shelf-deposits occurring throughout the whole Alpine Foreland Basin during the Early Burdigalian (Allen et al. 1985; Harzhauser and Piller, 2007). Many of these deposits are dominated by skeletal grains since along this narrow and shallow seaway carbonate factories flourished.

In Early Burdigalian time, slightly toward the east from the southern end of the Alpine Foreland Basin, in the north-central part of the Proto-Mediterranean, was located the Tertiary Piedmont Basin (Fig. 1.4.2). The Tertiary Piedmont Basin was a long lived depression that evolved from the Late Eocene to the Late Miocene over the inner part of the Alpine wedge. The basin was dominated by the sedimentation of the siliciclastic

material eroded from the Alpine chain. At the beginning of the Miocene the deformation caused by the rotation of the Alpine wedge uplifted a number of isolated banks and islands in the middle of the basin (Clari et al. 1994; Maffione et al. 2008). During the Early Burdigalian along these shallow banks and islands, protected from the main siliciclastic sedimentation, carbonate deposition was possible (Clari et al. 1994).
The bioclastic carbonate successions studied in this thesis project deposited in the Alpine Foreland Basin (Sommières Basin) and in the Tertiary Piedmont Basin (Pietra da Cantoni Basin), in the Lower Burdigalian, just before the beginning of the Monterey Event, under similar climatic conditions, but in very different hydrodynamic settings: a tide-dominated seaway the former and an isolated bank the latter. Both differences and similarities between the two basin are faithfully recorded in the fossil associations preserved and the changes in species assemblages and abundances are related to an environment gradient mainly created by different nutrients supply-rate.

2 – The Burdigalian of Tertiary Piedmont Basin

Transported rhodoliths witness the lost carbonate factory: a case history from the Miocene Pietra da Cantoni limestone (NW Italy)

Giovanni Coletti

Daniela Basso

Alfredo Frixa

Cesare Corselli

Published in : Rivista Italiana di Paleontologia e Stratigrafia, 2015, volume 121 (3): 345-368.

2.1 – Introduction

This work is aimed at improving our knowledge of fossil rhodalgal factories by emphasizing rhodoliths as a tool in the study of transported sediments. The Pietra da Cantoni Group (PDC; Lower Miocene) of the Tertiary Piedmont Basin (TPB) (Schüttenhelm, 1976; Vannucci et al. 1996; Bicchi et al. 2002; Bicchi et al. 2006) has been chosen as an example of a rhodalgal carbonate platform, where the main area of carbonate production is not flawless preserved in place. In this framework we analyze and integrate literature data and new observations on the paleontology and sedimentology of the PDC and we review the mechanisms and processes involved in rhodolith transport.

From the Oligocene onward, coralline algae have spread massively throughout the platform photic zone. Because they are well adapted to a broad range of climatic conditions and can thrive even in dim light, they are one of the most common and important carbonate producers in platform environment. Coralline algae dominate in the rhodalgal carbonate factories (Carannante et al. 1988) where they are the main carbonate producers. During the Miocene these carbonate factories were common in the Mediterranean area (Civitelli and Brandano, 2005), in the Indo-Pacific and in the Caribbean (Braga et al. 2010). They are a rich archive of past climatic and environmental information with a potential that is still underexplored (D'Atri, 1990; Carannante et al. 1996; Basso and Tomaselli, 1994; Basso et al. 1998; Pomar et al. 2002; Brandano et al. 2005 ; Civitelli and Brandan,o 2005; Halfar and Mutti, 2005; Vigorito et al. 2005 ; Bassi et al. 2006; Bassi et al. 2010; Brandano et al. 2007; Brandano et al. 2009; Brandano et al. 2010; Brandano et al. 2012; Checchoni and Monaco, 2008; Checconi et al. 2010; Braga et al. 2010; Puga-Bernabéu et al. 2010). They are also important hydrocarbon reservoirs with large oil and gas fields located in the Pacific and in the

Atlantic areas (Erlich et al. 1990; Heubeck et al. 2004; Neuhaus et al. 2004; Sattler et al. 2004; Vahrenkamp et al. 2004; Fournier and Borgomano, 2007; Borromeo et al. 2011; Coletti et al. 2016).

Unlike chlorozoan carbonate factories, rhodalgal factories may develop outside the tropical belt and in conditions (*e.g.,* tropical upwelling regions) where hermatipic coral growth is inhibited and the platform lacks a marginal rim (Schlager, 2003; Vigorito et al. 2005). Without this barrier to waves and currents, sediment transport and reworking may play an important role in the depositional architecture, and the platform often develops a ramp or a distally steepened ramp profile (Carannante et al. 1996; Pomar et al. 2002; Vigorito et al. 2005; Pomar and Kendall, 2007; Williams et al. 2011). Similar processes of transport and resedimentation are also recorded in other carbonate systems dominated by loose-grained production (e.g., Senonian rudist-bearing platforms, Carannante et al. 1999; and Cenozoic foraminifer-dominated ramps, Beavington et al. 2005). Sediments transported basinward may have a high preservation potential (Parson-Hubbard et al. 1999; Halfar et al. 2001); if the carbonate factory become lost or unobservable, the transported skeletal remains might provide information on the shallow-water environment where they were produced (Nebelsick et al. 2001; Rasser and Nebelsick, 2003). Therefore, when transport processes do not excessively alter the original composition of the sediment through mixing and selection, displaced materials can potentially be used to reconstruct the “lost” shallow-water environment (Nebelsick et al., 2001; Basso et al., 2012; Leszczyński et al., 2012). This could be especially useful in active, compressional tectonic settings, where short-lived small carbonate platforms develop on topographically high areas over thrust sheets and where resedimentation is frequent (Carannante et al., 1996; Bosence, 2005).

Rhodoliths have an added value for these paleoecological reconstructions. During their growth, they bind skeletal grains of their native environment preserving the record of the changing benthic associations through time or space (Basso, 1991; Basso and

Tomaselli, 1994; Basso et al. 1998; Checconi and Monaco, 2008). Other organisms may also overgrow them or bore and nest inside (*e.g.,* barnacles, bryozoans, encrusting foraminifers, mollusks, annelids, etc.) adding other fruitful details. These small and free-living “carbonate factories” can be regarded as “island habitats” (Lee et al. 1997) that retain all the information accumulated during their development and preserve them after transport and burial.

2.2 - Geological setting and regional evolution

The Pietra da Cantoni Group develops from the Burdigalian to Early Langhian (Novaretti et al. 1995), and outcrops in the eastern sector of the Monferrato area (Piedmont, Italy), which is part of the TPB. The TPB is a long-lived basin that evolved from the Late Eocene to the Late Miocene over the inner part of the Alpine wedge and it has recorded the complex interplay between the tectonic forces of the continental collision. During the Early Oligocene, sedimentation in the TPB was confined to small fault-bounded basins and continental and shallow marine facies prevailed (Mosca et al. 2009; Rossi et al. 2009). In the Oligocene, the basin became deeper and there was a transition toward open marine conditions (Mosca et al. 2009; Rossi et al. 2009). At the beginning of the Miocene (Aquitanian stage), the deformation caused by the rotation of the Alpine Wedge (Maffione et al. 2008) uplifted and divided the Monferrato area into an eastern and a western sector. The western sector was deeper and dominated by a slope to basin environment as indicated by the deposition of siliceous ooze (Bonci et al. 1990; Clari et al. 1994; Clari et al. 1995; Novaretti et al. 1995). The eastern Monferrato was uplifted resulting in the formation of an angular unconformity along which the Aquitanian-Early Burdigalian interval is missing. In the Burdigalian the deformation was completed in the eastern Monferrato and the PDC deposited at the top of the unconformity developed upon the underlying deposits (Casale Monferrato, Marne di M. Piano, Cardona, Antognola Formations). In the western Monferrato basin instead, the sedimentation was dominated by siliciclastic sand.

During the Burdigalian the rhodalgal carbonate factories developed in a shallow sea environment, which was, according to paleogeographical reconstruction, between

latitude 35° and 40° N (Meulenkamp et al. 2000). In the Early Miocene the Earth climate was globally warmer than present day, with tropical and subtropical climatic region extending to higher latitude (Adams et al. 1990; Billups et al. 2010). Reconstruction of the terrestrial climate of Europe, based on continental proxies, suggests temperatures up to 6°C warmer (Mosbrugger et al. 2005). Taking these elements into consideration a tropical climate is conceivable for the region, as testified by fossil assemblages (Vannucci et al. 1996). From the Langhian onward, the western and eastern Monferrato had similar subsidence rates, leading to uniform deposition of fine carbonate to mixed carbonate-siliciclastic sediments (the calcareous member of Tonengo sandstone Fm., Dela Pierre et al. 2003). After the Early Serravallian, a further deepening occurred, which is indicated by the deposition of the Marne di Mincengo Formation.
The PDC is divided into two sequences (Bicchi et al. 2006). The older Sequence 1 (Aquitanian-Lower Burdigalian) outcrops exclusively in the village of Rosignano Monferrato. It is composed of bioclastic wackestone and packstone with scattered rhodoliths. The boundary with the overlying Sequence 2 is a ravinement surface with small scattered lenses of rhodolith-rich, coarse bioclastic material (Bicchi et al. 2002). The second sequence is further divided into two units. The lower unit is the main subject of this work and outcrops only in the eastern part of the basin. It consists of coarse bioclastic limestone deposited in a shallow marine environment (Schüttenhelm 1976; Bicchi et al. 2006). The upper unit consists of marly packstones and marls deposited in a deeper environment (Schüttenhelm, 1976; Bicchi et al. 2006). Outcrops of the upper unit of Sequence 2 are present in the whole PDC basin. The two units are separated by a thin interval that shows heavily reworked and bioeroded bioclasts (mainly mollusk shells but also small rhodoliths and fish bones), pebbles and authigenic minerals (mainly glaucony and phosphate). According to literature (Novaretti et al. 1995; Bicchi et al. 2006), the lower unit is referred to Biozone N7a (*Globigerinoides trilobus* subzone, Blow, 1969). The base of this biozone is marked by the disappearance of *Catapsydrax dissimilis* and dated

at 17.62 Ma in the open ocean (Wade et al. 2011). In the TPB, an ash layer with an $^{40}Ar/^{39}Ar$ age of 18.7±0.2 Ma (Ruffini, 1995; D'Atri et al. 1999; D'Atri et al. 2001), located above the disappearance of *Catapsydrax dissimilis,* suggests a possible diachrony of the event. On these bases, the lower unit of Sequence 2 should have been deposited between about 19 and 18 Ma (Novaretti et al. 1995). Calcareous nannofossils, planktonic foraminifers and miogypsinds distribution in the Villa San Bartolomeo succession shows that in the studied area, the lower unit of Sequence 2 belongs to Biozone N7a (Schüttenhelm, 1976; Vannucci et al. 1996; Bicchi et al. 2002; Bicchi et al. 2006).

2.3 – Material and Methods

Currently, the PDC outcrops are scattered and discontinuous. The rock is poorly cemented and porous, therefore it weathers rapidly and is generally covered by thick soil and dense vegetation. Outcrops are visible in villages and dismissed quarries. The lower unit of PDC Sequence 2 was studied in the following dismissed quarries located near the villages of Rosignano and Terruggia (Fig. 2.3.1): Villa San Bartolomeo (VB), Castello di Uviglie (UV), Torre Veglio North (TN), Torre Veglio South (TS). Presently, VB is no longer accessible and TN and TS are buried.

The outcropping successions were measured, and described by grain-size and texture. The rhodolith size was measured, and nodules larger than 3 cm were extracted and broken to study their internal structure and composition. The rhodolith shape and structure were described following Bosellini and Ginsburg (1971), Bosence (1983a) Vannucci et al. (1996) and Basso (1998).

Since VB, UV, TN and TS outcrops did not offer a sufficiently large surface for sedimentological observations of large-scale structures, further fieldwork was performed in the other nearby PDC outcrops. In particular, the outcrop of Rosignano, which is very close to the studied area (Fig. 2.3.1), offers a very large exposure of the lower unit of PDC Sequence 2. Further observation were done in the Treville village, the westernmost outcrop of the rhodolith-bearing unit of PDC Sequence 2.

Thin sections of 115 samples collected by Vannucci et al. (1996) in VB and TN, and 85 samples collected in 2010 by the authors in UV and TS, were analyzed for this work. From these, 110 thin sections were obtained from isolated rhodoliths and 90 were dedicated to both rhodoliths and their embedding sediment. On 12 samples from UV and TS sections, X-ray diffraction (XRD; PANalytical's Xert PRO Materials Research Diffractometer) and X-Ray fluorescence (XRF; PANalytical's Eilon 3-XL energy

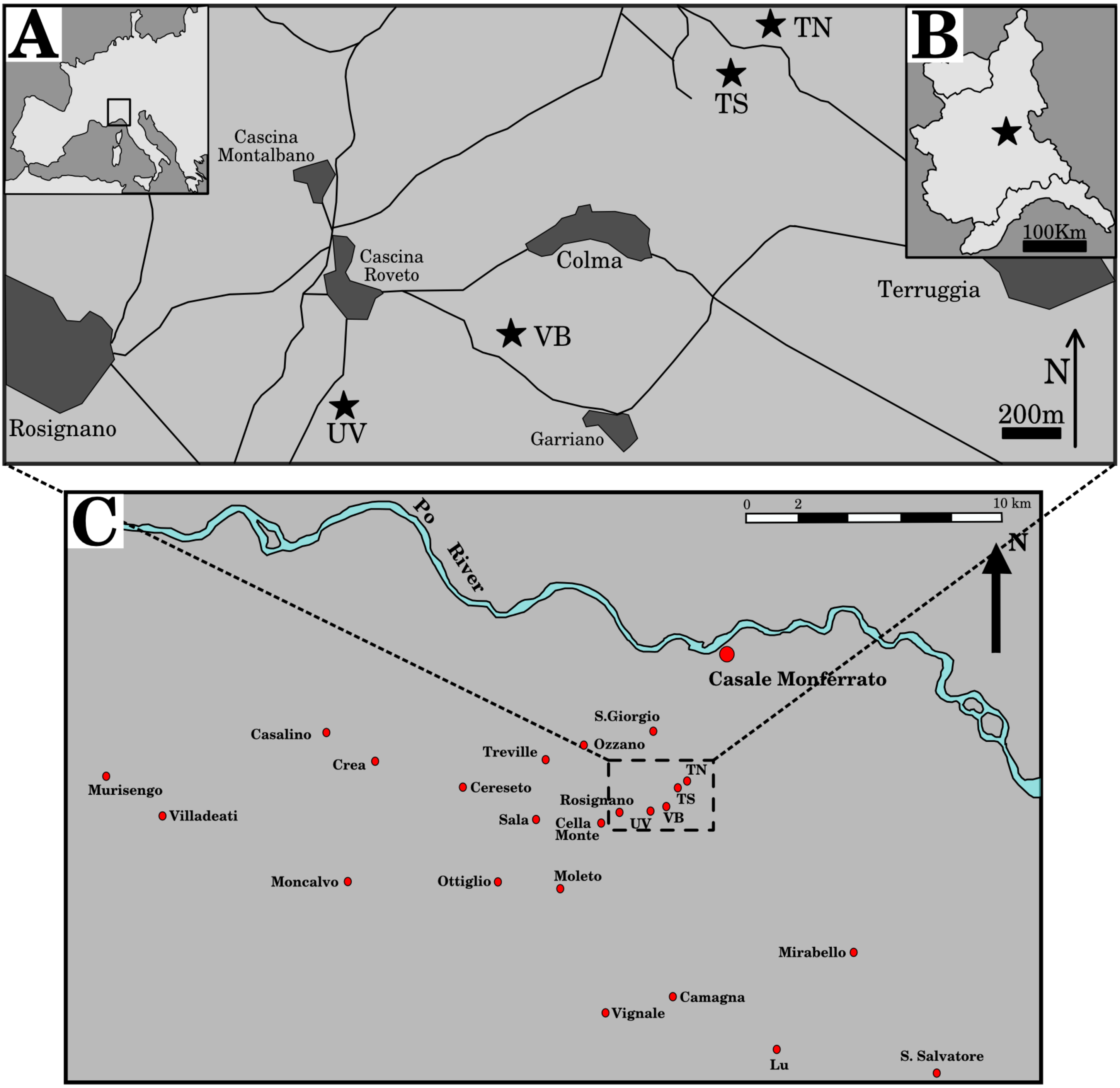

Figure 2.3.1 : Upper panel: sketch map of the investigated outcrops (stars); Uviglie (UV; 45° 4.70' N 8° 24.79' E); Villa San Bartolomeo (VB; 45° 4.82' N 8° 25.27' E); Torre Veglio North (TN; 45° 5.53' N 8° 25.85' E); Torre Veglio South (TS; 45° 5.25' N 8° 25.84' E). A) Simplified map of Europe with Northwestern Italy (black box). B) Simplified map of Northwestern Italy, with the studied area (star). C) Map of all the outcrops of PDC, modified after Schüttenhelm, 1976.

dispersive X-ray fluorescence spectrometer) analyses were performed to assess their mineralogical and chemical composition after rhodolith removal. The glaucony of the samples was qualitatively studied following the procedure of Amorosi (1997) to assess its autochthony and its maturity.

The texture, composition and bioclastic assemblage of the rhodolith-embedding material were quantified by point counting (Flügel, 2009) on digital photomicrographs of thin sections. A 150x150 µm grid was used and an average of 400 points was counted in each analyzed section. The recognized categories were: coralline algae, barnacles, benthic foraminifers, planktonic foraminifers, mollusks, bryozoans, echinoids, serpulids, ostracods, micrite, sparite, glaucony, authigenic phosphate and non-carbonate minerals. On suitable thin sections of the rhodoliths, point counting was also performed on the sediment patches trapped within the nodules to assess the differences between the material inside and outside the rhodoliths. Data from point-counting were statistically treated by hierarchical cluster analysis and non-metric multidimensional scaling ordination (MDS) based on the Bray-Curtis similarity with PRIMER 6 (Kruskal 1977; Field et al. 1982; Clarke and Gorley, 2006).

The growth-form and relative abundance of coralline algae were studied on thin sections. Coralline taxonomy follows Kato et al. (2011) and Bittner et al. (2011). The identification of foraminifers was conducted to the lowest taxonomic level possible (mostly genus or species), which required extraction of foraminifer tests from the sediment after disaggregation of rock samples. The foraminifers were identified under stereomicroscope and scanning electron microscope (SEM; TESCAN mega TS5136 XM). For SEM analysis, specimens were cleaned, mounted on SEM stubs by an adhesive conductive carbon disk and then gold-coated. With the exception of the SEM-prepared specimens, the remaining foraminifers were eventually embedded in epoxy resin, cut and prepared in thin sections. The taxonomic nomenclature follows Loeblich & Tappan's revision (1987). Among the other skeletal grains the most abundant taxa of barnacles, bryozoans and mollusks were also identified.

2.4 – Results

The results have been divided in two sections, a former with the presentation of the detailed paleontological and sedimentological data of the four main outcrops (Villa San Bartolomeo, Uviglie, Torre Veglio North and Torre Veglio South) and a latter dedicated to the sedimentological description of Rosignano and Treville outcrops.

Villa San Bartolomeo (VB), Uviglie (UV), Torre Veglio North (TN) and Torre Veglio South (TS)

Paloeontological and sedimentological analyses in these outcrops allowed the recognition of different facies, lithozones and the identification of the most abundant taxa of the fossil association.

Facies description. Four facies were recognized, based on rock characteristics, texture, and statistical treatment of compositional data (Fig. 2.4.1). Each facies includes one or more lithozones, identified in the outcrop on the basis of their rock texture, mineralogy and macroscopic fossiliferous content. Lithozones were numbered from 1 to 6, from the oldest to the youngest (Figs 2.4.2; Fig. 2.4.3).
Facies 1 is a typical rhodalgal assemblage (sensu Carannante et al. 1988) characterizing lithozones 1 to 4a. The coarse skeletal elements are composed of rhodoliths, large benthic foraminifers and barnacle plates. The fine fraction is dominated by fragments of coralline algae, barnacles, benthic foraminifers, bryozoans, echinoids and mollusks. In the

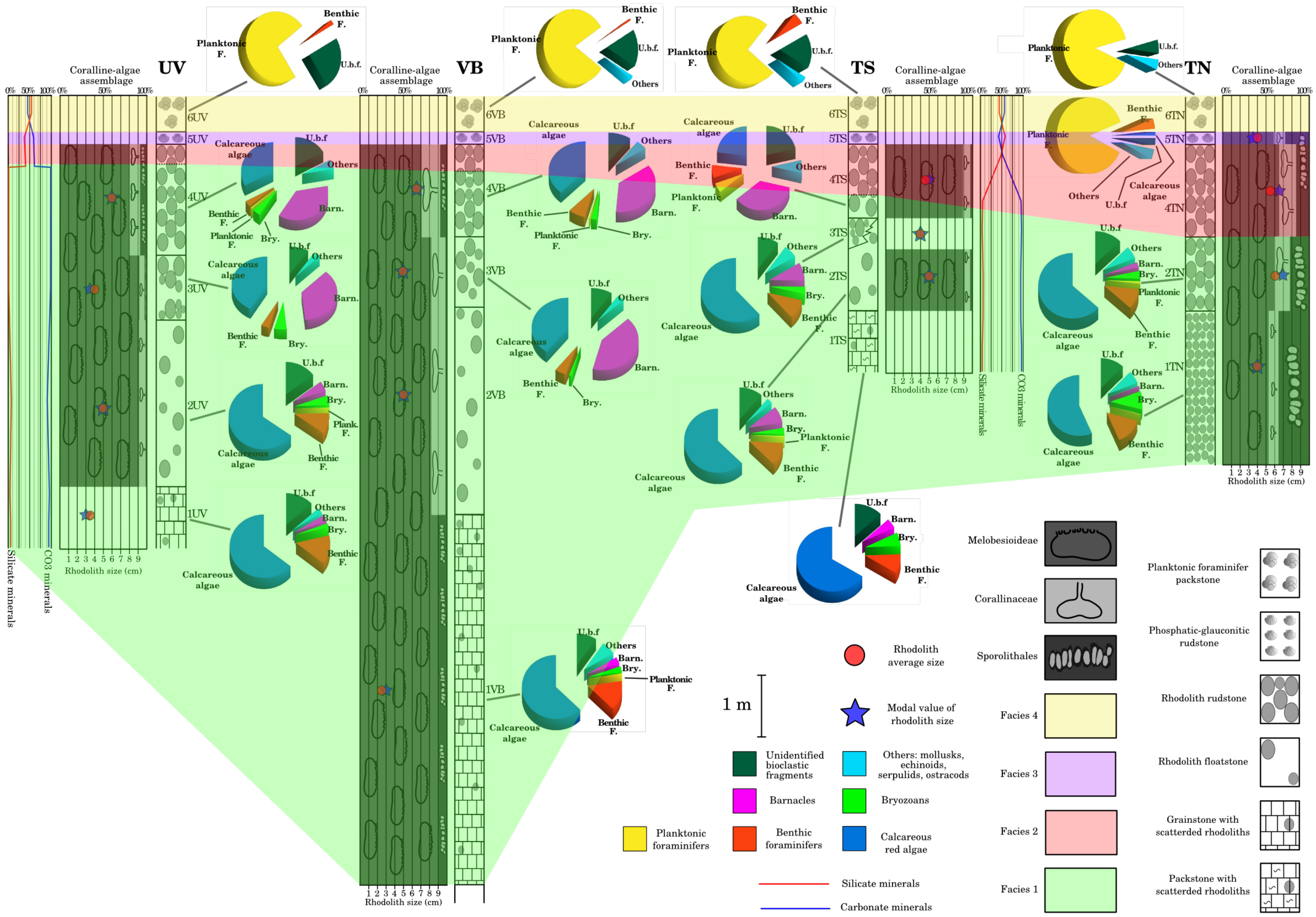

Figure 2.4.1 : Simplified stratigraphic log of the studied PDC sections summarizing bioclastic composition, mineralogical composition, general attributes of sampled rhodoliths, coralline-algae assemblages and facies distribution. In lithozones 1UV, 1TS, 3TS, coralline algae were insufficiently studied due to poor preservation.

hierarchical cluster analysis and MDS ordination, samples of Facies 1 gather in Clusters 1 and Cluster 2. The rock is an almost pure limestone with a siliciclastic fraction primarily composed of silt-sized and sand-sized grains of quartz.

UV		VB		TS		TN	
6	Glauconitic, planktonic foraminifers marly-packstone. Micrite is abundant	6	Glauconitic, planktonic foraminifers marly-packstone. Micrite is abundant	6	Glauconitic, planktonic foraminifers marly-packstone. Micrite is abundant	6	Glauconitic, planktonic foraminifers marly-packstone. Micrite is abundant
5	Phosphatic-glauconitic rudstone. Micrite is abundant	5	Phosphatic-glauconitic rudstone. Micrite is abundant	5	Phosphatic-glauconitic rudstone. Micrite is abundant	5	Phosphatic-glauconitic rudstone. Micrite is abundant
4b	Glauconitic rhodolith rudstone. Micrite is present	4b	Glauconitic rhodolith rudstone. Micrite is present	4b	Glauconitic rhodolith rudstone. Micrite is present	4b	Glauconitic, reverse graded, rhodolith rudstone. Micrite is present
4a	Rhodolith rudstone. Without interstitial material	4a	Rhodolith rudstone. Without interstitial material	4a	Rhodolith rudstone. Without interstitial material	4a	Absent
3	Barnacle and rhodolith rudstone. Without interstitial material	3	Barnacle and rhodolith rudstone. Without interstitial material	3	Rhodolith rudstone with barnacle fragments. Without interstitial material	3	Absent
2	Bedded rhodolith floatstone. Almost without interstitial material	2	Bedded rhodolith floatstone. Almost without interstitial material	2	Bedded rhodolith floatstone. Almost without interstitial material	2	Rhodolith rudstone. Almost without interstitial material
1	Lepidocyclinid grainstone with scattered rhodoliths. Without interstitial material	1	Lepidocyclinid grainstone with scattered rhodoliths. Without interstitial material	1	Coralline-algae packstone with scattered rhodoliths. Micrite is abundant	1	Rhodolith rudstone. Micrite is abundant

Figure 2.4.2 : Lithozones characteristics

Facies 2 characterizes the upper part of the fourth lithozone (4b). Large skeletal elements are rhodoliths and barnacle plates. The fine fraction is mainly composed of planktonic foraminifers and grains of authigenic minerals. The rock is an impure limestone: it is rich in silicate minerals constituting up to 40% of the fine-grained fraction. Samples of this facies are included in the Cluster 3.

Facies 3 characterizes lithozone 5. The coarse fraction of the rock is composed of abraded,

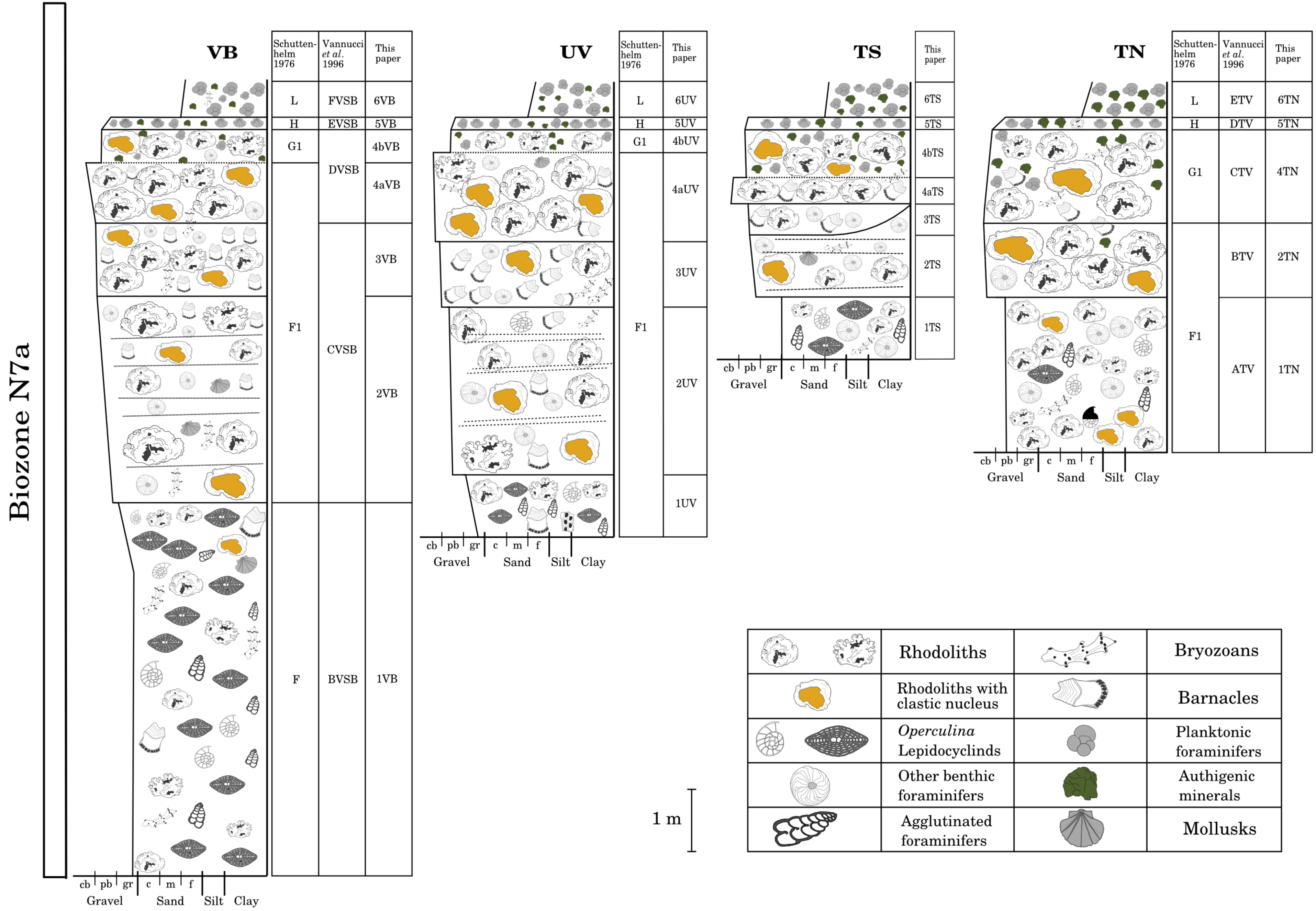

Figure 2.4.3 : Stratigraphic log of the studied sections in PDC and comparison with previous works; f: fine; m: medium; c: coarse; gr: gravel; pb: pebble; cb: cobble; Biozone N7a according to Blow (1969).

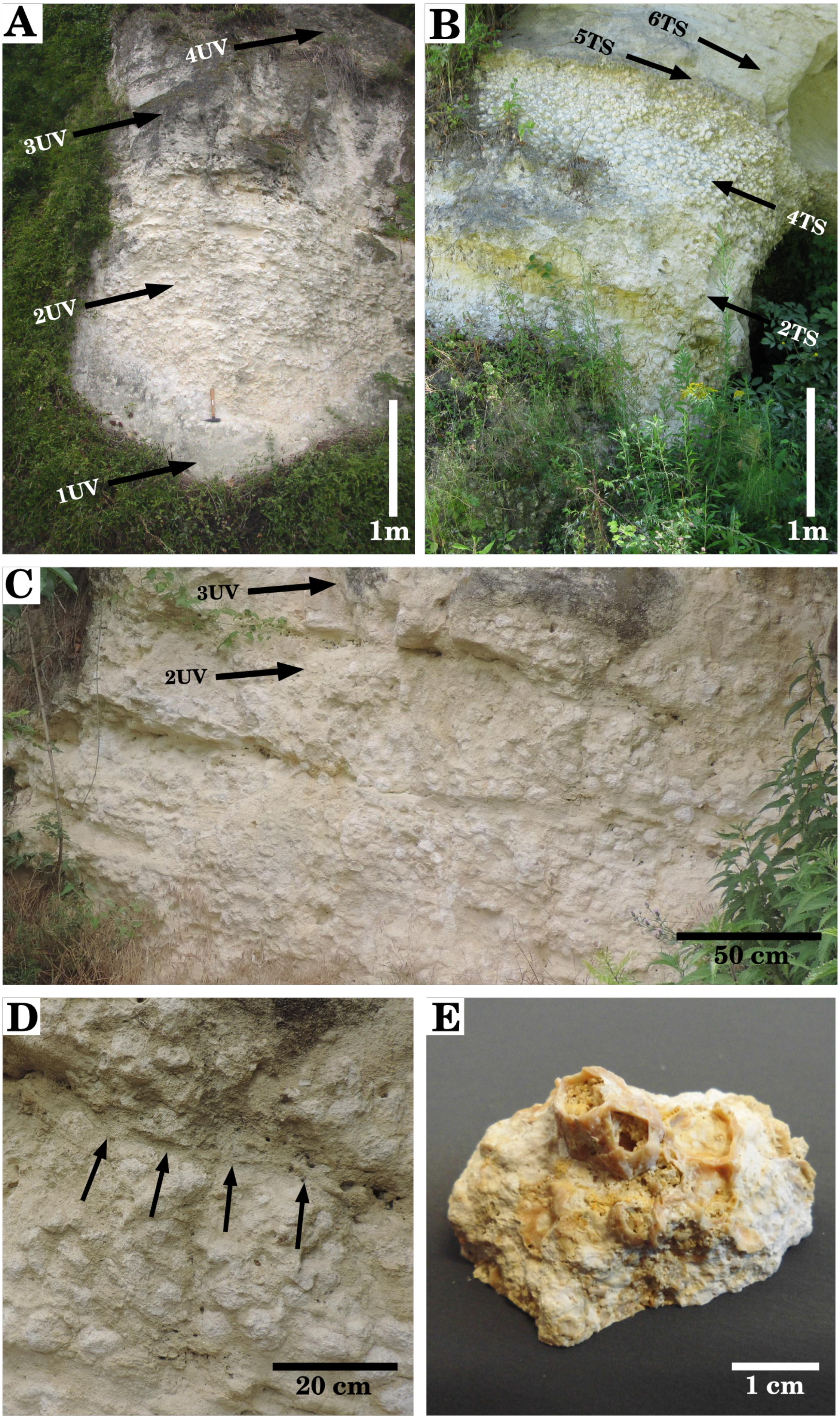

Figure 2.4.4 : Field pictures of the studied successions. A) Lithozones from 1 to 4 of UV quarry. B) Lithozones from 2 to 6 of TS quarry. C) Lithozone 2UV structures and the lower part of the overlaying lithozone 3UV. D) Lens of rhodolith floatstone at the boundary between lithozone 2UV and lithozone 3UV; arrows = base of the lens. E) Barnacle encrusting rhodolith surface.

winnowed and often phosphatized bioclasts (mainly pebble-size rhodoliths and mollusk shells). The finer material embedding the large elements is almost entirely composed of planktonic foraminifer tests, glaucony and authigenic phosphate grains. In the hierarchical cluster analysis and MDS ordination the samples of Facies 3 and 4 are grouped in Cluster 4. The rock is a marly limestone, and nearly half of the material is composed of silicate minerals.

Facies 4 characterizes lithozone 6. Large skeletal elements are almost absent, and most of the rock is composed of planktonic foraminifer tests; glaucony grains are frequent and phosphate grains occur. The rock is a marly limestone with abundant clay minerals. In the hierarchical cluster analysis and MDS ordination the samples of this facies are encompassed in Cluster 4, together with Facies 3.

Lithozones description. In the outcrops on the basis of their rock texture, mineralogy and macroscopic fossiliferous content different lithozones were identified. The lithozones were numbered from 1 to 6, from the oldest to the youngest (Fig. 2.4.3), their characteristics are summarized in Table 1. The thickness and characteristics of the lithozones slightly vary among the quarries, and certain lithozones do not occur in all quarries. These lithozones can be correlated with those used by previous authors (Fig. 2.4.3).

1VB, the basal lithozone of the VB section, is a lepidocyclinid-rich grainstone with scattered small rhodoliths. The rock is characterized by a weak fabric with common orientation of the large and flat skeletal elements. This lithozone is overlain by a bedded rhodolith floatstone (2VB), which is then followed by a rudstone composed of barnacle fragments and rhodoliths (3VB). The fourth lithozone (4VB) is a rhodolith rudstone. The material in which the rhodoliths are embedded at the base is composed of coarse skeletal fragments (mainly barnacle and coralline debris) (4aVB), whereas at the top is mainly composed of planktonic foraminifers and grains of glaucony and phosphate (4bVB).

The base of the UV succession (Fig. 2.4.4A), 1UV, is a lepidocyclind-rich grainstone, with scattered small rhodoliths. The overlying 2UV lithozone is composed of several 30-50 cm thick beds of rhodolith floatstone alternated with thin beds of coralline-rich grainstone (Fig. 2.4.4A, C). The thickness of these beds is variable and most of them are laterally discontinuous. In the upper part of this lithozone, near the boundary with the overlaying 3UV lithozone, small, lens-shaped bodies of rhodolith floatstone are present (Fig.2.4.4D). The boundary between 2UV and the overlaying 3UV is sharp and probably erosional (Fig. 2.4.4C). 3UV is a rudstone composed of barnacle debris and rhodoliths. The base of the lithozone is rich in rhodoliths while upward they are less common. The rock presents a weak fabric with a common orientation of the large and flat skeletal elements. The lithozone 4UV is a rhodolith rudstone that is rich in bioclastic fragments at the base (4aUV) and in planktonic foraminifers, glaucony and phosphate grains at the top (4bUV). 1TS, the first lithozone of the TS succession (Fig. 2.4.4B), is a rhodolith packstone. 2TS is a bedded rhodolith floatstone, alike 2UV. The 3TS is a laterally discontinuous rhodolith rudstone rich in barnacle debris. The lithozone 4TS, similarly to 4VB and 4UV, is subdivided in two part: 4aTS and 4bTS.

The basal lithozones of TN, 1TN and 2TN are massive rhodolith rudstone (in 2TN rhodoliths are larger than in 1TN).

The TN quarry lacks a lithozone characterized by barnacle abundance and without glaucony and phosphate grains (the lithozone 3 of the other quarries). The lithozone 4TN is a rhodolith rudstone. Since rhodolith-embedding material in 4TN, from the base to the top, is principally composed by planktonic foraminifers, glaucony and phosphate grains, the whole lithozone was correlated with the upper part of the fourth lithozone (4b) of the other quarries.

Lithozones 5 and 6 have the same characteristics in all of the studied quarries (Fig 2.4.2; Fig. 2.4.3). The lithozone 5 (lag deposit) is a thin bed of winnowed, phosphatized and glauconized material, mollusk shells, small rhodoliths, fish skeletal remains and rock

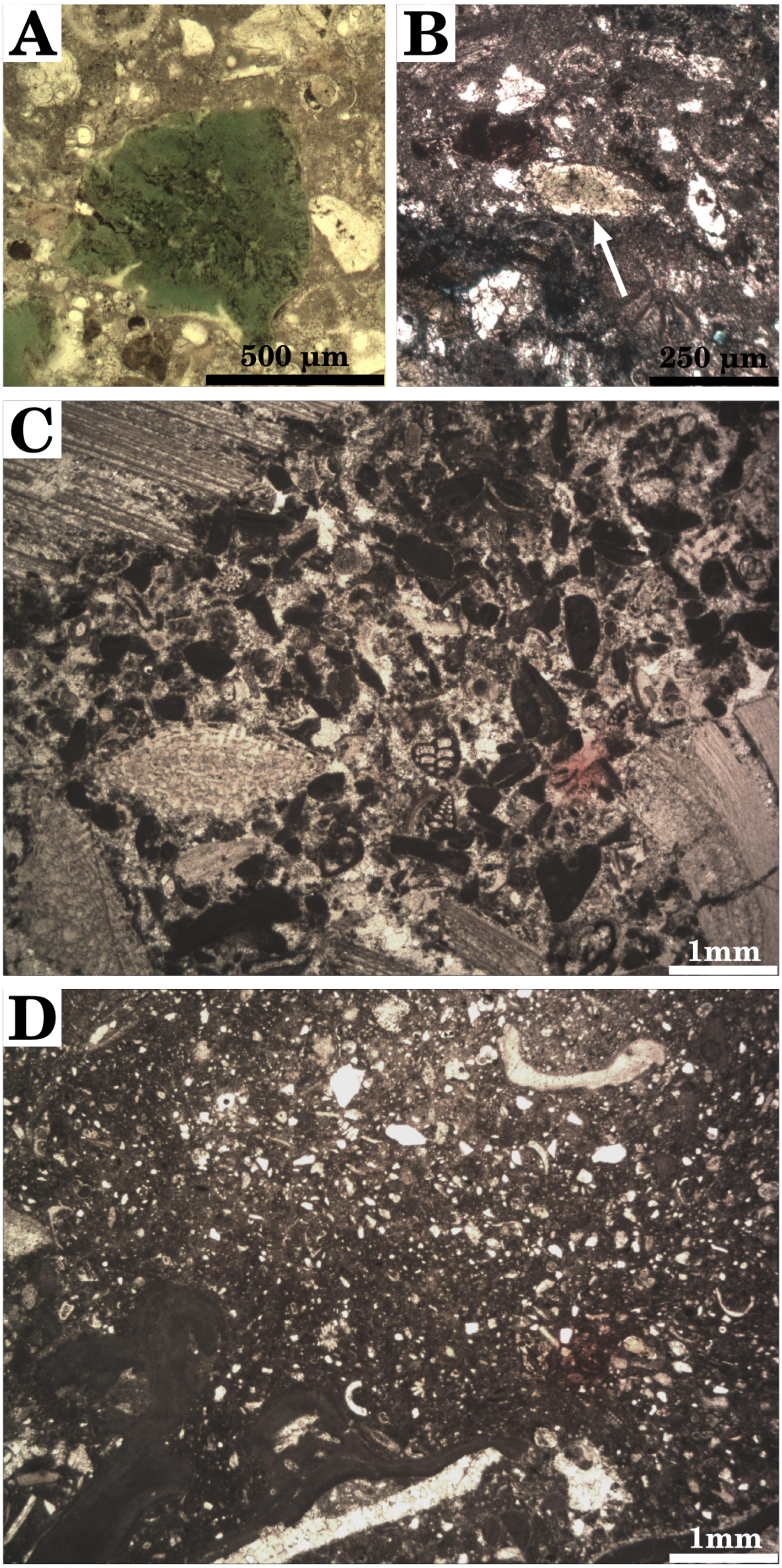

Figure 2.4 5 : Glaucony grains. A) Highly mature glauconite. B) Glaucony grain with an average degree of maturity (arrow). C) Shallow-water skeletal grains inside the rhodolith from Treville outcrop. D) Deeper water sediment outside the same rhodolith from Treville outcrop.

fragments from the Casale Monferrato Fm. This lithozone is easily recognizable and separates the lower and the upper units of Sequence 2. It belongs to the uppermost part of Biozone N7a (Bicchi et al. 2006). The lithozone 6 is a planktonic-foraminifers-rich marly packstone; this lithozone is the base of the upper unit of Sequence 2.
From a chemical and mineralogical perspective, lithozones 1 to 4a are almost pure limestone (90-98% carbonate minerals) while 5 and 6 are marly limestone (60% carbonate minerals; Fig. 2.4.1). The 4b is an impure limestone because the rhodolith embedding material is mainly composed of authigenic minerals and clays (Fig. 2.4.1). Calcite has a low magnesium content (Mg/Ca$\approx$0,01); quartz is the most common silicate mineral found in lithozones 1 to 4a, while clay minerals become abundant upward. The phosphorous concentration increases and phosphatized bioclasts become more frequent from part b of the lithozone 4 upward. Glaucony is present in the whole succession. In lithozones 1, 2, 3 and 4a, glaucony is rare and is mainly present as the filling of skeletal-grain porosity; the grains are small, without cracks and of a pale-green color. Upward it is common and especially abundant in lithozones 5 and 6. In the latter lithozones the glaucony grains are larger and of a deep-green color, they also present cracks filled with pale-green glaucony (Fig. 2.4.5A, B). The angular shape of the grains and their occurrence as the filling of intraparticle porosities, suggest an *in situ* origin for these minerals in all the lithozones. The abundance of authigenic minerals peaks in lithozone 5.

Multivariate Statistical Analyses. Data from point-counting analyses of biogenic components, performed on both the material inside and outside of the rhodoliths, were classified by a hierarchical cluster analysis and ordinated by non-metric multidimensional scaling (MDS). This procedure identified three large groups and a smaller group at 60% of Bray-Curtis similarity (Fig 2.4.6; Fig 2.4.7). Clusters 1 and 2 include all of the samples from Facies 1 (lithozones from 1 to 4a), including also samples

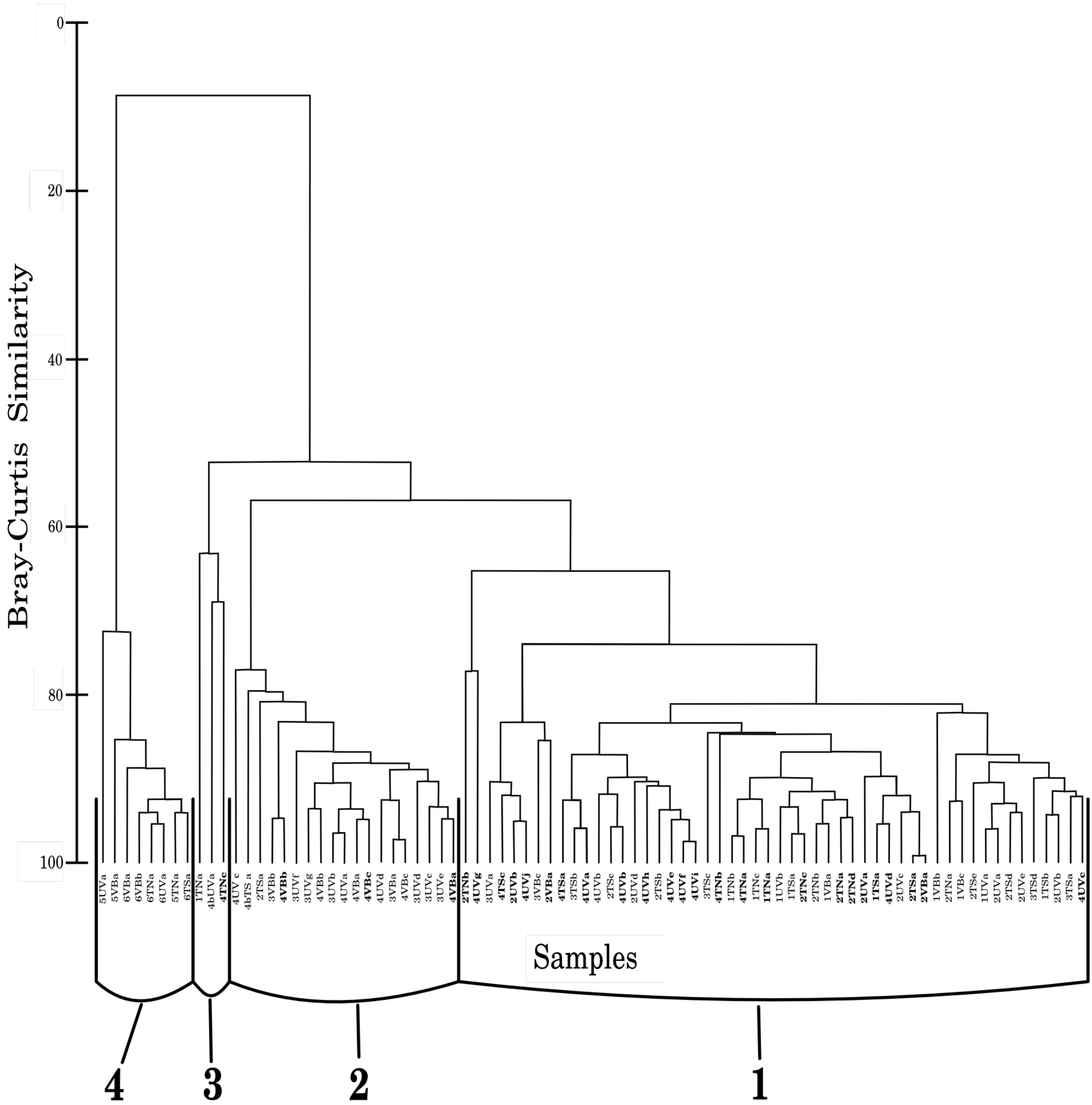

Figure 2.4.6 : Hierarchical agglomerative dendrogram based on Bray-Curtis similarity of the bioclastic composition of samples. Point counts of bioclastic composition were standardized and then analyzed for Bray-Curtis similarity. The samples are grouped in clusters 1 to 4 at 60% of Bray-Curtis similarity. Samples from inside rhodoliths are in bold.

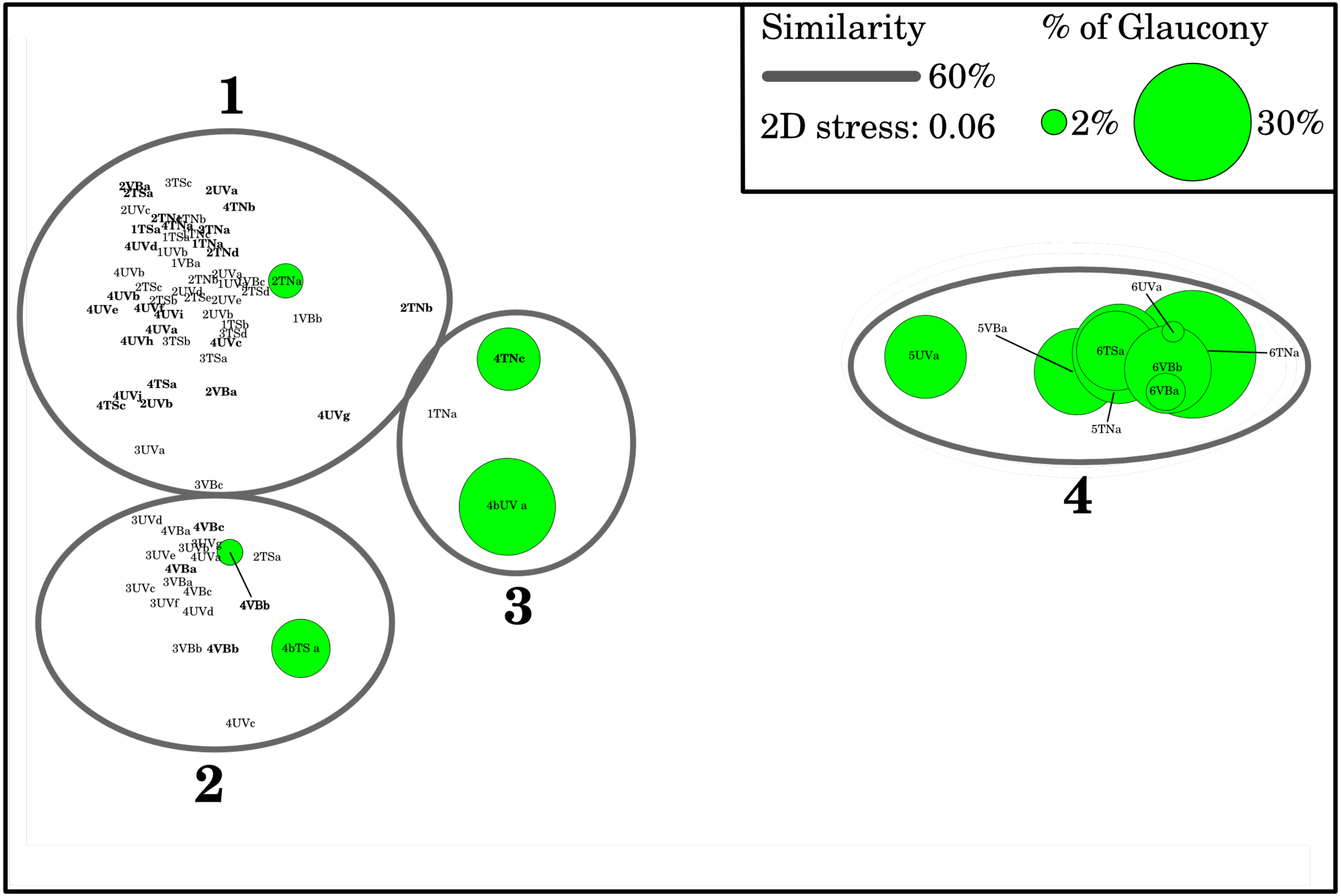

Figure 2.4.7 : MDS (2D) ordination of the samples, based on the same Bray-Curtis similarity as Figure 6. 2D stress indicates the displacement of the sample in the representation from its actual position in the multidimensional space. Circles represent the amount of glaucony in samples, with circle radius proportional to glaucony.

from inside the rhodoliths. Cluster 1 encompasses samples rich in coralline algae debris and benthic foraminifers, whereas samples with abundant barnacle fragments are in Cluster 2.

The small Cluster 3 stands in the central part of the plot, slightly closer to Cluster 1 and 2; this cluster includes samples from Facies 2 (lithozone 4b) together with samples with peculiar assemblages. In sample 1TNa, bryozoans are more abundant than in any other sample, whereas in samples **4TNc** (a bioturbation of the outer layer of a rhodolith) and 4bUVa, coralline algae and barnacle fragments are mixed with planktonic foraminifers.

Cluster 4 includes all of the samples from Facies 3 and 4 (lithozones 5 and 6).

Glaucony is far more abundant in Clusters 4 and 3 than in Clusters 1 and 2 (Fig. 2.4.6; Fig. 2.4.7).

Rhodoliths. According to pebble shape classification (Zingg 1935; adopted for the algal nodules by Bosence 1983a), most of the studied rhodoliths are spherical, discoidal specimens are rare. This result is confirmed by the quantitative sphericity analysis (Sneed & Folk 1958): most rhodoliths have sphericity > 0.8. Rhodoliths are small, pebble-sized (long axis less than 6.5 cm) in lithozone 1 and generally large, cobble-sized (long axis more than 6.5 cm) from lithozone 2 upward (Fig. 2.4.1).

The coralline growth form is almost always encrusting to lumpy and has an internal laminar structure made of closely stacked overgrowing crusts. Some rhodoliths with a columnar structure have been observed in 5TN.

Melobesioideae dominate the rhodolith algal assemblages, with abundance ranging from 60% to 90% (Fig. 2.4.1). Corallinaceae and Sporolithales are common accessories. Among Corallinaceae, *Spongites* and *Lithoporella* are the most frequent genera.

Lithophylloideae are rare and were only identified in 4VB, 4UV and 5TN. The most abundant species are *Lithothamnion moretii*, *Lithothaminion gianmarinoi*, *Lithothamnion* sp., *Phymatholiton* sp., *Mesophyllum roveretoi*, *Sporolithon* sp., *Spongites fruticulosus* and *Lithoporella melobesioides*.

Rhodolith nucleus is generally composed of bioclastic material. Some nodules grow as coated grains (Steneck, 1986; Basso et al., 2009) around large angular to sub-angular pebbles issued from the Casale Monferrato Fm.

In Facies 1, the bioclastic debris trapped inside the rhodoliths is composed of coralline fragments (50-70%), barnacle detritus (10-30%), benthic foraminifers (5-10%) and rare fragments of mollusks, bryozoans, echinoids and serpulids. The same association of skeletal grains is also observed in all of the boreholes of the algal nodules. In Facies 2, the very same association of skeletal grains is observed trapped inside the rhodoliths, whereas, planktonic foraminifers and glaucony grains are found in the boreholes of the outer layer of the rhodoliths. Rhodolith surfaces are often encrusted by bryozoans, barnacles (Fig. 2.4.4E) and serpulids; rhodoliths with barnacle-encrusted surfaces are especially common in lithozones 3 and 4.

Other skeletal grains: distribution and preservation. Coralline fragments are the main component of the studied lower unit of Sequence 2 (Facies 1 and Facies 2; lithozones 1 to 4); in lithozones 1 and 2 they represent up to 60%-65% of the skeletal grains. In the lithozones 3 and 4a, in the UV and VB quarries, the percentage of coralline algae debris is lower (30-40%) and barnacle fragments are more abundant (40%). Entire individual barnacles encrusting the rhodoliths have been observed in lithozones 2, 3 and 4 (Fig. 2.4.4E). The studied specimens have been identified as *Balanus* sp. and placed in the *Balanus trigonus* group (sensu Newman & Ross 1976) on the basis of their similarity to *B. spongicola* and *B. calidus* (Buckeridge pers. comm., 2013).

Benthic foraminifers are generally common (10%) but in the lithozones 3 and 4, in the UV and VB quarries, they are scarce. Textulariidae comprise 20-25% of the total observed benthic foraminifers in lithozone 1, their numbers decrease upward. In VB and UV quarries, in lithozone 1, large lepidocyclinids (*Nephrolepidina tourneri* and

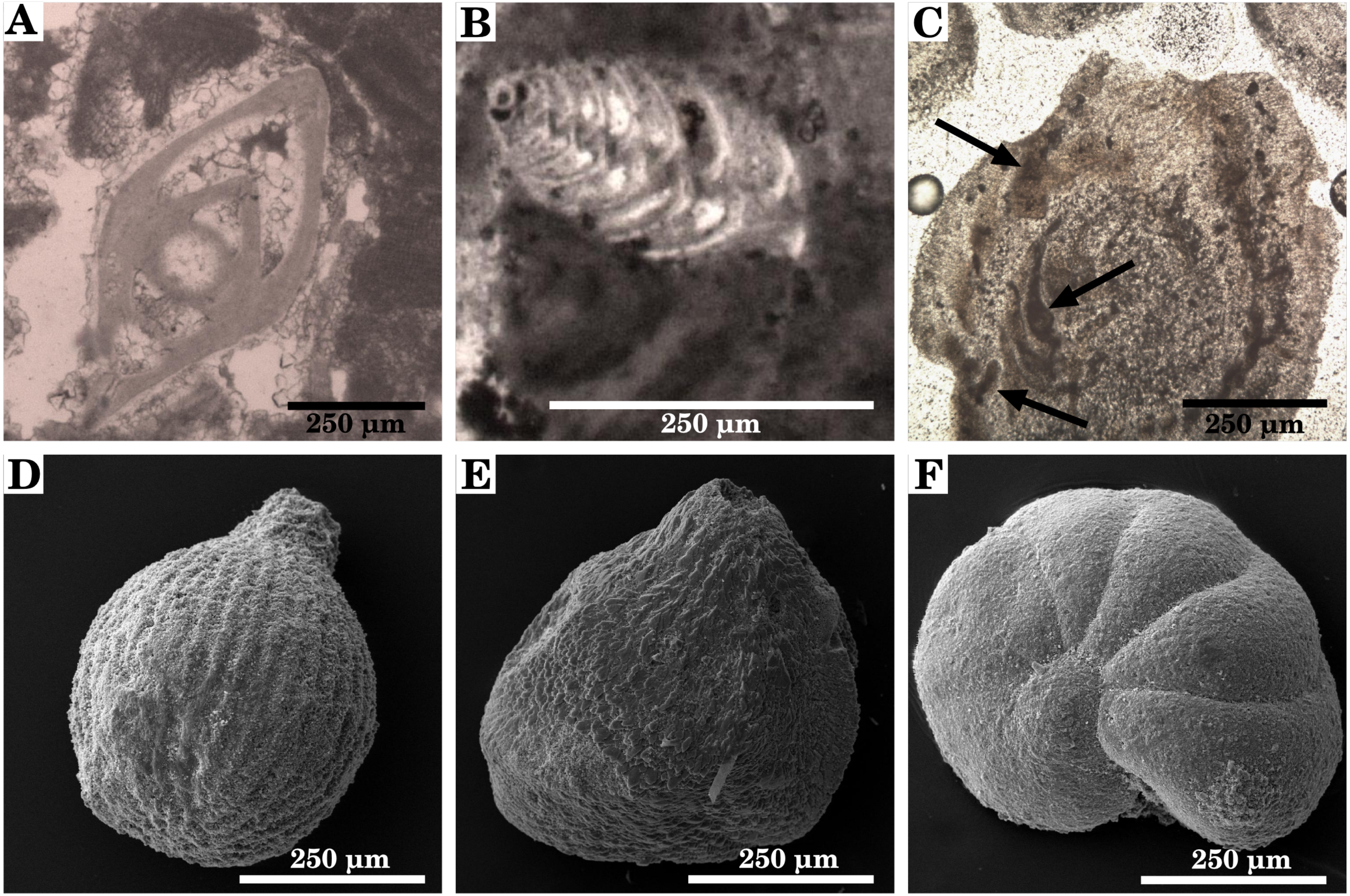

Figure 2.4.8 : Microfossils. A) *Lenticulina* B) Bolivinidae sp.. C) *Amphistegina* with chambers filled by glaucony; arrows = glaucony. D) *Lagena* E) *Bifissurinella lindenbergi*. F) *Lobatula lobatula*.

Eulepidina dilatata according to Schüttenhelm 1976) dominate the association. In lithozone 2, 3 and 4, and in lithozone 1 in the TN and TS quarries, the association is dominated by *Lobatula lobatula* (Fig. 2.4.8F), *Amphistegina* cf. *radiata* (identified following O'Herne 1974 description) and *Elphidium crispum*. *Operculina complanata*, *Miogypsina* spp., *Rosalina* sp., *Eponides repandus*, *Sphaerogypsina globulus*, *Stomatorbina torrei* and *Neoconorbina orbicularis* are common accessories.

In Facies 1 and Facies 2, specimens of *Lenticulina calcar*, *Lagena* and Bolivinidae (Fig. 2.4.8A, D, B) were found in association with the previously mentioned shallow-water foraminifers despite their typical distribution in deeper waters.

Planktonic foraminifers are uncommon in Facies 1, they become more frequent in Facies 2. and they are extremely abundant in Facies 3 and Facies 4. Among them, *Globigerina ciperoensis*, *Globigerina praebulloides*, *Globigerinoides trilobus*, *Globigerinoides quadrilobatulus*, *Zeaglobigerina woodi woodi* and *Globaquadrina dehiscens* are common species (Bicchi et al. 2006).

Bryozoans are present as minor components and are slightly more frequent in TN and TS than in the VB and UV quarries. In Facies 1 and Facies 2, the articulated bryozoan of the Bicorniferidae family, *Bifissurinella lindenbergi* (Fig. 2.4.8E) commonly occurs.

Mollusks and echinoids are less frequent than bryozoans, except in Facies 3 where bivalve shells are abundant. Bivalve identification is hindered by poor preservation, and whenever complete specimens are found (generally large *Pecten*), the shells are too brittle for extraction; no articulated specimens were observed. Specimens of the genera *Pecten*, *Flabellipecten*, *Amussium*, *Cardita*, and *Ostrea* have been recognized. Serpulids and ostracods are rare. Deep-water ostracods have been reported by previous authors (Schüttenhelm 1976). Gastropods were not directly observed but gastropod borings were observed on barnacle shells.

Breakage and abrasion are the most common biostratinomic processes observed on skeletal grains; rounding is negligible, and most of the bioclasts retain their angular shape. Barnacle opercular plates are thinned, and their superficial features are abraded. Parietal plates are highly fragmented and abraded, and only their upper and thicker edges are usually preserved. In lithozones 2 to 4, *Amphistegina* tests are frequently eroded and the innermost whorl of the chamber can be exposed; *Elphidium* and lepidocyclinid tests are also often deeply abraded. Bivalve shells are generally fragmented. Borings are common in rhodoliths, and gastropod perforations are frequent on barnacle opercular plates. Encrusting bryozoans, although not abundant, are scattered on barnacle plates and coralline algae; coralline algae encrust both barnacle plates and bryozoan colonies. Rare and poorly preserved specimens of *Amphistegina*, *Lepidocyclina* and *Miogypsina* with chamberlets filled by glaucony are present in lithozones 2 to 4 (Fig. 2.4.8C). Bryozoan zoecia and other skeletal porosities in Facies 1 are also infrequently filled by glaucony. Phosphatization and glaucony fillings of skeletal grains are common in Facies 3.

Rosignano and Treville

Rosignano outcrop dominates the top of the hill where the village was built. It is long several hundreds of meters and over 15 meters high. The base of the succession is massive (Fig. 2.4.9A); the central and upper portions are bedded, with each bed 2 to 20 cm thick, frequently showing an erosive base (Fig. 2.4.9C). In the upper part of the outcrop, several channels are present (Fig. 2.4.9A; Fig. 2.4.10A, B). In the western part of the outcrop the succession is thinner and bedded, with beds 5 to 40 cm thick (Fig. 2.4.9B). Thick beds are continuous while thin beds are composed by small lens-shaped bodies cutting each other (Fig 2.4.9D). Cut samples show a weak fabric of the bioclasts. Small mud-clasts are abundant. The rock is a grainstone with large benthic foraminifers, echinoderm plates, bryozan colonies and scattered rhodoliths. Rhodoliths are abundant

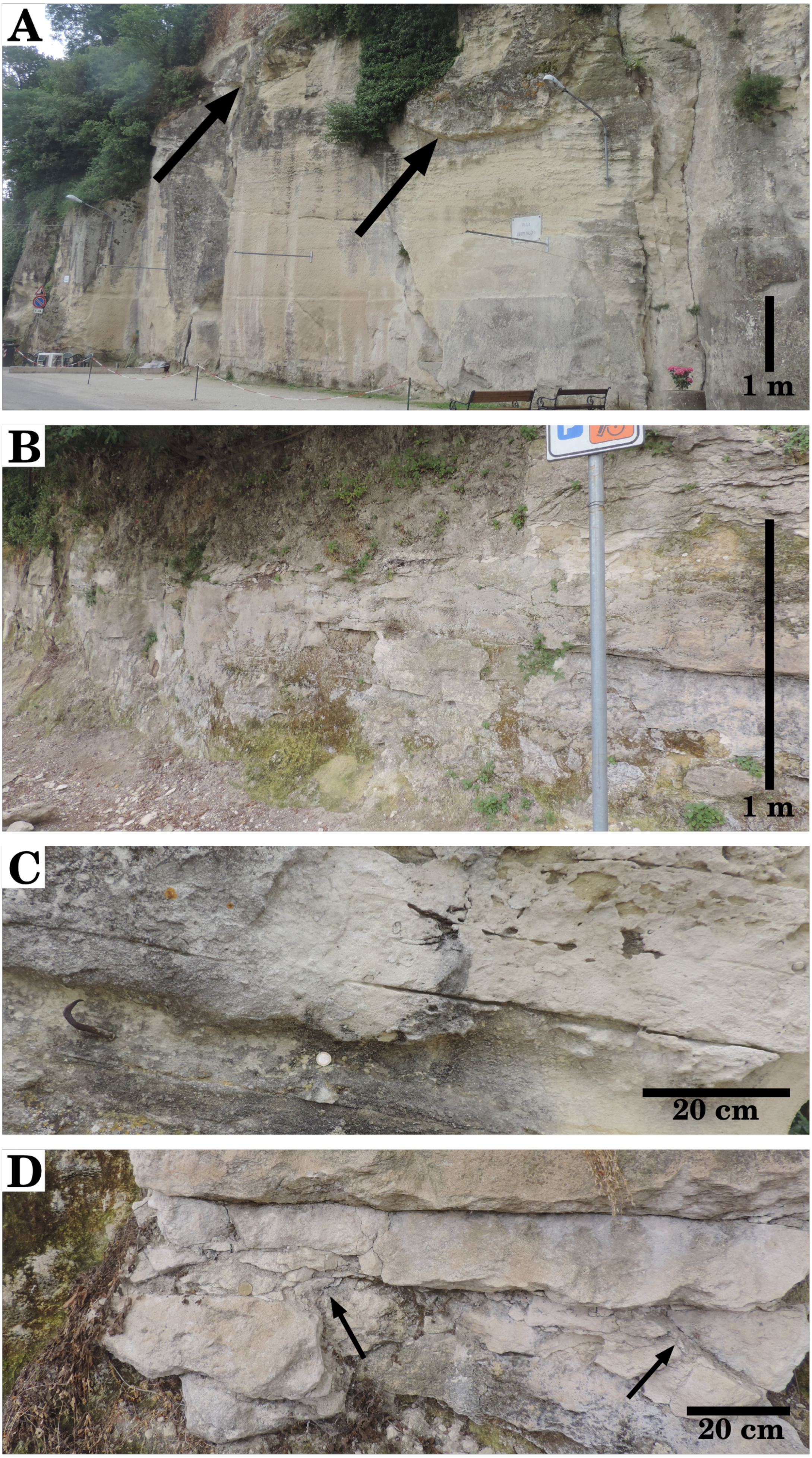

Figure 2.4.9 : Rosignano outcrop (45° 4.85' N 8° 24' E). A) Overview of the outcrop; arrows=channels. B) Western part of the outcrop. C) Lens shaped bodies in the western part of the outcrop. D) Detail of the erosive base of the beds.

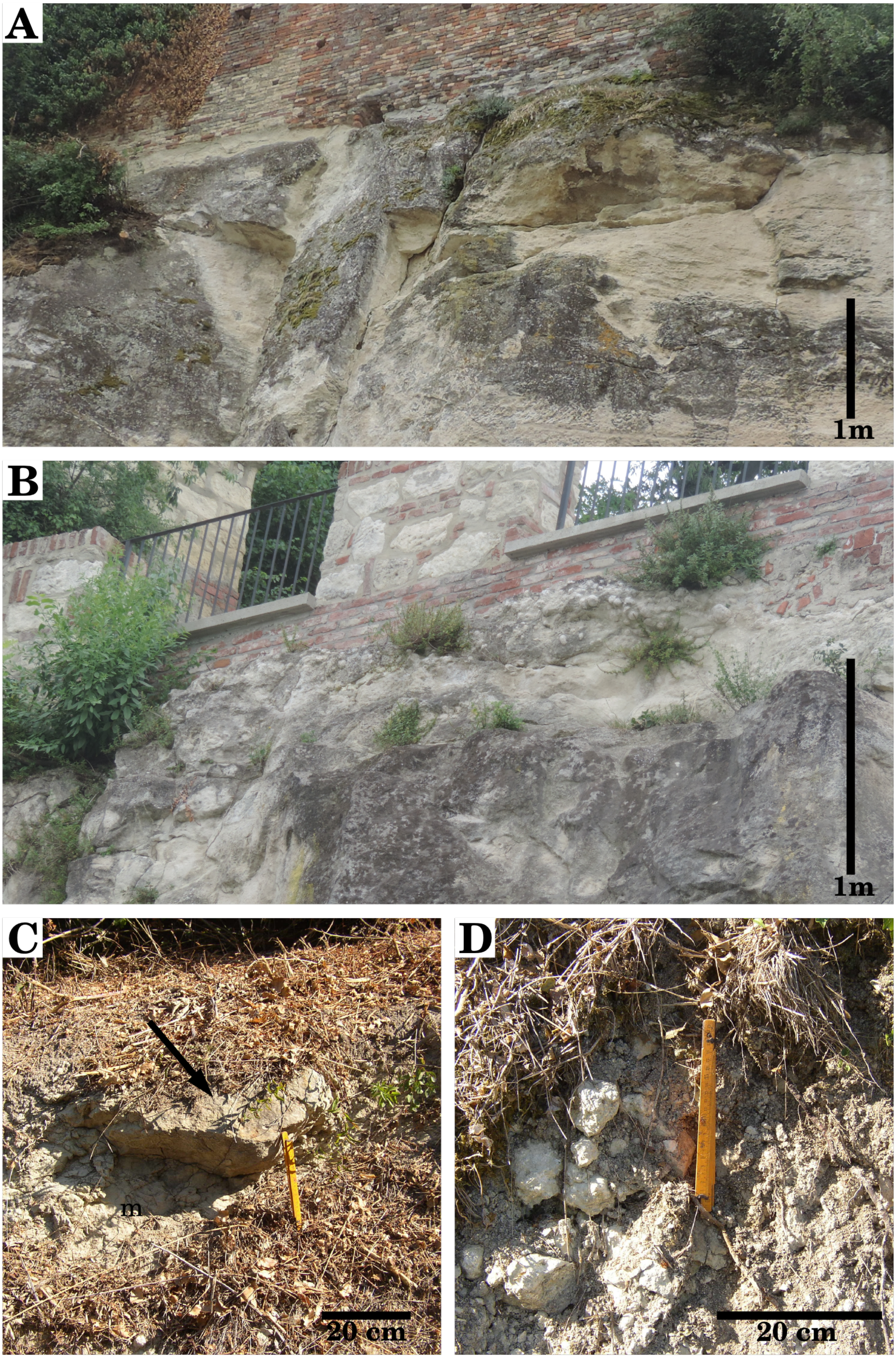

Figure 2.4.10 : A) Detail of a large channel in Rosignano outcrop. B) Detail of a rhodolith-filled channel in Rosignano outrcop. C) Coarse bioclastic limestone (arrow) interbedded in marls (m), in Treville outcrop (45° 5.81'N 8° 22' E). D) Rhodoliths scattered within the marls in Treville outcrop.

just in the uppermost part of the succession, in a channel deposit (Fig. 2.4.10B).
Treville outcrop is located on the hill of the village graveyard, and consists of marls interbedded with skeletal grainstone (Fig. 2.4.10C). Rhodoliths-rich beds are also present (Fig. 2.4.10D). The skeletal assemblage observed within the rhodoliths of these beds is composed by coarse, shallow-water, skeletal fragments (Fig. 2.4.5C). The marls in which the rhodoliths are embedded are mainly composed of clay, micrite and tests of planktonic foraminifers (Fig. 2.4.5D). Both Treville and Rosignano outcrops belongs to biozone N7a (Schüttenhelm, 1976; Bicchi et al. 2006).

2.4.5 – Discussion

The Burdigalian PDC Platform

Several sedimentological and paleontological evidences suggest that the carbonate sediment of the lower unit of PDC Sequence 2 moved from their shallow-water original environment toward slightly deeper waters.

1. The coarse skeletal layers, interbedded in marls in Treville, were also deposited by sediment gravity-flows, but in a deeper environment, probably on the slope of the platform. According to a previous reconstruction of the basin (Schüttenhelm, 1976) Treville was closer than UV, VB, TN, TS and Rosignano to the basin depocenter (Fig. 2.5.1). Being the westernmost outcrop of coarse skeletal limestone, it represents the distal margin of a submarine deposit formed by skeletal grains that were produced by the shallow-water rhodalgal carbonate factory of the PDC platform (Fig. 2.5.1).
2. The channels and the erosional scars in the Rosignano outcrop suggest that the sediment was probably transported by sediment gravity-flow. The common presence of mud clasts and the lack of a strong fabric support this interpretation (Major, 1998; Mutti et al. 2009). These events may have been triggered by the impact of storm currents. Strong currents generated by storm waves can provide enough energy to trigger sediment motion (Paull et al. 2003). Each channel scour probably represents a single event in which the sediment gravity-flow erodes the underlying substrate and then fill the depression. The presence of a rhodolith-filled channel at the top of Rosignano succession is an evidence that flows, mainly composed by rhodoliths, were common in the

3. PDC platform (Fig. 2.4.10B). The beds in the western part of Rosignano outcrop (Fig. 2.4.10B, D) were also deposited by gravity-flows. The nearby VB, UV, TN and TS deposits probably originated in a similar way, as suggested by the presence of lensoidal beds (Fig. 2.4.4C, D). However, due to the small exposed surface, it was impossible to observe any large-scale structure.

4. No fossil in life position was observed in the studied outcrops. Bivalve shells and colonies of articulated bryozoans (*Bifissurinella lindenbergi*) were always disarticulated, suggesting remobilization of the thanatocenosis before the final burial.

5. Skeletal grain porosities filled by glaucony commonly occur in all of the studied layers of UV, VB, TN and TS outcrops. This mineral forms in marine water below 50-60 m (Odin and Matter 1981; Odin and Fullagar, 1988; Carozzi, 1993; Amorosi, 1997); however, since the fossil association suggests a shallower environment, a transport toward slightly deeper waters is assumed.

6. The presence of deeper-water foraminifers (e.g. *Lenticulina calcar*, Goubert et al. 2001; Murray, 2006; Fiorini, 2015) and ostracods (Schüttenhelm, 1976) mixed with inner platform benthic foraminifers, also suggests a transport toward slightly deeper waters.

Resedimentation is common in rhodalgal platforms and is widely recorded in the fossil record (Pomar et al. 2002; Vigorito et al. 2005; Puga-Bernabéu et al. 2014). Currently, similar processes have also been recorded from the southern tip of Baja California (Mexico), where rhodalgal carbonate is produced in the inner part of the platform and transported into the basin by sediment gravity-flows (Schlanger and Johnson, 1969; Halfar et al. 2001). The skeletal composition of the transported material is still similar to the *in situ* assemblage (Van Andel, 1964; Schlanger and Johnson, 1969). Similar to the PDC limestone, the Baja California carbonate platform also lacks important framework builders (coral are only present in small patches fringing the shoreline) and it is exposed to strong currents. Unlike the Baja California platform, the PDC shallow-water skeletal

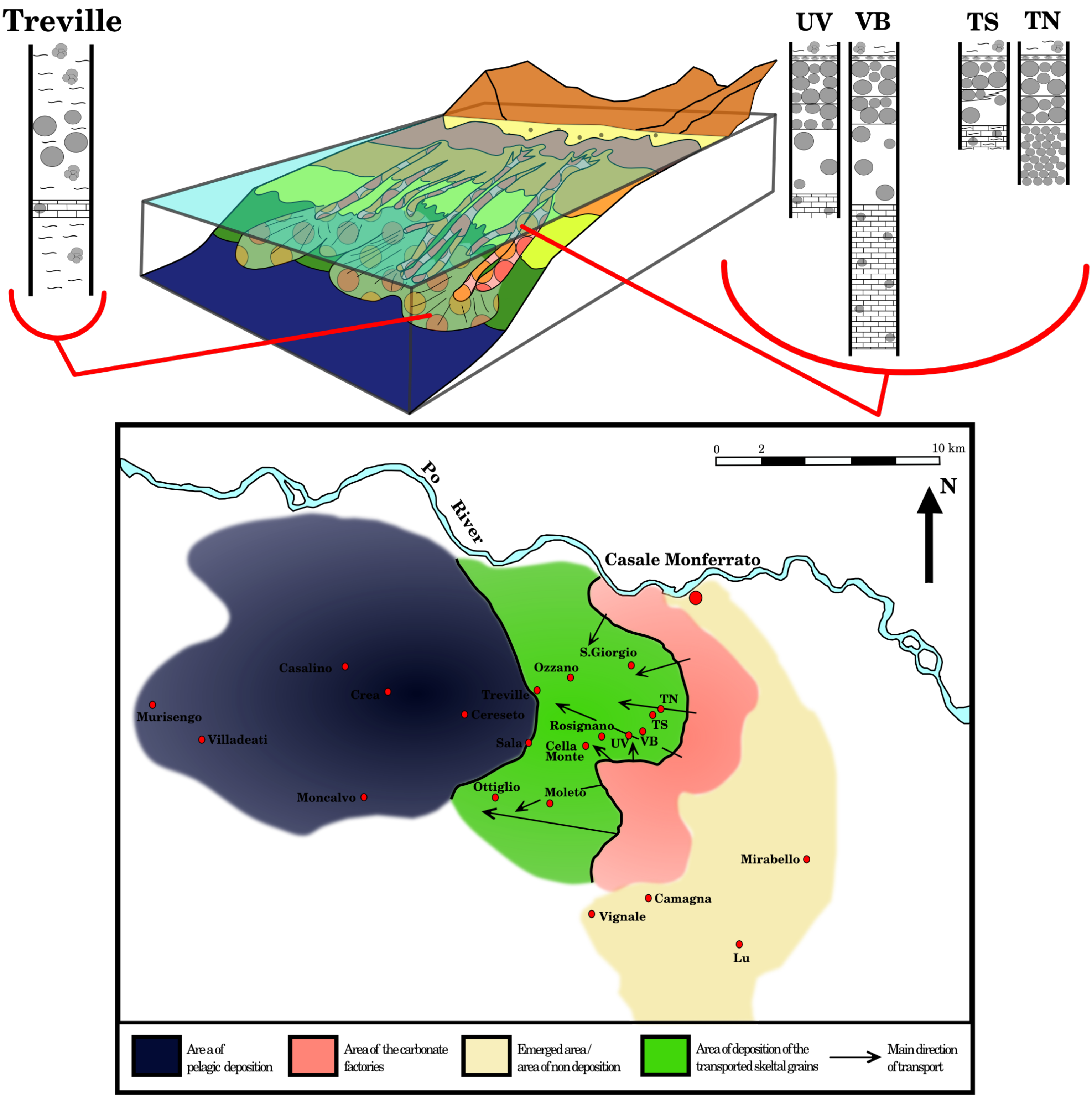

Figure 2.5.1 : Reconstruction of PDC basin during the deposition of Sequence 2, lower unit. The position of the main localities of PDC and the depositional environments of the carbonate ramp are shown. Modified after Schüttenhelm (1976).

grains were transported just slightly deeper than their original formation environment. They were moved from inner-middle ramp settings toward at least the lowermost part of the middle ramp, were glaucony formation could take place. Treville gravity-flow deposited in an even deeper environment, probably on the slope.

The transport rate and the carbonate factory exert a significant control over the long-term evolution of the carbonate platform (Pomar and Kendall 2007; Williams et al. 2011). The high transport rate and the presence of a rhodalgal carbonate factory fostered the development of a distally steepened ramp profile in the PDC system. Inherited topographic elements such as elevated areas and depressions must have locally warped this simple profile. According to regional-scale studies, the PDC complex deepens westward and is characterized by NW-SE oriented troughs and highs arranged parallel to the main tectonic lineaments (Schüttenhelm, 1976; Dela Pierre et al. 1995). Channels crossing the productive areas of the inner-middle ramp exerted significant control over the facies distribution and the depositional architecture of the system. Sediments were funneled along a VB-Treville northern depression and a Moleto-Ottiglio southern depression (Schüttenhelm, 1976; Fig. 2.5.1). Angular clasts from the Casale Monferrato Fm. (Early-Middle Eocene) are common rhodolith cores, indicating that those rocks were exposed on nearby areas that also influenced the sediment distribution.

Rhodolith Transport

Rhodoliths are precious tools in paleoecological reconstruction of environment with high rate of sediment transport, since they preserve the record of the changing benthic associations through time or space (Basso and Tomaselli, 1994; Basso et al. 1998; Checconi and Monaco, 2008). Therefore, it is useful to provide a brief overview encompassing the known examples of rhodolith transport from past and present-day oceans.

Transport may be a single or a multiple stage process (Fig. 2.5.2). In the latter, rhodoliths and other skeletal grains produced in shallow-water carbonate factories are first moved across the platform under the action of strong currents (Kamp et al. 1988; Puga-Bernabéu et al. 2010; Brandano et al. 2012) (Fig. 2.5.2, case 1). Sediment then accumulates on the slope-break and it may eventually move again as sediment gravity-flow (Fig. 2.5.2, case 2) (Schlanger and Johnson, 1969; Halfar et al. 2001).

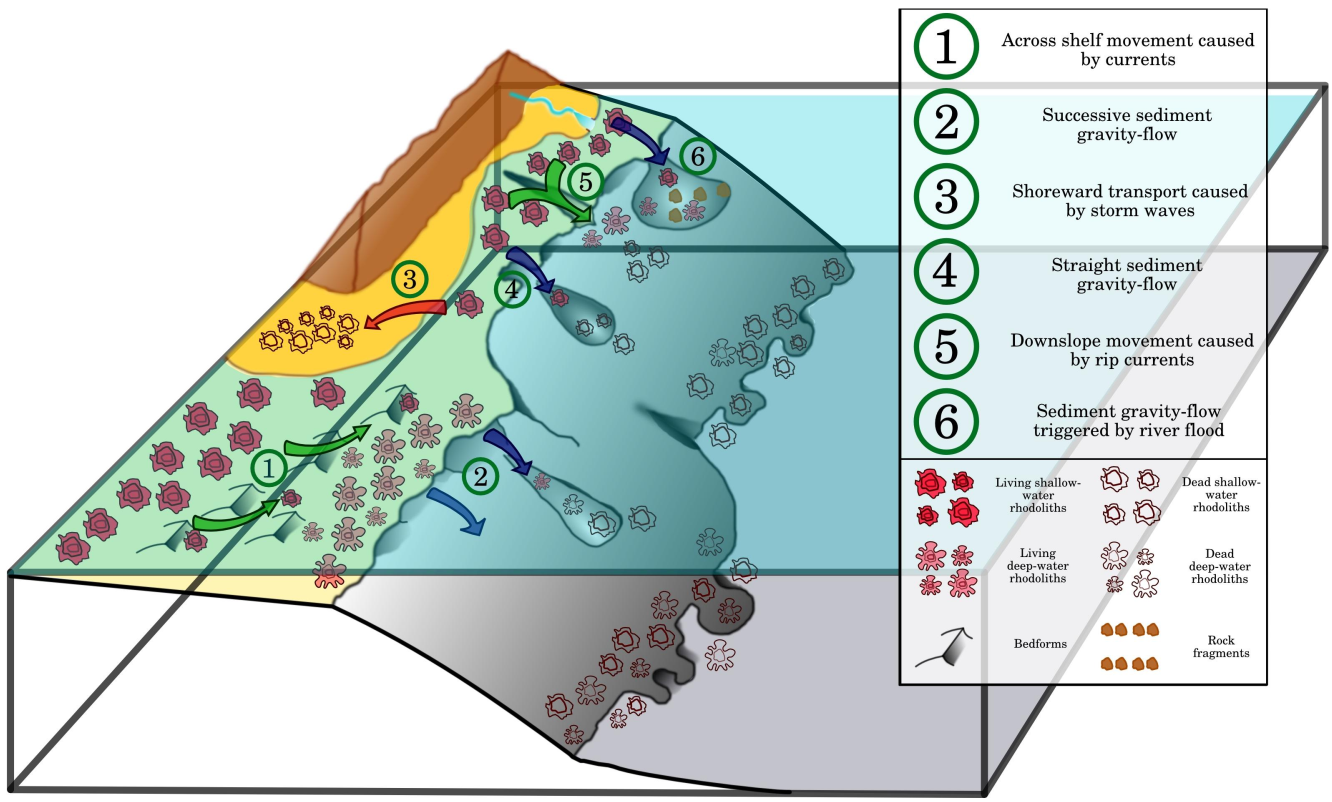

Figure 2.5.2 : Block-diagram summarizing the six main cases of rhodolith transport.

During across-platform transport, bioclasts undergo a suite of destructive biostratinomic processes, the most important of which are fragmentation, abrasion, corrosion, size-selection, and biodestruction (Johnson, 1962; Staff et al. 1986; Brett and Baird, 1986;

Wilson, 1988; Basso et al. 2009). Rhodoliths may continue to grow by further coralline encrustation or by other constructive biostratinomic processes, which is indicated by sharp contrasts of bioturbation and microfaunal assemblages between the rhodolith nucleus and the rhodolith surface (Basso, 1991; Checconi and Monaco, 2008; Checconi et al. 2010). Further development of rhodoliths may occur in the time between the deposition near the slope-break and later movements. This period of growth is marked by a sharp change in the algal association of the rhodoliths, with deep water species systematically on the outer layer of the rhodoliths and shallow-water species near the core.

During the subsequent process of sediment gravity-flow, skeletal assemblages may undergo further selection and additional breakage. If the final resting place is within the photic zone, rhodoliths may slowly grow until they are eventually buried. In this situation, a change in both algal assemblage and algae growth form should be detected, with growth forms (of shallow-water species) at the rhodolith nucleus recording frequent overturning, and growth forms (of deep-water species) in rhodolith outer layers that record a less turbulent setting.

During all the stages of the process, skeletal grains may become trapped inside the rhodoliths by either algae binding or by seeping through borings. Although seeping may happen any time, binding only occurs during coralline life. The distribution of skeletal grains inside the rhodoliths is therefore useful to understand whether or not they have formed in the same environment of the algae (Basso, 1991).

Single-stage transport is also possible, especially on narrow shelves. Strong storm-induced currents may sweep shallow-water rhodoliths and move them directly into deeper-waters (Fig. 2.5.2, case 5) (Checconi et al. 2010; Brandano and Ronca, 2014). Also a straight gravity-driven process may carry the rhodoliths directly into the basin (Fig. 2.5.2, case 4) (Fravega and Vannucci, 1982). The flow may be triggered by seismic activity, strong currents but also by exceptional river floods (Brandano and Ronca, 2014) (Fig. 2.5.2, case 6). As in the two-stage transport, both destructive biostratinomic processes and new encrustation are always possible until the final burial.

The transport of lithified or partially lithified sediment may also occur. Rhodoliths can be exposed to erosion as a result of uplift or sea-level fall, and the detached elements might move basinward (Leszczyński et al. 2012) similar to other rock fragments (Fig. 2.5.2, case 6). The rhodolith-bearing intraclast-rich limestone is likely related to the erosion of lithified or partially lithified sediment.

Channel networks may funnel sediments downslope, leading to the development of channel and channel-related depositional bodies (Cherchi et al. 2000; Vigorito et al. 2005; Vigorito et al. 2006; Bassi et al. 2006).

Shoreward transport, in which shallow-water rhodoliths are moved to the shore by hurricane-generated waves (Johnson et al. 2011), cannot be ruled out (Fig. 2.5.2, case 3) since it is known in present-day environments and in the fossil record.

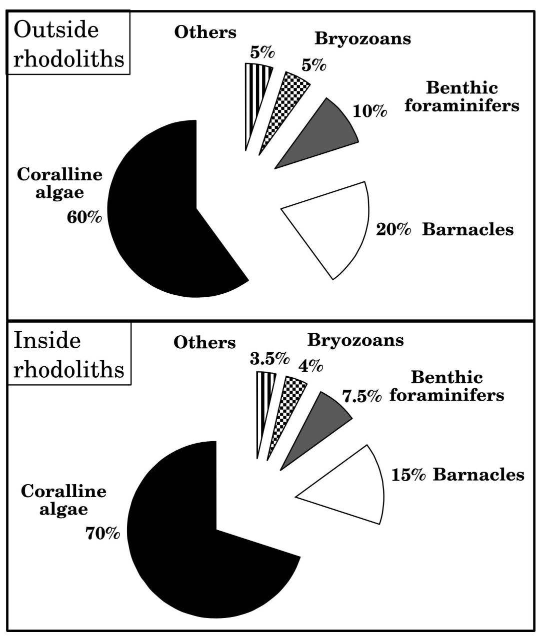

Figure 2.5.3 : Circle charts showing a comparison between the bioclastic composition of the sediment inside and outside rhodoliths; Facies 1.

As a general rule, long transport in space and time increases the chance of mixing different materials; longer times also enhance the effects of biostratinomic processes. Transport by gravity flow is likely to be less selective than transport by currents and may allow both rhodoliths and associated skeletal grains to reach deeper settings as a recognizable unit.

In this framework, it is possible to sketch the processes that moved the PDC rhodoliths. The skeletal assemblage observed inside rhodoliths is characterized by shallow-water elements: barnacle fragments, large benthic foraminifers (lepidocyclinids, *Amphistegina*) and small, shallow-water, benthic foraminifers (*E. crispum*, *L. lobatula*). In Facies 1 this assemblage is present both inside the borings at the rhodolith cores (which is generally the oldest part of the coated grain) and within the coralline thalli. The similarity between the skeletal assemblages inside and outside the rhodoliths, in VB, UV, TN and TS outcrops (Fig. 2.5.3), indicates negligible mixing effects, which is consistent with a transport mainly caused by sediment gravity-flow. Negligible mixing also point-out to a short distance transport from the formation environment to the final resting place. In Facies 2 the shallow water assemblage is present within coralline thalli and in some bore holes, but glaucony and planktonic foraminifers are present in the borings of the rhodolith outer layers. The lack of planktonic foraminifers and authigenic minerals bound by coralline thalli implies that the final depth of deposition was below the photic zone where rhodoliths could no longer grow. The seeping of deeper water sediment in the bore holes occurred after the death of the rhodoliths.

The absence of a recurring pattern in coralline species assemblages and in growth forms suggests a situation closer to the single-stage transport (Fig. 2.5.2, case 4), where rhodoliths are moved directly by sediment gravity-flow.

The rhodoliths of Treville, which are interbedded in marls, preserve inside their core the same shallow-water assemblage of skeletal grains of the rhodoliths of UV, VSB, TN and

TS (Fig. 2.4.5C), testifying that they originated in the same environment. The clear difference between the skeletal assemblage inside the rhodolith and the skeletal assemblage outside the rhodoliths (Fig. 2.4.5C, D) is an evidence that the rhodoliths of Treville, unlike those of VB, UV, TN, TS, were transported in a deeper environment, probably on the slope. Obviously coralline-algae growth was impossible in this environment too, and therefore no deep-water material was bound by coralline-algae.

Facies interpretation

Facies 1. The presence of coralline algae and large symbiont-bearing benthic foraminifers (lepidocyclinids, *Amphistegina*, *Operculina*, *Miogypsina*) indicates a formation environment within the photic zone for Facies 1. *E. crispum* is one of the most common benthic foraminifers in all of the lithozones of Facies 1. This species lives between 0 to 50 m (Murray, 2006). The other commonly occurring benthic foraminifers *A. radiata* (20-90 m, Murray 2006); *L. lobatula* (0-150 m, Holcova and Zagorsek, 2008), *O. complanata* (50-90 m, Murray, 2006) and *Miogypsina* (0-50 m, Geel, 2000) indicate a similar depth. Considering the abundance of barnacle encrustation between coralline layers inside the rhodoliths and on the rhodolith surfaces, environmental conditions were clearly suitable for both coralline algae and barnacles. Large internally compact spherical rhodoliths and the low micrite content suggest the important role of bottom currents in sweeping the ramp on a regular basis. This high-energy environment is also consistent with the barnacle abundance of Facies 1. The growth rate of barnacle has been directly correlated to water turbulence and plankton abundance (Sanford and Menge, 2001); barnacle-rich fossil sandstones have been related to turbulent and food-rich environments (Kamp et al. 1988).

The high phosphate content (represented by authigenic phosphate) in lithozone 4 and 5 suggests mesotrophic to eutrophic conditions. The widespread occurrence of authigenic phosphate and glaucony also indicate nutrient-rich waters (Pufahl, 2010). Therefore, the studied associations might have developed in non-oligotrophic, high-energy waters. The increase in particulate organic carbon, driven by nutrient abundance, reduces the water transparency and moves the entire benthic zonation shoreward (Hallock and Schlager, 1986; Vannucci et al. 2003; Hallock, 2005). Hapalidiales dominate the PDC coralline algae association (Fig. 2.4.1). Currently, similar assemblages are generally found in clear oceanic waters deeper than 60 m (Braga and Aguirre, 2001). According to the supposed nutrient abundance and the related water turbidity, we suggest a water-depth of less than 40 m, in the inner-middle ramp, for the formation environment of the rhodoliths of Facies 1. A depth shallower than 40m is also in accordance with the bathymetric range of the benthic foraminifers association. The final depth of deposition should be placed slightly deeper, in the middle ramp, below 50-60m, the shallowest depth for the formation of glaucony (Odin and Matter, 1981; Odin and Fullagar, 1988; Carozzi, 1993; Amorosi, 1997). Although they were transported, Facies 1 skeletal elements compose a coherent assemblage. Both rhodoliths and most of the smaller bioclastic fragments indicate the same formation environment, as testified by the presence of the same grain association outside and inside rhodoliths (Fig. 2.5.3).

The different skeletal compositions within Facies 1 may be interpreted as variability in sediment supply. The barnacle-dominated rudstone (3UV and 3VB), characterized by the abundance of hard-bottom dweller foraminifers (*Amphistegina* and *Lobatula*), formed in current-exposed areas. The assemblage of the grainstone, rich in lepidocyclinds, epiphytic foraminifers and agglutinated foraminifers (1UV and 1VB), originated in more sheltered zones, possibly with seagrass or other non-calcareous seaweeds.

Facies 2. Facies 2 indicates the inception of sediment starvation after the final drowning of the rhodalgal factory by relative sea-level rise. According to regional studies, this sea-level change initially had a main eustatic component, however, it occurred at the beginning of a long period of tectonic subsidence driven by regional geodynamic processes (Dela Pierre et al. 1995; Bicchi et al. 2006). Therefore, it is difficult to precisely locate this transgression event on the global eustatic curves because of the complex local interplay between tectonic and sea-level fluctuations.

The sea-level rise reduced the sediment supply, by drowning the rhodalgal carbonate factory and by reducing the transport of skeletal material toward the lower parts of the middle ramp. According to the low-stand shedding model (Carannante et al. 1996), in carbonate systems dominated by heterozoan production, there is a decrease in sediment transport during high-stand, since the carbonate factory is well below the wave base and therefore wave action is no longer able to move the sediment.

The qualitative analyses suggest that glaucony of this facies has an average degree of maturity. The occurrence of abundant glaucony grains, which are more mature than the light-green grains of Facies 1, is an evidence for the reduced sedimentation rate. Bioturbation processes and long exposure on the seafloor, caused by the low sedimentation rate, allowed fine planktonic sand and glaucony to seep inside the coarse, rhodolith-dominated, underlying deposits.

The rhodoliths of Facies 2 and Facies 1 are similar (shape, size, coralline algae composition, skeletal assemblage inside rhodoliths), suggesting that both rhodolith groups formed in the same environment in the inner-middle ramp and were later transported in the lower middle ramp.

Facies 3. Facies 3 corresponds to a major sedimentation break in the area. The carbonate production and the sedimentation rate are at their lowest. The massive reduction in carbonate supply is recorded by the transition from the limestone/impure limestone of

Facies 1 and Facies 2 to the marly limestone of Facies 3 and 4. Small highly phosphatized rhodoliths swept away from the shallow-water area testify the last transport episodes. Sediment deposited at depth well below 50-60 m, on the lower boundary of the middle-ramp and were exposed for a long time on the sea floor before the final burial, promoting glaucony and phosphate development. Observations of the glaucony grains indicate a high degree of maturity (Fig. 2.4.5A). This facies probably represents the maximum flooding surface of the initial marine transgression. According to Amorosi (1995) model, high concentration of mature glaucony in a condensed bed, at the boundary between shallow marine deposits and outer ramp, marks the maximum flooding surface of a marine transgression.

Facies 4. Facies 4 indicates the onset of hemipelagic sedimentation dominated by calcareous foraminifers, nannofossils and clays. Glaucony occurs in large, deep-green, angular grains and glaucony-filled planktonic foraminifers are common, testifying a still low sedimentation rate. The complete disappearance of coarse, shallow-water skeletal grains suggests a further deepening of the depositional environment.

2.6 – Conclusions

The studied Burdigalian section (lower unit of Sequence 2, sensu Bicchi et al. 2006) of the PDC represents a carbonate platform developed in a compressional setting where the inner ramp facies are unknown because they were either dismantled and not preserved in place, or buried under younger sediments. The inherited topography exerted a strong control over the facies distribution, depositional profile and pathways of sediment transport. Based on rock texture, mineralogy, chemical composition and fossil content, four main facies were recognized in the studied area. These facies record the evolution of the carbonate factory from maturity to final drowning and dismantling. The relative sea-level rise drowned the ramp and stopped the rhodalgal carbonate factory. This caused a progressive decrease in basinward sediment transport from facies 1 to 3, with the latter testifying the complete starvation.

The limestone of Facies 1 was composed of large skeletal elements formed in a rhodalgal-dominated inner-middle ramp setting. Currents moved the sediments across the ramp, supplied the energy for rhodolith overturning and produced the water turbulence that the barnacles required to thrive. Sediment gravity-flows carried the sediment basinward in a slightly deeper environment.

The impure limestone of Facies 2 was characterized by an increased contribution of pelagic components and authigenic minerals, indicating the inception of sediment starvation.

The complete sediment starvation was marked by the deposition of the condensed glauconitic-phosphatic limestone of Facies 3. Finally, the sedimentation of the marly limestone of Facies 4, dominated by the planktonic foraminifer tests, prevailed over the entire area.

The study of the skeletal assemblages trapped inside the rhodoliths and of rhodolith characteristics allowed a better reconstruction of the carbonate ramp and its processes. The PDC sediments deposited at a slightly greater depth than their original environment, after a short-lived transport.

Where only rhodoliths are left to witness the presence of a carbonate factory, the material stored inside these nodules may be sufficient to draft the characteristics of that environment. A reconstruction of the platform assemblage and of the major carbonate producers may be achieved based on sedimentary bodies consisting of transported grains as long as it is supported by detailed paleoecological analyses and taphonomy (Nebelsick et al. 2001; Rasser and Nebelsick, 2003). The investigation of rhodolith algal assemblages, structure, encrusting organisms and rhodolith-trapped sediment proved to be helpful since rhodoliths are free-living archives that retain all of the information accumulated during their development. Rhodoliths may store a record of their original environment, the platform across which they moved, and their final resting place. When buried and preserved in deeper settings, they may survive the platform and retain a fragment of its history.

3 – The Burdigalian of the Sommières Basin

Coralline algae as depth indicators in the Sommières Basin (Lower Miocene, Southern France)

Giovanni Coletti

(Article in preparation)

3.1 – Introduction

In paleoenvironmental reconstructions establishing the water depth is extremely important (Perrin et al. 1995). This determination is generally based on both paleontological and sedimentological evidences but the results are always relative since neither criteria have proxies directly related to water depth. Actually the only physical variable directly related to water depth is pressure and pressure does not strongly influence organisms distribution or depositional processes. Taxa distribution is rather controlled by light penetration, water turbulence, temperature, salinity and nutrient concentrations, which in turn are controlled by water depth. Sedimentological processes are mainly influenced by the proximity to the coastline (identified as the main source of detritus) and water turbulence, which are once again related to water depth. Due to these limitation, the integrated approach, based on the comparison of independent biological and sedimentological proxies, are favored over single-instrument studies. Coralline are a powerful instrument since they may provide information on both light penetration and hydrodynamic energy. Actually their distribution is deeply connected to light availability and their growth morphology is tightly related to the hydrodynamic energy (Steneck, 1986; Lund, 2000). Furthermore coralline algae are among the major contributors to carbonate production in shelf environment during the Cenozoic and they are widespread from the poles to the tropics and from the intertidal zone to the lower limit of the photic zone (Adey and Macintyre, 1973; Aguirre et al. 2000).
Although crustose coralline algae are among the most abundant marine carbonate producers and can potentially provide a wealth of information, they are relatively underemployed in paleoecological reconstruction. This is due in part to difficulties in identification since strong similarities in appearance exist among phylogenetically distant taxa (Adey and Macintyre, 1973; Steneck, 1986). The introduction of anatomical

characters used by modern phycologist lead to important and valuable changes in fossil-coralline taxonomy, but also created additional problems since the vast majority of fossil species discovered in the past is poorly described and type specimens are partially missing. Even though there have been several taxonomic revisions based on the modern approach, most of fossil species cannot be identified with confidence (Bassi, 1998; Rasser and Nebelsick, 2003). As a result of these problems, many scientists are reluctant to undertake detailed studies involving fossil coralline algae, and their potential in paleoenvironmental reconstruction is insufficiently exploited.

The aim of this work is to prove the usefulness of quantitative analyses on coralline distribution. Within a well constrained sedimentological and paleontological context, the abundance of corallines, both at order, genus and species level, is quantified in the form of the area occupied by the different taxa. The various species identified are thoroughly described in order to make potential future taxonomic revisions as easy as possible. The distribution patterns are then studied along a bathymetric gradient to assess the overall response of the group and identify the species that are more susceptible to variations in water depth, which have the potential to be used as proxies in paleoenvironmental reconstruction, at least on the local scale. Although it is very difficult with coralline algae to safely generalize local findings, this line of work may produce interesting results and can be repeated in many different context, hopefully laying the foundations for large-scale conclusions on fossil coralline distribution and a renewed interest in the subject.

3.2 - Geological setting and depositional Environment

In the Early Burdigalian the sea flooded the Alpine Molasse Basin (also know as Perialpine Foreland Basin), creating a narrow seaway, connecting the Western Mediterranean with the Parathetys, which lasted till the Early Langhian (Allen et al. 1985; Rögl, 1998; Dercourt et al. 2000; Reynaud and James, 2012; Fig 3.2.1). This narrow seaway (about 100 Km wide and about 1000 Km long; Allen et al. 1985) was dominated by tidal currents (Allen et al. 1985; Harzhauser and Piller, 2007). Atlantic tide entered the basin from a southwesterly direction, becoming progressively amplified by the narrow and shallow passage, promoting vigorous currents reflected in the tidally controlled shelf-deposits occurring throughout the whole Alpine Molasse Basin during the Early Burdigalian (Allen et al. 1985; Harzhauser and Piller, 2007).
Near the Rhône River delta, in Southeastern France, the marine transgression in the Molasse Basin lead to the deposition of extensive, tide-controlled, shelf deposits over the folded Mesozoic and Paleogene strata (Besson et al. 2005; Reynaud et al. 2006; Reynaud and James, 2012). The Sommières Basin was one of the many sub-basin of the Molasse Basin in SE France, located near the junction of the seaway with the Western Mediterranean (Reynaud and James, 2012; Fig. 3.2.1). The basin was a depression near 15 Km wide, connected to open sea through a corridor 6 km long and 2 km wide (Reynaud and James, 2012). Inside the basin three main unit are recognized: Sandy Molasse, Sandy Marls and Calcareous Molasse (Demarcq, 1970; Reynaud and James, 2012; Fig. 3.2.1). These units are respectively, lower, middle and upper Burdigalian in age and they represents two different depositional sequences (Berger, 1974; Reynaud

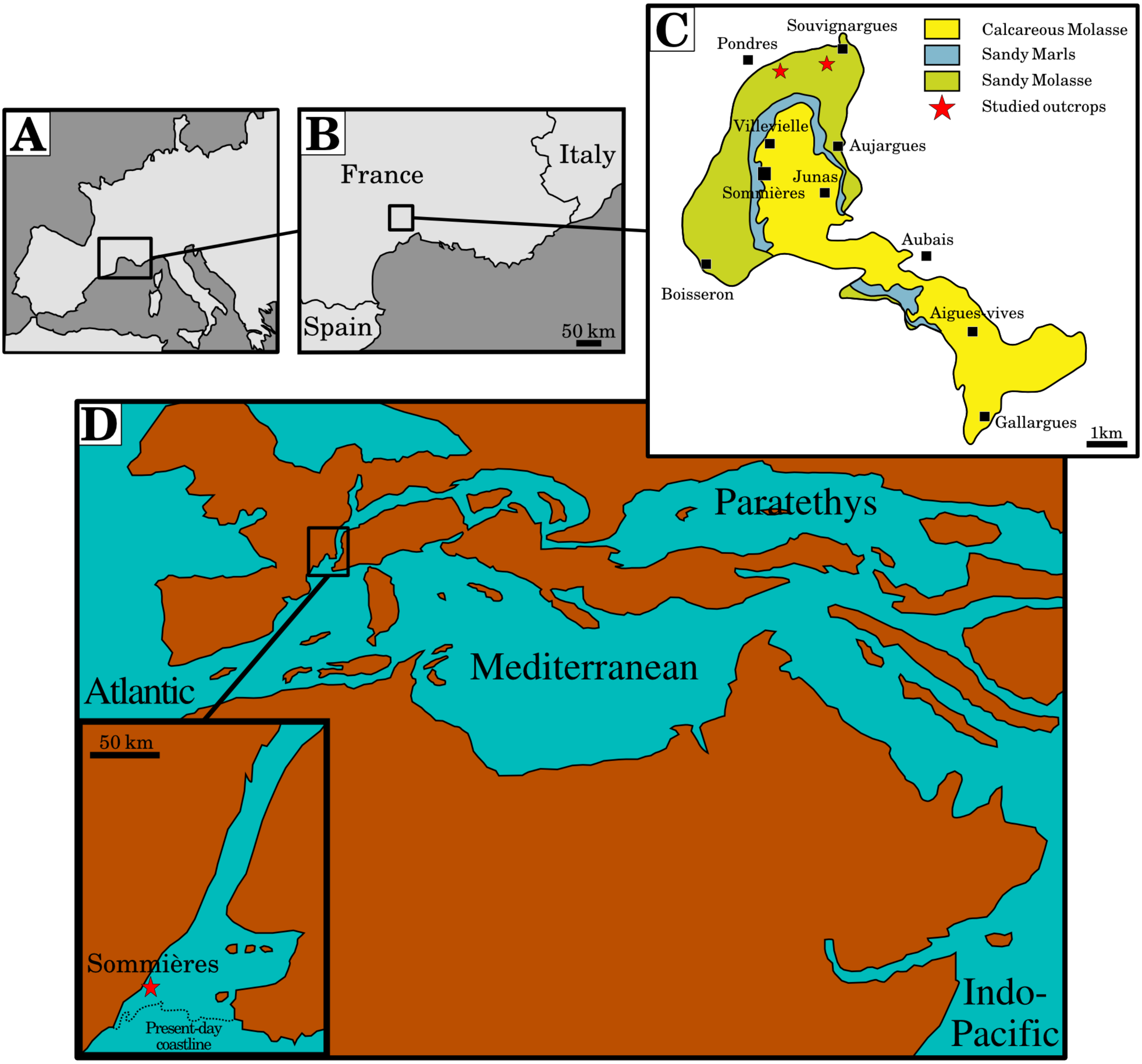

Figure 3.2.1 : Geographic and paleogeographic position of the Sommières Basin. A) Position in present-day Western Europe. B) Position in present-day France. C) Geological map of Sommières Basin (modified after Reynaud and James, 2012). D) Paleogeograhic reconstruction of the Mediterranean basin during the Early Burdigalian (modified from Meulenkamp et al. 2000); left panel present the detailed reconstruction of the Rodanian area of Alpine Molasse Basin, where Sommières Basin was located (modified from Besson, 2005; Reynaud and James, 2012).

and James, 2012). The first one is a transgressive sequence that records the flooding of the Sommières Basin. The beginning of the deposition of Sandy Molasse Unit testifies the beginning of the transgression (Transgressive System Tract) while the Sandy Marls Unit represent the maximum highstand of the succession (Highstand System Tract; Reynaud and James, 2012). At the end of the deposition of the HST an abrupt sea level fall is indicated by a major shift in facies distribution. The overlaying second sequence, is composed of the Calcareous Molasse Unit and deposited during the second marine transgression of the basin (Reynaud and James, 2012). The coarse grained base of the unit corresponds to the low standing deposition (Lowstand System Tract), while the overlaying beds are interpreted as the TST of the second sequence (Reynaud and James, 2012). This succession is similar to those in most of the other Burdigalian embayments of Molasse Basin in SE France (Rubino et al. 1990; Reynaud et al. 2006; Reynaud and James, 2012). By the end of the Burdigalian the basin was uplifted, due to the reactivation of the Nîmes fault and, as a consequences of that, the basin was filled up by sediments (Seranne et al. 2002; Reynaud and James, 2012).

The basin depositional system was largely controlled by tidal currents and within the system six main depositional environments are recognized by Reynaud and James (2012): marginal conglomerate, tidal bars and channels, open-coast tidal deposits, subtidal dunes, basinal bioclastic beds and basinal muds. Marginal conglomerates are recognized mainly within Sandy Molasse Unit, at the basin edge near Souvignargues and Boisseron villages, bordering the basin paleocoast (Fig. 3.2.1). They are characterized by coarse grained rocks with a remarkable detrital fraction issued from the erosion the bedrock of the basin and a bioclastic fraction with abundant fragments of barnacles and other encrusting biota. The tidal bars environment is mainly recorded in the Sandy Molasse Unit near the village of Pondres (Fig. 3.2.1), it developed slight basin-ward than the marginal conglomerates, in a still shallow-water setting dominate by large tidal bars draped by smaller subaqueous dunes and cut by swatchway channels. Coarse-grained bioclastic grainstones, with abundant bryozoans and coralline algae dominate the environment. Open coast tidal deposits are principally found in the outcrops of the Calcareous Molasse Unit near the village of Gallargues (Fig. 3.2.1), and developed in a more distal setting. They are composed of alternating mudstones, composed of lime mud created by the disintegration of skeletal grains, and bioclastic packstones transported basin-ward from shallow areas during storms. Subtidal dunes environment is widespread in the basin and is recorded both in the Sandy and Calcareous Molasse units, with the best outcrops near the Junas quarry (Fig. 3.2.1). It is dominated by the deposition of thoroughly cross-bedded coarse-grained bioclastic sediments with abundant bryozoans, coralline algae and echinoids. Basinal bioclastic beds are recorded in the Calcareous Molasse unit and outcrop in the village of Sommières (Fig. 3.2.1). These beds are made up by fining-up packages with bryozoan-rich rudstone at the base and mudstone at the top. They deposited into an offshore low-energy environment near the center of the basin, occasionally affected by storm events. The basinal muds, composed of minute shell fragments, sponge spicules, ostracods and fine-grained quartz-grains, deposited in a low energy and relatively deep environment. This environment is largely recorded in the Sandy Marls Unit, with scattered outcrop in the central part of the basin (Fig. 3.2.1).

The basin hosted an heterozoan carbonate factory where the most important carbonate producers were bryozoans, barnacles, coralline algae, echinoids and mollusks (Reynaud and James, 2012). Lesser contributors were benthic foraminifers, serpulids, brachiopods and ostracods (Reynaud and James, 2012). Barnacles and other hard-substrate biota were more common along the coast of the basin while soft-substrate taxa thrived more offshore (Reynaud and James, 2012).

3.3 – Material and Methods

The Sandy Molasse Unit, of lower Burdigalian age, is the main subject of this work. The outcrop studied are located near the village of Souvignargues, near an old dismissed quarry (43° 48.387'N; 4° 7.147'E), and near the village of Pondres in the active quarry of La Garenne (43° 48.466'N; 4° 5.94' E).

Since the rock is coarse-grained, very large (5kg each) volumes of rock were taken in order to obtain compositionally representative samples. Samples were taken after the removal of the upper and probably weathered rock surface.

A small tile (approximately 10x10cm) was produced from each sample, over the tile surface the gravel-sized elements were analyzed and quantified by point-counting, using a grid with a mesh size of 2 mm. The recognized categories were: rock fragments, macroscopic skeletal grains and sand-sized elements (< 2 mm).

For each sample X-ray diffraction analyses (XRD; PANalytical's Xert PRO Materials Research Diffractometer) were performed to better quantify the mineralogical composition of the rock.

From each sample 2 to 3 thin sections (35 thin sections in total) were prepared to study texture, mineralogical and bioclastic composition of the rock by point-counting (Flugel, 2009). In each thin section 6 digital photomicrographs were captured, the photos were captured in a random position and with no overlap between them. A digital grid with a mesh-size of 300 μm was used and more than 300 hundred points were identified for each photomicrographs. The recognized categories were: void, sparitic cement, micrite, rock-fragments, silicate minerals, authigenic minerals, coralline algae, bryozoans, barnacles, mollusks, echinoids, larger benthic foraminifers, smaller benthic foraminifers, planktonic foraminifers, brachiopods, ostracods and serpulids.

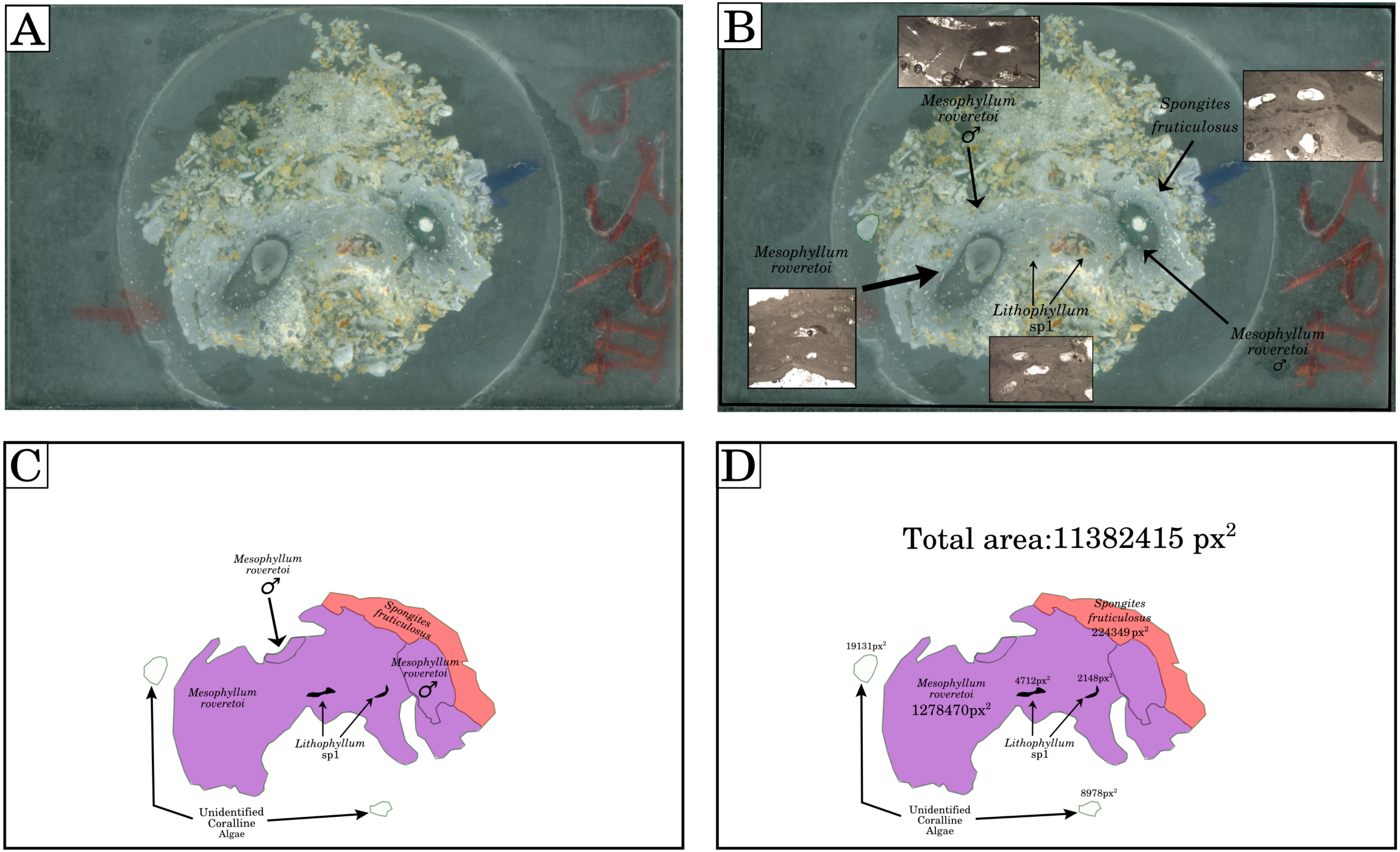

Figure 3.3.1 : the procedure used to quantify coralline algae abundance. A) scanning of the whole thin section. B) Identification of the species. C) Delimitation of the area occupied by the various species in the vector grahic editor. D) Calculation the surface occupied by the algae; the program calulate the surface in px^2 but this result can easily converted in mm^2 since the total area of the thin section is known.

Thin sections for to the identification and study of coralline algae were produced from each sample. Forty thin sections (separated from the previous group) were produced and analyzed for this purpose. Thin sections of coralline algal were observed under light microscope to study and measure their anatomical features. Growth-forms terminology follows Woelkerling et al. (1993). Vegetative anatomy was measured along longitudinal radial section (Quaranta et al. 2007; Vannucci et al. 2008). The diameter of the cells was measured including the cell wall; cell length was measured as the distance between two primary pit connections and includes the cell wall (Basso et al. 1996). Conceptacles were measured along their axial section (*i.e.* the longitudinal section that cuts a conceptacle medially resulting in the pore canal being completely visible Afonso-Carillo et al. 1984), in accordance to Quaranta et al. (2007) and Vannucci et al. (2008) methodology.
Coralline taxonomy at higher taxonomic ranks follows Woelkerling (1988) adapted to the paleontological use by Braga et al. (1993) and later modified by Harvey et al. (2003), Kato et al. (2011), Bittner et al. (2011) and Nelson et al. (2015).
Coralline algae abundance was quantified by scanning whole thin sections, importing the raster image in a vector graphics editor, defining in the vectorial environment the area occupied by coralline taxa (coralline were previously identified under light microscope) and finally querying the program for the extension of the area, therefore quantifying in mm^2 the coralline abundance in each section (Fig. 3.3.1). These results allowed to determine accurately the contribution of each species to the total assemblage and its distribution in the studied sequences.

3.4 – Results

Paleontological, petrographical and mineralogical analyses allowed the recognition of different lithozones and the identification of the dominant coralline algae species (Fig. 3.4.1; Tab. 3.4.1; Tab. 3.4.2). The presentation of the results is divided in two sections, a former with the information relative to the Souvignargues succession and a latter dedicated to the Pondres succession. Detailed descriptions of the coralline algae presented in this chapter are delivered in the taxonomic appendix (Chapter 6).

Souvignargues

Lithozone description. The studied succession of Souvignargues has not been further divided in to various lithozones since paleontological and petrological characteristics of the rock are homogeneous (Fig. 3.4.1; Tab. 3.4.1; Tab. 3.4.2).

The rock is an impure rudstone with 20% of silicate minerals and traces of authigenic phosphate. A crude lamination can be seen due to the common orientation of skeletal elements (Fig. 3.4.2 A-B). Half of the elements are gravel-sized, among them coralline-algal branches (group I and II, sensu Bosence, 1976) and bryozoans colonies are fairly common, very small rhodoliths (less than 2 cm in diameter) are less frequent (Fig. 3.4.2 C). Small rounded pebbles of limestone and quartz are present (Fig. 3.4.2 C).

Point count analyses show that bryozoans are the most common skeletal grains, occurring either as small fragments or as whole colonies (with branched and nodular morphologies); coralline algae are also very abundant (Fig. 3.4.2 D-E; Tab. 3.4.1).

Lithozone	Souvignargues	Pondres				
		Lithozone 1	Lithozone 2	Lithozone 3	Lithozone 4	Lithozone 5
Calcite minerals (XRD)	79%	73.3%	68%	86.2%	84.5%	78.3%
Silicate minerals (XRD)	20.5%	26.7%	32%	13.8%	15.5%	21.7%
Gravel-sized elements						
Elements <2mm	49.8%	85.2%	96%	95.2%	81.4%	85.1%
Bioclastic fraction	46.2%	14.4%	3.9%	4.8%	18.6%	14.8%
Detrital fraction	4%	0.4%	0.1%	0%	0%	0.1%
Point counting						
Bioclastic elements	69.2%	66.4%	61.3%	77.3%	78.1%	76%
Silicate grains	12.1%	25.5%	30.7%	16.4%	15.1%	20%
Rock fragments	18.7%	8.1%	8%	6.3%	6.8%	4%
Point counting (bioclastic fraction)						
Bryozoans	51%	43.2%	44.3%	56.6%	35.2%	40%
Coralline algae	32.4%	24.7%	16.1%	15.7%	43.7%	30%
Mollusks	9.5%	4.8%	6.5%	5.2%	7%	11.9%
Echinoids	5%	19.1%	23.2%	19.1%	10.2%	14.4%
Barnacles	2%	6.2%	6.5%	1%	2.3%	1.4%
Benthic foraminifers	0.1%	1.8%	2.6%	2.2%	1.5%	1.8%
Planktonic foraminifers	0%	0%	0%	0%	0%	0%
Brachiopods	0%	0.2%	0.8%	0.2%	0.1%<	0.4%
Others	0%	0.1%<	0%	0%	0.1%<	0.1%

Table 3.4.1 : Petrographic and bioclastic characteristics of the analyzed lithozones in the Sommières Basin

Lithozones	Souvignargues	Pondres				
		Lithozone 1	Lithozone 2	Lithozone 3	Lithozone 4	Lithozone 5
Hapalidiales	85%	92.8%		99.5%	95.2%	100%
Corallinales	9.5%	7.2%		0.5%	4.8%	0%
Sporolithales	5.5%	0%		0%	0%	0%
Identified species						
Sporolithon sp. 1	8.7%	0%		0%	0%	0%
Lithophyllum sp. 1	2.6%	1.8%		0.6%	1%	0%
Spongites fruticulosus	0%	2.4%		0%	3%	0%
Spongites sp. 1	0%	4.6%		0%	0%	0%
Spongites sp. 2	0%	0.3%		0%	0%	0%
Lithoporella melobesioides	0.1%	0.1%<		0.1%<	0.1%<	0%
Lithoporella minus	0.1%<	0%		0%	0.1%<	0%
Mesophyllum roveretoi	15.9%	67.6%		16.5%	42.6%	11.1%
Mesophyllum galettoi	4.5%	0%		0%	0%	0%
Mesophyllum ishijimai	4%	0.4%		0%	0%	0%
Mesophyllum sp. 1	17.3%	0%		0%	0%	0%
Lithothamnion ponzonense	19%	13.4%		0%	20.5%	0%
Lithothamnion crispatum	5.2%	0%		0%	0%	0%
?*Lithothamnion* sp. 2*	8.2%	0%		0%	18.3%	0%
Lithothamnion/Phymatolithon sp. 1	9.8%	0%		0%	1.6%	0%
Lithothamnion/Phymatolithon sp. 2	0%	6.9%		0%	0%	39%
Phymatolithon calcareum	0%	2.6%		0%	1.2%	0%
Phymatolithon sp.*	4.7%	0%		59.4%	11.7%	19.3%
Phymatolithon sp. 1	0%	0%		23.4%	0%	30.6%

Table 3.4.2 : Coralline algae association in the studied lithozones of the Sommières Basin; *= ?*Lithothamnion* sp. 2 and *Phymatolithon* sp. are both sensu Hrabovský et al. 2015.

Figure 3.4.1 : Stratigraphic log of the Sommières Basin and of the studied sections. The general log of the basin is modified from Reynaud and James (2012). f: fine; m: medium; c: coarse; gr: gravel; pb: pebble; cb: cobble

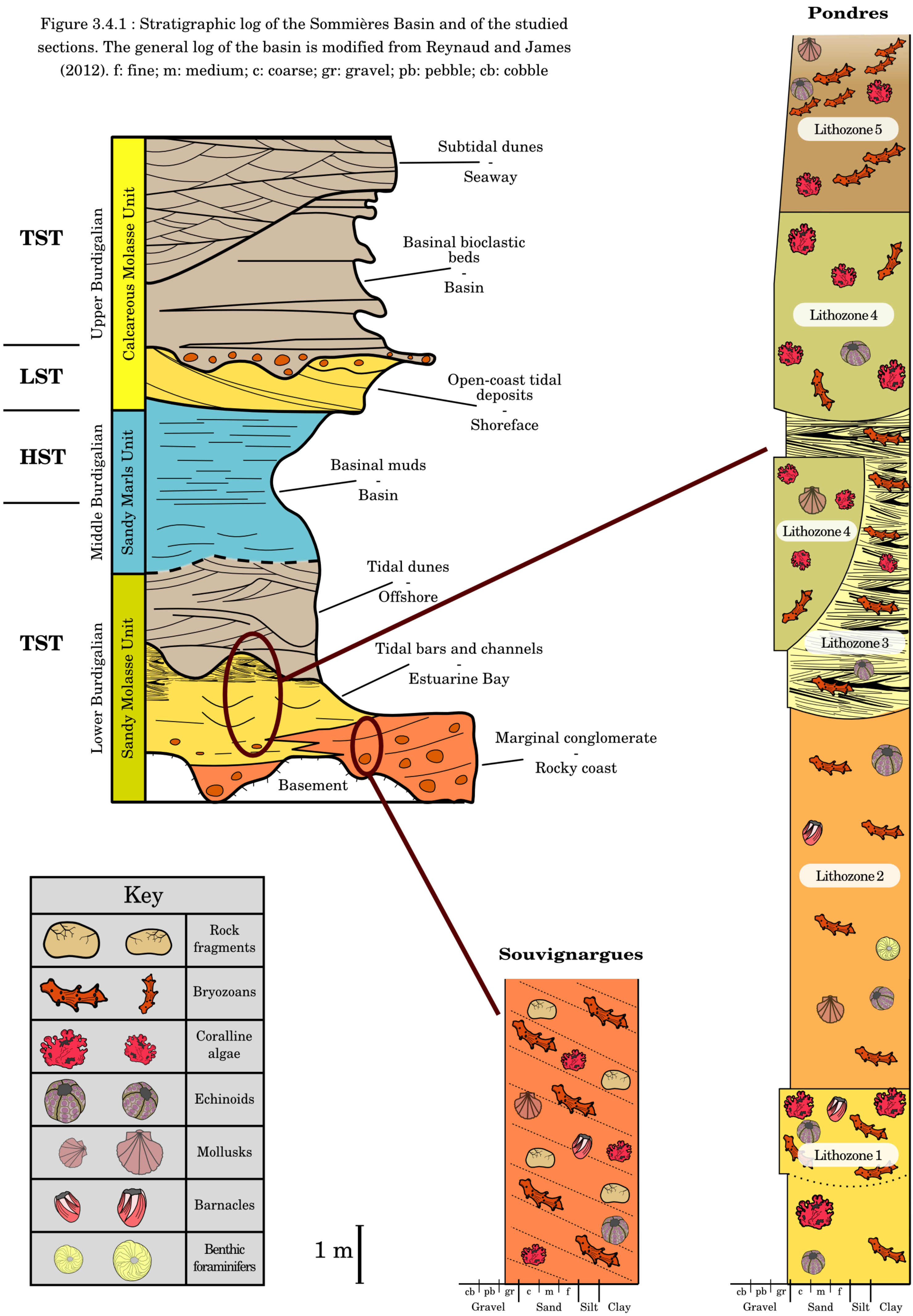

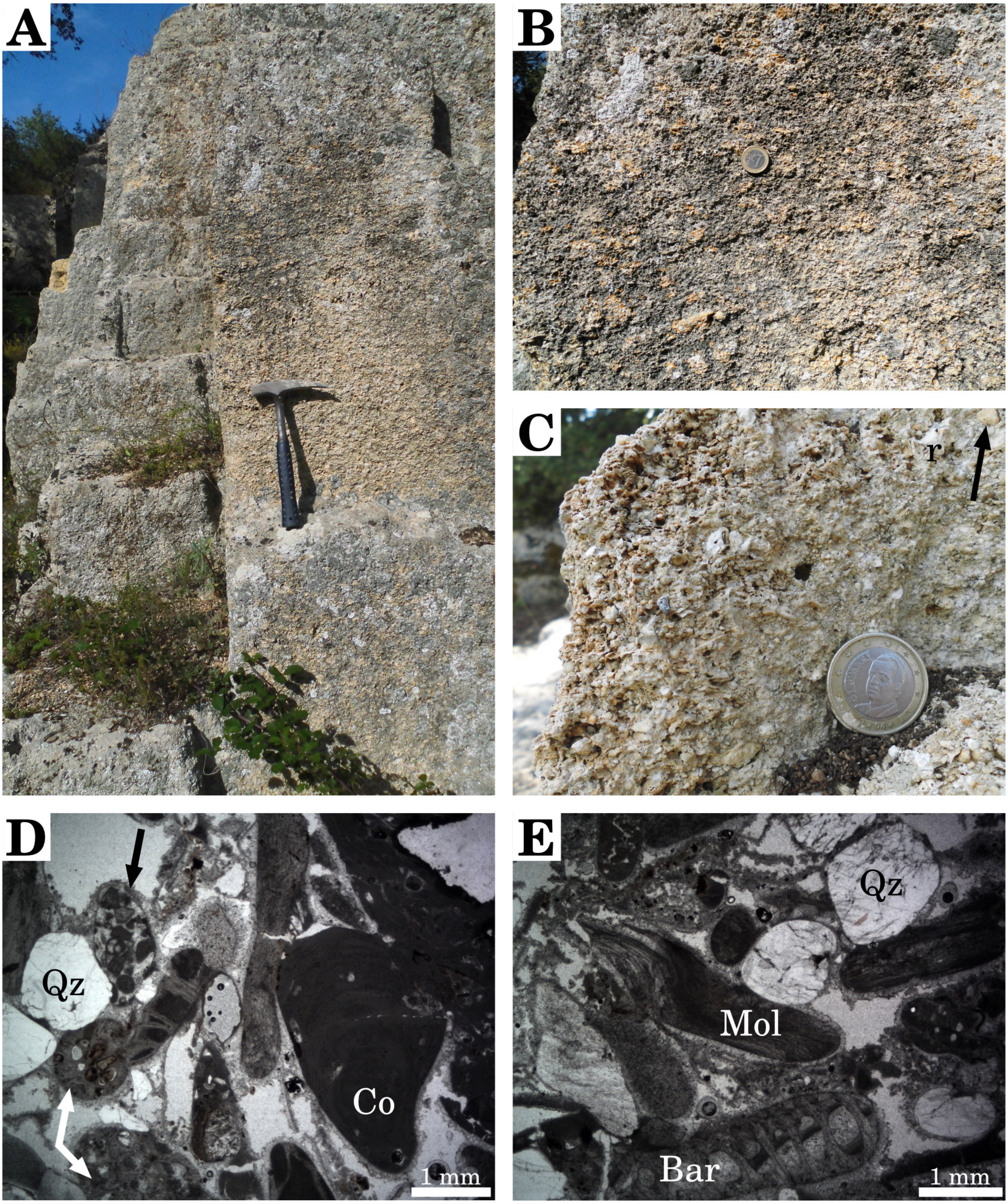

Figure 3.4.2 : Souvignargues outcrop. A) Old quarry of Souvignargues. B) Detail of the lamination. C) Detail of the rock texture; black arrow=rock fragment; r=very small rhodolith. D) Thin section of a sample from Souvignargues; Qz=rounded quartz grain; white arrows=bryozoans; black arrow=limestone rock fragment; Co=coralline algal branch. E) Thin section of a sample from Souvignargues; Qz=rounded quartz grain; Mol=mollusk; Bar=barnacle.

Mollusks, especially oyster fragments, are common while echinoids and barnacles are minor components (Fig. 3.4.2 D-E; Tab. 3.4.1). Benthic foraminifers, both larger and small are extremely rare, the former group is entirely represent by a few rare specimens of *Amphistegina* (Tab. 3.4.1). The siliciclastic fraction is mainly composed of rock fragments, but quartz grains are also very common (Fig. 3.4.2 D-E; Tab. 3.4.1). Authigenic minerals are also present, especially authigenic phosphates.

Coralline algae assemblage. Coralline algae association is dominated by members of the order of the Hapalidiales, while Corallinales and Sporolithales are minor components in most of the samples (Tab. 3.4.2).

Among recognized Hapalidiales the genus *Mesophyllum*, is the most common and is represented by four different species: *Mesophyllum* sp. 1, *Mesophyllum roveretoi*, *Mesophyllum ishijimai* and *Mesophyllum galettoi* (Tab. 3.4.2). Among them *Mesophyllum* sp 1 is most abundant and occurs in most of the samples, *M. roveretoi* covers an overall high percentage of surface but occurs only in one sample. *M. galettoi* and *M. ishijimai* are minor components. The genus *Lithothamnion* is represent by two species, *Lithothamnion ponzonense*, which is the most important species of the whole association, and *Lithothamnion crispatum* which instead occurs just in one sample (Tab. 3.4.2). The only species allocated with certainty in the genus *Phymatolithon* is *Phymatolithon* sp. (sensu Hrabovský et al. 2015), which occur just in one sample. Other two Hapalidiales species, with uncertain generic placement were recognized ? *Lithothamnion* sp.2 (sensu Hrabovský et al. 2015) and *Lithothamnion/Phymatolithon* sp. 1; neither of the two species are very abundant (Tab. 3.4.2).

Taxa of the order Corallinales occur in the majority of samples from Souvignargues. Among identified Corallinales the encrusting species *Lithophyllum* sp. 1 is the most common (Tab. 3.4.2). In some samples very small crusts of *Lithoporella melobesioides* are present and only in one sample *Lithoporella minus* was observed.

The overall area covered by Sporolithales is low but *Sporolithon* sp1, the only recognized species of the order, occurs in approximately 25% of the samples (Tab. 3.4.2).

Pondres

Lithozone description. In the quarry of La Garenne, on the basis of their rock texture, mineralogy and macroscopic fossiliferous content different lithozones were identified, the lithozones are numbered from 1 to 5 from the oldest to the youngest (Fig. 3.4.1).
Lithozone 1 is an impure coarse grainstone with more than 25% of silicate minerals (Tab. 3.4.1). The rock shows locally a thin lamination, but is generally massive. Small, 1m thick and 2-3m wide, channel structures are present in the upper part of the lithozones, the sediments filling the channels are coarser-grained with abundant large skeletal elements.
Most of the elements are sand-sized and only 15% is gravel-sized, mainly bryozoans, either nodular and branched colonies, but also coralline-algal branches (group I and II) (Fig 3.4.3 A-C; Tab 3.4.1). Rare rhodoliths do also occur in Lithozone 1 (Fig 3.4.3 B). They are mostly pebble-sized and elliptical in shape, some of them are box-work rhodoliths and they entrained a remarkable amount of sediment between their crusts. Some large nodules are composed of both coralline-alga crusts and bryozoans.
The point count results from lithozone 1 samples shows that bryozoans are again the most common skeletal elements, coralline algae and echinoids are very abundant, lesser amount of barnacles and mollusks are also present (Fig. 3.4.3 D; Tab 3.4.1). Both larger and smaller benthic foraminifers are rare, among the former *Amphistegina* is the only recognized genus, the latter are mainly represented by *Cibicides* and *Elphidium*. The terrigenous fraction is mainly composed of sand-sized quartz grains with lessere amount of rock fragments. Authigenic glaucony is also present, albeit not abundant (Tab. 3.4.1).

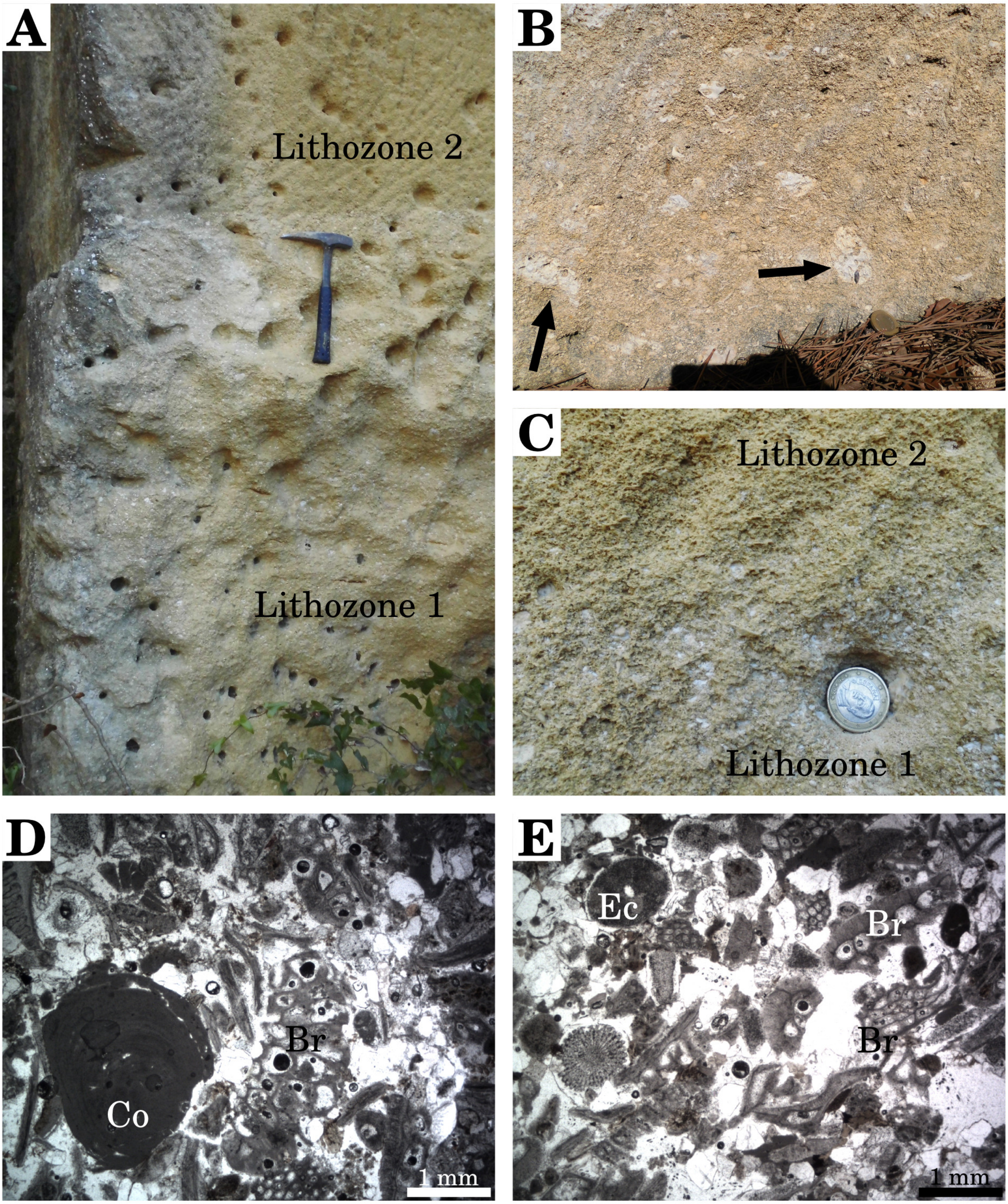

Figure 3.4.3 : The lower part of the outcrop of Pondres in the quarry of La Garenne. A) Lithozone 1 and lithozone 2. B) Rhodoliths in lithozone 1; black arrows=rhodoliths. C) Sharp transition between lithozone 1 and lithozone 2. D) Coralline-rich lithozone 1; Co=coralline alga; Br=bryozoans. E) Coralline-poor lithozone 2; Ec=echinoids; Br=bryozoans.

Lithozone 2 is an impure bioclastic-grainstone with silicate minerals composing over 30% of the rock (Tab. 3.4.1). The rock is massive, the grains are well sorted, present a common orientation and their overwhelming majority is sand-sized (Fig. 3.4.3 E; Tab. 3.4.1).

Bryozoans dominate the skeletal assemblage, echinoids are abundant and coralline algae are present in lower proportion relatively to lithozone 1 (Fig. 3.4.3 E; Tab. 3.4.1). Mollusks and barnacles are also present. Benthic foraminifers are more common than in Lithozone 1. Larger benthic foraminifers are rare and represented by specimen of *Amphistegina*. *Cibicides*, *Elphidium* and various agglutinated forms are common among the smaller benthic foraminifers. Rare brachiopods also occur in this Lithozone. The siliciclastic fraction is mainly composed of sand-sized quartz grains and rare rock fragments. Authigenic minerals also occur.

Lithozone 2 upper boundary is an erosive surface and the overlying Lithozone 3 is characterized by a pervasive herringbone cross-stratification with mud drapes (Fig. 3.4.4 A-C). The rock is an impure grainstone with a small amount of silicate minerals. Gravel-sized elements are rare, albeit some coralline-algal branches occur (Tab. 3.4.1).

There is a higher proportion of bryozoans compared to the underlying lithozone 2, echinoids and coralline algae are common while mollusks are not (Fig. 3.4.4 D; Tab. 3.4.1). Barnacles, benthic foraminifers and brachiopods are rare. Larger benthic foraminifers are absent in this lithozone, smaller benthic foraminifers are mainly represented by *Cibicides*, *Elphidium* and agglutinated forms. The siliciclastic fraction is composed by small sand-sized quartz grains, rock fragments are present in lesser amount relatively to the previous lithozones (Tab. 3.4.1). Authigenic minerals occur also in this lithozone.

Lithozone 3 is cut by small and large channel. These channels are massive and they are filled by coarser-grained elements relatively to the surrounding lithozone 3. The fillings of these channels as been defined as lithozone 4 (Fig. 3.4.4 A, C). Lithozone 4 channels

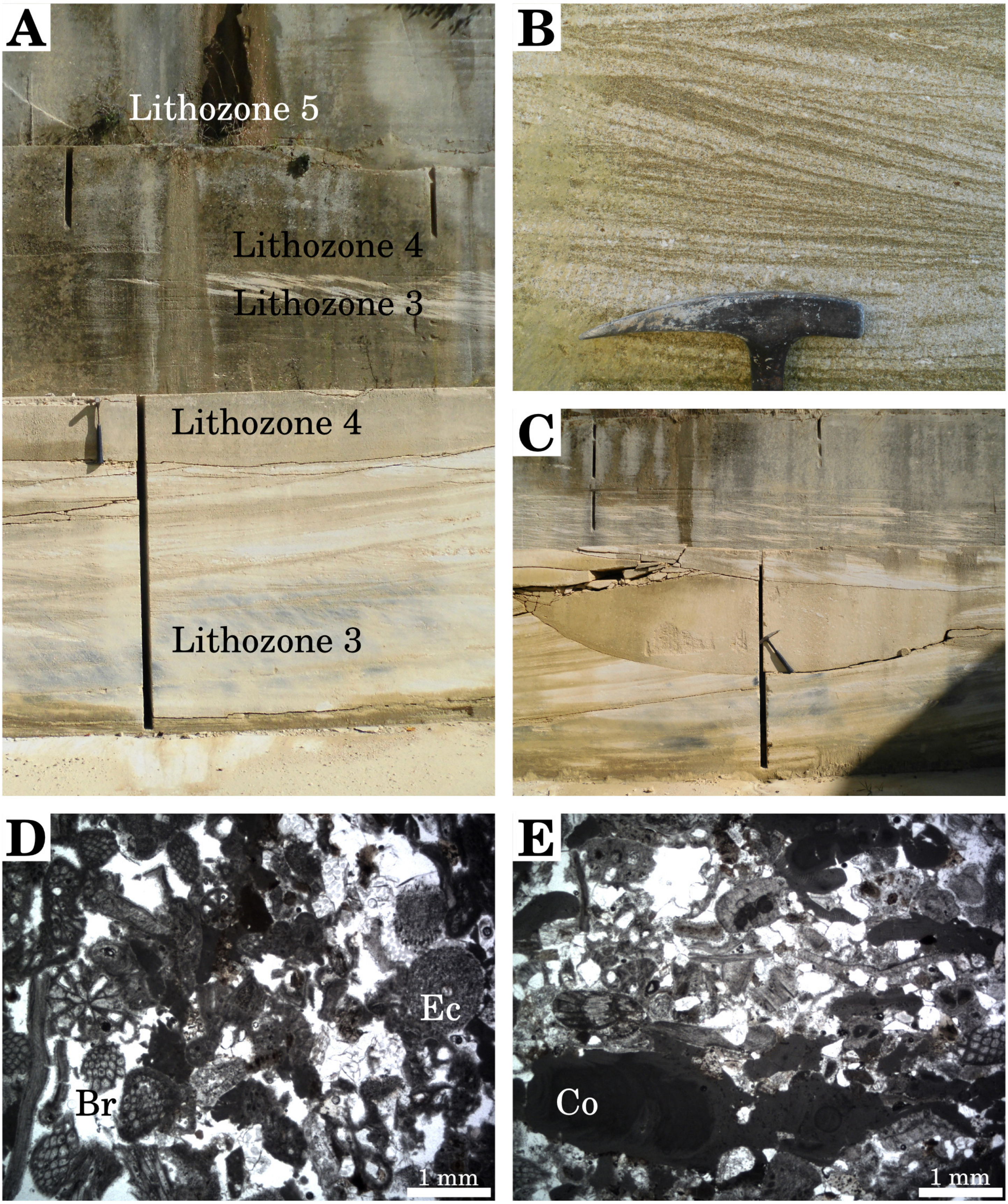

Figure 3.4.4 : The upper part of the outcrop of Pondres in the quarry of La Garenne. A) Lithozone 4 channels cutting through lithozone 3; in the upper part lithozone 5 is visible. B) Herringbone cross-stratification in lithozone 3. C) Lithozone 4 channel within lithozone 3. D) Bryozoans-rich lithozone 3; Br=a group of small bryozoan colonies; Ec=echinoids. E) Coralline-rich lithozone 4; Co=coralline alga.

are scattered and discontinuous at the base of lithozone 3 but became a continuous layer toward the top (Fig. 3.4.4 A). The rock is a coarse impure grainstone with 15% of silicate minerals (Tab. 3.4.1). The majority of the elements are sand-sized but nearly 20% are gravel-sized, mainly coralline algae branches (group I and II) but also bryozoan colonies and some rare barnacle plates (Tab. 3.4.1). Rare rhodoliths also occurs in this lithozone, generally pebble-sized and elliptical in shape.

In this lithozone, according to point counting analyses, the skeletal association is dominate by coralline algae, bryozoans are also very common but they are present in lesser amount compared to the previous lithozones (Fig 3.4.4 E; Tab. 3.4.1). Echinoids and mollusks are common while barnacle are are, albeit they are more abundant that in the surrounding lithozone 3. Benthic foraminifers are are rare, they are mainly represent by *Cibicides* and *Elphidium*, some agglutinated taxa are also present; only one specimen of *Amphistegina* was observed in this lithozone. The siliciclastic fraction is mostly composed of sand-sized quartz grains but some rock fragment also occur; authigenic minerals are present (Tab. 3.4.1).

Still upward coralline algae become less common while bryozoans increase in abundance and bryozoan macroids become very common. This lithozone, lithozone 5, is an impure grainstone with more than 20% of silicate minerals (Tab. 3.4.1). The base of the lithozone is massive, but moving upward a faint planar lamination appears (Fig. 3.4.4 A). Most of the elements are sand sized, gravel-sized elements are mainly bryozoans colonies and extremely rare, very-small rhodoliths and coralline-algal branches.

Skeletal assemblage is dominated by bryozoans, but coralline algae are very common (Fig. 3.4.5 B; Tab. 3.4.1). Mollusks and echinoids are common, while barnacle are rare and in lesser amount relatively to the previous lithozone. Some very rare brachiopods were also observed in this lithozone. Benthic foraminifers are rare, the most common species belong to genera *Elphidium* and *Cibicides* but agglutinated forms are also present. Also within this lithozone no larger benthic foraminifer was observed.

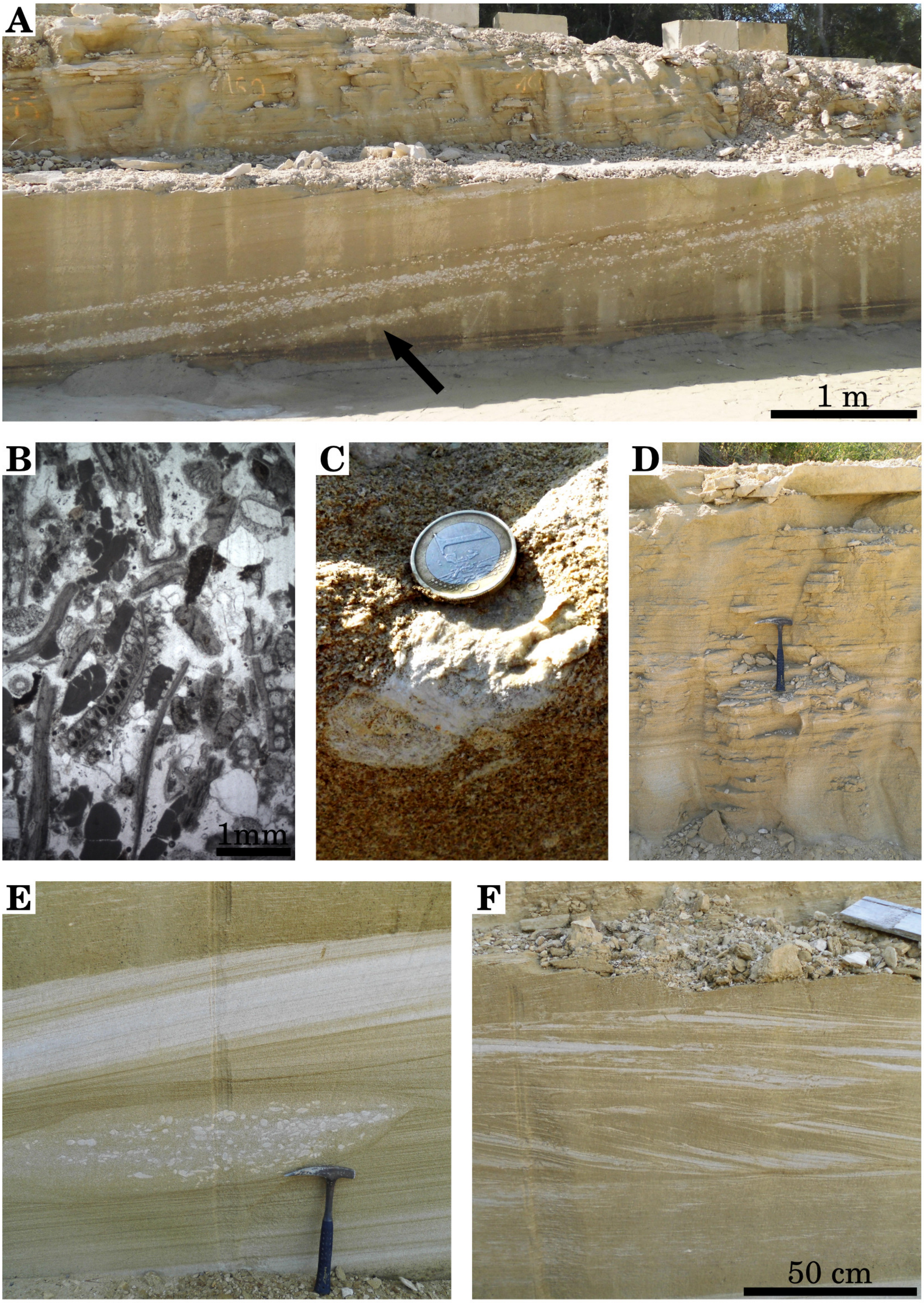

Figure 3.4.5 : The uppermost part of the Pondres outcrop in the quarry of La Garenne. A) Layers with abundant bryozoans macroids; black arrow=layers with bryozoans macroids. B) thin section of a sample of the uppermost part of lithozone 5. C) Detail of a bryozoan macroid. D) Clear parallel lamination in fine-grained sediments, further upward than the layers with macroids. E) Further upward large bryozoan macroids are once again present. F) Locally also cross lamination is once again present.

The siliciclastic fraction is almost entirely composed of sand-sized quartz grains, rock fragment are less abundant that in other lithozones; authigenic minerals are present (Tab. 3.4.1).

Still upward the rock is clearly parallel laminated with decimeter thick layers rich in large bryozoans macroids (Fig 3.4.5 A, C). Moving upward the mud content increase and large skeletal elements are absent, but the overlying layers are again characterized by the presence of bryozoans macroids and herringbone cross-stratification (Fig 3.4.5 D-F). This upper intervals of the succession of Pondres were not studied in detail in this work since they lack almost entirely coralline algae.

Coralline algae assemblage. Hapalidiales dominate coralline algae assemblage in lithozone 1 (Tab. 3.4.2). Corallinales are minor components but they are present in almost every sample. Among recognizable Hapalidiales the genus *Mesophyllum* is the most common and it is almost entirely represented by *M. roveretoi*, the most abundant and common species of the association (Tab. 3.4.2). *L. ponzonense* is another common Hapalidiales and is the only representative of its genus. *Phymatolithon calcareum* is rare and is the only representative of genus *Phymatolithon*. Corallinales are represented by five different species, three species included in the genus *Spongites*, *L. melobesioides* and *Lithophyllum* sp. 1 (Tab. 3.4.2).

In lithozone 2 coralline algae are not common especially rhodoliths and large branches. The small fragments present always lack the taxonomic elements essential for their classification and therefore their identification was impossible.

Lithozone 3 coralline association is dominated by Hapalidiales, Corallinales are very rare and represented only by small crusts of *Lithophyllum* sp. 1 (Tab. 3.4.2). Hapalidiales are mainly represented by the genus *Phymatolithon,* with two different species: *Phymatholithon* sp., which is the most common species of the association and *Phymatholithon* sp. 1 (Tab. 3.4.2).

Genus *Mesophyllum* is entirely represented by *M. roveretoi* and genus *Lithothamnion* is absent.

In lithozone 4 Hapalidiales still dominate the association but Corallinales are more abundant (Tab. 3.4.2). Among the latter *Spongites* fruticulosus is the most common, *Lithophyllum* sp. 1 increases in importance relatively to the previous lithozone. *L. melobesioides* and *L. minus* are also present (Tab. 3.4.2). Among Hapalidiales *Mesophyllum* and *Lithothamnion* have similar importance, but the former is more abundant. In this lithozone the only recognized species of the genus *Mesophyllum* is *M. roveretoi* that is also once again the dominant species of the association (Tab. 3.4.2). *Lithothamnion* is mainly represented by two species of equal importance *L. ponzonense* and ?*Lithothamnion* sp.2 . *Phymatholithon* is present in lower proportion and is represent by the species *Phymatholithon* sp. (common) and *P. calcareum* (rare).

Coralline association of lithozone 5 is entirely composed by Hapalidiales, among them *Phymatolithon* is most important genus (Tab. 3.4.2). The encrusting-foliose species *Phymatolithon* sp. 1 dominate the association together with an other species of uncertain generic placement *Lithothamnion/Phymatolithon* sp. 2; *Phymatolithon* sp. is also abundant (Tab. 3.4.2). Genus *Mesophyllum* is uncommon and its only representative in this lithozone is *M. roveretoi* (Tab. 3.4.2).

3.5 – Discussion

General interpretation

Heterozoan skeletal assemblages dominate the basin, bryozoans and coralline algae are the main carbonate producers in the studied successions while barnacles dominate on the other side of the basin (near the village of Boisseron; Fig. 3.2.1; Reynaud and James, 2012). These assemblages are typical of temperate latitudes in present-day oceans but many of the recognized species suggest warmer waters. Among benthic foraminifers the presence of *Amphistegina* suggests average annual temperatures around 20 °C (Geel, 2000; Langer and Hottinger, 2000; Beavington-Penney and Racey, 2004). Among coralline algae *Sporolithon* and *Lithoporella* are both genera of remarkable tropical affinity (Adey, 1979; Fravega et al. 1989; Vannucci et al. 1996; Braga and Aguirre, 2001). North-western Europe during the Early Miocene, was characterized by a warm-tropical climate (Adams et al. 1990; Mosbrugger et al. 2005; Billups et al. 2010), therefore a warm water setting is coherent with the general paleoclimatic reconstruction of the region. High nutrient supply to the basin could have caused the more temperate style of the assemblage. Abundance of nutrients may actually cause a decrease in water clarity and drive out taxa related to tropical and oligotrophic reef environment, thus “cooling” the “look” of the assemblage (Hallock and Schlager 1986; Vannucci et al. 2003; Hallock 2005; Halfar et al. 2006; Coletti et al. 2013). The presence of abundant trophic resources in the seawater of Sommières Basin during the Early Burdigalian is proved by the widespread presence of authigenic phosphate and by the high biomass of suspension-feeders (barnacles and bryozoans) in the Sandy Molasse Unit (Reynaud and James, 2012). Therefore taking into account both the nutrient "cooling" effect and the rarity of tropical species, a sub-tropical climate for the Sommières Basin during the Early Burdigalian is suggested.

The depositional environments of Souvignargues and Pondres successions were different. Souvignargues area during the Early Burdigalian was very close to the rocky coastline as testified by the common rounded pebbles and rock fragments issued from the erosion of basement of the basin (Tab. 3.4.1). Rock texture and fabric suggest an high-energy environment close to the shore (Tab. 3.4.1; Fig. 3.4.2). Moving further toward the shore (toward the village of Souvignargues) the impure rudstone of the studied outcrop grade in to conglomerates deposited in high-energy conditions as pocket beaches or spits against the rocky shoreline of the basin (Reynaud and James, 2012). Therefore a very shallow sub-tidal environment is assumed for the Souvignargues succession.

Pondres succession, as suggest by the lower abundance of rock fragments and the general texture of the rock (Tab. 3.4.1), deposited further away from the coast, in a tidal estuary with large tidal bars cut by tidal channels (Reynaud and James, 2012).

The channel structures in lithozone 1 represent ephemeral channels, along which skeletal grains were drifted off-shore. These bioclastic elements originated in slightly shallower water, as testified by coralline algae which are more common in the fillings than in the surroundings. Lithozone 4 deposited within larger and more important channels. The skeletal assemblage characterized by coarser-grained fragments, more abundant coralline algae and barnacles, and the more frequent rock fragments than in the surrounding lithozone 3, testifies that also lithozone 4 elements formed in a proximal environment and were later transported into deeper-waters (Tab. 3.4.1). The pervasive herringbone cross-stratification of lithozone 3 was instead generated by the migration of smaller bedforms created by tidal currents, over the larger tidal-bars.

Pondres succession records a transgressive trend from lithozone 1 to 5. This is suggested by the decrease of the detrital fraction, especially rock fragments, the decrease of barnacles and larger benthic foraminifers and the replacement of rhodoliths by bryozoans macroids (Tab. 3.4.1). This deepening upward is in accordance with the general interpretation of the basin which reconstruct the Sandy Molasse Unit as the transgressive system tract of a depositional sequence (Reynaud and James, 2012). Therefore Pondres lithozone 1 deposited in a shallow-water tidal setting, but at greater depth than Souvignargues rudstone; lithozones 2, 3 and 5 deposited further deeper, but still within the photic zone. Lithozone 4 skeletal assemblages formed in shallow water, like lithozone 1, but was later transported into deeper conditions.

Coralline algae distribution

Coralline-algae distribution in the studied succession is closely related to the paleobathymetric setting. In present-day oceans Corallinales are generally dominant in shallow water settings, while Hapalidiales characterize deeper waters, the very same trend has been recognized throughout the Neogene (Adey and Macintyre, 1973; Adey, 1979; Adey et al. 1982; Minnery et al. 1985; Adey, 1986; Perrin et al. 1995; Lund et al. 2000; Braga and Aguirre, 2001; Braga et al. 2009). Accordingly Corallinales abundance peaks in Souvignargues samples and decreases in the Pondres succession following the deepening-upward trend (Tab. 3.4.2). It should be pointed out that even though both Pondres and Souvignargues succession both deposited in a relatively shallow-water setting, Hapalidiales always dominate coralline-algal assemblages (Tab. 3.4.2). This is a consequence of the high nutrient supply-rate. Increased plankton biomass, caused by nutrients, increases the amount of particulate organic carbon in the ecosystem which in turn reduces water transparency and light availability to the benthic community, therefore moving shoreward the whole benthic zonation (Hallock and Schlager, 1986; Vannucci et al. 2003; Hallock, 2005).

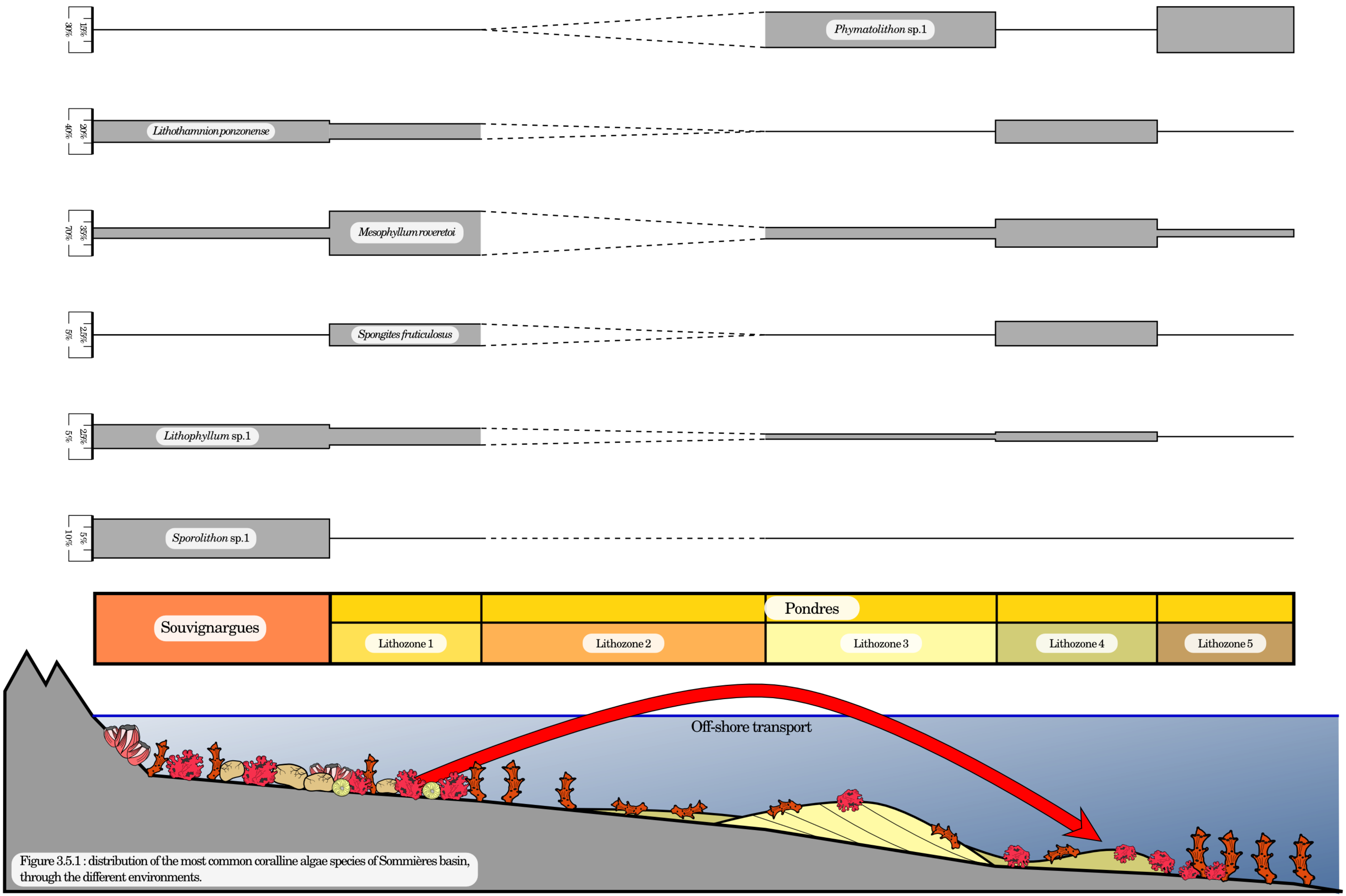

Figure 3.5.1 : distribution of the most common coralline algae species of Sommières basin, through the different environments.

Coralline-algal species distribution is also heavily influenced by water depth and among the species identified in the flora of the Sommières Basin, many of them seem to be tightly related to the availability of light at the sea-floor.

Lithophyllum sp.1 is an encrusting species characterized by very thin thalli with a growth morphology that closely resemble that of the modern *Titanoderma pustulatum*. It commonly occurs in samples close to the paleo-shoreline of the basin and become more rare moving toward deeper waters (Fig. 3.5.1). *Lithophyllum* is typically a shallow-water genus which require strong light to thrive (Adey and Macintyre, 1973; Adey, 1979; Adey et al. 1982; Minnery et al. 1985; Adey, 1986; Perrin et al. 1995; Braga and Aguirre, 2001; Braga et al. 2009). Morphologies with thin adherent crusts and raised conceptacles, are common in fast developing coralline algae which dominate habitats with intense physical disturbance, like the shore-line (Steneck, 1986). Therefore is likely that *Lithophyllum* sp.1 can actually be used in the context of the Sommières Basin and elsewhere as a proxy of shoreline proximity.

Like *Lithophyllum* sp. 1 also *Spongites fruticulosus* is more common in shallow-water samples (Fig. 3.5.1). This species commonly occur in shallow-water assemblages and is frequent in the coralline algae assemblages of the Mediterranean area since the Oligocene (Vannucci et al. 1996; Braga et al. 2001; Braga et al. 2009).

In the context of Sommières Basin also *Sporolithon* sp. 1 shows a remarkable preference toward shallow-water conditions (Fig. 3.5.1). While the Corallinales are typically shallow-water dwellers, most of the modern species of the order Sporolithales are more common in to deep-water assemblages (Adey and Macintyre, 1973; Adey, 1979; Adey et al. 1982; Adey, 1986; Perrin et al. 1995; Lund et al. 2000; Braga and Aguirre, 2001). However some species of *Sporolithon* prefer instead shallow waters (Minnery et al. 1985; Adey, 1986; Perrin et al. 1995), this situation is frequently observed in climatic condition at the boundary between temperate and tropical realm (Basso et al. 2009; Neill et al. 2015). Since light limitation is a primary ecological factor in coralline, they can be used to reconstruct the water depth of the paleo-environment, but coralline fragments may be transported and whenever a substrate heterogeneity is present low-light algae may occur close to high-light algae (Adey, 1986). Taking this into account, although shore-ward transport sometimes occurs (Johnson et al. 2011), the lack of *Sporolithon* into Pondres samples rule out the possibility that the specimens were transported in to Souvignargues are from somewhere else. Whether *Sporolithon* sp. 1 is a cryptic species inhabiting a shallow-water environment or is a coralline algae which thrive in well-lit superficial waters cannot be distinguished, but in the context of the Sommières basin the species can be used as a proxy of near-shore conditions.

Mid-depth and deeper-water conditions in the basin are dominated by Hapalidiales (Tab. 3.4.2). Among them *Mesophyllum roveretoi* is the most common species, its abundance peaks at middle-depth (Lithozone 1 of Pondres; Fig. 3.5.1) and this kind of depth-distribution is frequent within the genus *Mesophyllum* (Minnery et al. 1985; Adey, 1986). *Lithothamnion ponzonense* shows a slight preference toward deeper waters but thrive also in shallow-water (Fig 3.5.1), suggesting a rather large tolerance to various light conditions.

Phymatolithon sp. 1 is a readily recognizable species, it is characterized by very thin leafy crusts and produces rhodoliths, with a loose laminar arrangement. In the Sommières basin is remarkably restricted to deep water conditions (Fig. 3.5.1). *Phymatholithon* sp. 1 is also known from the Tertiary Piedmont Basin Pietra da Cantoni Limestone (as *Lithothamnion crispithallus*), where its abundance peaks just before the drowning of the carbonate ramp (Vannucci et al. 1996). *Phymatholithon* sp. 1 morphology is potentially well adapted to a life under low-light conditions, actually in present-day oceans coralline living near the algal extinction depth, have similar morphology to maximize their area/volume ratio and consequently capture more light (Steneck, 1986; Lund et al. 2000). Therefore it might be possible to use this species in Miocene carbonates, as a proxy of deep-waters, near the lower limit of the photic zone.

3.6 - Conclusions

During the lower Miocene the area of the Rhone River mouth (Southeastern France) hosted the junction of the Alpine Molasse Basin with the Western Mediterranean. In that area was located the Sommières Basin, a tide-controlled Burdigalian embayment connected to the Molasse sea through a narrow seaway. Along its coastline an heterozoan carbonate factory, dominated by bryozoans, barnacles, coralline algae and echinoids, flourished, notwithstanding the warm climate, thanks to high level of nutrient availability. Within this basin the impure rudstone of Souvignargues's succession deposited in an high-energy environment nearby the shoreline. They are composed of bryozoans, coralline algae and an abundant detrital fraction of rounded pebbles and sand-sized quarz grains. The coarse-grained grainstones of Pondres succession deposited further away from the coast in a tidal estuary dominated by the interplay of tidal bars and tidal channels. This succession records, in its different lithozones, a deepening-upward trend coherent with the general transgressive trend of the lower Burdigalian unit. The skeletal assemblage is dominated by bryozoans, coralline algae and echinoids. Coralline algae and in particular rhodoliths are more common in the shallow-water part of the Pondres succession while bryozoan macroids become more important in the deeper-water part.

Coralline-algal associations were quantitatively studied along this well constrained bathimetric gradient. Hapalidiales largely dominate the coralline-algal flora of the basin, but they are significantly more abundant in deeper waters. Corallinales conversely are remarkably more common in shallow water environment (albeit they are always less abundant than Hapalidales).

The very same distribution is commonly observed in modern oceans.

Among the most common identified species many taxa shows a distribution remarkably related to water depth. *Mesophyllum roveretoi* is the most common species in the basin and its abundance peaks at middle depth. *Lithothamnion ponzonense* is frequent and abundant in most of the sample and show a slight preference toward deeper waters. The easy recognizable leafy crusts of *Phymatholithon* sp.1 dominate in deep-water rhodoliths. Among Corallinales the encrusting species *Lithophyllum* sp. 1 is preferentially distributed in shallow waters near the shore-line. Also *Spongites fruticulosus* is more common in shallow-water environment.

While these species follow a pattern similar to those of their modern relatives, the distribution of *Sporolithon* sp. 1 is more peculiar. Actually in the Sommières Basin this species is restricted into shallow waters while in modern oceans *Sporolithon* more commonly dwells into low-light, deep-water environment. Nonetheless shallow-water species of *Sporolithon* also occur, especially at the transition between the tropics and the temperate realm (eg. Northern New Zealand), a climatic situation probably very close to that of lower Burdigalian Sommières Basin.

These results prove that quantitative analyses of coralline algae distribution, within a well constrained paleoenivronmental framework, are useful to detect and understand coralline autoecological preferences. Further studies performed with the same approach will make it possible to strengthen these findings and establish new coralline-based paleoecological proxies. The distribution of the three order of crustose coralline algae is an important source of information on the paleoenvironment but a more accurate reconstruction can be achieved through species-level identification.

4 – Nutrients Influence

Nutrients influence on Miocene carbonate factories

Giovanni Coletti

(Article in preparation)

4.1 – Introduction

Nutrient availability is an important control in the distribution of carbonate forming biota in modern oceans (Hallock and Schalger, 1986; Hallock, 1988a; Hallock, 2005; Carannante et al. 1988; Wood, 1993; Holmes et al. 1997; Brasier, 1995a; Brasier, 1995b; Halfar et al. 2004; Wilson and Vecsei, 2005; Jessen et al. 2014). High nutrient supply increases plankton biomass and provide more organic matter to heterotrophs, moreover the abundance of plankton and of organic matter suspended in the water column reduces water clarity and further influences benthic communities (Chapter 1). The most visible result of nutrient influence on carbonate factories is a shift from autotrophs-dominated, light-dependent association toward a heterotrophs-dominated, light-independent association. Therefore nutrients influence has been often used to justify the presence of Heterozoan carbonates (sensu James, 1997), which commonly occur in cool climates, in an otherwise warm-water context (e.g. Carannante et al 1988; Brandano and Corda, 2002; Cunningham and Collins, 2002; Vannucci et al. 2003; Reynaud and James, 2012; Coletti et al. 2015; Brandano et al. 2016). However, nutrients influence, in the vast majority of paleoenvironmental reconstructions, is just assumed on the basis of fossil assemblages, without direct measurement of the concentrations of phosphorous, the ultimate limiting nutrient, whose rate of supply regulates primary production over long timescales (Tyrrel, 1999). Most of techniques actually can measure only proxies related to phosphorous abundance or the total amount of phosphorous present in the rock. The latter is not a direct expression of biologically-available phosphorous since it considers also unaltered grains of detrital apatite of igneous and metamorphic origins, which are not a viable source of phosphate. Therefore classical geological techniques (e.g. X-ray fluorescence) are not suitable to study nutrients abundance in the fossil record. The aim of this contribution is to use SEDEX sequential extraction, a methodology devised to separate and measure biologically-available phosphorous from the total mass of phosphorus, for a paleonvironmental reconstruction of two lower Miocene carbonate successions: the Pietra da Cantoni Group of Tertiary Piedmont Basin and the Sandy Molasse Unit of the Sommières Basin (details of the geological setting are present in Chapter 2 and Chapter 3). The skeletal assemblages of these two sequences are dominated by coralline algae, bryozoans and barnacles, but developed in climatic conditions that should have supported a more classical warm-water association (Chapter 2; Chapter 3). In this study SEDEX phosphorous extraction is combined with detailed paleontological analyses of the skeletal assemblages and of coralline algae flora to provide direct evidences of nutrient influence on Miocene carbonate factories.

4.2 – Material and Methods

The sequence of Uviglie was selected as representative of the Pietra da Cantoni group and the sequences of Souvignargues and of Pondres were selected as representative for the Sandy Molasse Unit of the Sommières Basin (Chapter 2; Chapter 3, for details on the geological setting of the two basins). Very large and representative samples were taken from each lithozone in the selected outcrops (Chapter 2; Chapter 3, for the summary of the various lithozones and their characteristics). The samples were taken after the removal of the superficial part of the rock that might have been altered by weathering. Using the same procedure a sample was picked from the outcrop of Boisseron (Sandy Molasse Unit, Fig. 3.2.1), which was located on the opposite shore (relative to Souvignargues and Pondres) of the Sommières Basin, to further study nutrient dynamics within the basin. Serving as internal reference of low phosphorous concentration, a sample of coral-reef limestone of Miocene age (Balza di Rocca Limata, Terravecchia Formation, Sicily, Grasso and Pedley, 1988) was also included in the analyses.
Rock samples were grounded in an agate mortar to <125 µm and a dry weight of 0.08 g from each sample was used in the sequential extraction. The remaining of the grounded samples was used for quantitative x-ray powder diffraction, total organic carbon analysis, CHN analysis and a portion was stored as archive. The extraction was performed according to Ruttenberg et al. 2009, which proposed an improved version of the original SEDEX sequential extraction (Ruttenberg, 1992) aimed to reduce procedural flaws (excessive sample manipulation and loss of material; Fig. 4.2.1; Fig. 4.2.2). The extraction, through a series of chemical reactions, dissolves all P-bearing minerals and allows for an accurate quantification of P separated in its different sedimentary

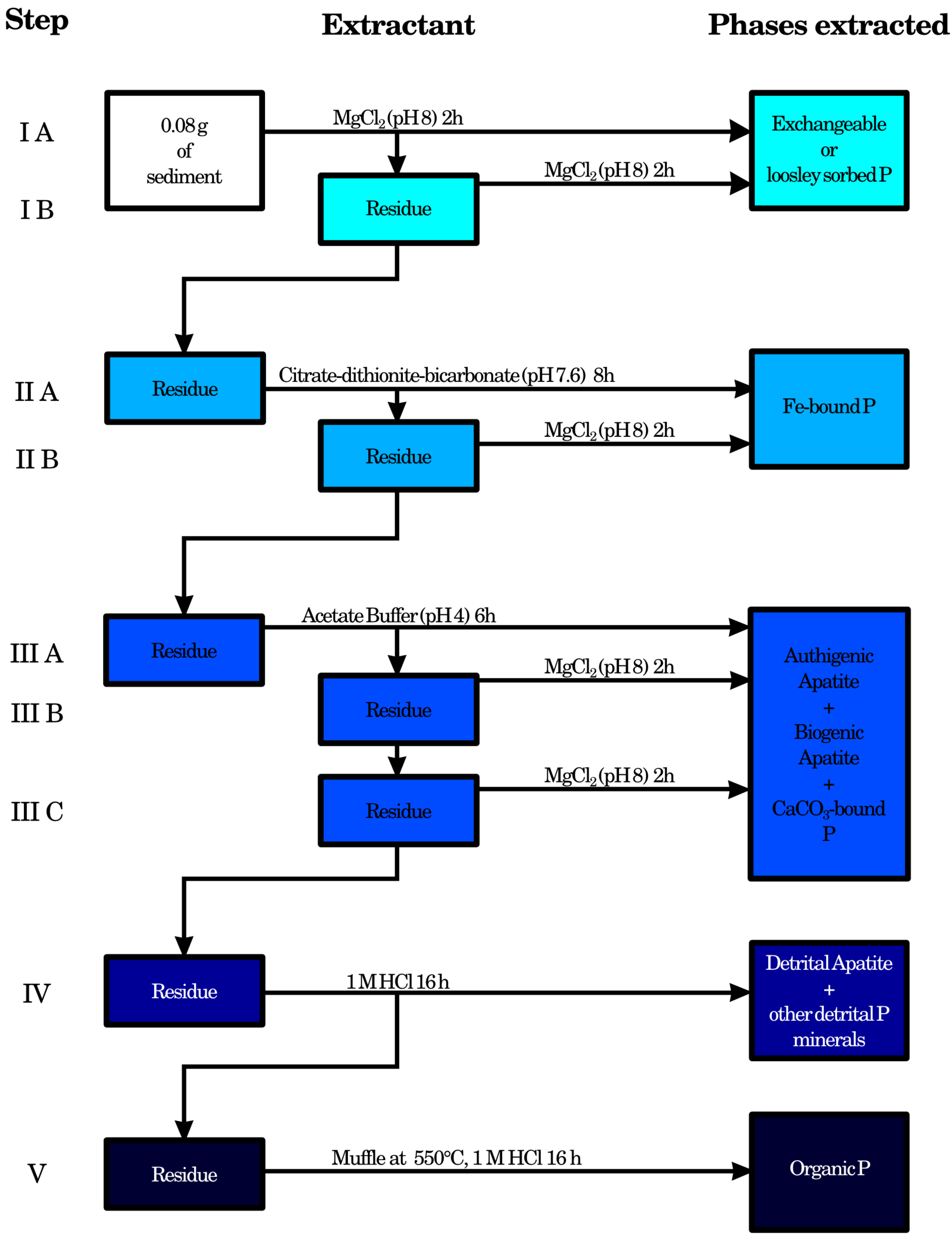

Figure 4.2.2 : improved SEDEX extraction line; modified after Ruttenber et al. 2009

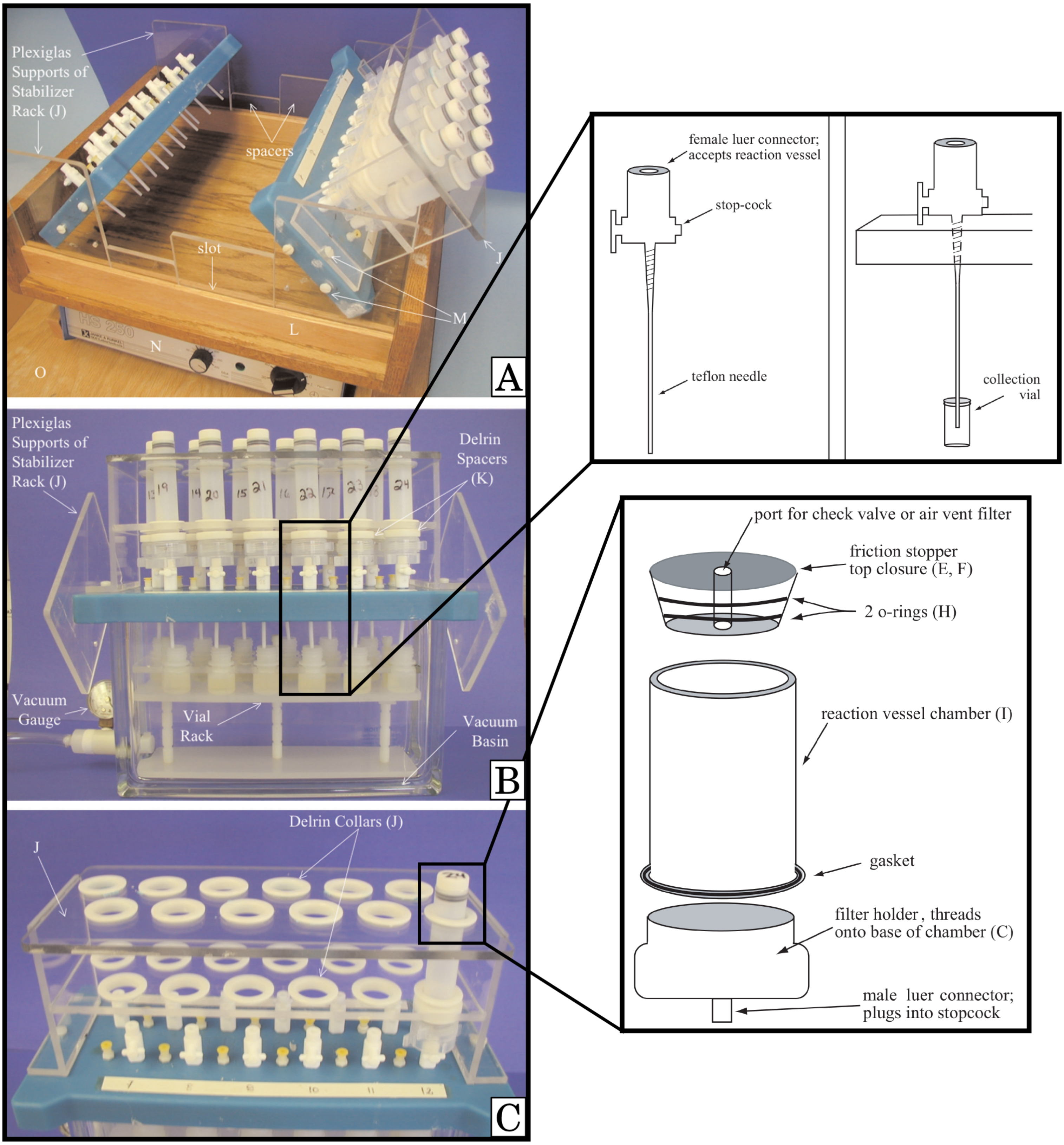

Figure 4.2.2 : SEDEX reaction vessels, from Ruttenber et al. 2009.
A) Two sample holders for SEDEX extraction, the one on the right is fully loaded with the teflon reaction vessel while the other one is void; both sample holders are mounted on the shaker table for the reaction step.
B) Sample holder fully loaded and seated on the vacuum chamber for supernatant collection; on the right panel the details of the structure of the stopcocks of the reaction vessels.
C) The structure of the sample holder, only in the right-lower bottom of the sample holder a single reaction vessel is mounted; on the right panel details of the structure of the reaction vessel.

reservoirs (Fig. 4.2.1). These are exchangeable (or loosely-bound) P, Fe-oxyhydroxides-bound P, authigenic and biogenic Ca-P minerals, organic P and detrital apatite (Ruttenberg, 2004). All these reservoirs, except detrital apatite, are sinks for the reactive P present in the water (Ruttenberg, 1992); therefore, the sum of their contribution to the total phosphorous pool, in this study, has been used as a proxy for nutrients availability in the paleoenvironment.

Petrographic characteristics and skeletal assemblages of the limestones were studied with point-counting technique performed on digital photomicrographs of thin sections (Flügel, 2009). To further study authigenic minerals, scanning electron microscope observations (SEM) and energy-dispersive X-ray spectroscopy (EDS) analyses were performed on carbon-coated thin sections.

Coralline distribution was studied by direct measurement, with a vector graphics editor, of the area covered by the different taxa of coralline-algae in the thin sections. Coralline algae identification follows Woelkerling (1988), adapted for paleontological use by Braga et al. (1993) and modified by Harvey et al. (2003), Kato et al. (2011), Bittner et al. (2011) and Nelson et al. (2015) (further details on the point-count technique and taxa identification are present in Chapter 2.3 and Chapter 3.3).

4.3 – Results

Skeletal assemblages

Pietra da Cantoni Group. In lithozones UV1 to UV4 skeletal fragments derives from a benthic carbonate factory while in lithozones UV5 and UV6 the main carbonate producers are planktonic foraminifers (Fig. 4.3.1; Tab. 4.3.1). The transition from benthic carbonate production to the planktonic carbonate factory occurs at the top of lithozone UV4 (sub-zone UV4b; Tab. 4.3.1). The benthic production system is dominated by coralline algae, benthic foraminifers and barnacles. Mollusks, echinoids and bryozoans are minor components; ostracods and serpulids are rare (Tab. 4.3.1). Coralline algae are especially abundant in lithozone UV1 and UV2 (>>50% of the skeletal grains). Coralline still dominate in lithozone UV3 and UV4 but they are less common (Tab. 4.3.1). Coralline nodules (rhodoliths; Fig. 4.3.1B) are also very common in all the lithozones, further emphasizing the importance of coralline as carbonate producers in the Pietra da Cantoni Group.

Benthic foraminifers are a major component of the skeletal assemblages of lithozones UV1, UV2 and UV4, while in lithozone UV3 they are less abundant (Tab. 4.3.1). Lithozones UV1 and UV2 are dominated by larger benthic foraminifers of the genera *Nephrolepidina*, *Eulepidina*, *Miogypsina, Sphaerogypsina, Amphistegina* and *Operculina* (Fig. 4.3.1D). In lithozones UV3 and UV4 smaller benthic foraminifers (*Elphidium*, *Lobatula*, *Rosalina*, *Eponides*, *Stomatorbina* and *Neoconorbina*) are more common; the larger forms, albeit rarer, are still present (further details of benthic foraminifers distribution are presented in Chapter 2.4).

Skeletal assemblage	Lithozones [Point counting]												
	UV1	UV2	UV3	UV4a	UV4b	UV5	UV6	PON1	PON2	PON3	PON4	PON5	SOUV1
Coralline algae	74%	75.1%	47%	47.1%	27.4%	12.8%	0%	24.7%	16.1%	15.7%	43.7%	30%	32.4%
Bryozoans	2.3%	4.6%	6.4%	4.5%	4.7%	0%	0%	43.2%	44.3%	56.6%	35.2%	40%	51%
Barnacles	3.6%	4.4%	41.4%	37.7%	25%	0%	0%	6.2%	6.5%	1%	2.3%	1.4%	2%
Benthic foraminifers	17%	10.7%	3.4%	3.7%	10.8%	12.5%	2.9%	1.8%	2.6%	2.2%	1.5%	1.8%	0.1%
Planktonic foraminifers	0%	0.2%	0%	0.6%	17.5%	66.4%	97%	0%	0%	0%	0%	0%	0%
Echinoids	1.8%	2.5%	1%	2.2%	5.6%	0%	0%	19.1%	23.2%	19.1%	10.2%	14.4%	5%
Mollusks	0.3%	1.9%	0.7%	3.1%	7.1%	8.3%	0%	4.8%	6.5%	5.2%	7%	11.9%	9.5%
Brachiopods	0%	0%	0%	0%	0%	0%	0%	0.2%	0.8%	0.2%	0.1%<	0.4%	0%
Ostracods	0%	0.1%	0%	0.6%	1.4%	0%	0.1%	0.1%<	0%	0%	0.1%<	0%	0%
Serpulids	1%	0.5%	0.1%	0.5%	0.5%	0%	0%	0%	0%	0%	0%	0.1%	0%
Phosphorous content (μmol P /g of sample)													
Bioavailable P	25.38	26.2	23.62	24.48	69.01	121.95	83.39	31.64	34.51	24.2	34.31	33.71	44.44
Detrital P	0.37	0.98	0.48	0.76	48.76	75.76	70.22	2.15	2.15	1.83	3.27	2.13	2.03
Detrital and authigenic fractions [Point counting]													
Detrital fraction	0.4%	1.6%	0.5%	2.1%	10.7%	19.5%	10.6%	33.5%	38.7%	22.7%	22%	26%	30.8%
Bioclastic fragments	99.5%	98.3%	99.5%	97.8%	75.3%	46.4%	68.2%	66.4%	61.2%	77.3%	78%	75.9%	69.2%
Authigenic minerals	Traces	Traces	Traces	Traces	14%	34.1%	21.2%	Traces	Traces	Traces	Traces	Traces	Traces
Quantitative X-ray powder diffraction													
Silicate minerals	4.9%	8.9%	2.3%	2%	42.5%	52.6%	37.8%	26.7%	32%	13.8%	15.4%	21.6%	20.4%
Carbonate minerals	95.1%	91.1%	97.3%	97.7%	55.8%	43.5%	57.8%	73.3%	67.9%	86.2%	84.5%	78.3%	79.2%
Carbonate-Apatite	Traces	Traces	Traces	Traces	1.4%	3.7%	4.4%	Traces	Traces	Traces	Traces	Traces	Traces

Table 4.3.1 : Skeletal assemblages, phosphorous content, petrographic characteristics and mineralogical composition of the lithozones of the studied successions.

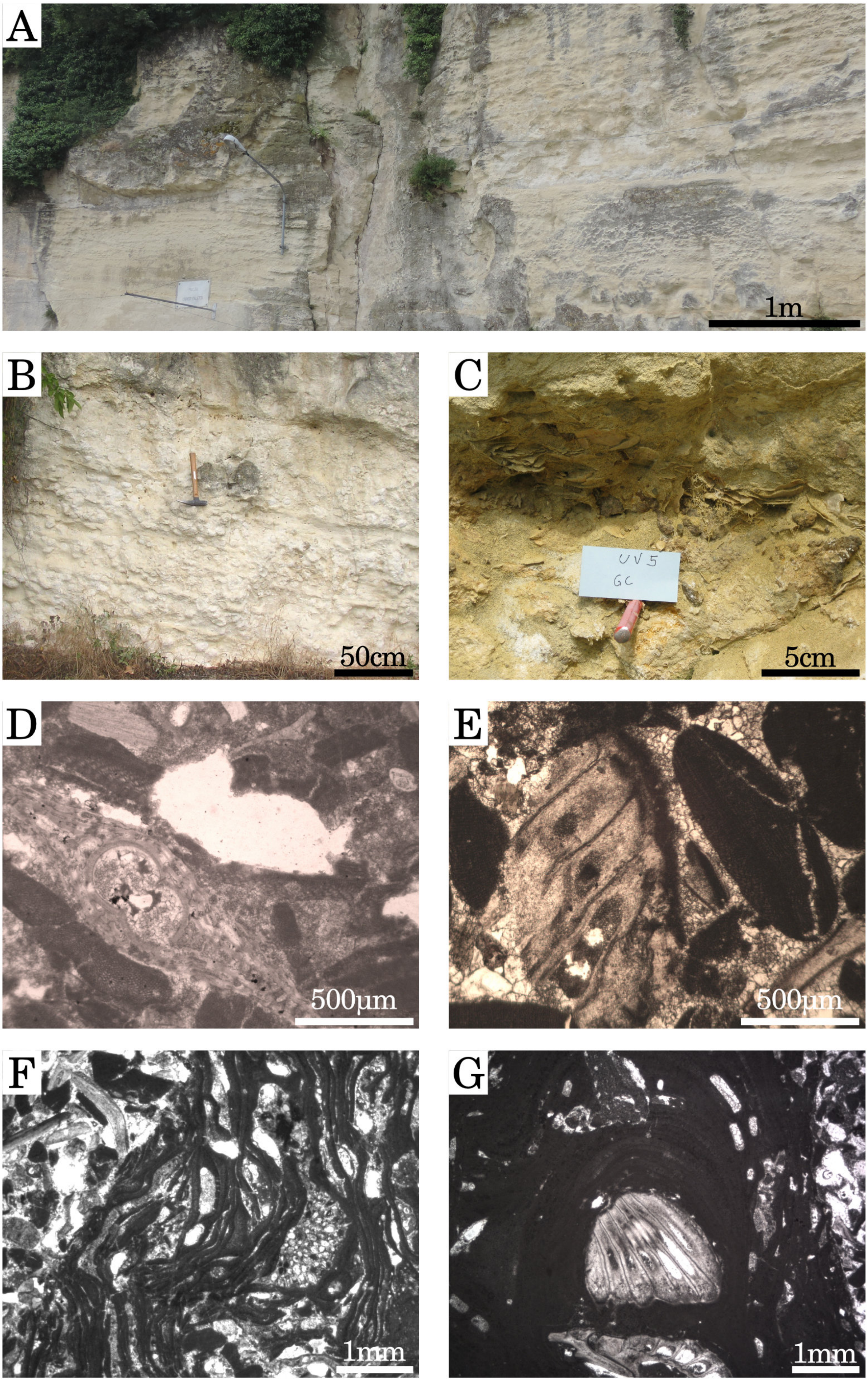

Figure 4.3.1 : Pietra da Cantoni Group. A) Channels in the Pietra da Cantoni limestone. B) Uviglie, rhodolith floatstone, lithozone 2. C) Uviglie, lithozone 5, impure limestone rich in authigenic phosphates. D) Uviglie, lithozone 1, larger benthic foraminifers. E) Uviglie, lithozone 3, barnacles fragments. F) Uviglie, lithozone 4, *Phymtolithon* sp. 1. G) Uviglie, lithozone 4, *Lithothamnion crispatum*.

Barnacles are extremely abundant in lithozones UV3 and UV4 and fragments of barnacle plates are almost just as common as coralline algae fragments (Fig. 4.3.1E; Tab. 4.3.1). In these lithozones barnacle-encrusted rhodoliths are also very common (further details on the skeletal assemblages of the Pietra da Cantoni Group are presented in Chapter 2.4).

Sommières Basin. The carbonate factory of the Sommières Basin, during the lower Burdigalian, was dominated by bryozoans, coralline algae, barnacles and echinoids (Fig. 4.3.2). In the studied sections of Souvignargues and Pondres the vast majority of skeletal grains derives from bryozoans and coralline algae, echinoids are abundant, barnacles and mollusks common, benthic foraminifers rare, brachiopods, serpulids and ostracods very rare (Fig. 4.3.2B-D; Tab. 4.3.1). Bryozoans are almost always the main producers, only in lithozone PON3 coralline algae are slightly more abundant (Fig. 4.3.2D; Tab. 4.3.1). Both rhodoliths and bryozoans macroids occurs in both successions and the latter are common at the top of Pondres succession (Fig. 4.3.2B-C; further details on the skeletal assemblages of the Sommières Basin are presented in Chapter 3.4). Benthic foraminifers, both larger and small are rare, the former group is entirely represent by a few rare specimens of *Amphistegina*; *Cibicides*, *Elphidium* and agglutinated forms occur within the latter (Fig. 4.3.2E).
The skeletal assemblage of Boisseron outcrop is largely dominated by barnacles and mollusks fragments (mainly oysters), bryozoans and echinoids are common and coralline algae and benthic foraminifers rare.

Coral-reef limestone of Balza di Rocca Limata. The Messinian coral-reef of Balza di Rocca Limata (NE Sicily, Southern Italy) belong to the Terravecchia Formation (Grasso and Pedley 1988). It consist of a large (45m high and 2km wide) in situ deposition formed by

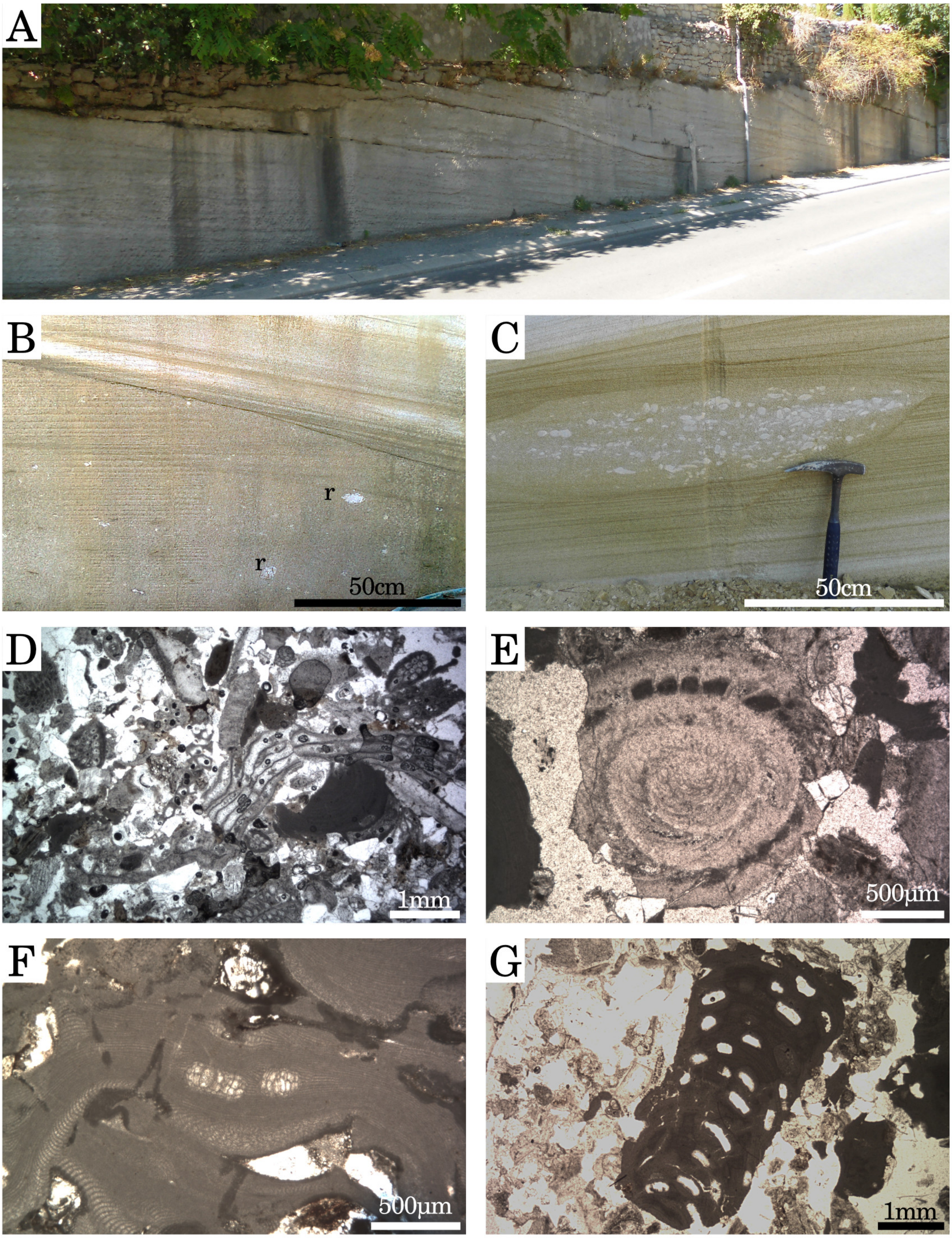

Figure 4.3.2 : Sommières Basin. A) Boisseron outcrop. B) Pondres, Lithozone 4; r=rhodoliths. C) Pondres, above Lithozone 5, bryozoans macroids. D) Pondres, Lithozone 3. E) Pondres, Lithozone 4, *Amphistegina*. F) Pondres, Lithozone 1, *Mesophyllum roveretoi*. G) Pondres, Lithozone 4, ?*Lithothamnion* sp.2.

branched colonies of *Tarbellastrea* and some, scattered, both massive and branched, colonies of *Porites*. The skeletal assemblages is largely dominated by fragments of hermatypic corals.

Coralline algae distribution

The detailed descriptions of the morphology of the coralline algae described in this paragraph is presented in the taxonomic appendix (Chapter 6).

Pietra da Cantoni Group. Hapalidiales dominate coralline association of all the lithozones. Within lithozones UV1-3 Corallinales and Sporolithales contribution is minimal, while in lithozone UV4 they are more important, albeit not common (Tab. 4.3.2). Actually in UV4, Corallinales and Sporolithales occur associated together and in large quantities, in few samples but they are almost completely absent in most of the others.
The most common and frequently occurring species are: *Lithothamnion giammarinoi*, *Lithothamnion ponzonense*, *Lithothamnion crispatum*, *Lithothamnion/Phymatolithon* sp. 3, *Phymatolithon* sp.1, *Mesophyllum roveretoi* and *Lithoporella melobesioides* (Fig. 4.3.1F-G). *Mesophyllum galettoi*, *Mesophyllum ishijimai*, *Spongites fruticulosus* and *Sporolithon* sp.1 are locally abundant but they do not frequently occur in the association. Other species, like *Lithophyllum* sp.1, *Lithophyllum* sp.2, contribute only marginally to the association.

Sommières Basin. The coralline association of the Sandy Molasse Unit of the Sommières Basin is also largely dominated by Hapalidiales. Corallinales occur in all lithozones except lithozone PON5 were only Hapalidiales are present. Albeit Corallinales contribution is small they actually occur in almost every sample; they are especially

Orders	Lithozones											
	UV1	UV2	UV3	UV4	UV5	UV6	PON1	PON2	PON3	PON4	PON5	SOUV1
Hapalidiales	99.7%	98.6%	98.2%	83.2%			92.8%		99.5%	95.2%	100%	85%
Corallinales	0.3%	1.4%	0.8%	8.6%			7.2%		0.5%	4.8%	0%	9.5%
Sporolithales	0%	0%	1%	8.2%			0%		0%	0%	0%	5.5%
Identified species												
Sporolithon sp. 1	0%	0%	0%	7.7%			0%		0%	0%	0%	8.7%
Sporolithon sp. 2	0%	0%	1.5%	0%			0%		0%	0%	0%	0%
Lithophyllum sp. 1	0%	0%	0.4%	0.5%			1.8%		0.6%	1%	0%	2.6%
Lithophyllum sp. 2	0%	0.1%	0%	0.1%			0%		0%	0%	0%	0%
Spongites fruticulosus	0%	0%	0%	7.2%			2.4%		0%	3%	0%	0%
Spongites sp. 1	0%	0%	0%	0%			4.6%		0%	0%	0%	0%
Spongites sp. 2	0%	0%	0%	0%			0.3%		0%	0%	0%	0%
Lithoporella melobesioides	0.3%	1.3%	0.8%	1.5%			0.1%<		0.1%<	0.1%<	0%	0.1%
Lithoporella minus	0%	0%	0%	0%			0%		0%	0.1%<	0%	0.1%<
Mesophyllum roveretoi	19.4%	2.9%	0%	13.9%			67.6%		16.5%	42.6%	11.1%	15.9%
Mesophyllum galettoi	0%	19.5%	0%	0%			0%		0%	0%	0%	4.5%
Mesophyllum ishijimai	19%	0%	0%	0%			0.4%		0%	0%	0%	4%
Mesophyllum sp. 1	0%	0%	0%	0%			0%		0%	0%	0%	17.3%
Mesophyllum sp. 2	0%	1.7%	0%	0%			0%		0%	0%	0%	0%
Lithothamnion ponzonense	5.8%	38.8%	0%	6.5%			13.4%		0%	20.5%	0%	19%
Lithothamnion crispatum	0%	18.7%	0%	8.5%			0%		0%	0%	0%	5.2%
Lithothamnion giammarinoi	47.3%	4.9%	32.8%	6%			0%		0%	0%	0%	0%
?*Lithothamnion* sp. 2*	0%	0%	0%	0%			0%		0%	18.3%	0%	8.2%
Lithothamnion/Phymatolithon sp. 1	0%	0%	0%	0%			0%		0%	1.6%	0%	9.8%
Lithothamnion/Phymatolithon sp. 2	0%	0%	0%	0%			6.9%		0%	0%	39%	0%
Lithothamnion/Phymatolithon sp. 3	0%	2.9%	9%	14.3%			0%		0%	0%	0%	0%
Phymatolithon calcareum	0%	0%	0%	0%			2.6%		0%	1.2%	0%	0%
Phymatolithon sp.*	0%	0%	0%	0%			0%		59.4%	11.7%	19.3%	4.7%
Phymatolithon sp. 1	0%	7.6%	55.6%	24.4%			0%		23.4%	0%	30.6%	0%
Phymatolithon sp. 2	0%	0%	0%	3.9%			0%		0%	0%	0%	0%

Table 4.3.2 : Coralline algae association; in lithozones UV5, UV6 and PON2 due to paucity of coralline the association has not been studied; *= ?*Lithothamnion* sp. 2 and *Phymatolithon* sp. are both sensu Hrabovský et al. 2015.

abundant in lithozone SOUV1. Sporolithales only occur in SOUV1, but is remarkable that in this lithozone they are very frequent.

The most abundant and frequently occurring species are: *Mesophyllum roveretoi*, Lithothamnion *ponzonense*, ?*Lithothamnion* sp. 2, *Phymatolithon* sp. (sensu Hrabovský et al. 2015), *Phymatolithon* sp. 1 and *Lithophyllum* sp.1 (Fig. 4.3.2F-G).

Mesophyllum sp.1 and *Sporolithon* sp.1 are common only in SOUV1, the former is quite abundant in this lithozone. *Lithothamnion crispatum*, *Phymatolithon calcareum*, *Mesophyllum galettoi*, *Mesophyllum ishijimai*, *Spongites fruticulosus* and *Lithoporella melobesioides* contribute only marginally to the association (further details on coralline distribution and trends in Sommières basin are presented in Chapter 3.4).

Phosphorous content, petrography and mineralogical composition

Pietra da Cantoni Group. The limestones of the Uviglie section of the Pietra da Cantoni Group may be separated in two groups from the mineralogical point of view: the pure limestones (with >90% of carbonate minerals) of lithozones UV1-UV4a and the impure limestones (with <90% of carbonate minerals) of lithozones UV4b-UV6 (Fig. 4.3.1C; Tab. 4.3.1). This difference in mineralogical composition, resulting from XRD analyses, is supported by point counting observations that show an increase in the detrital fraction and in the abundance of authigenic minerals, in particular glaucony but also authigenic phosphates (Fig. 4.3.3A-B; Tab. 4.3.1). Actually in lithozones UV1-UV4a glaucony grains are rare, small and pale green in color, while in lithozones UV4b-UV6 they are larger, of a deep-green color, and far more common (Fig. 4.3.3A).

The concentrations of both detrital phosphorous (Det-P from here onward) and biologically-available phosphorous (Bio-P from here onward) are far higher in the impure limestones than in the pure limestones (Tab. 4.3.1). The average Bio-P content from the

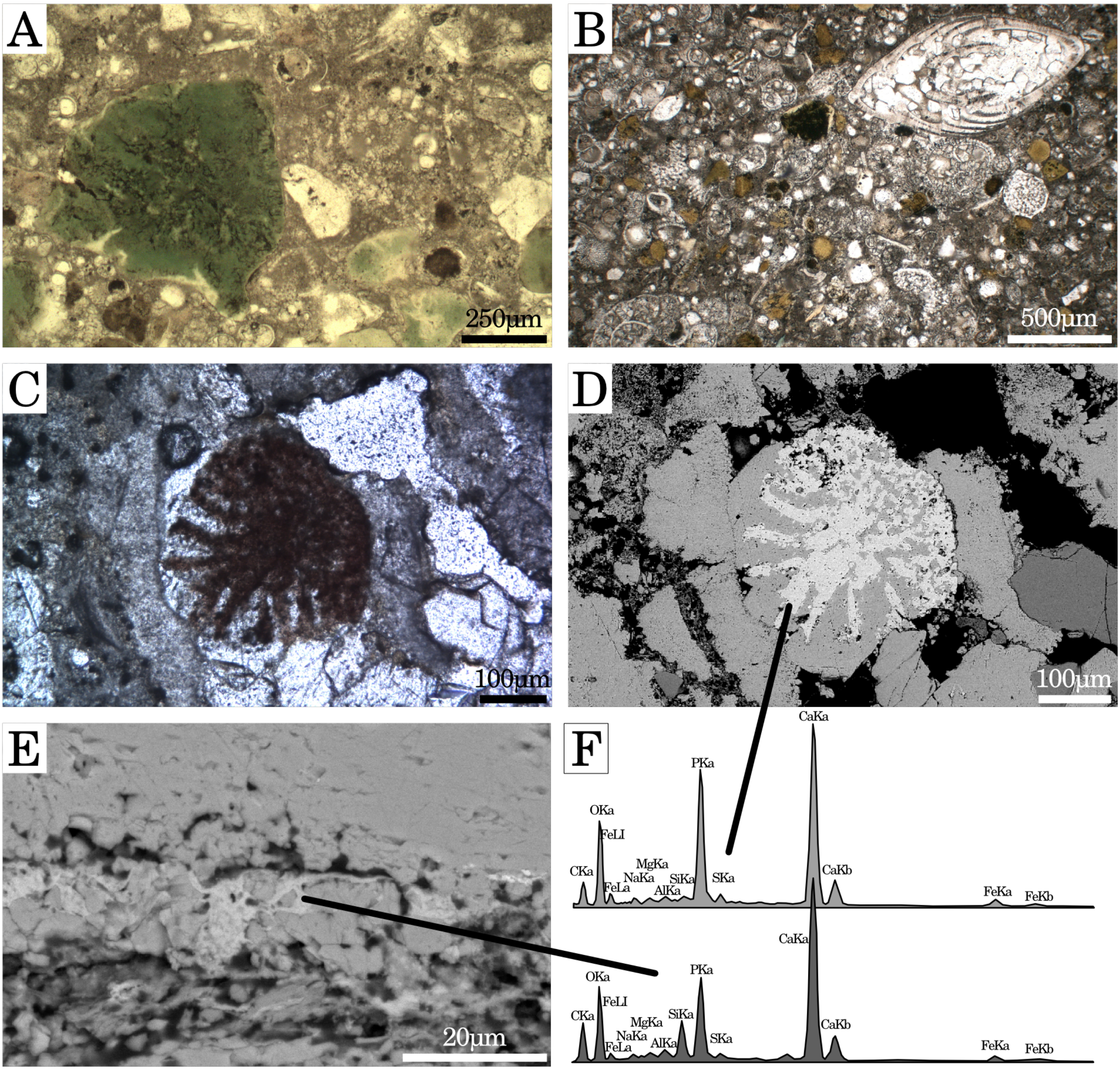

Figure 4.3.3 : Authigenic minerals. A) Pietra da Cantoni Group, glaucony and authigenic phosphates. B) Pietra da Cantoni Group, Uviglie, Lithozone 6, glaucony and authigenic phosphates. C) Sommières Basin, Pondres, Lithozone 3, transmitted light microscope, skeletal grain with authigenic phosphate. D) Sommières Basin, Pondres, Lithozone 3, SEM, backscattered electron image highlights the differences in density between calcite (dark grey) and the authigenic phosphate (light gray) in the skeletal grain. E) Sommières Basin, Souvignargues, detail of authigenic phosphates (light gray) interweaving with biogenic calcite (dark grey). F) EDS spectra of the authigenic phosphates.

pure limestones is 24.92 μmol/g of sample, Det-P contribution is neglible (0.65 μmol/g), on the other hand impure limestone sample have an average concentration of 91.45 μmol/g of Bio-P and of 64.91 μmol/g of Det-P. This difference is also supported by XRD analyses and that shows the abundant presence of Carbonate-Apatite in the impure limestones (Tab. 4.3.1).
Organic matter analyses show a negligible amount of organic carbon in all the samples.

Sommières Basin. Pondres and Souvignargues succession of the Sommières Basin are entirely composed of impure limestone (with <90% of carbonate minerals), this is supported by both XRD analyses and point-counting (Tab. 4.3.1). It must be stressed that in this instance detrital fraction is underestimated by XRD since limestone rock-fragments, eroded from the Oligocene and Cretaceous bedrock of the basin, are very common in the studied successions. Actually according to point-counting analyses the detrital fraction represents, on average, 1/3 – 1/4 of the rock (Tab. 4.3.1). Authigenic minerals, both glaucony and phosphates, occur in small amounts in all the lithozones (Fig. 4.3.3C-F; Tab. 4.3.1). The sample of Boisseron outcrop is also an impure limestone (79.4% of carbonate minerals, 20.1% of silicate minerals and traces of Carbonate-Apatite).
Phosphorous concentration is more uniform in Pondres and Souvignargues successions than in the succession of Uviglie of the Pietra da Cantoni group. The average value of Bio-P is 40.56 μmol/g, the highest values are recorded in SOUV1 and the lowest in PON3 (Tab. 4.3.1). The average value of Det-P is 2.26 μmol/g and only minor differences occur between the different lithozones (Tab. 4.3.1). Boisseron sample has a Bio-P concentration of 31.37 μmol/g and a Det-P concentration of 1.79 μmol/g.
Organic matter analyses show only negligible amounts of organic carbon in the samples.

Coral-reef limestone of Balza di Rocca Limata. The coral-reef limestone is a pure limestone with 93.7% of carbonate minerals and 6% of silicate minerals; it has a Bio-P content of 16.78 µmol/g and a Det-P content of 0.89 µmol/g.
According to organic matter analyses there is just a negligible amount of organic carbon in this sample.

4.4 – Discussion

Skeletal assemblages

Both Sommières Basin and Pietra da Cantoni Group benthic skeletal assemblages are temperate in character. They are dominated by bryozoans, coralline algae, barnacles and benthic foraminifers and they also lack skeletal elements which are usually common in tropical assemblages, like corals and abundant green-calcareous algae (Tab 4.3.1). On the other hand paleontological indicators of tropical climate occur in both sequences. Larger benthic foraminifers are abundant and diverse in the sequences of the Pietra da Cantoni Group; in the Sommières Basin they are less common and only *Amphistegina* occurs, but they are not completely excluded from the association (Fig. 4.3.1; Fig. 4.3.2). Their presence suggests warm waters with average annual temperature generally above 20°C (Beltzer et al. 1997; Geel, 2000; Langer and Hottinger 2000; Beavington-Penney and Racey, 2004) *Sporolithon* sp.1 and *Lithoporella melobesioides* occur both in the French and Italian samples and they are typical of warm waters (Adey 1979; Fravega et al. 1989; Vannucci et al. 1996; Aguirre et al. 2000). General paleoclimatic reconstructions also suggest warm climate during the lower Miocene and the persistence of tropical condition in the Mediterranean region during this stage (Zachos et al., 2001; Pomar et al. 2004; Mosbrugger et al. 2005). Furthermore during the Burdigalian there is even a slight northwards expansion of zooxanthellate corals in the Mediterranean, and symbiont-bearing corals are recorded even in the northern part of the Alpine Molasse Basin (Perrin and Bosellini, 2012). Therefore symbiont-bearing corals were present even further north than the two localities considered in this study.

Therefore there is an apparent contradiction between the temperate association of the Sommières Basin and of Pietra da Cantoni Group and the general warm-temperate/tropical climate of the Mediterranean region during the lower Burdigalian. Nutrients supply strongly affects carbonate producing organism (Hallock and Schalger, 1986; Wood, 1993; Mutti and Hallock, 2003); a shift from corals to coralline algae domination can occur in response to a modest increase in nutrient flux, while a shift from corals to a heterotroph-dominated biota can result from a substantial increase in nutrients flux (Hallock, 2001). In the present-day Gulf of California, consistently with a strong gradient in nutrients concentration, different carbonate factories exist: coral reefs dominate in oligotrophic-mesotrophic conditions, coralline algae in mesotrophic-eutrophic sectors, and bryozoans and mollusks in eutrophic environments (Halfar et al. 2004; Halfar et al. 2006). Along the eastern coasts of Australia experiments on the recruitment and the early growth of calcareous organism proved that coralline algae and corals are remarkably more abundant far away from terrestrial run off, while bryozoans are more common near shore, in nutrient-rich turbid waters (Holmes et al. 1997). Similar patterns also occur well within equatorial waters. Along the Spermonde shelf (Sulawesi, Indonesia) river run-off and nutrient abundance reduce water clarity and restrict hermatypic corals to clear and most shallow water of the shelf (Wilson and Vecsei, 2005). On the other hand larger benthic foraminifers thrive in the mesotrophic waters of the shelf and are a major component of the skeletal assemblage (Wilson and Vecsei, 2005). In situ nutrients-enrichment experiments in tropical waters further suggest that coral settlement is negatively impacted by an increase in nutrient supply, bryozoans recruitment is increased and coralline algae cover remains roughly constant (Jessen et al. 2014).

On the basis of the observable behavior of modern systems, nutrients influence on carbonate factories has been successfully recognized in the fossil record and has become a factor that must be taken into account in paleoenvironmental reconstructions (e.g.

Carannante et al. 1988, Brasier 1995b; Brandano and Corda, 2002; Cunningham and Collins, 2002; Hageman et al. 2003; Vannucci et al. 2003; Pomar et al. 2004; Reynaud and James, 2012; Brandano et al. 2016).

According to these strong lines of evidence it is reasonable to assume that nutrients played a major role in driving out hermatypic corals and fostering the dominance of heterotroph suspension-feeders (bryozoans and barnacles) and mesophotic and oligophotic carbonate producers (larger benthic foraminifers and coralline algae) in the Pietra da Cantoni Group and in the Sandy Molasse Unit of the Sommières Basin. During the Burdigalian the two localities were at the same latitude and they were separated just by a few hundreds of kilometers, so there was no room for large climatic differences. Therefore the existing differences between the two environments were, more than likely, caused by nutrients influence. The coralline-barnacle-larger benthic foraminifers association of the Pietra da Cantoni limestone probably developed in mesotrophic waters while mesotrophic-eutrophic conditions fit in perfectly with the bryozoans dominance of the Sommières Basin.

Coralline algae distribution

Hapalidiales largely dominate coralline-algae assemblages in all the lithozones of both areas (Tab 4.3.2). Most of the algal cover is produced by species of genera *Lithothamnion* and *Phymatolithon* and only in lithozones PON1 and PON4 *Mesophyllum* species are dominant (Tab 4.3.2). In tropical and warm-temperate waters the abundance of Hapalidiales, and of the group *Lithothamnion+Phymatholithon* in particular, peaks between middle-platform depth and the lower end of the photic zone (Adey, 1986; Aguirre et al., 2000). The paleobathymetric indicators in the two localities suggest instead more shallow-water. Souvignargues succession is characterized by the abundance of rock-fragments and the common presence of large rounded pebbles, suggesting a near-shore depositional environment (Chapter 3.5 for details). Pondres sequence deposited deeper but the presence of barnacles and rock-fragments still suggest a not so deep near-shore environment (Chapter 3.5 for details). In the Uviglie section the spherical morphology of the rhodoliths and the laminar growth form of coralline algae suggest frequent overturning, this, together with barnacle abundance, point once again to a not so deep middle-ramp environment for the area of rhodolith formation (Chapter 2.5 for details).

Therefore the presence of oligophotic algae in shallow and mid-depths waters on the plankton, strongly suggests a reduced light penetration in both localities. This is in agreement with nutrients abundance. Nutrients directly affect water clarity by increasing plankton biomass and consequently particulate organic carbon (Hallock and Schalger, 1986). Furthermore if the source of nutrients is river run off, water transparency is further reduced by river suspended-load.

Lithothamnion crispatum distribution gives further insight on water clarity in the two localities. Actually this coralline alga in present-day oceans shows a remarkable preference toward clear and well-lit waters (Pascelli et al. 2013; Neill et al. 2015). *L. crispatum* is common in Uviglie rhodoliths, but is quite rare in the Sommières Basin, occurring only in Souvignargues nodules (Tab. 4.3.2), suggesting that in the Sommières Basin water transparency was probably lower than in the Pietra da Cantoni area.

Phosphorous concentration

The concentrations of Bio-P measured with SEDEX extraction in the samples faithfully reflect benthic skeletal assemblages, supporting mesotrophic conditions for the Pietra da Cantoni Group and mesotrophic-eutrophic waters for the Sommières basin.

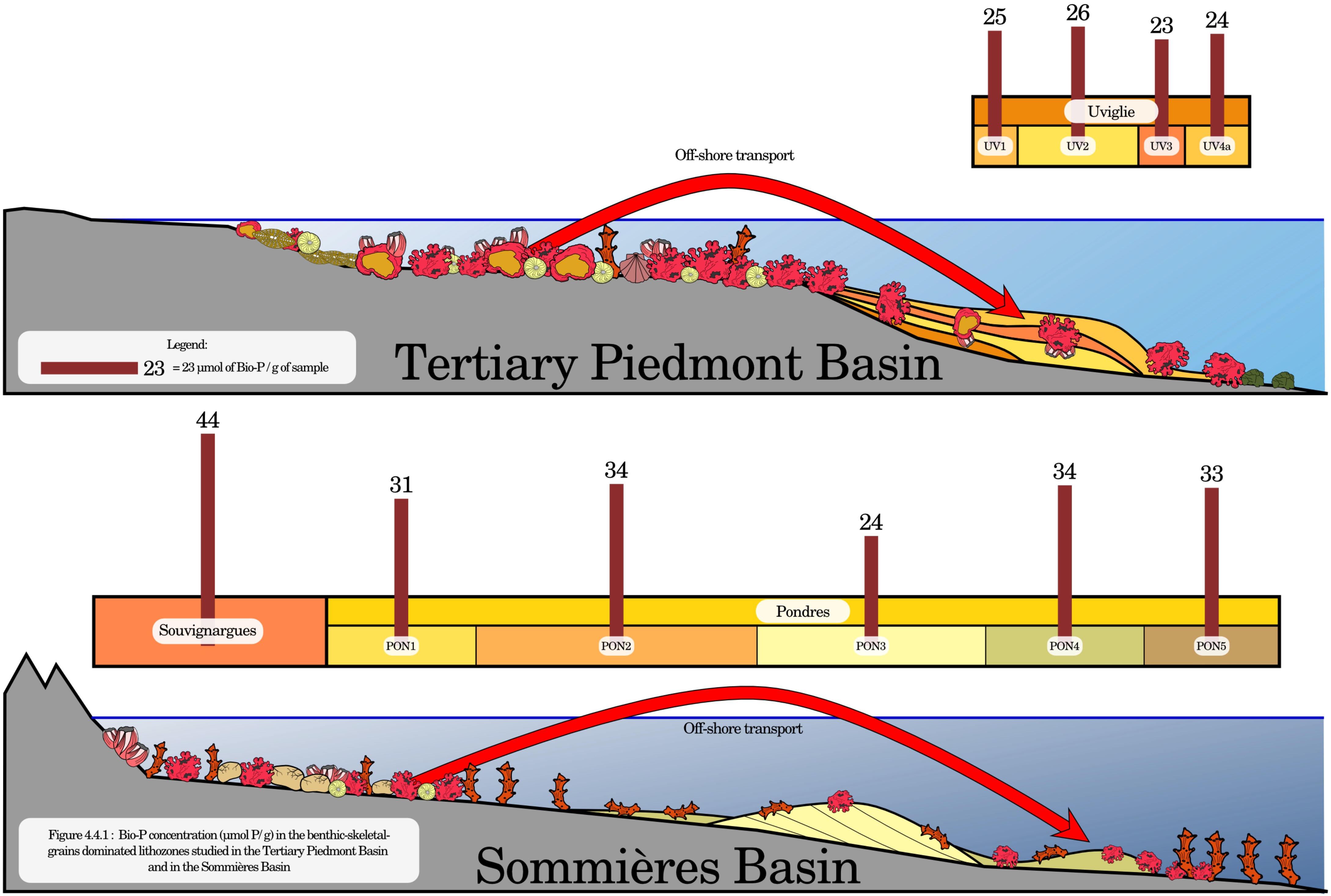

Figure 4.4.1 : Bio-P concentration (µmol P/ g) in the benthic-skeletal-grains dominated lithozones studied in the Tertiary Piedmont Basin and in the Sommières Basin

Actually Bio-P concentration in Sommières Basin samples is higher than in lower part of the Uviglie sequence (Tab 4.3.1; Fig. 4.4.1). Bio-P concentrations of both localities are higher than the Bio-P concentration in the coral-reef sample of Balza di Rocca Limata, which was supposed to have the lowest concentration of phosphorous since coral-reef are oligotrophic environments (Tab 4.3.1). The highest values of Bio-P are however recorded in the upper portion of the Uviglie section, dominated by pelagic sedimentation. These results are also in agreement with XRD analyses that indicate abundant authigenic phosphates in these samples.

It should be remembered that SEDEX extraction measure phosphorous concentration for a given weight of sample. This mass of rock corresponds to a volume of rock and consequently to a sedimentation rate. Bio-P concentrations in the samples are therefore directly proportional to the concentration of phosphorous in the paleoenvironment and inversely proportional to the sedimentation rate. Actually when the sedimentation rate is low, skeletal elements lie exposed at the water-sediment interface for a long time and authigenic phosphate minerals can develop. Glaucony abundance and maturity are also directly related to sedimentation rate (Amorosi, 1995; Amorosi, 1997). According to glaucony distribution and characteristics, the sedimentation rate was lower in the Pietra da Cantoni area than in the Sommières Basin. Glaucony is especially abundant and mature in lithozones UV4b and UV5, which correspond to a major sedimentation break in the area and to a period of extremely low sedimentation rate. Large and mature glaucony crystals also occur in lithozone UV6 (Fig. 4.3.3A), testifying a still low sedimentation rate during the deposition of this lithozone. Consequently the high Bio-P content of these samples is related to the very low sedimentation rate. Moreover, on these basis, the difference in Bio-P concentration measured between the Sommières Basin and the lower part of Pietra da Cantoni sequence, corresponds to an originally even larger difference of Bio-P concentration in the paleoenvironment.

Diagenesis is another factor that should not be underestimated since has the potential to change the original composition of the sediment through time. Authigenic Ca-P minerals (Carbonate-fluorapatite) are one of the major sink of Bio-P on continetal margins (Ruttenberg and Berner, 1993). These minerals are quite resistant to alteration, they are more resistant than carbonate minerals (calcite, magnesite and dolomite) and display the same dissolution rate of albite (Guidry and Mackenzie, 2003). Moreover in these minerals P is preferentially retained in the crystal lattice during the early stages of dissolution (Guidry and Mackenzie, 2003). Only in the acid condition present within soils, these minerals can dissolve and lose their phosphorus. However, during organic carbon analyses no remarkable amount of organic matter was detected, thus ruling out plant and soil related alteration. Fe-oxyhydroxides are a relatively less stable sink for P. Under anoxic condition, near the sediment-water interface, the P adsorbed to these mineral surfaces is released back in to the water column (Krom and Berner, 1981). In both successions there are no paleoecological indicators that suggest anoxic conditions at the sea floor, therefore also this phosphorous sink should have not been compromised. Finally it should also been stressed that the two studied sequences are characterized by a similar history of short and very shallow burial, limited tectonic deformation and meteoric diagenesis. Rock texture is also rather uniform and since they have the same age, also the length of the exposure to meteoric alteration (within the very same climatic zone) is similar. Therefore if any alteration occurred, it should have modified the original composition in the same way in both localities, therefore preserving the original differences.

Taking in to account all these evidences is unlikely that the measured concentrations of Bio-P are just the random result of different diagenetic alteration. The observed Bio-P concentrations reflect instead the original differences in nutrients supply which are also faithfully recorded by the skeletal assemblages and coralline algae association (Fig. 4.4.1).

Nutrients supply line

The Pietra da Cantoni carbonate system developed on an isolated bank uplifted by the rotation of the Alpine Wedge (Maffione et al. 2008) and therefore protected from the siliciclastic detritus eroded from the Alps. The presence of angular rock fragments, issued from older formations, suggests the existence of small and low-lying emerged lands. These small islands however were clearly not a large source of detritus and nutrients. Actually the lower portion of Uviglie sequence is composed only of very pure limestone with minimal siliciclastic contribution (Tab. 4.3.1). Accordingly also the Det-P fraction of total P concentration is minimal (Tab. 4.3.1). After the drowning of the carbonate platform the detrital fraction become more important since the bioclastic contribution of the benthic carbonate factory was reduced to almost zero (Tab. 4.3.1). Within this setting is unlikely that nutrients were supplied by river runoff during the development of Pietra da Cantoni benthic carbonate factory. An upwelling source is more consistent with the very low concentration of Det-P in the lower part of the sequence. The deposition of siliceous ooze westward (and basin-ward) from Pietra da Cantoni area support this hypothesis (Bonci et al. 1990). The increase of Det-P in the upper part of Uviglie sequence is simply related to the increased importance of the detrital fraction due to the low sedimentation rate caused by the decrease of carbonate production. Differently from the Pietra da Cantoni, the Sommières Basin was almost completely enclosed by land and was connected to the open sea by a flooded paleo-incised valley (Reynaud and James, 2012). Accordingly the contribution of the detrital fraction is remarkably more important than in Pietra da Cantoni limestones. Det-P concentration is also higher than in the lower part of the Uviglie sequence and there is a correlation between the detrital fraction and the total phosphorous concentration (Tab 4.3.1). The near-shore area of Souvignargues actually has higher phosphorous concentration than the more off-shore area of Pondres (Tab 4.3.1). It is therefore likely than in the

Sommières Basin the source of nutrient was land based, either due to small rivers or directly from the runoff of the land.

Paleoenvironmental reconstruction

The carbonate factories of Pietra da Cantoni of the Tertiary Piedmont Basin and of the Sandy Molasse Unit of the Sommières Basin developed during the Burdigalian in the Northern part of the Mediterranean region. The climate in the period was warm (sub-tropical to warm-temperate) in the whole area and symbiont-bearing corals were present even in the Northern part of Alpine Molasse Basin (Pomar et al. 2004; Mosbrugger et al. 2005; Perrin and Bosellini, 2012; Fig. 1.4.2). However these two carbonate systems are characterized by "temperate" carbonate factories due to nutrients influence.

In the Tertiary Piedmont Basin (Fig. 1.4.2), the mesotrophic condition along the Pietra da Cantoni ramp foster the development of a rhodalgal carbonate factory (sensu Carannate et al. 1988), dominated by crustose coralline algae, with important contribution of larger benthic foraminifers and barnacles. The source of nutrients is the moderate upwelling of water from the deeper western sector of the Tertiary Piedmont Basin. Since they have low-light requirements coralline and larger benthic foraminifers are not affected by the reduced water clarity and can thrive along the ramp. Barnacle abundance is promoted by the high concentration of particulate organic matter suspended in the water column and by the strong currents that sweep the ramp, ensuring turbulence.

The Sommières Basin is located a few hundreds of kilometers westward, on the other side of the rising mountains range of the Alps, along the coasts of the Alpine Molasse Basin, near its junction with the Western Mediterranean (Reynaud and James, 2012; Fig. 1.4.2). In this tide-dominated inlet a bryo-rhodalgal (sensu Carannate et al. 1988) carbonate factory develops. Small ephemeral rivers and direct terrestrial runoff provide the strong injection of nutrients in the basin that foster bryozoans dominance. The mesotrophic-eutrophic turbid waters of the basin favor suspension-feeders heterotrophs over light-dependent organism. Larger benthic foraminifers are almost driven out from the association and only the stress-resistant taxa are able to survive. Coralline algae, which can live even with very-low levels of light, are still present and locally abundant but alway less common than in the mesotrophic Pietra da Cantoni ramp.

4.5 – Conclusions

The carbonate factories of the lower part Pietra da Cantoni Group of Tertiary Piedmont Basin and of the Sandy Molasse Unit of the Sommières Basin developed in the Mediterranean region in the Burdigalian, during a period of warm climate in the area. Due to the abundant nutrients supply, most sub-tropical taxa were driven out from the association. Low-light coralline algae were able to thrive in these shallow turbid-waters and heterotrophs suspension feeders flourished thanks to the plentiful supply of particulate organic carbon.

The rhodalgal carbonate factory of the Pietra da Cantoni grew up in mesotrophic waters on an isolated bank affected by upwelling currents. At the same latitude, mesotrophic-eutrophic waters fostered the development of a bryo-rhodalgal carbonate factory in the semi-enclosed Sommières Basin. In this inlet nutrients supply was land-based and its high rate favored bryozoans dominance over coralline algae and almost completely wiped out larger benthic foraminifers and the nutrient-sensitive coralline algae species like *Lithothamnion crispatum*.

Paleontological results are in complete agreement with geochemical analyses on phosphorus content. The latter actually indicates remarkably higher abundance of biologically-available phosphorous in the bryo-rhodalgal association than in the rhodalgal association. This proves that SEDEX sequential extraction is a viable instrument to investigate paleo-nutrient levels in neritic carbonates, opening new research possibilities in the field of paleoenvironmental reconstructions.

The integrated approach of this study has revealed a clear ecological distribution of Miocene Mediterranean carbonate-factories, based on nutrients abundance:

- Hermatypic corals in oligotrophic environment.

- Coralline algae, larger benthic foraminifers and heterotrophs supension feeders in mesotrophic environment.

- Bryozoans, coralline algae and other heterotrophs suspension-feeders in mesotrophic-eutrophic environment.

Nutrients availability, like temperature and hydrodynamic energy, strongly influences benthic organisms and controls carbonate facies associations. Their influence is preserved within the fossil record and paleontological and geochemical analyses can extract these information, improving the knowledge of Earth past.

5 – Conclusive Remarks

The integrated and detailed analyses of the two Miocene carbonate sequences studied in this thesis has produced remarkable scientific results which can be applied in different geographical areas and other epoch of Earth History.

- The investigation of the Pietra da Cantoni Group suggested that the observed rhodalgal facies in a warm-water context could be connected to a non-oligotrophic environment. The study also proved that rhodoliths are useful tools in the reconstructions of carbonate system with a high rate of sediment transport. Rhodoliths during their growth bind skeletal grains of their native environment and preserve them after transport and burial in deeper settings. In the event that the carbonate factory is lost or unobservable, the transported rhodoliths may provide information on the shallow-water environment where they grew up.

- Bryozoans dominance in the Sandy Molasse Unit of the Sommières Basin was probably related to non-oligotrophic conditions. The wealth of particulate organic carbon suspended in the waters of the basin fostered heterotrophs dominance at the expenses of water clarity. The paleontological study also proved that quantitative analysis of coralline distribution is useful for bathymetric reconstructions. Order-level distribution is an important source of information, and a more accurate reconstruction can be achieved through species-level identification. Within the Sommières Basin three species proved to be good proxy of shoreline proximity (*Spongites fruticulosus*, *Lithophyllum* sp.1, *Sporolithon* sp.1), another to be a deep-water dweller (*Phymatolithon* sp.1), and other two to be able to thrive over most of the photic zone (*Mesophyllum roveretoi* and *Lithothamnion ponzonense*).

- The comparison of the two sequences based on paleontological and geochemical evidences, highlighted the potential of SEDEX extraction in studying paleo-nutrient levels and the sensitivity of benthic organism to nutrients influence. Nutrients supply-rate had a major influence over the distribution of Miocene skeletal assemblages in the Mediterranean, fostering hermatypic corals in oligotrophic waters, coralline algae and larger benthic foraminifers in mesotrophic conditions and bryozoans in mesotrophic-eutrophic waters. Within this context the complete dominance of Hapalidiales in a shallow warm-water setting, appears to be an important indicator of turbidity and a clue of nutrients abundance.

These two carbonate sequences were chosen to minimize climatic and geographical variability and to concentrate over productivity. However, it would not have been possible to study nutrients influence, without having first thoroughly investigated both environments. Only with a sound understanding of the whole benthic community and its evolution through time and space, is possible to identify the effects of a single variable, which, together with many others, shapes the environment of a carbonate platform. This works proves that with this integrate and accurate approach is possible to unveil precious information stored in coarse-grained shallow-water limestones.
Nutrients have left a clear imprint on marine biota through time, and the results of this influence are preserved within the fossil record. Dig up these information will improve our knowledge of Earth past and of the future evolution of modern ecosystems.

6 – Appendix

Coralline Algae Taxonomical Remarks

This chapter is dedicated at the detailed description of the most common and abundant species of coralline algae identified in the Pietra da Cantoni Group of Tertiary Piedmont Basin and in the Sandy Molasse Unit of the Sommières Basin. Details of their distribution in the above mentioned carbonate sequences, are presented in Chapter 2, Chapter 3 and Chapter 4.

The description of *Lithothamnion crispatum* is presented in the form of the paper with which the fossil species has been synonymized with its modern relatives.

6.1 – *Sporolithon* sp. 1

Systematic Paleontology

Class Florideophyceae CRONQUIST, 1960

Sub-class Corallinophycidae LE GALL & SAUNDERS, 2007

Order Sporolithales LE GALL et al. 2009

Family SPOROLITHACEAE VERHEIJ, 1993

Genus *Sporolithon* HEYDRICH, 1897

Description

Encrusting to warty-fruticose growth form (Fig. 6.1.1A-B). Protuberances cylindrical up to 8 mm long and 6 mm wide (Fig. 6.1.1A). Thalli with monomerous organization, with crustose portions 500 µm to over 1mm in thickness (Fig. 6.1.1C). Non-coaxial ventral core up to 200 µm but generally thinner; interposed secondary ventral core are present in the protuberances (Fig. 6.1.1D-F). Ventral core cells are rectangular, 7 to 14 µm in diameter and 11 to 25 µm in length (Tab. 6.1.1). Peripheral zone cells are rectangular, 7 to 14 µm in diameter 5 to 23 µm in length (Fig. 6.1.1D; Tab. 6.1.1). Cell fusions are present. Trycocytes have not been observed. Epithallial cells have not been observed.
Compartments are grouped into slightly raised sori (Fig. 6.1.1E-H). Sori are 300 to 1750 µm in length (Fig. 6.1.1C). No layer of elongated cells occur below the sori. The compartments are elliptical in shape; they are 33 to 59 µm in diameter and 76-115 µm in height (Tab. 6.1.1). Compartments are separated by 1 or 2 filaments of cells (very rarely 3-4) composed of 4 to 5 cells (Fig. 6.1.1E-H). No calcified stalk-cell was observed within compartments.

	Diameter	Height
Ventral core (hypothallus) cells [µm]	7-14 [9.7 mean; 2.1 s.d.]	11-25 [16 mean; 2 s.d.]
Peripheral zone (perithallus) cells [µm]	7-14 [11 mean; 2 s.d.]	5-23 [13.5 mean; 4 s.d.]
Sporangial compartments [µm]	33-59 [49 mean; 8 s.d.]	76-115 [91 mean; 11 s.d.]

Table 6.1.1 : biometry of *Sporolithon* sp. 1

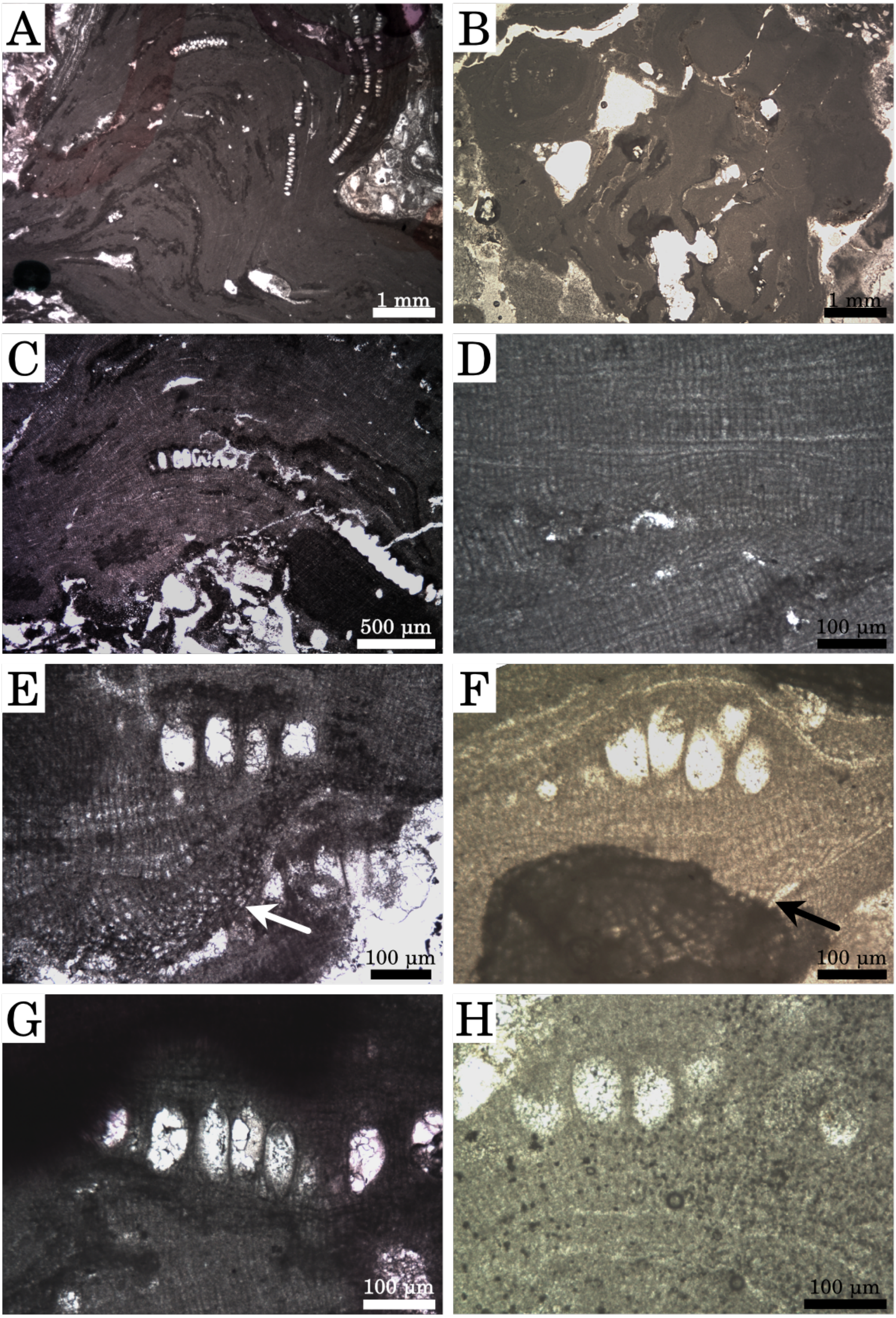

Figure 6.1.1 : Sporangial thallus of *Sporolithon* sp. 1. A) TPB, Lithozone 4, thallus overview. B) Sommières, Souvignargues, thallus overview. C) TPB, Lithozone 4, thallus overview. D) TPB, Lithozone 4, detail of the peripheral zone. E) TPB, Lithozone 4, vegetative and reproductive anatomy; white arrow=ventral core. F) Sommières, Souvignargues, vegetative and reproductive anatomy; black arrow=ventral core. G) TPB, Lithozone 4, detail of sporangial cavities. H) Sommières, Souvignargues, detail of sporangial cavities.

6.2 – *Lithophyllum* sp. 1

Systematic Paleontology

Class Florideophyceae CRONQUIST, 1960

Sub-class Corallinophycidae LE GALL and SAUNDERS, 2007

Order CORALLINALES SILVA and JOHANSEN, 1986

Family Corallinaceae LAMOUROUX, 1812

Sub-family Lithophylloideae SETCHELL, 1943

Genus *Lithophyllum* PHILIPPI, 1837

Description

Encrusting growth form (Fig. 6.2.1). Thalli with dimerous organization 100 to 300 µm in thickness (Fig. 6.2.1). Ventral layer of cells composed of cells square in section, slightly larger than the cells of the peripheral zone, 10 to 19 µm in diameter and 9 to 20 µm in height (Tab. 6..2.1; Fig. 6.2.1C). Peripheral zone cells are rectangular to square in section, well-defined cell walls separate adjacent filaments and cell fusion have not been observed. There is a clear lateral alignment of cells of adjacent filaments and the thallus has a net-like appearance, cells are 7 to 16 µm in diameter and 8 to 19 µm in length (Tab. 6.2.1; Fig. 6.2.1C-F). Trycocytes have not been observed. Epithallial cells have not been observed. Uniporate conceptacles chambers are 140 to 215 µm in diameter and 50 to 85 µm in height (Tab. 6.2.1: Fig. 6.2.1D-F). The conceptacles protrude from the surrounding thallus surface, the pore canal is conical in shape, tapering toward the conceptacle roof (with a base of up to 50 µm in diameter and a length of up to 35 µm). The central part of the floor of the conceptacle is slightly raised (Fig. 6.2.1D-E). The roof of the conceptacles is characteristically formed by one or two rows of cells longer than the surrounding cells, measuring 20-25 µm in length (Fig. 6.2.1E-F).

	Diameter	Height
Ventral layer (hypothallus) cells [µm]	10-19 [14 mean; 3 s.d.]	9-20 [14 mean; 4 s.d.]
Peripheral zone (perithallus) cells [µm]	7-16 [11 mean; 2 s.d.]	8-19 [13 mean; 4 s.d.]
Conceptacles [µm]	140-215 [185 mean; 40 s.d.]	50-85 [70 mean; 10 s.d.]
H/D ratio	0.37 mean; 0.08 s.d.	

Table 6.2.1 : biometry of *Lithophyllum* sp. 1

Remarks

This species is remarkably similar to *Lithophyllum nitorum*, a modern Atlantic species, reported by Braga and Aguirre (1995) in the Neogene of Spain. The holotype (Adey and Adey, 1973) is characterized by a thin thallus with a dimerous structure and conceptacles raised above the surrounding surface of the thallus. *Lithophyllum* sp.1, the Atlantic holotype of *L. nitorum* and *L. nitorum* of the Neogene of Spain have the same general morphology. Conceptacles are similar: they are small, with a slightly raised floor that can be interpreted as a columella and they have short conical pore canal. Furthermore, they all have a layer of cells longer than the peripheral-zone average, in the conceptacle roof. However significant differences exist in both reproductive and vegetative anatomy. The cells of the peripheral zone of the modern Atlantic species are smaller (5 to 13 µm of diameter and 5 to 11 µm of length) than those of Lithophyllum sp. 1. On the other hand conceptacles are significantly larger (255 to 385 µm of diameter and 100 to 135 µm height; Adey and Adey, 1973). The *L. nitorum* of the Neogene of Spain has similar cell size but larger conceptacles, the chambers are 216 to 396 µm in diameter and 84 to 168 µm height (Braga and Aguirre, 1995). Therefore, albeit *Lithophyllum* sp. 1 may be related to *L. nitorum*, it cannot be consider a conspecific.

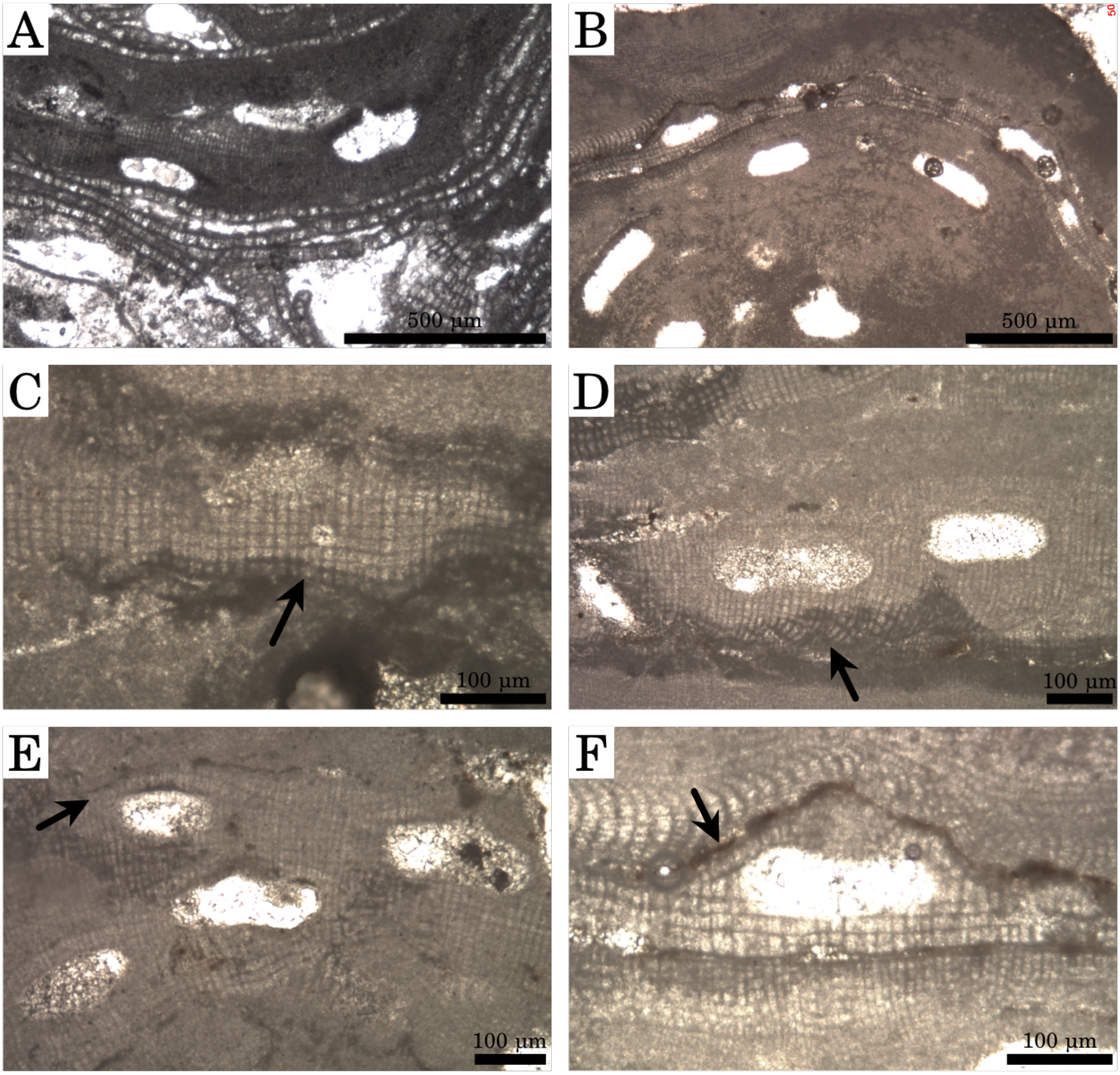

Figure 6.2.1 : *Lithophyllum* sp1. A) BTP, Lithozone 4, thallus overview. B) Sommières, Pondres, Lithozone 1, thallus overview. C) Sommières, Pondres, Lithozone 1, vegetative anatomy; black arrow=dimerous hypothallus. D) Sommières, Pondres, Lithozone 1, vegetative and reproductive anatomy; black arrow=dimerous hypothallus. E) Sommières, Pondres, Lithozone 1, conceptacles; black arrow=row of enlongated cells on conceptacle roof. F) Sommières, Pondres, Lithozone 1, detail of an asexual conceptacle; black arrow=row of enlongated cells on conceptacle roof.

6.3 – *Spongites fruticulosus*

Systematic Paleontology

Class Florideophyceae CRONQUIST, 1960

Sub-class Corallinophycidae LE GALL and SAUNDERS, 2007

Order CORALLINALES SILVA and JOHANSEN, 1986

Family Corallinaceae LAMOROUX, 1812

Genus *Spongites* KÜTZING, 1841

Spongites fruticulosus KÜTZING, 1841

Description

Thallus encrusting or warty to fruticose (Fig. 6.3.1). Crustose portions up to 1 mm thick. (Fig 6.3.1A). Protuberances up to 2 mm in diameter and more than 2 mm in length. Dimerous and monomerous organizations coexist on the same thallus (Fig. 6.3.2). In portion with monomerous organization the ventral core is non-coaxial, plumose and composed of large rectangular cells, 10 to 40 µm in length and 8-18 µm in height (Tab. 6.3.1; Fig. 6.3.1D). The ventral layer of cells, in portion with dimerous organization, is composed of large cells with the shape of a parallelogram, 10 to 21 µm in diameter and 15 to 17 µm of height (Tab. 6.3.1; Fig. 6.3.1E). The peripheral zone has growth lines and cell shapes range from rectangular to pentagonal. The cells of the peripheral zone have a diameter of 6 to 13 µm and they are 9-24 µm high (Tab. 6.3.1; Fig. 6.3.1). The fusions between cells of adjacent filaments are extremely common and therefore the peripheral zone has a messy appearance (Fig. 6.3.1). Each cell filament terminates at the thallus surface with a single, dome-shaped, epithallial cell, like in the modern species (Fig. 6.3.2A-B). Trichocytes have not been observed.

Uniporate conceptacles slightly protrude above the surrounding thallus surface (Fig. 6.3.1C). Conceptacles chambers are flask-shaped, 230 to 550 µm in diameter and 95 to 185 µm in height (Tab 6.3.1; Fig. 6.3.1A-C). The base of the pore canal is 60 to 100 µm wide (80 µm on average) and the canal is 75 to 170 µm long (120 µm on average; Fig. 6.3.1B-C). The roof of the conceptacles is 40 to 65 µm thick (50 µm on average) and is composed of 3 to 6 layers of cells. The remnants of a short columella can be observed on the floor of some conceptacles (Fig. 6.3.1B-C).

	Diameter	Height
Ventral layer (dimerous organization) cells [µm]	10-21 [16.5 mean]	15-19 [17 mean]
Ventral core (monomerous organization) cells [µm]	8-18 [12.6 mean; 3 s.d.]	10-40 [21.5 mean; 7 s.d.]
Peripheral zone (perithallus) cells [µm]	6-13 [10.5 mean; 2 s.d.]	9-24 [13 mean; 2.5 s.d.]
Conceptacles [µm]	230-500 [335 mean; 60 s.d.]	95-185 [135 mean; 30 s.d.]

Table 6.3.1 : biometry of *Spongites fruticulosus*.

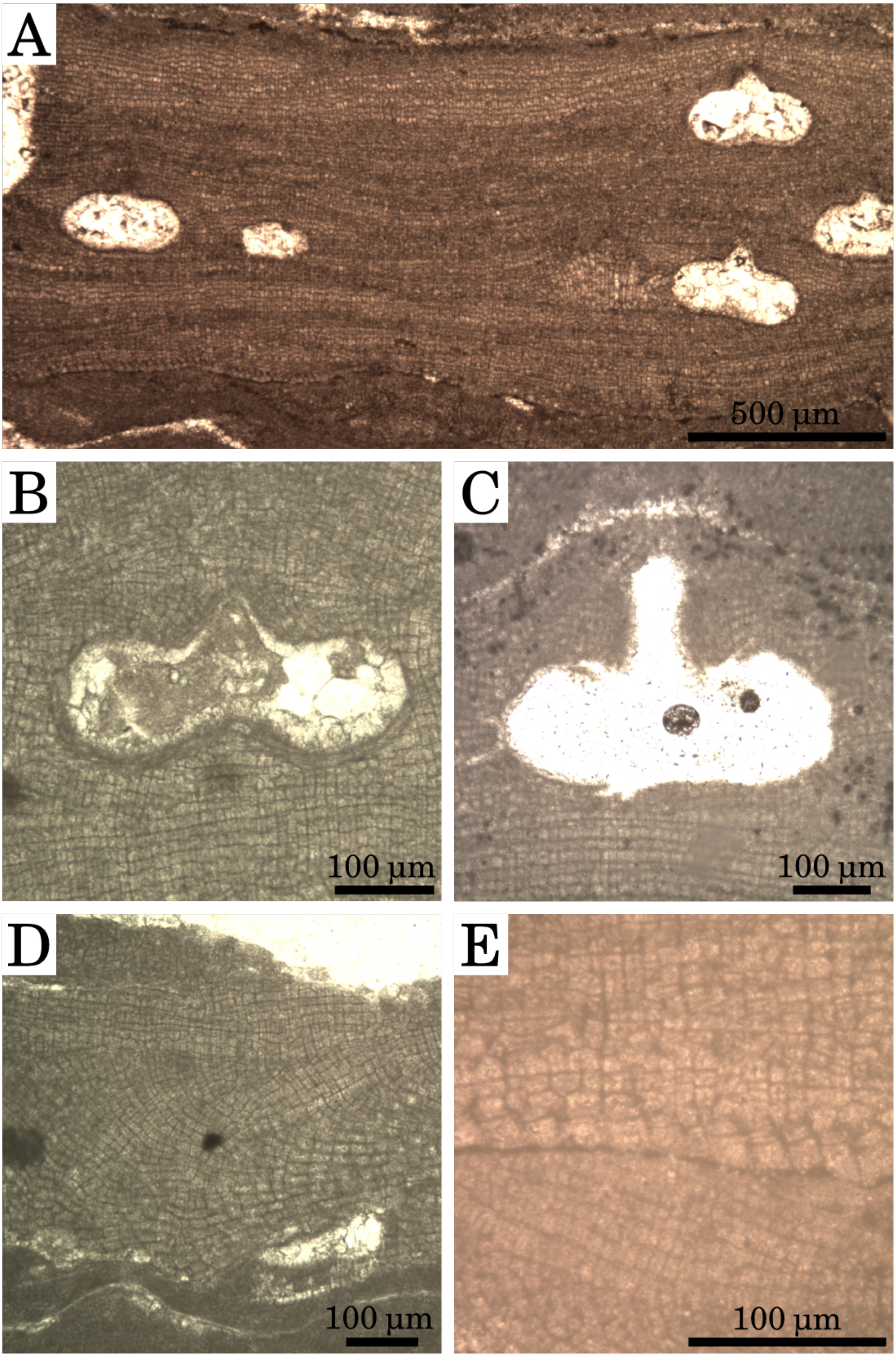

Figure 6.3.1 : *Spongites fruticulosus*. A) BTP, Treville, thallus overview. B) BTP, Torre Veglio Nord, uniporate conceptacle. C) Sommières Basin, Pondres, Lithozone 4, uniporate conceptacle. D) BTP, Torre Veglio Nord, non-coaxial ventral core in a part of the thallus with monomerous organization. E) BTP, Treville, monostromatic ventral core in a part of the thallus with dimerous organization.

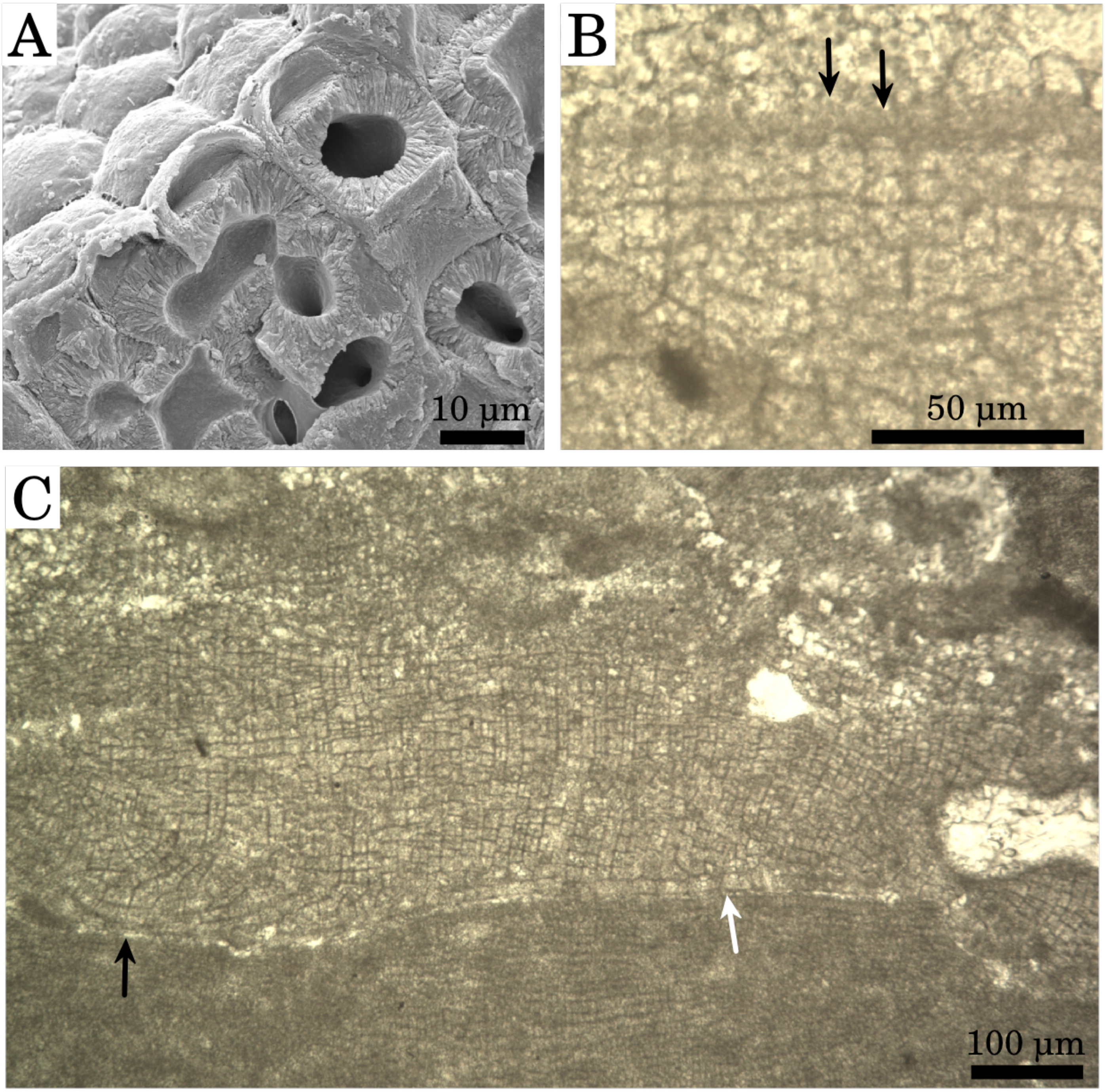

Figure 6.3.2 : *Spongites fruticulosus*, details of vegetative anatomy. A) Epithallial cells of a modern *S. fruticulosus* of Elba Island. B) BTP, Torre Veglio Nord, epithallial cells; black arrows=epithallial cells. C) BTP, Torre Veglio Nord, thallus with both dimerous and monomerous organization; black arrow=monomerous organization with non-coaxial ventral core; white arrow=dimerous organization with monostromatic ventral core.

6.4 – *Lithoporella melobesioides*

Systematic Paleontology

Class Florideophyceae CRONQUIST, 1960

Sub-class Corallinophycidae LE GALL and SAUNDERS, 2007

Order CORALLINALES SILVA and JOHANSEN, 1986

Family Corallinaceae LAMOROUX, 1812

Genus *Lithoporella* FOSLIE, 1909

Lithoporella melobesioides FOSLIE, 1909

Description

Thallus encrusting, consisting of a single, thin, layer of large cells, with a diameter of 11 to 36 µm and 11.5 to 44 µm high (Tab. 6.4.1; Fig. 6.4.1). The thallus sprouts radially from a basal disk that can be observed along section parallel to the surface on which *L. melobesioides* grow (Fig. 6.4.1F). The vegetative cells are covered by small, dome-shaped epithallial cells. Adjacent cells are connected by cell fusions (Fig. 6.4.1B). Trichocytes have not been observed.

Uniporate conceptacles are remarkably raised above the surrounding thallus surface, they are 315 to 320 µm in diameter and 200 to 245 µm high (Tab. 6.4.1; Fig. 6.4.1E). The pore canal is cone-shaped, tapering toward the floor of the conceptacle, the canal is around 70 µm wide at its opening and is near 130 µm long (Fig. 6.4.1E). The roof of the conceptacle is composed of irregularly arranged cells and is near 50 µm thick (Fig. 6.4.1E).

	Diameter	Height
Vegetative cells	11-36 [24 mean; 7.5 s.d.; 27 mode]	11.5-44 [25 mean; 6.5 s.d.; 26 mode]
Conceptacles [μm]	315-320	200-245

Table 6.4.1 : biometry of *Lithoporella melobesioides.*

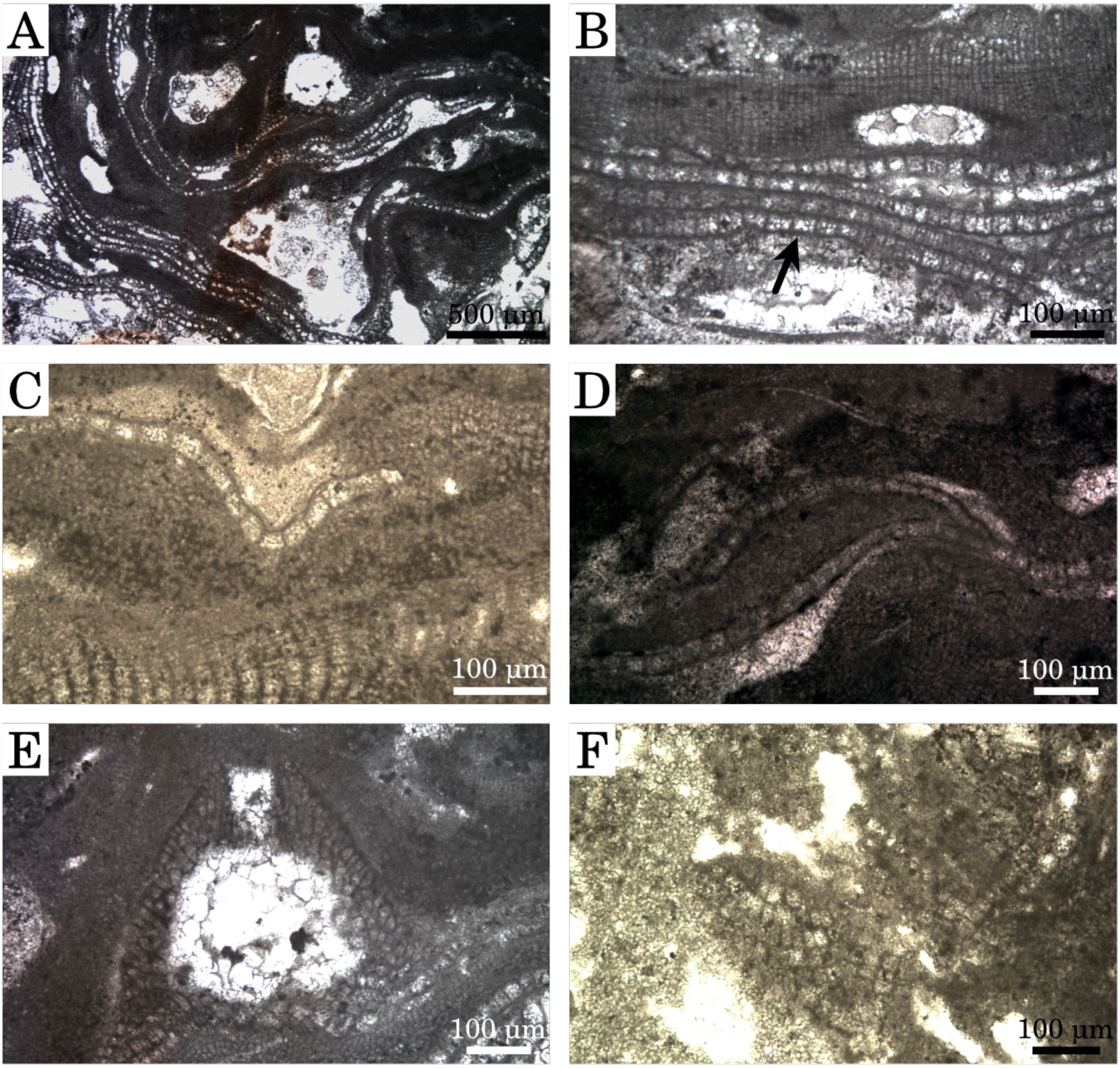

Figure 6.4.1 : *Lithoporella melobesioides*. A) BTP, Uviglie, Lithozone 4, thallus overview. B) BTP, Uviglie, Lithozone 4, detail of a series of thalli of *L. melobesioides*; black arrow=thallus of L. melobesioides. C) BTP, Uviglie, Lithozone 2, monostromatic thallus. D) Sommières, Souvignargues, monostromatic thallus. E) BTP, Uviglie, Lithozone 4, detail of the reproductive anatomy. F) BTP, Uviglie, Lithozone 2, detail of the basal disk.

6.5 – *Lithoporella minus*

Systematic Paleontology

Class Florideophyceae CRONQUIST, 1960

Sub-class Corallinophycidae LE GALL and SAUNDERS, 2007

Order CORALLINALES SILVA and JOHANSEN, 1986

Family Corallinaceae LAMOROUX, 1812

Genus *Lithoporella* FOSLIE, 1909

Lithoporella minus JOHNSON, 1964

Description

Thallus encrusting, consisting of a very thin single layer of cells, with a diameter of 8 to 19 µm and 11 to 21 µm high (Tab. 6.5.1; Fig. 6.5.1). Crusts are commonly formed by various thalli stacked on each other (Fig 6.5.1). The thallus sprouts radially from a basal disk that can be observed along section parallel to the surface on which *L. minus* grow (Fig. 6.5.1C). Adjacent cells are connected by cell fusions. Trichocytes have not been observed. All the observed specimens were infertile.

	Diameter	Height
Vegetative cells	8-19 [12 mean; 3 s.d.; 27]	11-21 [14.5 mean; 2.5 s.d.]

Table 6.5.1 : biometry of *Lithoporella minus*.

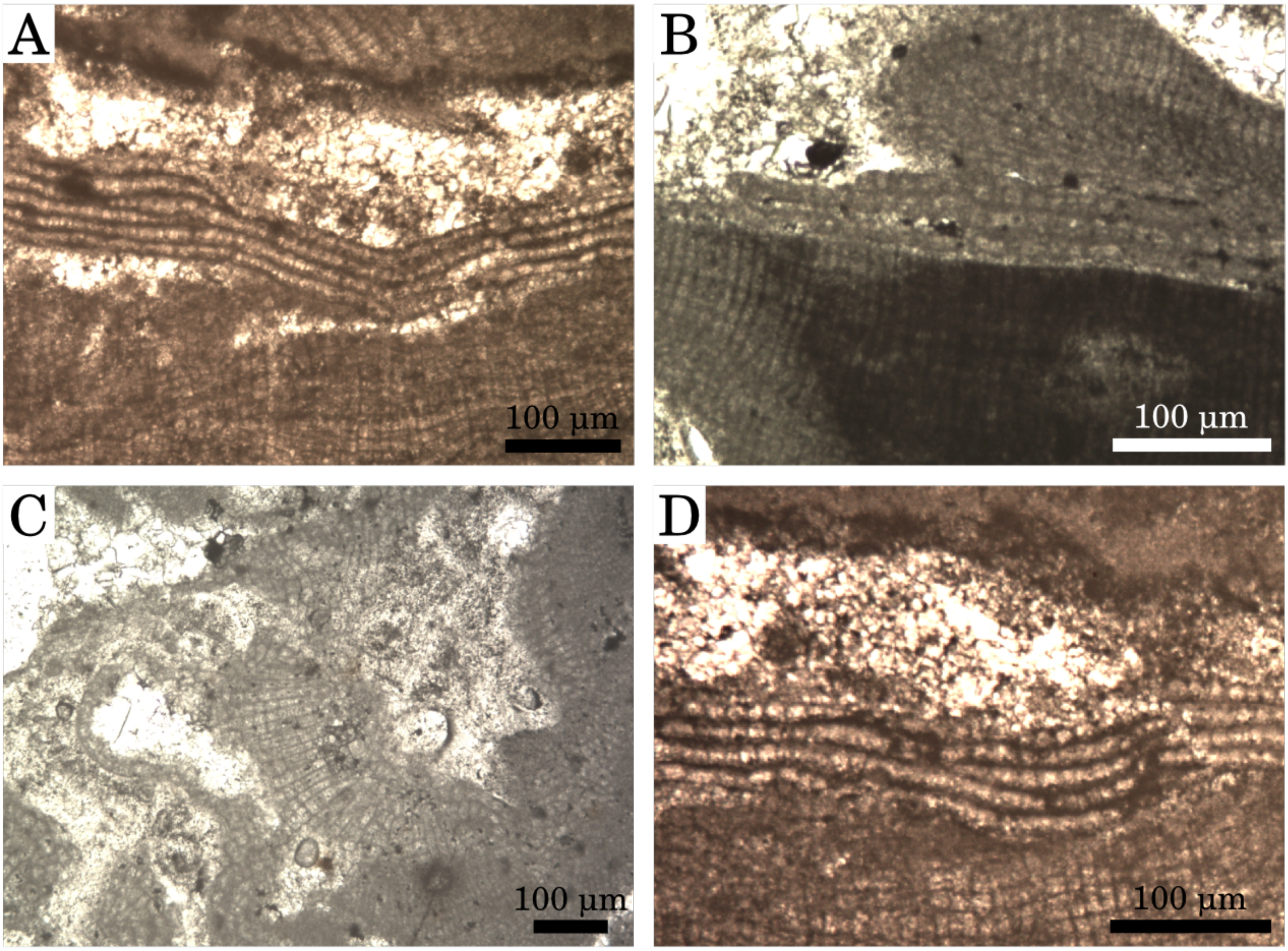

Figure 6.5.1 : *Lithoporella minus*. A) BTP, Treville. B) Sommières Basin, Pondres, Lithozone 4. C) Sommières Basin, Pondres, Lithozone 4, basal disk D) BTP, Treville.

6.6 – *Mesophyllum roveretoi*

Systematic Paleontology

Class Florideophyceae CRONQUIST, 1960

Sub-class Corallinophycidae LE GALL and SAUNDERS, 2007

Order Hapalidiales NELSON et al., 2015

Family Hapalidiaceae GRAY, 1864 (emended HARVEY et al., 2003)

Subfamily Melobesioideae BIZZOZERO, 1885

Genus *Mesophyllum* LEMOINE, 1928

Mesophyllum roveretoi CONTI, 1943

Description

Encrusting to warty growth form (Fig. 6.6.1). Protuberances are formed by various thalli stacked onto each other. Crusts 200 to 800 µm thick (Fig. 6.6.1B-D). Monomerous organization, coaxial ventral core 100 to 150 µm thick (Fig. 6.6.2A-B). Ventral core cells elongated and rectangular in section, 5 to 12 µm in diameter and 10 to 30 µm in length; the shortest cells are at the periphery while the longest are at the center of the ventral core (Tab. 6.6.1; Fig. 6.6.2A-B). Peripheral zone with the irregular alternation of larger cells and smaller cells (Fig. 6.6.2C). The cells of the peripheral zone are elongated and rectangular in section, 5-10 µm in diameter and 6-15 µm in height; larger and longer cells (up to 35-50 µm) border multiporate conceptacles (Tab. 6.6.1; Fig. 6.6.2). Cells of adjacent filaments are connected by cells fusion, the fusion are very common in both the peripheral zone and the ventral core (Fig. 6.6.2). Trichocytes have not been observed.

Epithallial cells have not been observed.

Multiporate sporangial conceptacles are moderately raised above the surrounding thallus surface (Fig. 6.6.2D-F). Conceptacle chambers are elliptical in shape, 190 to 450 μm in diameter and 90 to 250 μm high (Tab. 6.6.1: Fig. 6.6.2D-F). The chambers are very often filled by large adventitious cells (Fig. 6.6.2F). The roof of the conceptacles is flat, 25 to 60 μm thick (Tab. 6.6.1). The pore canals are conical and taper toward the roof; they are 10 to 20 μm wide and 30-40 μm long (Tab. 6.6.1).

Gametangial plants are dioecious.

The male gametangial thallus has the same vegetative anatomy of the sporangial thallus (Tab. 6.6.1; Fig. 6.6.3). Uniporate male gametangial conceptacles are slightly raised from the surrounding thallus surface, the chambers are very narrow and flask-shaped, they measure 170 to 325 μm of diameter and they are 40 to 120 μm high (Tab. 6.6.1; Fig. 6.6.3D-E). The pore canals are narrow (about 30 μm wide) and short. Conceptacle roof is 30 to 40 μm thick.

The female gametangial plant vegetative anatomy is similar to those of the male gametangial and sporangial plants (Tab. 6.6.1; Fig. 6.6.4). Unfertilized uniporate female conceptacles are raised from the surrounding thallus surface, the chambers are narrow and flask-shape, they measure 180 to 250 μm in diameter and they are 50 to 100 μm high (Tab. 6.6.1; Fig. 6.6.4C). The pore canals are cone-shaped, narrow (about 30 μm wide) and short (Fig. 6.6.4C). The roof of the conceptacle is 35 to 70 μm thick. After presumed karyogamy, carposporophytes develop within female conceptacles and the chambers become larger, 380 to 500 μm in diameter and 135 to 155 μm high (Tab. 6.6.1; Fig. 6.6.4D-E). The floor of the carposporangial conceptacles generally presents a central columella (Fig. 6.6.4D-E).

Sporangial thallus		
	Diameter	Height
Ventral core (hypothallus) cells [µm]	5-12 [7.5 mean; 2 s.d.]	10-30 [19.3 mean; 5 s.d.]
Peripheral zone (perithallus) cells [µm]	5-10 [6.85 mean; 1 s.d.]	6-15 [11.1 mean; 2 s.d.]
Conceptacles [µm]	190-450 [305 mean; 50 s.d.]	90-250 [165 mean; 25 s.d.]
H/D ratio	0.35-0.69 [0.55 mean; 0.09 s.d.]	
Roof thickness [µm]	25-60 [45 mean]	
Pore canal	10-20 [13.5 mean]	30-40 [35 mean]
Male gametangial thallus		
Ventral core (hypothallus) cells [µm]	5-9 [7 mean; 1 s.d.]	10-30 [18.1 mean; 6 s.d.]
Peripheral zone (perithallus) cells [µm]	4-8 [5.7 mean; 1 s.d.]	7-15 [11 mean; 2.5 s.d.]
Conceptacles [µm]	170-325 [265 mean; 55 s.d.]	40-120 [80 mean; 25 s.d.]
H/D ratio	0.18-0.4 [0.3 mean; 0.06 s.d.]	
Female gametangial thallus		
Ventral core (hypothallus) cells [µm]	5-10 [7.5 mean; 2 s.d.]	10-37[18.5 mean; 7.5 s.d.]
Peripheral zone (perithallus) cells [µm]	5-9 [6.75 mean; 1 s.d.]	5-17 [11.1 mean; 2.5 s.d.]
Conceptacles unfertilized [µm]	180-250 [220 mean; 60 s.d.]	50-100 [70 mean; 25 s.d.]
Carposporangial conceptacles [µm]	380-500 [425 mean]	135-155 [145 mean]

Table 6.6.1 : biometry of *Mesophyllum roveretoi*.

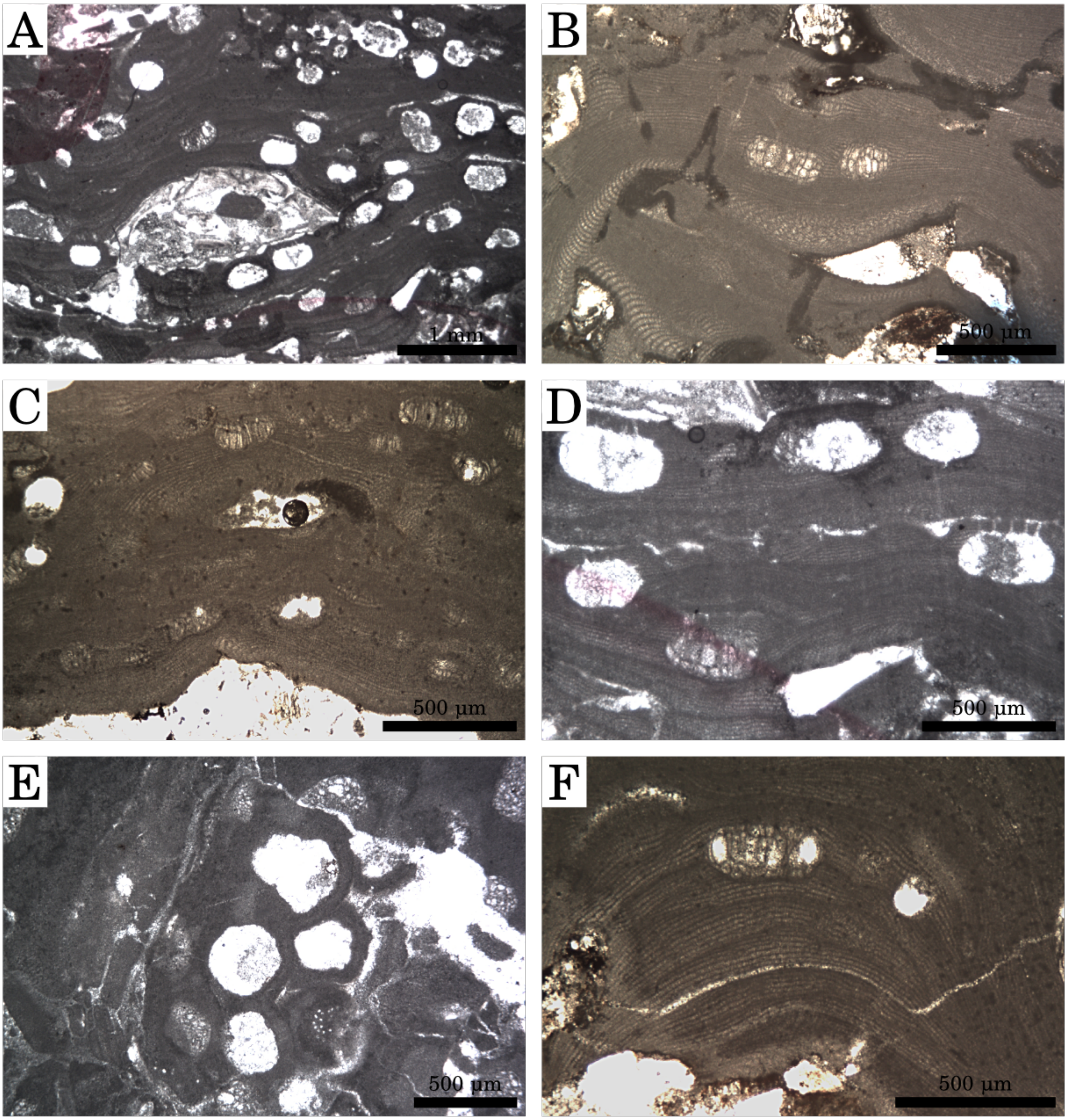

Figure 6.6.1 : *Mesophyllum roveretoi*. A) BTP, Uviglie, Lithozone 4, thallus overview. B) Sommières Basin, Pondres, Lithozone 1, thallus overview. C) Sommières Basin, Pondres, Lithozone 1, thallus overview. D) BTP, Uviglie, Lithozone 4, reproductive anatomy. E) BTP, Uviglie, Lithozone 4, equatorial section of multiporate conceptacles. F) Sommières Basin, Pondres, Lithozone 4, reproductive anatomy.

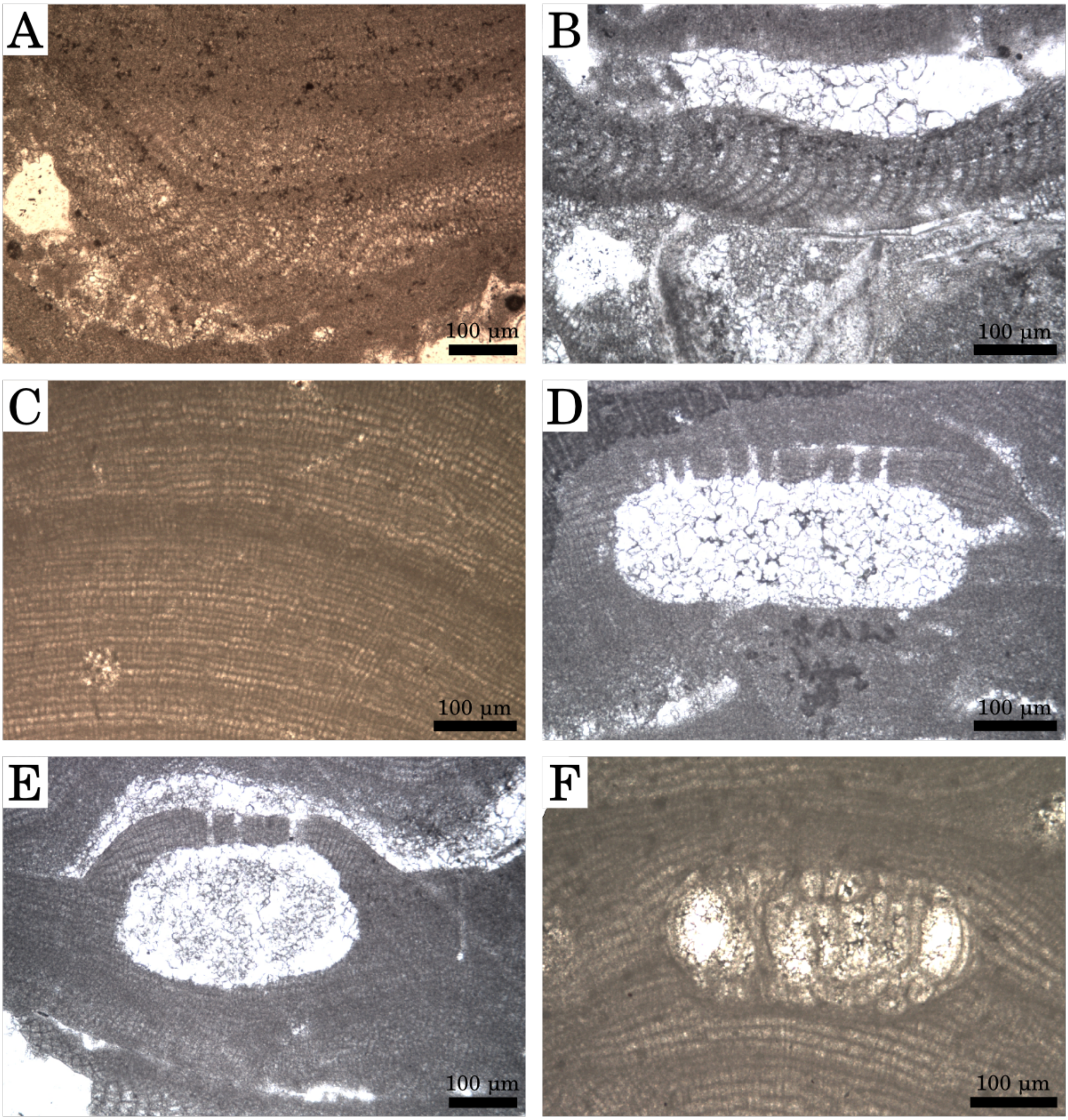

Figure 6.6.2 : *Mesophyllum roveretoi*. A) BTP, Uviglie, Lithozone 2, coaxial ventral core. B) BTP, Uviglie, Lithozone 4, coaxial ventral core. C) BTP, Treville, detail of the peripheral zone. D) BTP, Uviglie, Lithozone 4, multiporate conceptacle. E) BTP, Uviglie, Lithozone 4, multiporate conceptacle. F) Sommières Basin, Pondres, Lithozone 4, multiporate conceptacle.

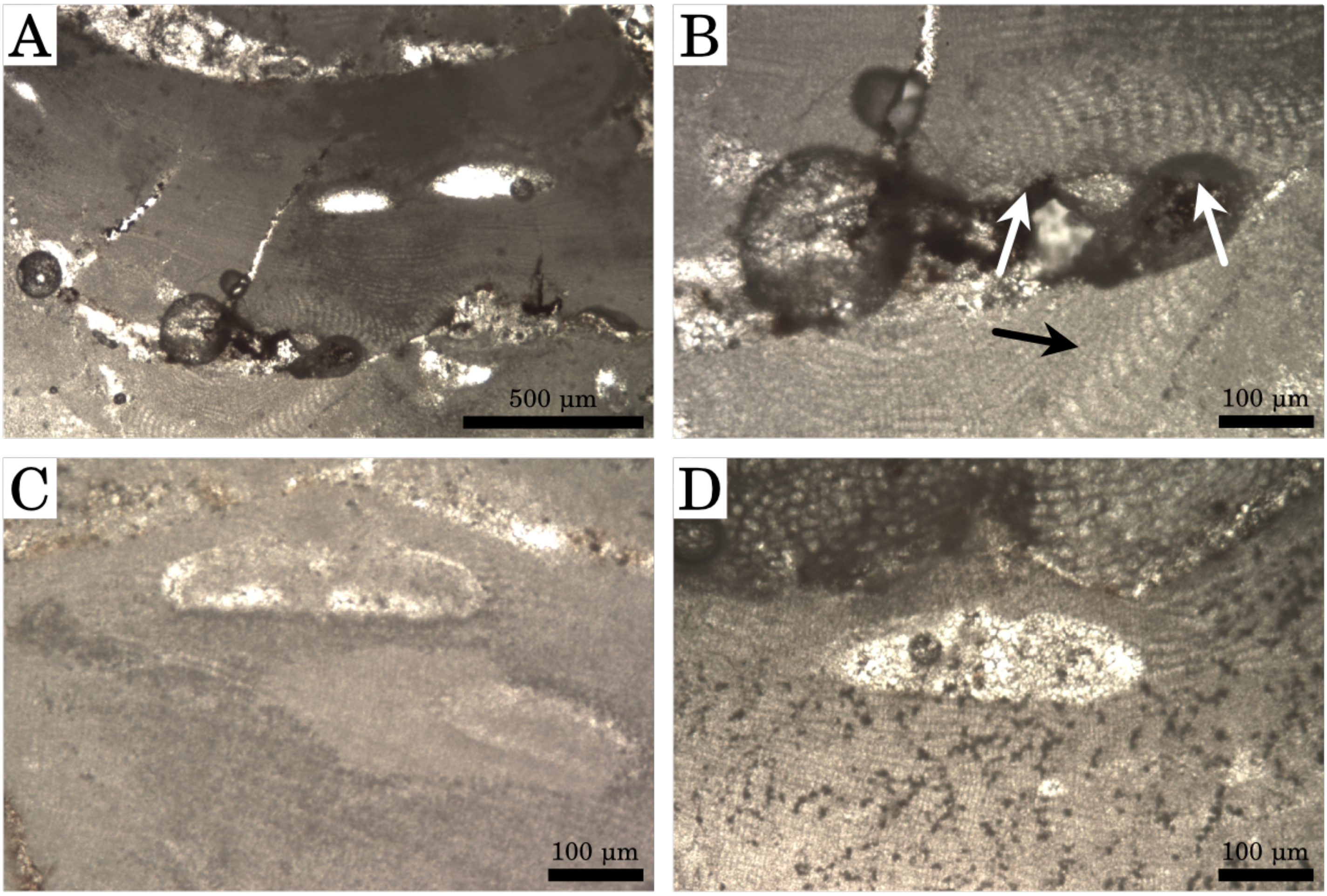

Figure 6.6.3 : *Mesophyllum roveretoi*, gametangial male thallus. A) Sommières Basin, Pondres, Lithozone 1, thallus overview. B) Sommières Basin, Pondres, Lithozone 1, coaxial ventral core; white arrows=coaxial ventral core of male *M. roveretoi*; black arrow= coaxial ventral core of an asexual *M. roveretoi* thallus. C) Sommières Basin, Pondres, Lithozone 1, uniporate conceptacles. D) Sommières Basin, Pondres, Lithozone 1; uniporate conceptacle.

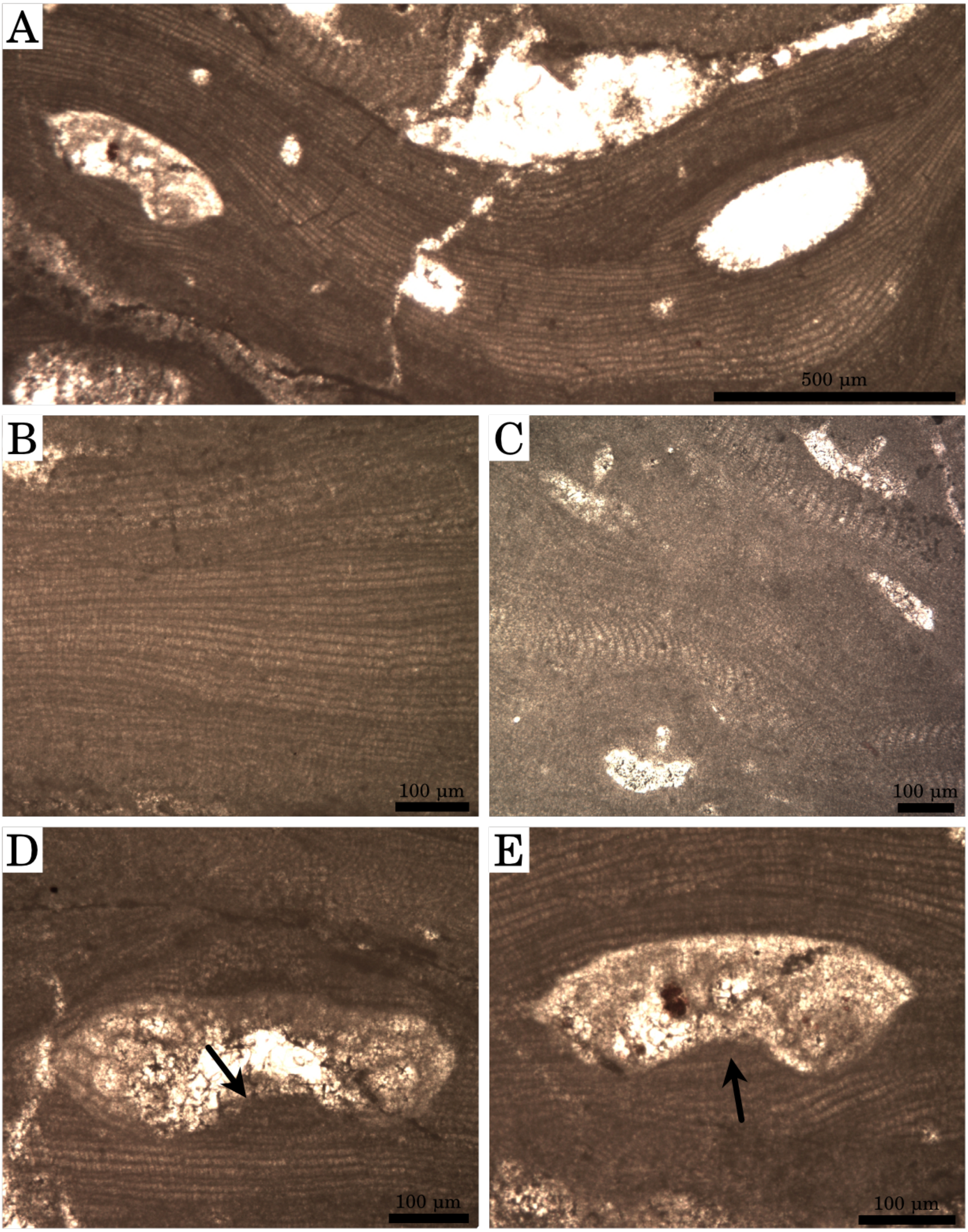

Figure 6.6.4 : *Mesophyllum roveretoi*, gametangial female thallus. A) BTP, Treville, thallus overview. B) BTP, Treville detail of zone peripheral zone. C) Sommières, Pondres, Lithozone 4, unfertilized female conceptacles. D) BTP, Treville, carpsporangial conceptacle; black arrow=columella. E) BTP, Treville, carpsporangial conceptacle; black arrow=columella.

6.7 – *Lithothamnion ponzonense*

Systematic Paleontology

Class Florideophyceae CRONQUIST, 1960

Sub-class Corallinophycidae LE GALL and SAUNDERS, 2007

Order Hapalidiales NELSON et al., 2015

Family Hapalidiaceae GRAY, 1864 (emended HARVEY et al., 2003)

Subfamily Melobesioideae BIZZOZERO, 1885

Genus *Lithothamnion* HEYDRICH, 1897

Lithothamnion ponzonense CONTI, 1943

Description

Encrusting to warty growth form (Fig. 6.7.1; Fig. 6.7.2). The protuberances (2. mm in diameter and more than 2.5 mm of length) are formed by various thalli stacked onto each other. Thalli have a thickness of 200 µm to 1 mm (Fig. 6.7.1; Fig. 6.7.2). Plants with monomerous organization with a non-coaxial ventral core 50 to 150 µm thick (Fig. 6.7.1C); interposed, thin, secondary ventral core are common between stacked thalli. Ventral core cells are rectangular in section, 11 to 23 µm in length and 6-15 µm in diameter (Tab. 6.7.1; Fig. 6.7.1C). Peripheral zone is characterized by lensoid zones created by the irregular alternation of larger and smaller cells (Fig. 6.7.1; Fig. 6.7.2). Peripheral-zone cells are square to rectangular in section, 7 to 17 µm high and 6 to 12 µm wide (most common values around 10x10µm; Tab. 6.7.1). At the sides of the conceptacle chambers, cells are significantly longer (Fig. 6.7.1; Fig. 6.7.2). Cells of adjacent filaments in the thallus are connected by cell fusions. Trichocytes have not been observed. Epithallial cells have not been clearly observed.

Multiporate sporangial conceptacles are slightly raised above the surrounding thallus surface (Fig. 6.7.1; Fig. 6.7.2). Conceptacle chambers are rectangular to elliptical in shape, 190 to 500 µm in diameter and 70 to 150 µm high (Tab. 6.7.1; Fig. 6.7.1; Fig. 6.7.2). Conceptacles with a remarkably larger diameter, created by the merging of two nearby conceptacles, were observed in most of the specimens (Fig. 6.7.1A; Fig. 6.7.2.D). Conceptacles chambers are sometimes filled by large adventitious cells (Fig. 6.7.2). The roof of the conceptacles is 20 to 40 µm thick (Tab. 6.7.1; Fig. 6.7.1; Fig. 6.7.2).

Description of the Holotype

Encrusting to warty growth form (Fig. 6.7.3). The protuberances (2mm in diameter and 3 mm of length) are formed by various thalli stacked onto each other. The thallus has a thickness of 200 µm to 1 mm. Plants with monomerous organization with a non-coaxial ventral core 50 to 150 µm thick; interposed, thin, secondary ventral core are common between stacked thalli (Fig. 6.7.3D). Ventral core cells are rectangular in section, 9 to 21 µm in length and 8-13 µm in diameter (Tab. 6.7.1; Fig. 6.7.3D). Peripheral zone characterized by lensoid zones created by the irregular alternation of larger and smaller cells (Fig. 6.7.3). Peripheral-zone cells are square to rectangular in section, 7 to 16 µm high and 8 to 13 µm wide (Tab. 6.7.1; Fig. 6.7.3). At the sides of conceptacle chambers cells are remarkably longer. Cells of adjacent filament in the thallus are connected by cell fusions. Epithallial cells are flattened; sub-epithallial initials are long as or slightly longer than their inward derivatives (Fig. 6.7.3F).

Multiporate sporangial conceptacles are slightly raised above the surrounding thallus surface (Fig. 6.7.3G-H). Conceptacle chambers are rectangular to elliptical in shape, 315 to 470 µm in diameter and 90 to 120 µm high (Tab. 6.7.1; Fig. 6.7.3G-H). Larger conceptacles, created by the merging of two nearby conceptacles, were observed (Fig. 6.7.3C). Conceptacles chambers are often filled by large adventitious cells (Fig. 6.7.3E). The roof of the conceptacles is 15 to 35 µm thick.

In the holotype a female gametangial thallus is also preserved (Fig. 6.7.4). The plant has the same vegetative anatomy of the sporangial thallus (Fig. 6.7.4). Unfertilized uniporate female conceptacles are small and narrow (Fig. 6.7.4D). After presumed karyogamy, carposporophytes develop within the female conceptacles, the chambers become larger, 495 to 500 µm in diameter and 110 to 140 µm high (Tab. 6.7.1; Fig. 6.7.4A-C). The pore canal is cone-shaped and broad, 100 µm wide and 150 µm long. The floor of carposporangial conceptacles may presents a central columella (Fig. 6.7.4A).

Sporangial thallus (Sommières Basin and Pietra da Cantoni Group)		
	Diameter	Height
Ventral core (hypothallus) cells [µm]	6-15 [9.8 mean; 2 s.d.]	11-23 [16.5 mean; 2.5 s.d.]
Peripheral zone (perithallus) cells [µm]	6-12 [9.4 mean; 1.5 s.d.]	7-17 [10.9 mean; 2 s.d.]
Conceptacles [µm]	190-500 [320 mean; 80 s.d.]	70-150 [115 mean; 20 s.d.]
H/D ratio	0.22-0.47 [0.34 mean; 0.06 s.d.]	
Roof thickness [µm]	20-35 [26 mean]	
Holotype Sporangial thallus (Ponzone, NW Italy)		
Ventral core (hypothallus) cells [µm]	8-13 [10.3 mean]	9-21 [15 mean]
Peripheral zone (perithallus) cells [µm]	8-13 [10 mean; 1.2 s.d.]	7-16 [11.9 mean; 2.2. s.d.]
Conceptacles [µm]	315-470 [390 mean]	90-120 [105 mean]
H/D ratio	0.21-0.35 [0.28 mean]	
Roof thickness [µm]	15-35 [25 mean]	
Holotype Female gametangial thallus (Ponzone, NW Italy)		
Carposporangial conceptacles [µm]	495-500	110-140

Table 6.7.1 : biometry of *Lithothamnion ponzonense.*

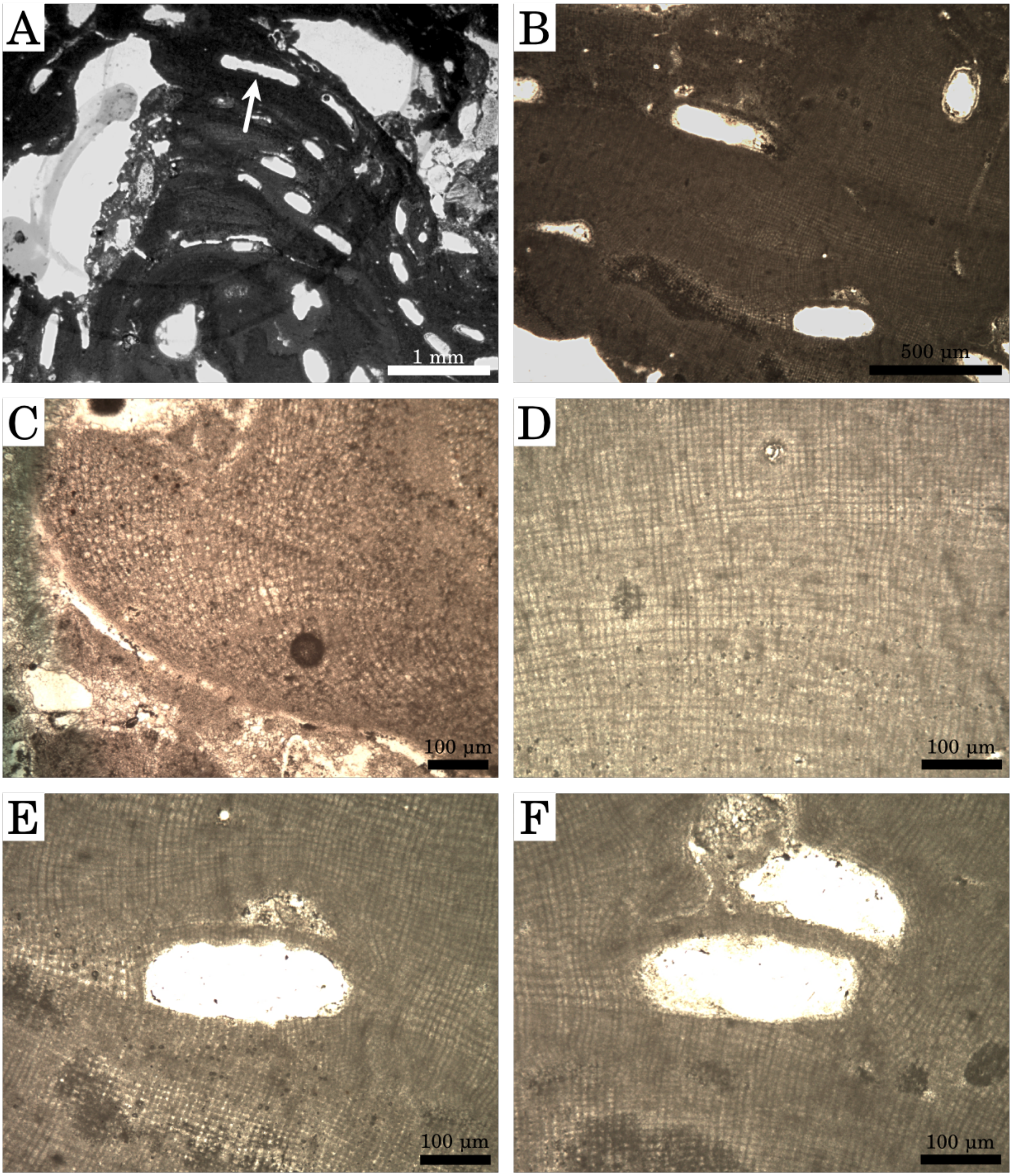

Figure 6.7.1 : *Lithothamnion ponzonense*, BTP, Uviglie, Lithozone 2. A) Thallus overview; white arrow=fused (double) conceptacles. B) Vegative and reproductive anatomy. C) Non-coaxial ventral core. D) Detail of the peripheral zone. E) Multiporate conceptacle. F) Multiporate conceptacle.

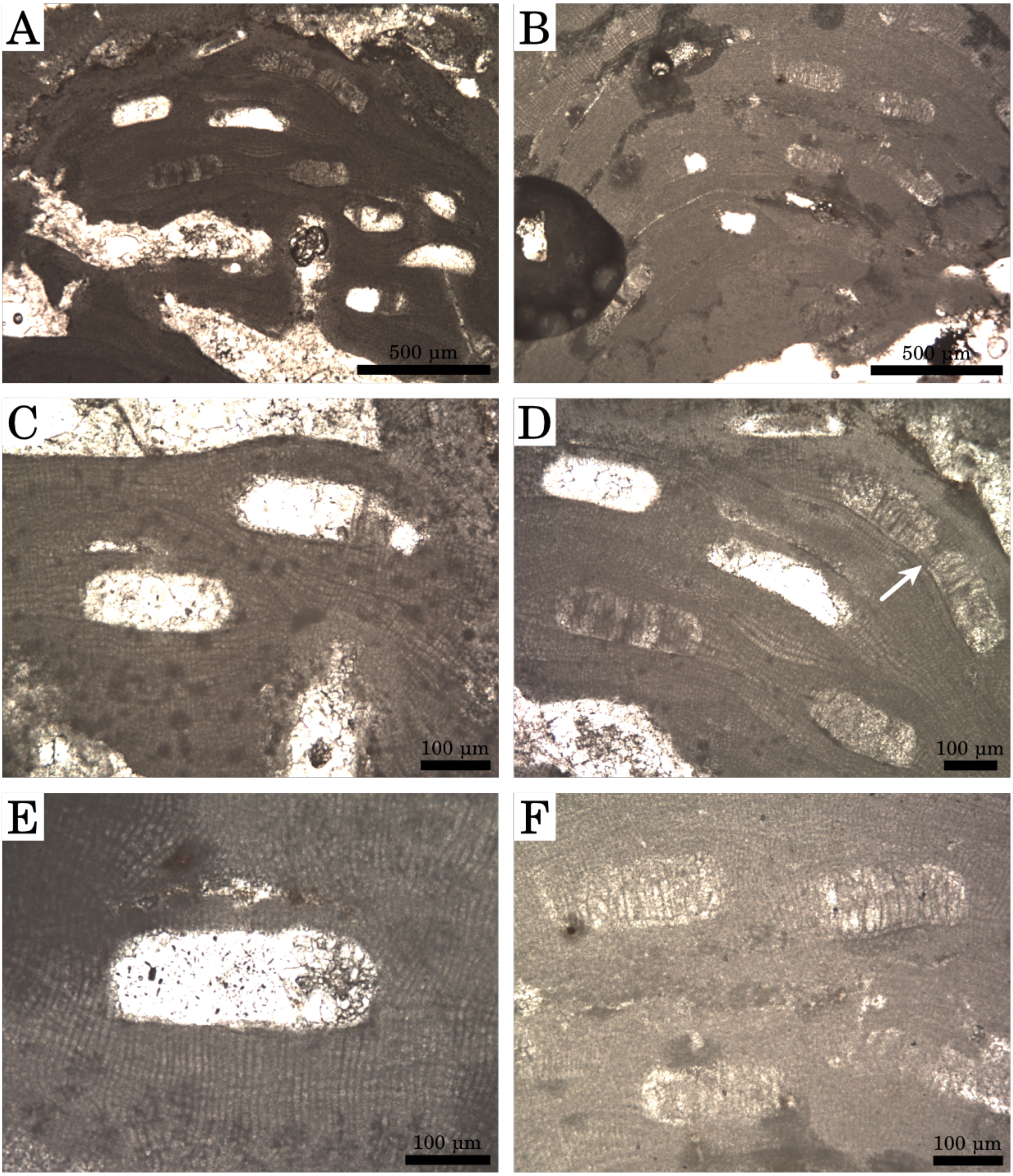

Figure 6.7.2 : *Lithothamnion ponzonense*, Sommières Basin, Pondres. A) Lithozone 1, thallus overview. B) Lithozone 4, thallus overview. C) Lithozone 4, multiporate conceptacles. D) Lithozone 1, multiporate conceptacles; white arrow= conceptacles in the process of fusing together. E) Lithozone 1, detail of a multiporate conceptacle. F) Lithozone 1, couple of multiporate conceptacles filled by adventitious cells.

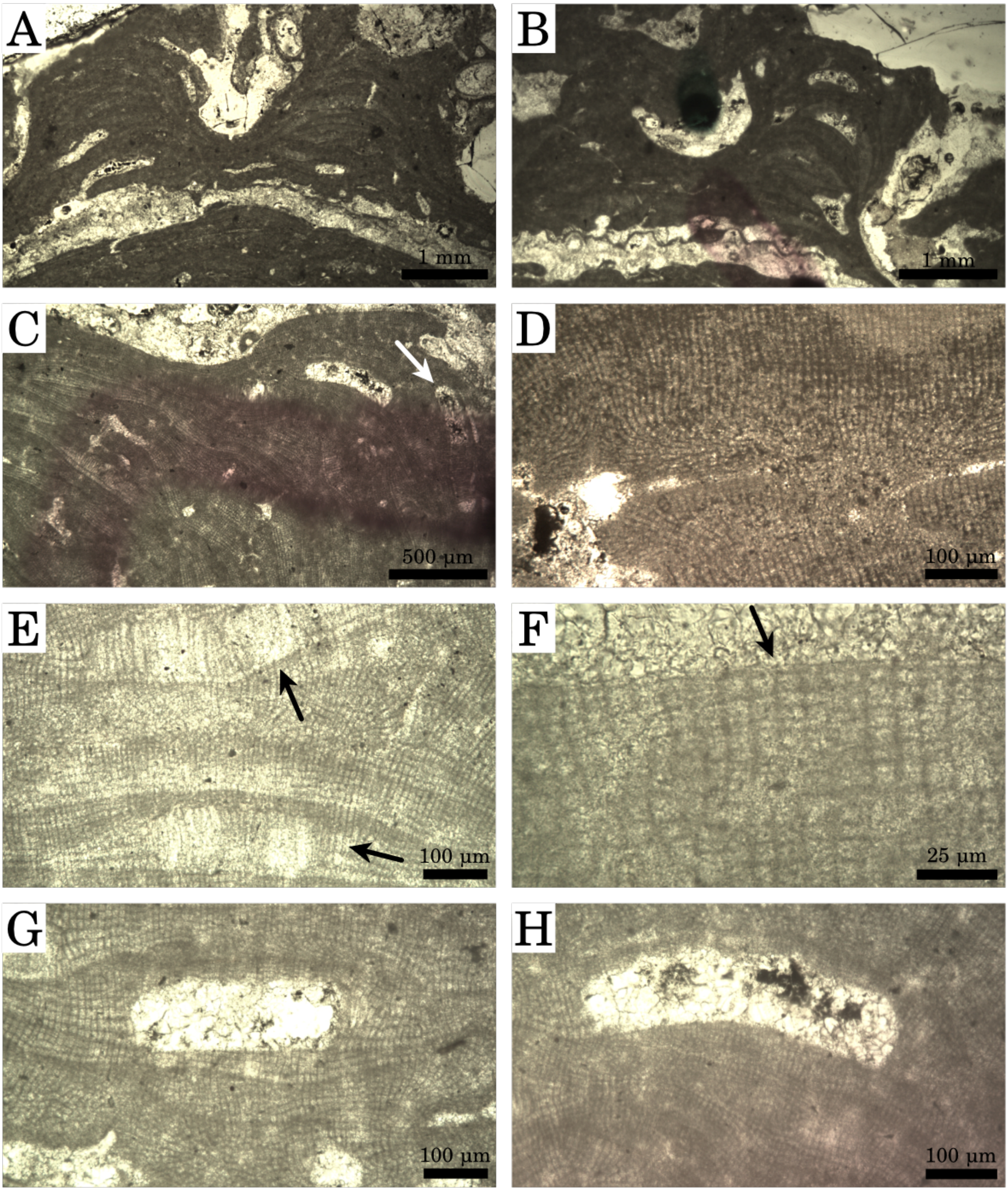

Figure 6.7.3 : *Lithothamnion ponzonense*, holotype, Miocene, Ponzone, NW Italy. A) Thallus overview. B) Overview of the female gametangial thallus. C) Vegetative and reproductive anatomy; white arrows=fused (double) conceptacles. D) Secondary ventral core. E) Zoned peripheral zoned with conceptacles filled by adventitious cells; black arrows=conceptacles filled by long cells. F) Epithallial layer, with sub epithallial intial slightly longer that their invard derivatives; black arrow= epithallial layer G) Multiporate conceptacle. H) Multiporate conceptacle.

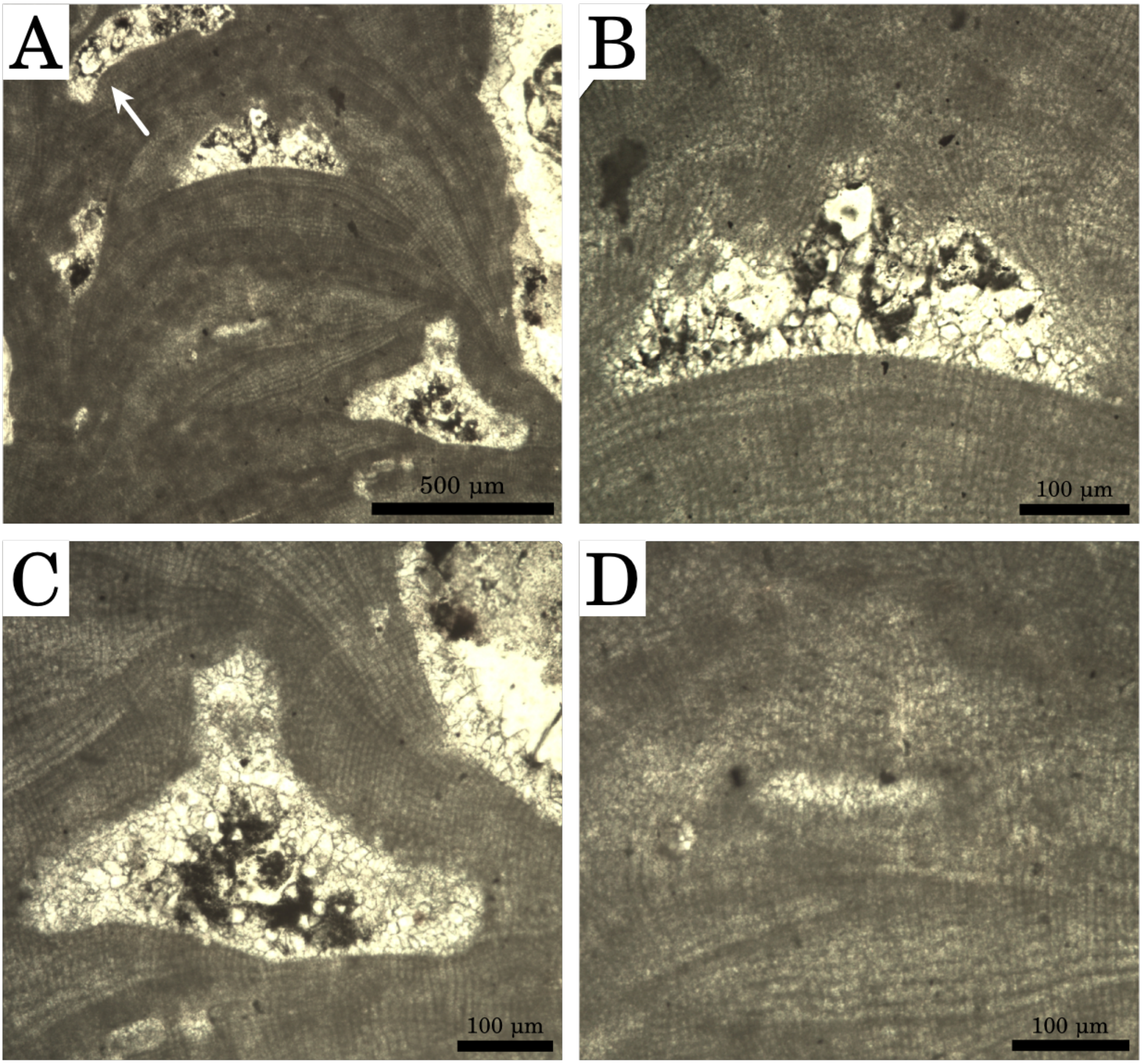

Figure 6.7.4 : *Lithothamnion ponzonense*, female gametangial plant; holotype, Miocene, Ponzone, NW Italy. A) Overview of the female gametangial thallus; white arrow=central columella of a carposporangial conceptacle. B) Carposporangial conceptacle. C) Carposporangial conceptacle. D) Unfertilized female conceptacle.

6.8 – *Lithothamnion crispatum*

Lithothamnion crispatum **: long-lasting species of non-geniculate coralline algae (Rhodophyta, Hapalidiales)**

Giovanni Coletti

Juraj Hrabovský

Daniela Basso

Carnets de Geologie – Notebooks on Geology (2016, under review).

Introduction

According to taxonomic uniformitarianism it is possible to extrapolate the ecological significance of modern species to their fossil counterparts. In most cases this core principle of paleoecology can be safely applied at least for paleoenvironments not older than the Miocene (Haunold et al. 1997; Aguirre et al. 2000). To accomplish this goal, recent species need reliable identification in the fossil record achievable through the application of the same criteria used in biological classification. In this way, the biological and paleontological classifications can be made consistent as far as fossil preservation allows. For coralline algae this approach has been developed in various contributions (Braga et al. 1993; Basso et al. 1996; Basso et al. 1997; Rasser and Piller, 1999; Rasser and Piller, 2000; Bassi et al. 2009; Iryu et al. 2009; Aguirre et al. 2012; Woelkerling et al. 2014; Hrabovský et al. 2015).

The aim of this paper is to contribute to this development by introducing a new diagnostic character never seen nor described before in the fossil material: the presence of pits surrounding the pore canals in the roof of the sporangial conceptacles. This is the key morphological feature of the non-geniculate coralline *Lithothamnion crispatum* Hauck 1978, unknown as a fossil until now. Fossils from the Pleistocene and the Miocene have been compared with modern Mediterranean specimens of *L. crispatum* to assess and study their relationship. The modern cosmopolitan distribution of *L. crispatum* includes the Mediterranean (Bressan and Babbini, 2003; Basso et al. 2011), the Atlantic Ocean (Keats et al. 2000; Nóbrega-Farias et al. 2010), the Indian Ocean (Silva et al. 1996), the Pacific coast of Australia (Harvey et al. 2003) and the northern coast of New Zealand (Neill et al. 2015). Living specimens have been collected from 2 to 80 m of water depth, as rhodoliths or crusts attached on hard substrates, particularly in well lit waters

(Keats et al. 2000; Nóbrega-Farias et al. 2010; Basso et al. 2011; Pascelli et al. 2013; Neill et al. 2015).

This species has a complex taxonomic history (details in Basso et al. 2011). In 2000 Keats et al. established that *Lithothamnion superpositum* is conspecific with *Lithothamnion indicum*. Subsequently Nóbrega-Farias et al. (2010) merged *L. superpositum* with *Lithothamnion heteromorphum*. Finally, in 2011 Basso et al. synonymized *L. heteromorphum* with *L. crispatum*, the Mediterranean species with nomenclatural priority. As a consequence of these taxonomic revisions, the geographic and ecological distribution of the species has become very broad, encompassing all the oceans and both hemispheres. The key feature that allowed synonymizing these species is the occurrence of pits over the roof of the multiporate conceptacles, a unique feature among Hapalidiales and a diagnostic feature in the delimitation of this *Lithothamnion* species (Wilks and Woelkerling, 1995). These roof pits are the consequence of the disintegration of the outermost cells in filaments surrounding the pore canals. In the resulting structure the pore canal is slightly raised in the center of a rosette of degenerate cells.

Material and methods

The specimens analyzed come from different localities, with some being studied in previous investigations (Table 1). Different specimens from the same sample or from the same outcrop were grouped together for analysis. Morphological data on Recent *L. crispatum* come from samples collected in the Egads Archipelago of the western Mediterranean (Marettimo Island, Basso et al. 2011).

Geographic Position	Age	N° of thin sections	Collector	Useful references
NW Italy-Tertiary Piedmont Basin-Villa San Bartolomeo	Burdigalian	1	Vannucci G.	Vannucci *et al.*, 1996 and Coletti *et al.*, 2015 for further details regarding the outcrop, the geological setting and coralline algae flora
NW Italy-Tertiary Piedmont Basin-Uviglie	Burdigalian	3	GC	
NW Italy-Tertiary Piedmont Basin-Torre Veglio	Burdigalian	2	Vannucci G.	
S France-Sommières Basin-Souvignragues	Burdigalian	1	GC	Reynaud and James, 2012, for further details on the geological setting of the basin
Czech Republic-Central Parathethys-Židlochovice	upper part of Lower Langhian	1	JH	Filipescu and Gìrbacea, 1997; Kováč *et al.*, 2005; Saint Martin *et al.*, 2007 Dolakova *et al.*, 2008; Hrabovský *et al.*, 2015, for information regarding the geological setting and coralline algae flora
Romania-Central Parathethys-Lopadea Veche	upper part of Lower Langhian	1	JH	
Slovakia-Parathethys-Stupava-Vrchná Hora	Upper Langhian	1	JH	
Slovakia-Parathethys-Sandberg	Lower Serravallian	1	JH	
S Italy-Sicily-Castelluccio	Pleistocene	3	DB	

Table 6.8.1 : Fossil samples analyzed.

Fossil samples were cut with an abrasive rock saw, and the porosity was then filled with epoxy resin. The surfaces were polished with silicon carbide and glued onto standard glass slides. The excess material was subsequently cut off and the thickness of the sample was reduced to less than 30 µm. The thin sections of coralline algal samples were then observed under light microscope to study and measure their anatomical features. Growth-forms terminology follows Woelkerling et al. (1993). Vegetative anatomy was measured along longitudinal radial sections (Quaranta et al. 2007; Vannucci et al. 2008). The diameter of the cells was measured including the cell wall; cell length was measured as the distance between two primary pit connections including the cell wall (Basso et al.

1996). Conceptacles were measured along their axial section (i.e., the longitudinal section that cuts a conceptacle medially so that the pore canal is completely visible Afonso-Carillo et al. 1984), in accordance to Quaranta et al. (2007) and Vannucci et al. (2008). Very large conceptacle chambers, clearly resulting from the merging of two nearby conceptacles, were not considered in statistical analyses. The diameter of the roof pits was measured either in the axial section of conceptacles or in the equatorial section tangential to the roof-top layer of cells. The length of the degenerate cells (i.e., the depth of the roof pit around the pore canal) was measured in the axial section of the conceptacles.

Analysis of variance (ANOVA) was employed to support the morphological comparison of the specimens and Levene's test was used to assess the equality of variances. Since ANOVA can analyze only one character at time, the H/D ratio of asexual conceptacle chambers was used, because it summarizes both conceptacle dimensions. In order to analyze differences and similarities between the samples further, multivariate statistics were performed with PRIMER 6 (Kruskal, 1977; Field et al. 1982; Clarke and Gorley, 2006). Bray-Curtis (B-C) samples similarity was calculated on average standardized values of the ventral core (hypothallium) and peripheral zone (perithallium) cell size, conceptacles diameter (D) and height (H), H/D ratio and roof thickness. The size of roof pits was not included in this analysis because of the small number of observations in the fossil and because no reference values was available for the modern specimens. Results, based on B-C similarity, were plotted as hierarchical agglomerative dendrograms.

Results

Systematic Paleontology

Class Florideophyceae Cronquist, 1960

Sub-class Corallinophycidae Le Gall & Saunders, 2007

Order Hapalidiales Nelson et al., 2015

Family Hapalidiaceae Gray, 1864 (emended Harvey et al., 2003)

Subfamily Melobesioideae Bizzozero, 1885

Genus *Lithothamnion* Heydrich, 1897

Lithothamnion crispatum Hauck, 1878

Habit and vegetative structure. Fruticose to foliose growth form (Fig. 6.8.1). Protuberances from cylindrical to lamellate, up to 6 mm long and 3 mm wide and commonly club-shaped. Thalli with monomerous organization, with crustose portions 100 to 500 µm thick (Fig. 6.8.2A-B). Ventral core up to 100 µm thick composed of plumose filaments that arch toward the thallus surface to form the peripheral zone (Fig. 6.8.2.C). Ventral core cells are rectangular, 9 to 28 µm in length and 6 to 12 µm in diameter (Tab. 6.8.2). Peripheral zone with alternation of larger cells and smaller cells (Fig. 6.8.2A). Peripheral zone cells rectangular, 8 to 31 µm in length and 8 to 15 µm in diameter (Tab. 6.8.2). Primary pit connections connect cells of the same filament while cells of adjacent filaments are connected by cells fusions (Fig. 6.8.2D); in Recent specimens secondary pit connections have not been observed (see Basso et al. 2011). Trichocytes have not been observed. It was not possible to observe clearly the shape of epithallial cells either due to the abrasion of the upper layer of cells or the excessive thickness of the sections. No significant difference in length was observed between the alleged sub-epithallial initials

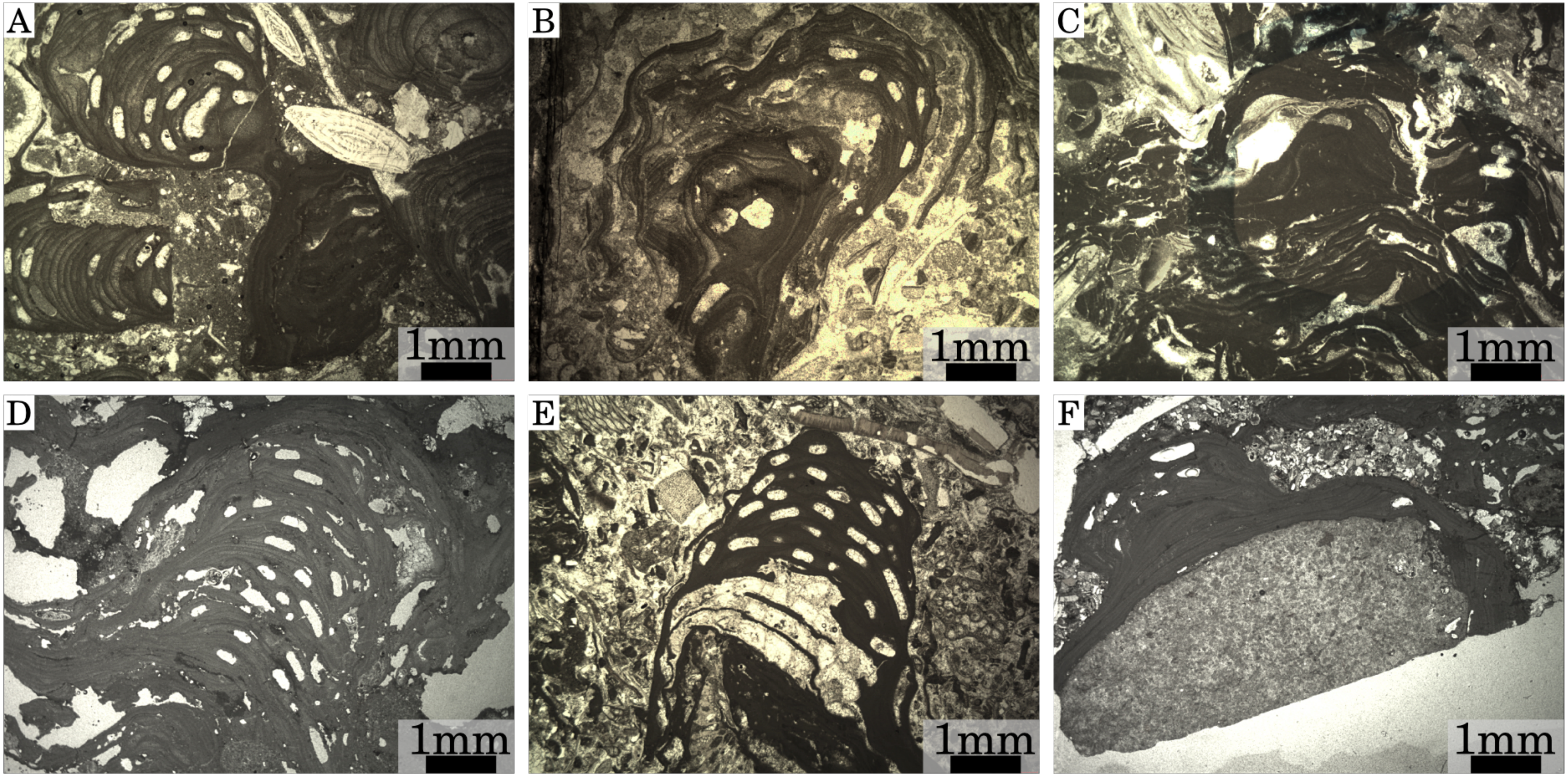

Figure 6.8.1 : Growth-forms of fossil specimens. A) Branches, Upper Langhian, Slovakia, Stupava-Vrchná Hora. B) Wavy crusts, upper part of Lower Langhian, Czech Republic, Židlochovice. C) Crusts in a rhodolith, Burdigalian, NW Italy, Tertiary Piedmont Basin, Villa San Bartolomeo. D) Branch formed by stacked crusts, Pleistocene, S Italy, Castelluccio. E) Branch formed by stacked crusts, upper part of Lower Langhian, Romania, Lopadea Veche. F) Epilithic crust, Pleistocene, S. Italy, Castelluccio.

	L.crispatum Burdigalian Tertiary Piedmont Basin NW Italy	*L.crispatum* Burdigalian Sommières Basin S France	*L.crispatum* upper part of Lower Langhian Židlochovice Czech Republic	*L.crispatum* upper part of Lower Langhian Lopadea Veche Romania	*L.crispatum* Upper Langhian Stupava Slovakia	*L.crispatum* Pleistocene Castelluccio S. Italy	*L.crispatum* Recent Marettimo S Mediterranean
Thallus organization	monomerous	monomerous	monomerous	monomerous	monomerous	monomerous	monomerous
Ventral core structure	Non coaxial plumose	Non coaxial plumose	Non coaxial plumose	Non coaxial plumose	Non coaxial plumose	Non coaxial plumose	Non coaxial plumose
VC cells length	11-28 µm [16 mean; 3.2 s.d.; n=80]	//	10-28 µm [16.8 mean; 4.5 s.d.; n=30]	9-26 µm [16.7 mean; 3.6 s.d.; n=32]	10-26 µm [16.9 mean; 3.5 s.d.; n=42]	13-25 µm [18 mean; n=10]	11-34 µm [18.6 mean; 4.2 s.d.; n=258]
VC cells height	7-12 µm [9.6 mean; 1.6 s.d.; n=80]	//	7-12 µm [10.5 mean; 1.5 s.d.; n=30]	7-11 µm [9.6 mean; 1.2 s.d.; n=32]	6-11 µm [9 mean; 1.5 s.d.; n=42]	7-11 µm [8.5 mean; n=10]	5.5-15 µm [9.5 mean; 2.2 s.d.; n=258]
PF zonation	yes	yes	yes	yes	yes	yes	yes
PF cells lenght	8-22 µm [13.3 mean; 2.3 s.d.; n=160]	10-15 µm [12.5 mean; 1.5 s.d.; n=30]	9-20 µm [13.7 mean; 3 s.d.; n=50]	8-31 µm [14.3 mean; 4.5 s.d.; n=50]	11-20 µm [13.8 mean; 2.4 s.d.; n=42]	9-19 µm [13.2 mean; 2.5 s.d.; n=90]	7-25 µm [15 mean; 3.1 s.d.; n=332]
PF cells diameter	8-14 µm [10.2 mean; 0.9 s.d.; n=160]	9-12 µm [10.5 mean; 1.5 s.d.; n=30]	9-13 µm [10.5 mean; 0.9 s.d.; n=50]	9-15 µm [11.2 mean; 1.2 s.d.; n=50]	9-12 µm [10.4 mean; 0.9 s.d.; n=42]	8-13 µm [10.4 mean; 1 s.d.; n=90]	7-16 µm [12 mean; 1.7 s.d.; n=332]
Conceptacle chamber diameter	265-425 µm [340 mean; 55 s.d.; n=30]	//	280-510 µm [355 mean; 60 s.d.; n=15]	265-415 µm [350 mean; 50 s.d.; n=14]	260-495 µm [390 mean; 80 s.d.; n=14]	290-550 µm [425 mean; 70 s.d.; n=22]	270-720 µm [430 mean; 128 s.d.; n=18]
Conceptacle chamber height	90-135 µm [115 mean; 10 s.d.; n=30]	//	95-140 µm [115 mean; 15 s.d.; n=15]	110-145 µm [130 mean; 10 s.d.; n=14]	110-150 µm [125 mean; 15 s.d.; n=14]	105-190 µm [140 mean; 20 s.d.; n=22]	100-315 µm [177 mean; 66 s.d.; n=18]
Conceptacle H/D ratio	0.29-0.47 µm [0.34 mean; 0.05 s.d.; n=30]	//	0.25-0.49 µm [0.33 mean; 0.07 s.d.; n=15]	0.29-0.5 µm [0.38 mean; 0.06 s.d.; n=14]	0.27-0.44 µm [0.33 mean; 0.06 s.d.; n=14]	0.26-0.39 µm [0.33 mean; 0.05 s.d.; n=22]	0.15-0.57 µm [0.41 mean; 0.11 s.d.; n=19]
Roof thickness	27-48 µm [36 mean; 6 s.d.; n=30]	//	36-50 µm [42 mean; 5 s.d.; n=15]	40-62 µm [50 mean; 6 s.d.; n= 14]	34-51 µm [40 mean; 5 s.d.; n=14]	38-54 µm [46 mean; 6 s.d.; n=22]	20-45 µm [30 mean]
Number of roof cells	3 to 4	//	3 to 4	3 to 6	3 to 4	3 to 5	4 to 6
Diameter of the pits	19-36 µm [28 mean; 5 s.d.; n=20]	//	26-47 µm [31 mean; 5 s.d.; n=17]	43-59 µm [49 mean; 6 s.d.; n=18]	26-44 µm [32 mean; 4 s.d.; n=20]	26-38 µm [34 mean; 3.5 s.d.; n=20]	//
Lenght of the degenerated cells	9-20 µm [14 mean; 4 s.d.; n=20]	//	15-26 µm [20 mean; 3 s.d.; n=17]	20-38 µm [29 mean; 5 s.d.; n=18]	12-24 µm [18.5 mean; 3 s.d.; n=20]	15-24 µm [19.3 mean; 2.5 s.d.; n=20]	//
Number of rosette cells	6 to 7	//	//	//	//	6	5 to 7
Conceptacles position	slightly raised	slightly raised	slightly raised	slightly raised	slightly raised	slightly raised	slightly raised

Tab. 6.8.2 : Comparison of features and biometry of modern and fossil *L. crispatum*. The specimens of *L. crispatum* from the Lower Serravallian of Slovakia, Sandberg locality, were poorly preserved. Since it was not possible to make an appropriate number of measurements for most of the parameters, they are omitted from the table; VC= ventral core; PF=peripheral zone; s.d. =standard deviation; //= insufficient data cover.

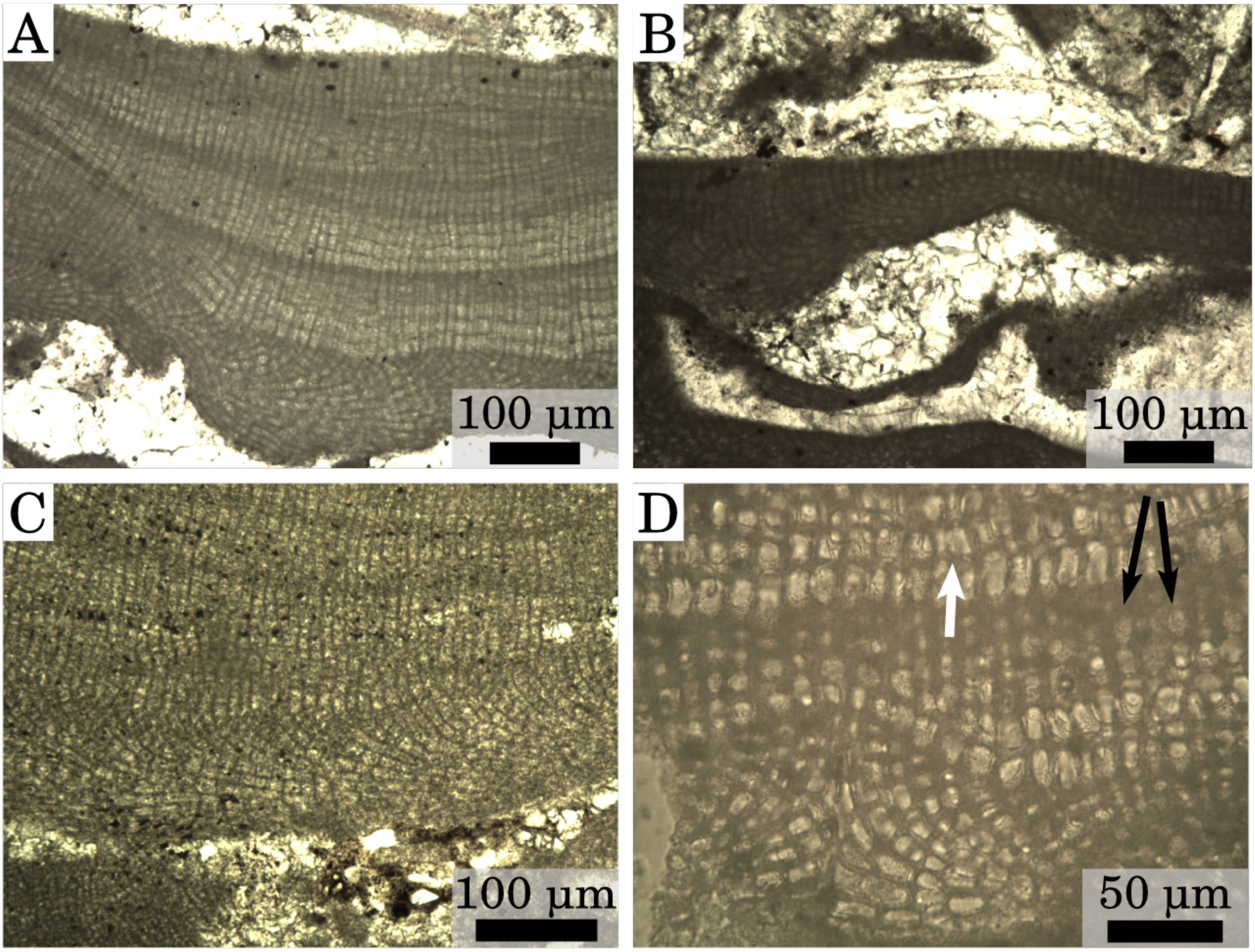

Figure 6.8.2 : Vegetative anatomy. A) Thick crust, upper part of Lower Langhian, Romania, Lopadea Veche. B) Thin crust, upper part of Lower Langhian, Romania, Lopadea Veche. C) Plumose ventral core, Burdigalian, NW Italy, Tertiary Piedmont Basin, Torre Veglio. D) High-magnification detail of a secondary ventral-core and of the overlying peripheral zone, Burdigalian, NW Italy, Tertiary Piedmont Basin, Uviglie, Lithozone 2; white arrow=cell fusion; black arrows=cell filaments with visible primary pits.

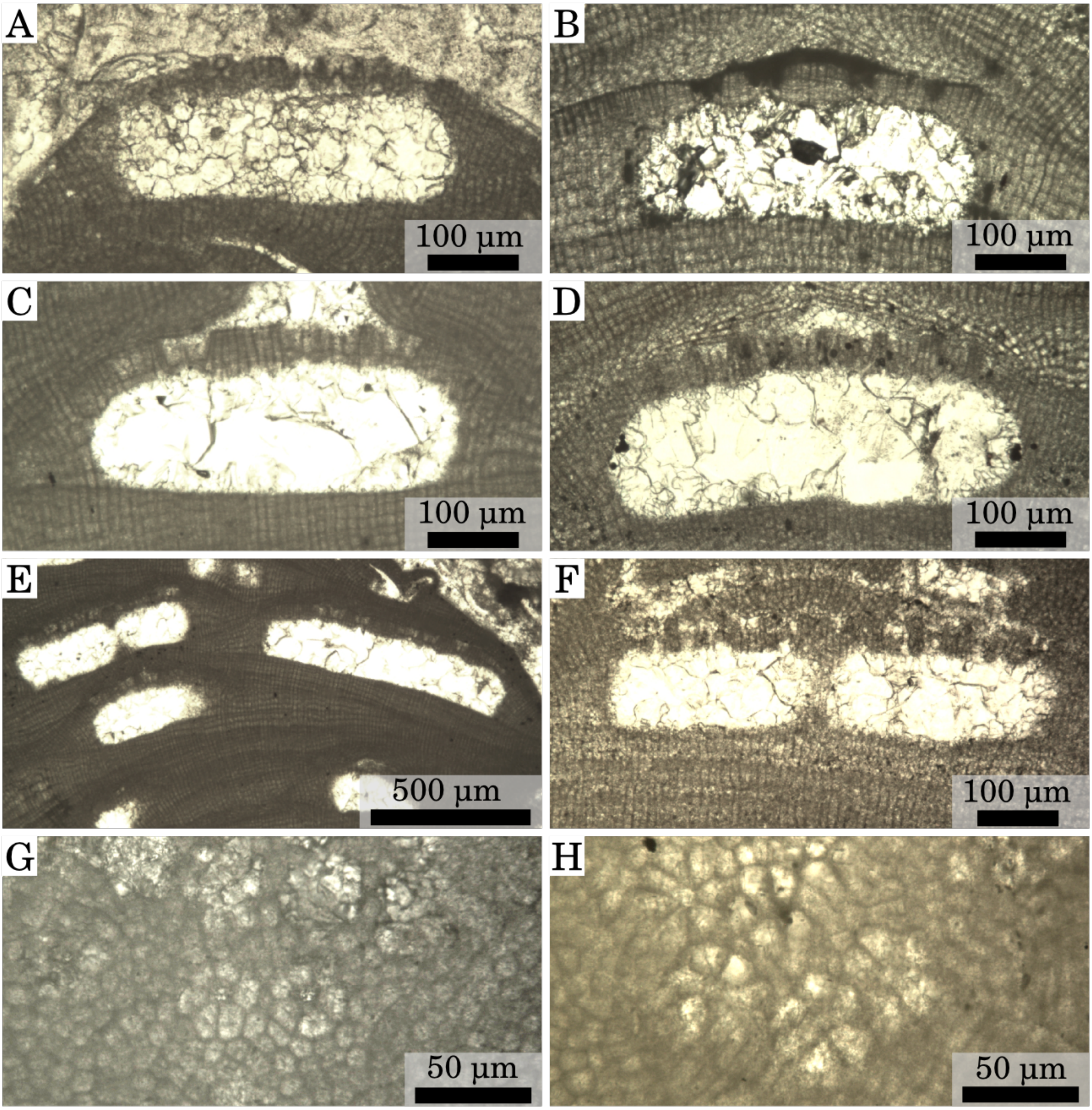

Figure 6.8.3 : Reproductive anatomy. A) Multiporate conceptacle, Burdigalian, NW Italy, Tertiary Piedmont Basin, Villa San Bartolomeo. B) Multiporate conceptacle, Pleistocene, S. Italy, Castelluccio. C) Multiporate conceptacle, upper part of Lower Langhian, Romania, Lopadea Veche. D) Multiporate conceptacle, Upper Langhian, Slovakia, Stupava-Vrchná Hora. E) Conceptacles almost merged (left) and conceptacles fully merged (right), upper part of Lower Langhian, Romania, Lopadea Veche. F) Conceptacles almost merged, upper part of Lower Langhian, Czech Republic, Židlochovice. G) Rosette of degenerated cells around the pore canals, Pleistocene, S. Italy, Castelluccio. H) Rosette of degenerate cells around the pore canals, upper part of Lower Langhian, Romania, Lopadea Veche.

and their inward derivatives, in agreement with the observations of Recent specimens of the species (Nóbrega-Farias et al. 2010, fig. 4; Basso et al. 2011, figs. 6, 10-11).

Reproductive anatomy. Only multiporate conceptacles have been observed in the specimens studied. Conceptacle chambers are generally subrectangular in shape, 260 to 550 µm in diameter and 90 to 190 µm in height (Tab. 6.8.2; Fig. 6.8.3A-D). Conceptacles with very large diameter (generally 700 µm but up to 1000 µm) may result from the merging of two nearby reproductive chambers, since such large structures were always observed close to adjacent couples of normal-sized conceptacles with the separating wall partially dissolved (Fig. 6.8.3E-F). The conceptacles protrude slightly above the surrounding thallus surface (Fig. 6.8.3A-F). The H/D (height/diameter) ranges between 0.25 and 0.5 (Tab. 6.8.2). The roof of the conceptacle is 27 to 62 µm in thickness and is composed of 3 to 6 cells (Tab. 6.8.2). The roof of the conceptacles is pitted with depressions, resulting from the disintegration of the uppermost cells of the filaments around the pore canals. The roof pits have a diameter ranging from 19 to 59 µm (Tab. 6.8.2; Fig. 6.8.3). The degenerate cells are 9 to 38 µm in length (Tab. 6.8.2). Rosettes of degenerate cells around the pore canal were observed in sections tangential to the roof of the conceptacles, with 6 to 7 cells counted around the pore canal (Tab. 6.8.2; Fig. 6.8.3G-H).

Statistical analysis. Levene's test verified that the variances of the H/D ratio of the samples are homogeneous, allowing the use of ANOVA (F distribution with 8 and 97 degrees of freedom). The calculated F-ratio is 1.64, so that we cannot reject the null hypothesis that the samples belong to a single population. That is, ANOVA demonstrates that there are no statistically significant differences between the mean H/D ratios of the conceptacles of the different samples. Multivariate statistical analysis of the main biometric variables of vegetative and reproductive anatomy shows that all the samples are grouped together at a very high level of B-C similarity (>90%). The dendrogram displays two main clusters: fossil and modern L. crispatum (Fig. 6.8.4). Within the fossils, the largest difference is recognized between the Romanian sample of Lopadea Veche and the remaining fossil samples (Fig. 6.8.4). This latter group is characterized by a >95% of B-C similarity and encompasses samples of different age and different geographical origin (Fig. 6.8.4).

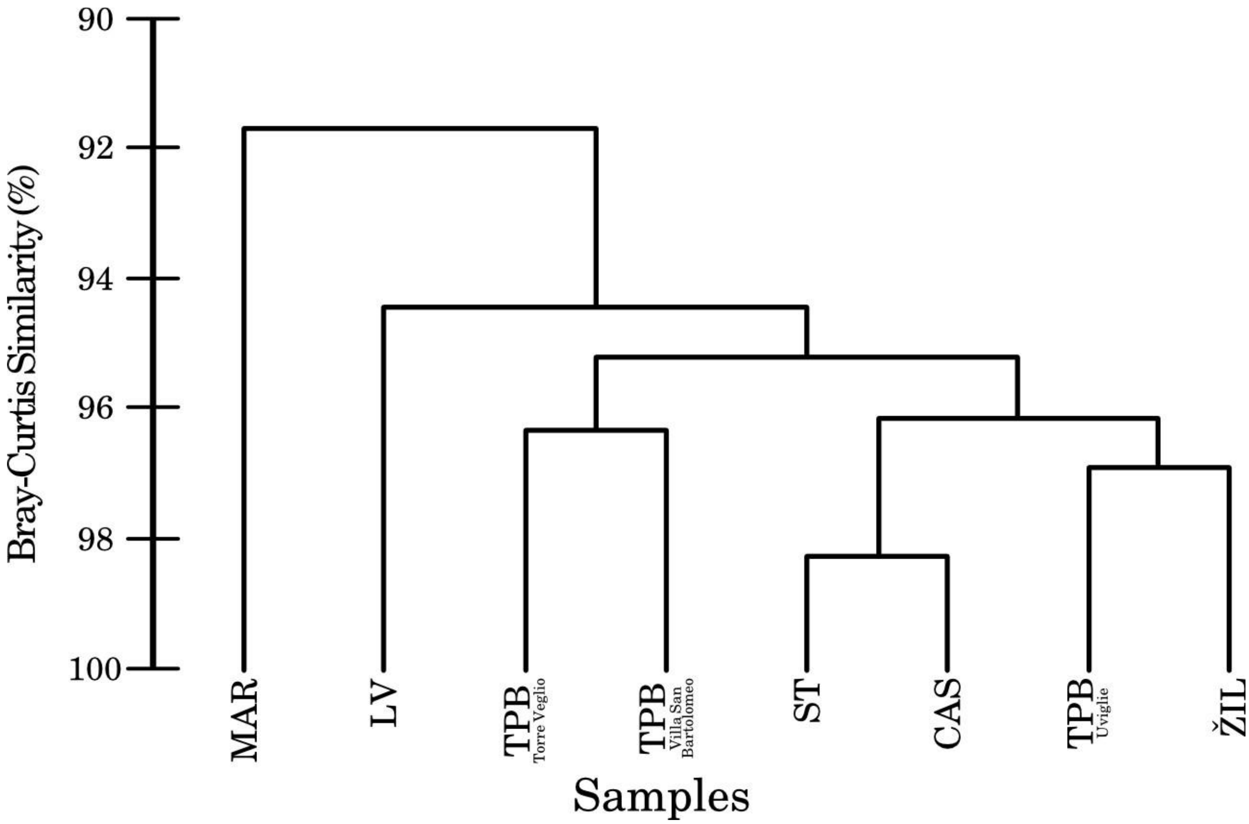

Figure 6.8.4 : Multivariate statistical analysis based on B-C similarity of the average value for each specimen of vegetative cell size and morphological characters of the multiporate conceptacles (see text for details); hierarchical agglomerative dendrogram. TPB=Tertiary Piedmont Basin, Burdigalian. ŽIL= Židlochovice, upper part of Lower Langhian, Czech Republic. LV=Lopadea Veche, upper part of Lower Langhian, Romania. ST=Stupava- Vrchná Hora , Upper Langhian, Slovakia. CAS=Castelluccio, Pleistocene, S. Italy. MAR=Marettimo, modern, Mediterranean.

Paleoecological distribution and associated skeletal assemblages. The fossils occur in various depositional environments and are associated with different benthic organisms.

In the outcrops of Tertiary Piedmont Basin, coralline algae dominate the skeletal assemblages, with barnacles and larger benthic foraminifers also very common. These rhodalgal carbonates were deposited in a mesotrophic, high-energy environment at tropical latitudes (Dercourt et al. 2000; Mosbrugger et al. 2005; Coletti et al. 2015).

The Sommières Basin was a small inlet of the Alpine Molasse Basin and located at the same latitude as the Tertiary Piedmont basin (Dercourt et al. 2000). Bryozoans, barnacles, echinoids and coralline algae were the main carbonate producers; larger benthic foraminifers were, in this case, very rare. These heterozoan carbonates were deposited in a tide-controlled environment under mesotrophic conditions as suggested by bryozoan dominance and the presence of authigenic phosphates (Reynaud and James, 2012).

Red algal limestones from Židlochovice were deposited in a stable shallow normal marine environment with low terrigenous input and seagrass meadows (Doláková et al. 2008, 2014). The section was deposited in a warm temperate to subtropical climate with marked seasonality (Doláková et al. 2014). Coralline algal to coralline algal-bryozoan limestones point to a cooler environment than the coral – coralline algal limestones of the southern sites of the Central Paratethys (Doláková et al. 2008, Kováč et al. 2005).

Limestones from Lopadea Veche correspond to the Gârbova de Sus Formation (Transylvanian Basin) that is characterized by nodular limestones (Filipescu and Gîrbacea, 1997). The foraminiferal associations suggest that limestones and marls were deposited in a shallow water-environment. Other common components are bivalves, bryozoans and rhodoliths (Filipescu and Gîrbacea, 1997). The occurrence of patch reefs in the distinct reefal Podeni Member (limestone of Gârbova de Sus Fm.) points to subtropical conditions (Saint Martin et al. 2007).

Sands, sandstones and limestones of the Stupava Member from the Vienna Basin contain the large benthic foraminifer *Amphistegina* (Hrabovský and Fordinál, 2013) in high abundance. Sandy limestones were deposited within a dynamic environment of normal salinity at the proposed depth of 35-80 m, affected by terrigenous input. The studied site was located in a warm, temperate to subtropical climatic zone (Hrabovský and Fordinál, 2013).

The Sandberg Member was proposed for marginal transgressive deposits of the Upper Langhian of the Vienna Basin (Baráth et al. 1994). Limestones were deposited in a circalittoral or infralittoral environment, on rises protected from terrigenous input (Baráth et al. 1994). Although terrestrial ecosystems suggest a subtropical climatic zone for these deposits, the marine microfauna indicates a cooling of the environment compared to the rest of the Langhian period (Kováč et al. 2005).

Heterozoan carbonates of the Pleistocene sequences of Castelluccio are largely dominated by bryozoans and coralline algae. The fossil association suggests a cool-temperate climate, probably just slightly colder than the modern Mediterranean's.

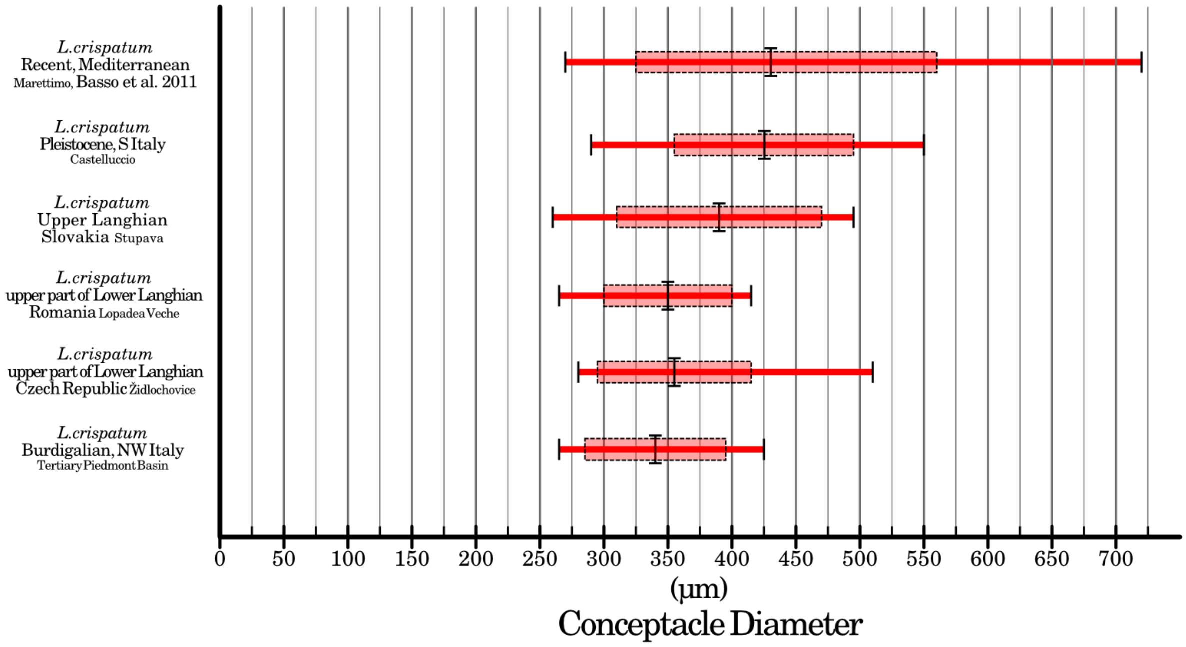

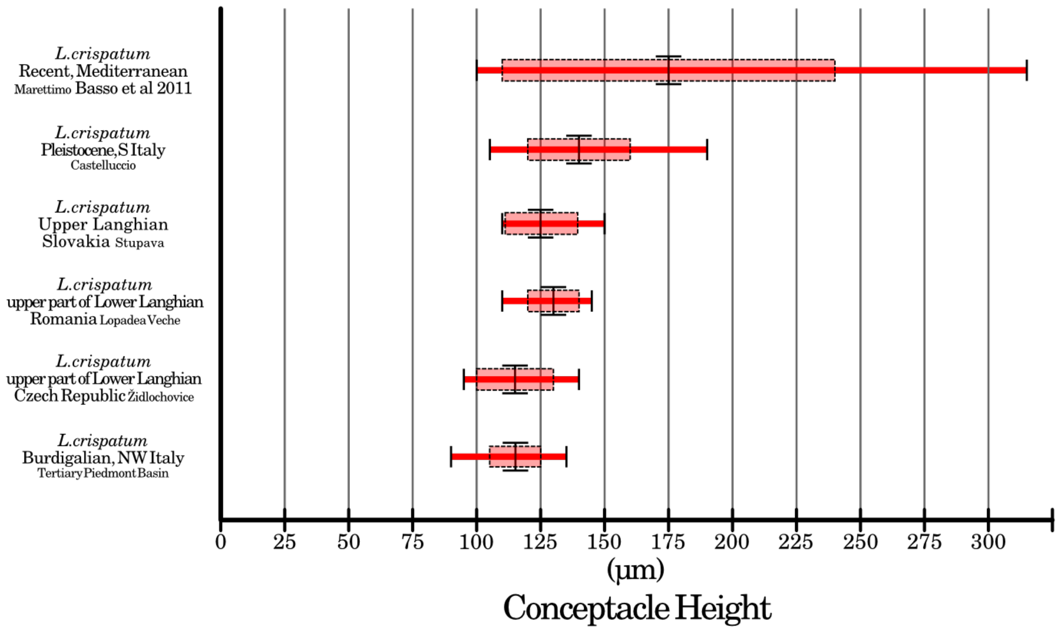

Figure 6.8.5 : Comparison of conceptacle chamber dimensions between fossil and recent samples. The long red bar indicates total range; the pale red rectangle indicates the standard deviation around the average which is represented by the large vertical black bar.

Discussion

Comparison between fossil samples. Fossil samples have a remarkably similar vegetative anatomy, without significant variation in thallus organization or the range and average size of vegetative cells (Tab. 6.8.2; Fig. 6.8.2).

Reproductive anatomy is also rather uniform among fossil samples (Tab. 6.8.2; Fig. 6.8.3). Both the total range and the average (± s.d.) interval overlap consistently, for both conceptacle diameter and conceptacle height (Fig. 6.8.5). Pleistocene specimens have the largest conceptacles among all the fossils, while those from the Tertiary Piedmont Basin have the smallest (Table 6.8.2; Fig. 6.8.5). Conceptacle H/D ratio is very consistent among the samples and most of the average values lie between 0.33 and 0.34 (i.e., conceptacle with diameter three times its height; Tab. 6.8.2). Only the sample from the upper part of the Lower Langhian of Lopadea Veche (Romania) is characterized by a slightly higher H/D ratio, due to its slightly higher than average conceptacle chambers (Tab. 6.8.2). ANOVA testing of this morphological parameter confirms that there is very little variation among the different samples and that they probably belong to the same statistical population.

Besides conceptacle size, all the other features of the reproductive anatomy of the fossil samples are remarkably similar. The number of cells that compose the roof and roof thickness are uniform. Large conceptacles, created by the merging of two nearby conceptacles, were observed in all the samples (Tab. 6.8.2).

Some differences may be observed in the morphology of roof pits (Fig. 6.8.3G-H). While the number of cells composing the rosette around the pore canals in the examined specimens is always 6 to 7, the diameter of the pits and the length of the degenerate cells are quite variable (Tab. 6.8.2; Fig. 6.8.6). Most of the samples, especially those of the Tertiary Piedmont Basin, have small and shallow pits (Fig. 6.8.3A-G), but the one from the upper part of the Lower Langhian of Romania has larger and deeper pits

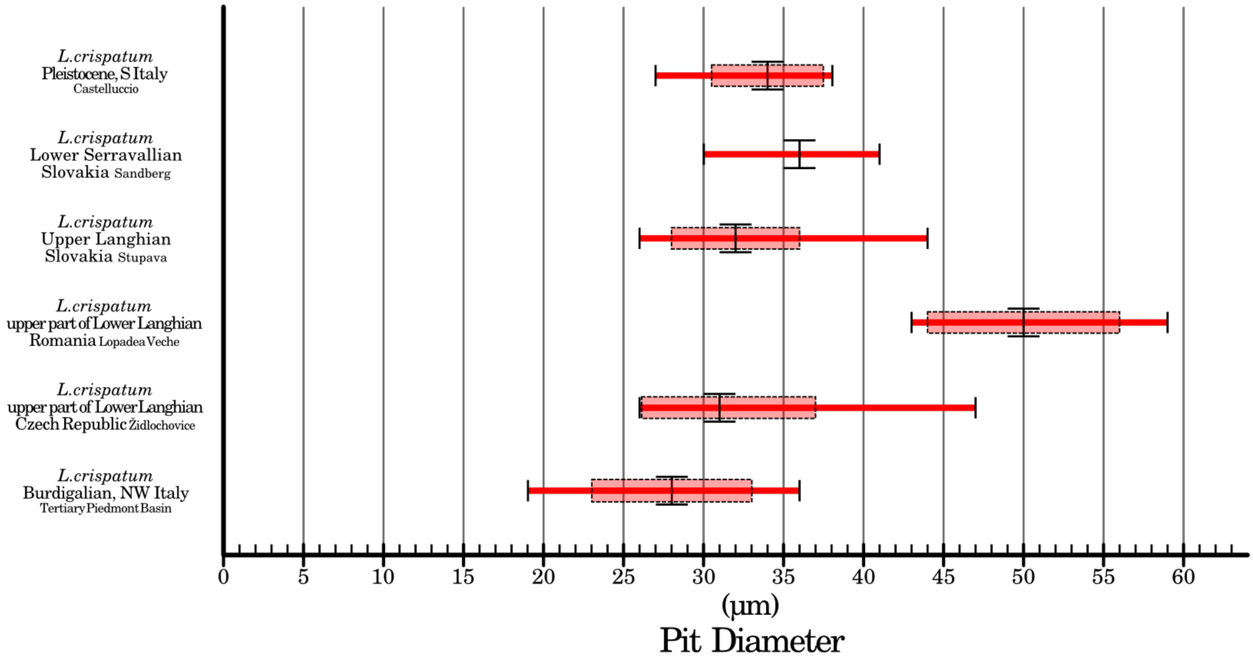

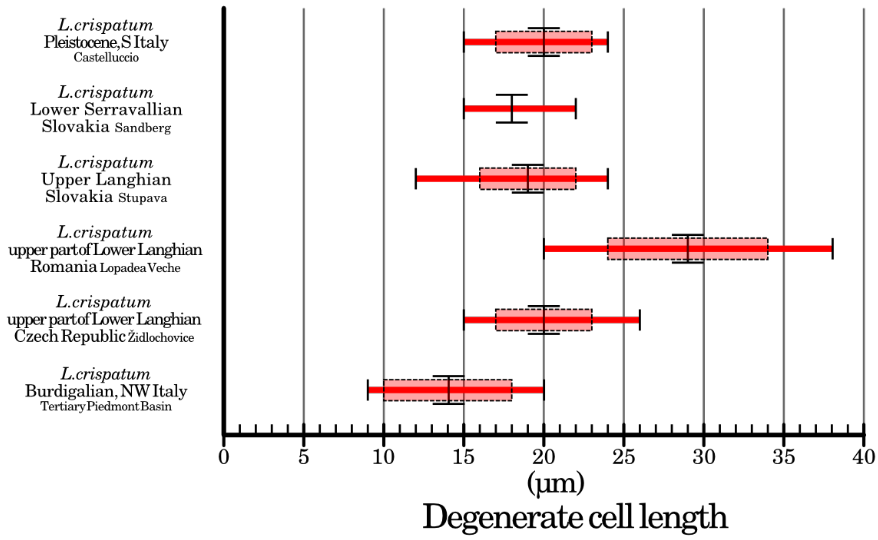

Figure 6.8.6 : Comparison of the size of roof pits between fossil samples. The long red bar indicates total range; the pale red rectangle indicates the standard deviation around the average which is represented by the large vertical black bar.

(Fig. 6.8.3C-H; Fig. 6.8.6). These differences cannot be related to differential preservation of the structures. Although mechanical and biological abrasion of coralline surfaces are common, the Romanian sample shows preserved walls between the cells forming the rosettes (Fig. 6.8.3H), so that abrasion processes must be ruled out. The internal details of these structures are very well preserved and it is possible to distinguish between the cavity of the central pore channel and the cavities of the surrounding degenerate cells (Fig. 6.8.3C). Differential dissolution would have resulted in blurred structures and therefore this process is also unlikely.

In the dendrogram (Fig. 6.8.4) the Romanian sample is separated from all other fossils indicating that, even setting aside the roof pits, this sample is somewhat different from the others. However taking in to account the other morphological variables, there is still an almost complete overlap between the ranges and the averages of this sample and those of the remaining fossils (Tab. 6.8.2). Since the differences are largely overwhelmed by the similarities and no comprehensive information exists on roof-pit morphological variability in modern *L. crispatum*, the Romanian specimens are considered conspecific with the other fossils examined.

In addition to the fossils discussed above, another specimen studied by Harlan Johnson (1962; 1964) deserves attention. The specimen is Eocene in age and was collected in the island of Ishigaki (Ryukyu, southern Japan). It was initially misidentified as *Lithothamnion vaughanii* Howe 1919 (Johnson, 1962) and later as *Mesophyllum vaughanii*. The published picture shows two conceptacles with clearly pitted roof (Johnson, 1962, pl. 13 fig. 1; Johnson, 1964, pl. 6, fig. 6). According to Johnson's description, the specimen has perithallial cells 10 to 19 µm in length and 8 to 11 µm in diameter, and conceptacles are 191 to 330 µm in diameter and 102 to 132 µm in height (Johnson, 1964). The vegetative anatomy is similar to that of the other fossils considered here, but its conceptacles have a significantly smaller diameter. Since a revision of Johnson's material is beyond the scope of this work it is impossible to assess with

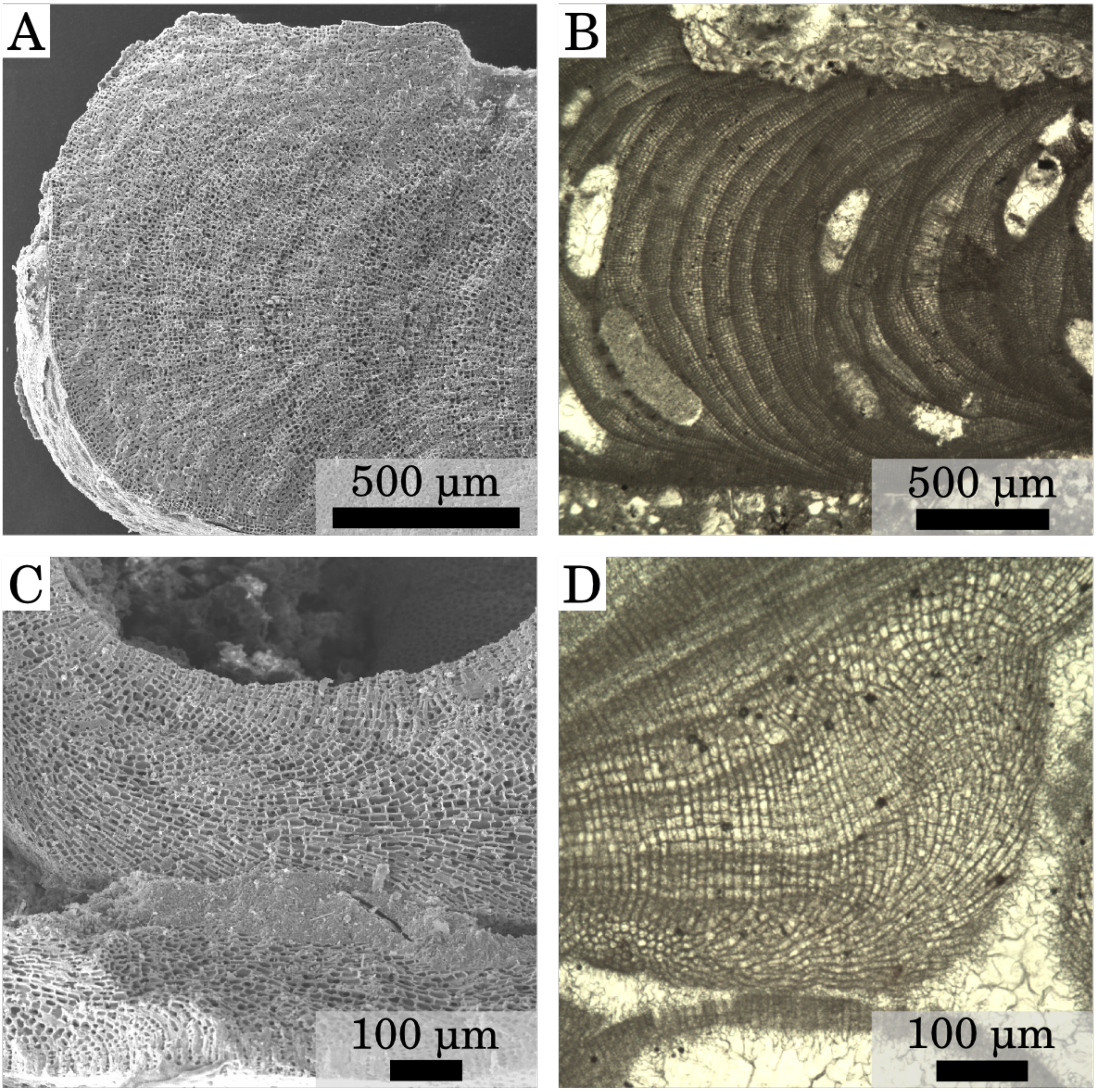

Figure 6.8.7 : Comparison of the vegetative anatomy of fossil and recent L. crispatum. (A) Zoned branch, Recent, Mediterranean, Egadi Islands, Marettimo. (B) Zoned branch, Upper Langhian, Slovakia, Stupava-Vrchná Hora . (C) Plumose ventral-core, L. crispatum lectotype, Recent, Rovigno, Mediterranean, Northern Adriatic, modified after Basso et al. (2011). (D) Plumose ventral-core, Upper Langhian, Slovakia, Stupava-Vrchná Hora.

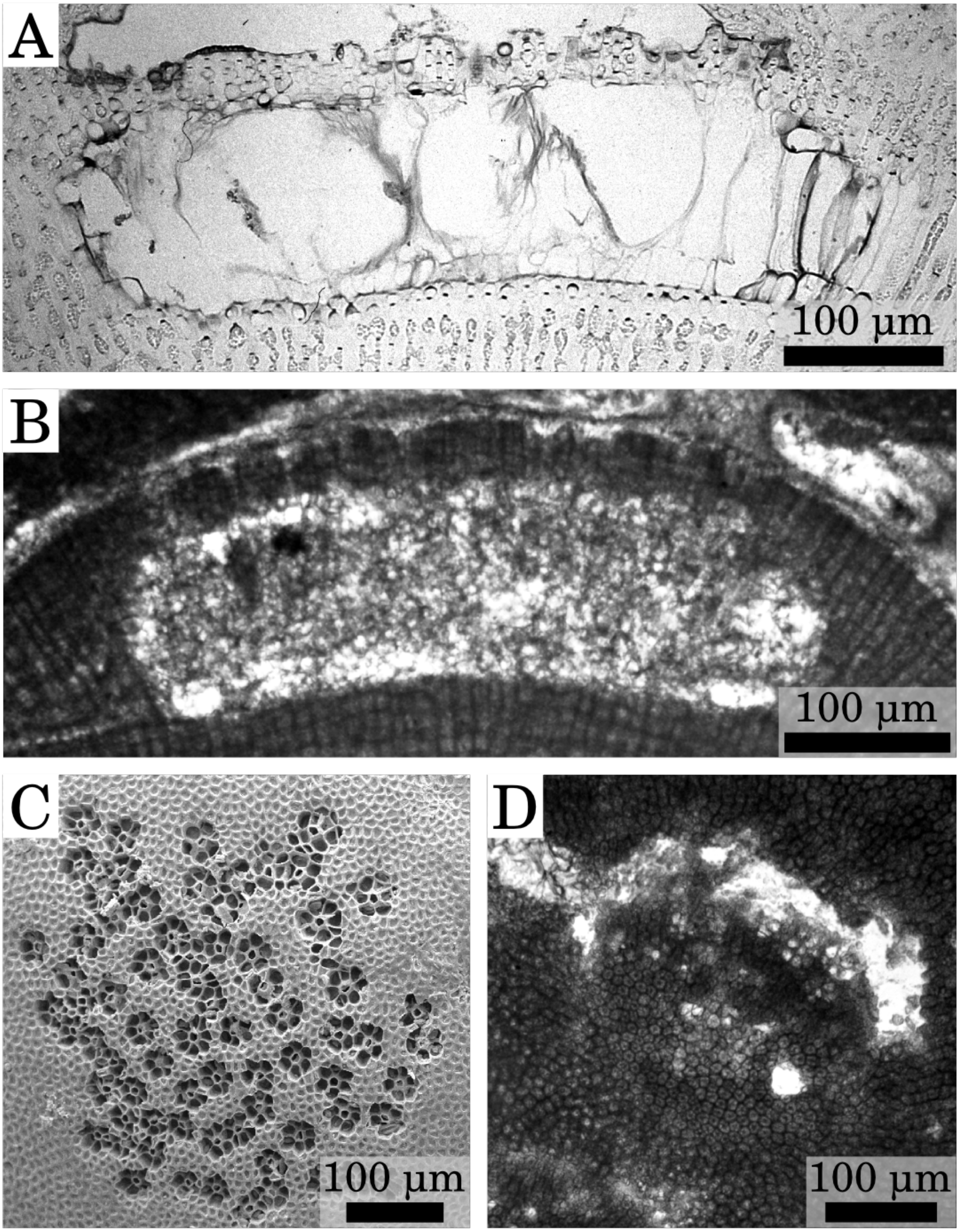

Figure 6.8.8 : Comparison of the reproductive anatomy of fossil and recent *L. crispatum*. A) Conceptacle chamber, Recent, Mediterranean, Egadi Islands, Marettimo. B) Conceptacle chamber, Burdigalian, NW Italy, Tertiary Piedmont Basin, Villa San Bartolomeo. C) Rosette of degenerate cells around pore canals, Burdigalian, NW Italy, Tertiary Piedmont Basin, Torre Veglio. D) Rosette of degenerate cells around pore canals, Recent, Mediterranean, Egadi Islands, Marettimo.

confidence its conspecificity with *L. crispatum* as circumscribed in this paper. However, we suggest that multiporate conceptacles with pitted roofs could have appeared as early as the Eocene.

Comparison with modern Lithothamnion crispatum. According to Wilks and Woelkerling (1995), Keats et al. (2000), Nóbrega-Farias et al. (2010) and Basso et al. (2011), the presence of pore canals bordered by a rosette of degenerate cells is a diagnostic feature that is unique to the genus *Lithothamnion*. It allows the identification of *Lithothamnion crispatum*, so that the fossil specimens examined must be included in this species. Setting aside this key feature, an accurate and direct comparison with the Mediterranean specimens (Marettimo, Egadi Islands, southern Tyrrhenian Sea) reveals that the fossil and modern groups are morphologically extremely similar (Fig 6.8.7; Fig. 6.8.8). The vegetative anatomy is almost identical in both ranges and average values (Tab. 6.8.2; Fig. 6.8.7). Reproductive anatomy is also similar: the conceptacles of modern *L. crispatum* are similar in size to the fossil ones, and so are the H/D ratio and the roof characteristics (Tab. 6.8.2; Fig. 6.8.8). The multivariate statistical analysis further emphasizes the similarity between Recent and fossil *L. crispatum*, since the two groups are clustered at more than 90% of B-C similarity. On the other hand, it must be recognized that the multivariate analysis separates the sample from Marettimo from its fossil counterparts (Fig. 6.8.4). This separation is caused by the larger average size of the conceptacles of the Recent specimens. The largest difference occurs between the lower Burdigalian samples of the Tertiary Piedmont Basin and the Marettimo sample, while the Pleistocene sample from Castelluccio is the closest to the modern one (Tab. 6.8.2; Fig. 6.8.5). However, since the total ranges of the two groups overlap completely, these differences should be considered within the natural variability of the species (Fig. 6.8.5). The outcome of the analysis of variance performed on the H/D ratio also strengthens this hypothesis. The Marettimo specimens and the fossils also share similar morphology and a common diameter of the roof pits, length of the degenerate cells, and number of cells in the rosette (Fig. 6.8.8C-D). Large roof pits, as large as those of the sample from Romania, were observed in the lectotype from the Adriatic Sea, Mediterranean (Basso et al. 2011, figs 13-14), suggesting that the size of the roof pits is a quite variable feature.

A general comparison with data from other papers on modern *L. crispatum* is more difficult since biometric data are usually provided just as total range, and not all the variables are measured every time. However, it should be pointed out that although all the modern specimens are grouped together by the presence of roof pits, minor morphological differences seem to exist amongst them (Basso et al. 2011, table 1). Therefore, the variability displayed by the different populations of *L. crispatum* in the world's oceans is comparable to, if not greater than, the variability observed amongst the various fossil populations.

Since no morphological evidence can be used to separate modern *L. crispatum* from the fossil corallines analyzed in this work, they must be considered conspecific, and consequently the stratigraphic range of *L. crispatum* is extended at least to the Burdigalian.

Conclusions

Fossil and modern specimens share the same vegetative and reproductive anatomy and are characterized by the same unique diagnostic feature: the presence of a rosette of degenerate cells (a pit in axial sections) around the multiporate conceptacle pore canals. Both qualitative comparison and statistical analyses show that their morphology is remarkably similar. The fossil specimens analyzed here are thus conspecific with modern *Lithothamnion crispatum*, whose stratigraphic range is extended back at least to the Burdigalian. The species has been found associated with markedly different skeletal assemblages and in very varied climatic conditions throughout the Cenozoic. The fossil record, consistent with its modern cosmopolitan distribution, suggests a remarkable adaptability. Although the morphofunctional significance of *L. crispatum* roof pits remains unknown, they seem to be a successful and persistent feature.

6.9 – *Lithothamnion giammarinoi*

Systematic Paleontology

Class Florideophyceae CRONQUIST, 1960

Sub-class Corallinophycidae LE GALL and SAUNDERS, 2007

Order Hapalidiales NELSON et al., 2015

Family Hapalidiaceae GRAY, 1864 (emended HARVEY et al., 2003)

Subfamily Melobesioideae BIZZOZERO, 1885

Genus *Lithothamnion* HEYDRICH, 1897

Lithothamnion giammarinoi FRAVEGA et al., 1993

Description

Encrusting thallus with crusts, 100 to 200 µm thick in portions without conceptacles, wherever conceptacles are present the thallus is thicker (Fig. 6.9.1). Thallus with monomerous organization and thin non-coaxial ventral core composed of small cells rectangular in section (Fig. 6.9.1C). Peripheral zone with the regular alternation of smaller and larger cells (Fig. 6.9.1D). Peripheral zone cells are square to rectangular in section, 5 to 13 µm in diameter and 6 to 14 µm high (Tab. 6.9.1). Cells of adjacent filaments are connected by cell fusions. Epithallial cells flat; sub-epithallial initial long as or longer than their inward derivatives. Trichocytes have not been observed Multiporate sporangial conceptacles rise remarkably from the surrounding thallus surface (Fig. 6.9.1E-F). Conceptacle chambers are elliptical in shape and very large, 450 to 750 µm in diameter and 170 to 320 µm high (Fig. 6.9.1E-F). The roof is convex and

50-90 µm thick. Pore canals are cone-shaped and tapers toward the roof, they are approximately 20 µm wide at the base and 40 µm long (Fig. 6.9.1F).

Female gametangial plants have the same vegetative anatomy of the sporangial plant (Tab. 6.9.1; Fig. 6.9.2). Carposporangial conceptacles are very large, 940 to 1090 µm in diameter and 250 to 295 µm high, with a pore canal up to 100 µm wide and 170 µm long (Tab. 6.9.1; Fig. 6.9.2). The floor of carposporangial conceptacles may presents a central columella (Fig. 6.9.2A).

Sporangial thallus		
	Diameter	Height
Peripheral zone (perithallus) cells [µm]	5-13 [8.25 mean; 1.5 s.d.]	6-14 [9.5 mean; 2 s.d.]
Conceptacles [µm]	450-750 [585 mean; 100 s.d.]	170-320 [225 mean; 40 s.d.]
H/D ratio	0.29-0.51 [0.38 mean; 0.06 s.d.]	
Roof thickness [µm]	50-90 [65 mean]	
Female gametangial thallus		
Ventral core (hypothallus) cells [µm]	6-13 [9 mean]	12-25 [15 mean]
Peripheral zone (perithallus) cells [µm]	5-10 [7.75 mean; 1 s.d.]	7-13 [9.5 mean; 2 s.d.]
Carposporangial conceptacles [µm]	940-1090 [1020 mean]	250-295 [280 mean]

Table 6.9.1 : biometry of *Lithothamnion giammarinoi*.

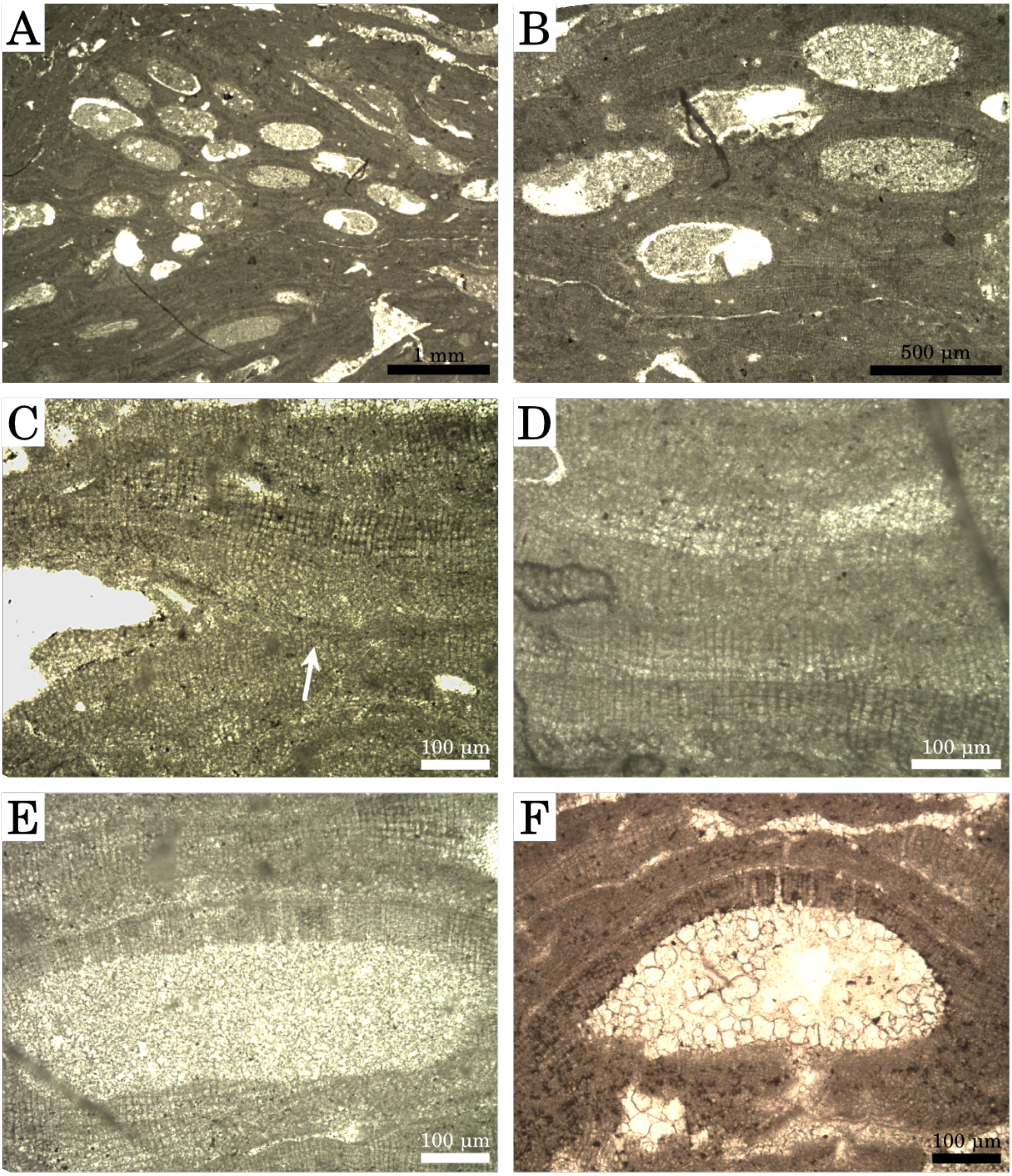

Figure 6.9.1 : *Lithothamnion giammarinoi*, BTP, Uviglie. A) Lithozone 1, thallus overview. B) Lithozone 1, thallus overview. C) Lithozone 1, non-coaxial ventral core; white arrow=non coaxial ventral core. D) Lithozone 1, zoned perithallus. E) Lithozone 1, multiporate conceptacle. F) Lithozone 4, multiporate conceptacle.

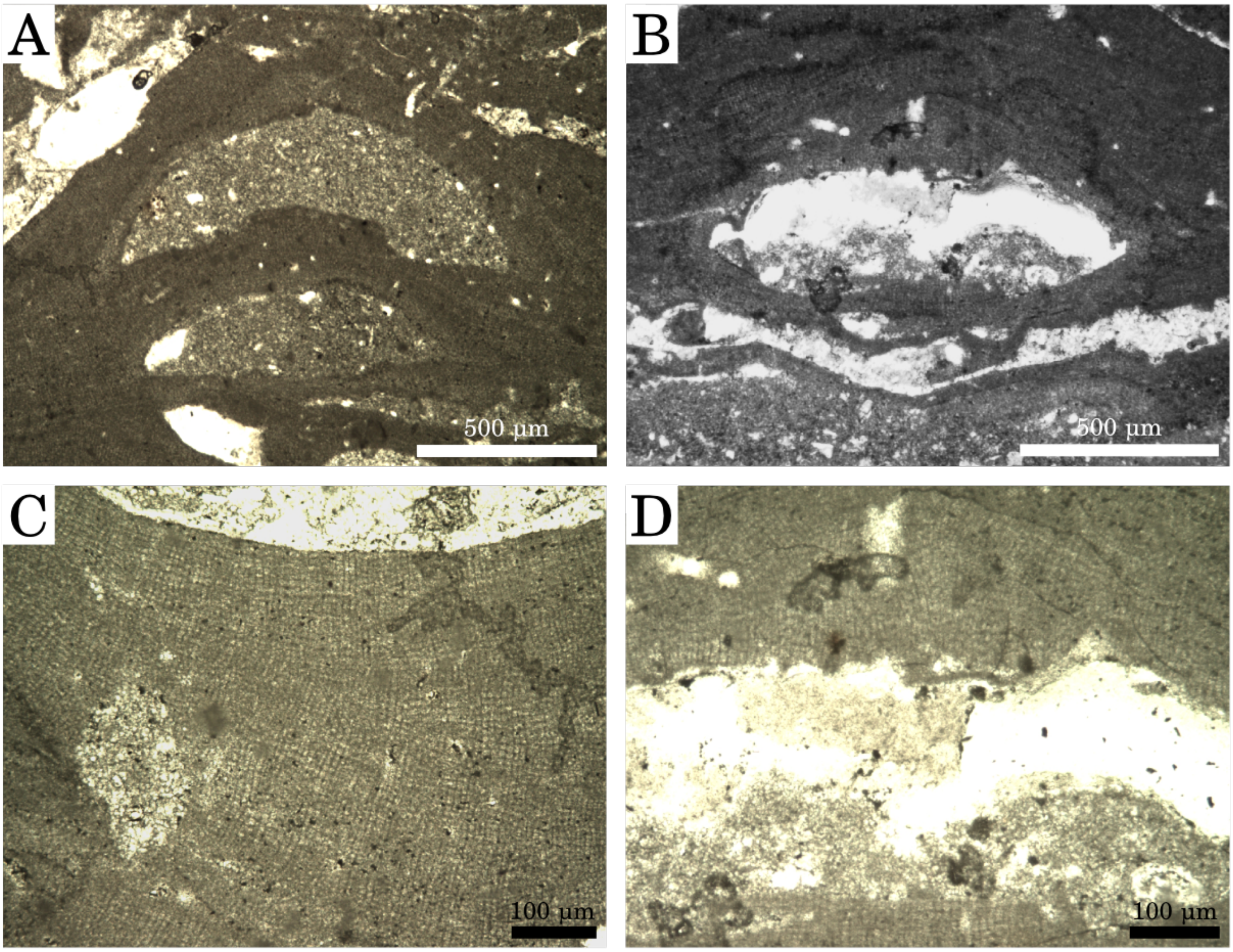

Figure 6.9.2 : *Lithothamnion giammarinoi*, female gametangial thallus, BTP, Uviglie, Lithozone 1. A) Reproductive anatomy. B) Uniporate female conceptacle. C) Peripheral zone. D) Detail of the pore canal of the uniporate female conceptacle in B).

6.10 – ?*Lithothamnion* sp. 2

Systematic Paleontology

Class Florideophyceae CRONQUIST, 1960

Sub-class Corallinophycidae LE GALL and SAUNDERS, 2007

Order Hapalidiales NELSON et al., 2015

Family Hapalidiaceae GRAY, 1864 (emended HARVEY et al., 2003)

Subfamily Melobesioideae BIZZOZERO, 1885

Genus *Lithothamnion* HEYDRICH, 1897

Description

Growth form fruticose, protuberances 2mm in diameter and several mm in length (Fig. 6.10.1A-C). Thallus with monomerous organization; only the secondary ventral core, formed above conceptacles, was observed (Fig. 6.10.1D-E). Ventral core organization is non-coaxial, the cells are rectangular in section, approximately 20 µm long and have a diameter of 11 µm (Fig. 6.10.1D-E). Peripheral zone with the irregular alternation of short and longer cells (Fig. 6.10.1F). Peripheral zone cells are rectangular, 6 to 12 µm in diameter and 9 to 20 µm high (Tab. 6.10.1). Cells of adjacent filaments are connected by cells fusions. Epithallial cells were not clearly observed. Trichocytes have not been observed. Multiporate conceptacles slightly raised above the surrounding thallus surface. Conceptacle chambers rectangular in shape, 200 to 660 µm in diameter and

100 to 160 µm high (Tab. 6.10.1; Fig. 6.10.1G-H). The roof is flat and 30 to 45 µm thick (Tab. 6.10.1; Fig. 6.10.1G-H).

Remarks

On the basis of both vegetative and reproductive anatomy the species observed in the Sommières Basin (Fig. 6.10.1) has been identified as a conspecific of ?*Lithothamnion* sp. 2 of the Lower Langhian of the Parathethys Basin, identified by Hrabovský et al. 2015 (Fig. 6.10.2).

Sporangial thallus		
	Diameter	Height
Peripheral zone (perithallus) cells [µm]	6-12 [8.5 mean; 1.5 s.d.]	9-20 [12.5 mean; 3 s.d.]
Conceptacles [µm]	200-660 [370 mean; 70 s.d.]	100-160 [125 mean; 20 s.d.]
H/D ratio	0.37	
Roof thickness [µm]	30-45 [40 mean]	

Table 6.10.1 : biometry of ?*Lithothamnion* sp. 2

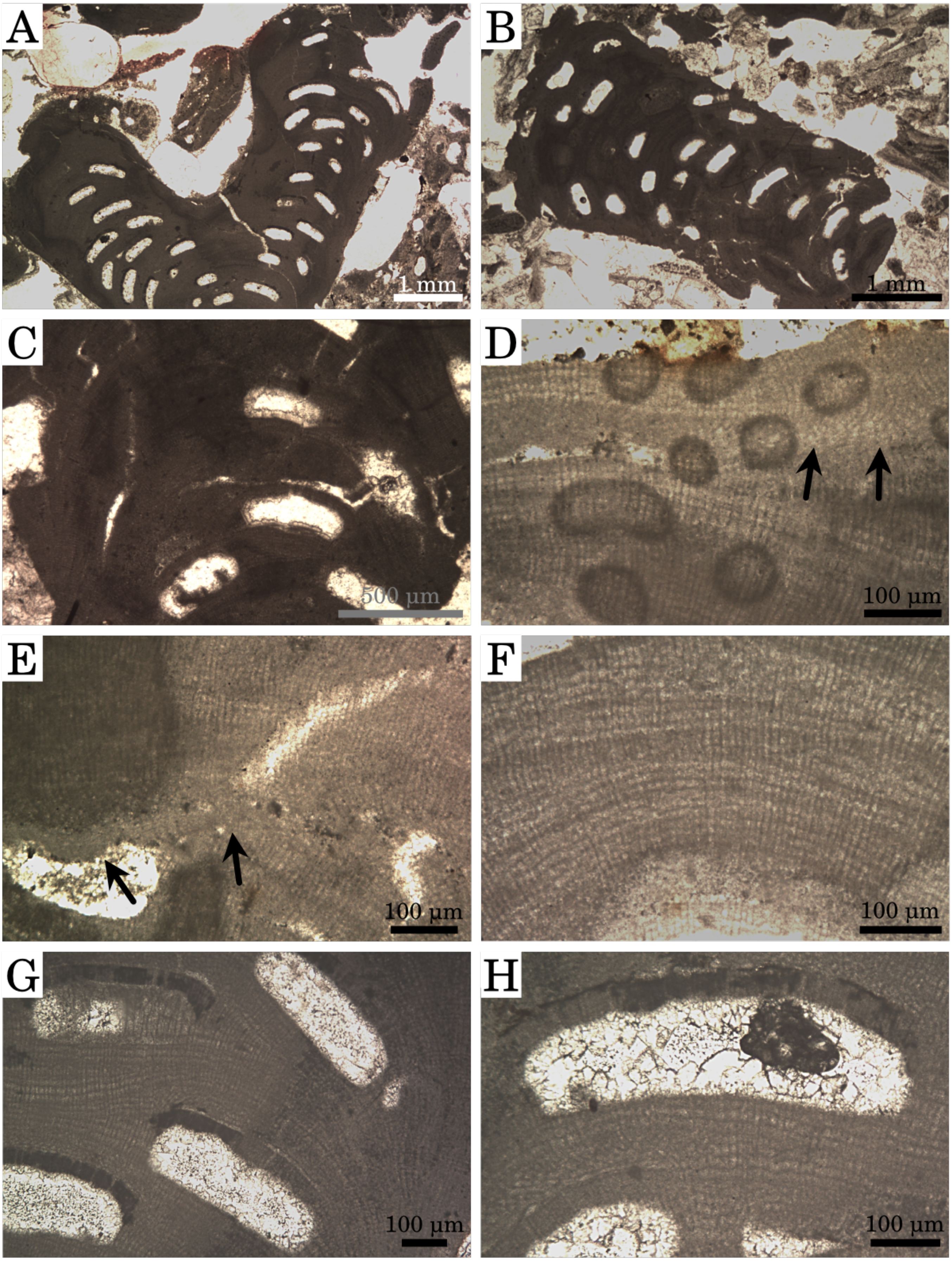

Figure 6.10.1 : ?*Lithothamnion* sp2. A) Sommières Basin, Sovignargues, free-living branch, thallus oveview. B) Sommières Basin, Pondres, Lithozone 4, free living branch, thallus overview. C) Sommières Basin, Pondres, Lithozone 4, reproductive anatomy. D) Sommières Basin, Pondres, Lithozone 4, secondary ventral core; black arrow=thin secondary ventral core. E) Sommières Basin, Pondres, Lithozone 4, secondary ventral core; black arrow=thin secondary ventral core. F) Sommières Basin, Pondres, Lithozone 4, peripheral zone. G) Sommières Basin, Souvignargues, multiporate conceptacles. H) Sommières Basin, Souvignargues, multiporate conceptacle.

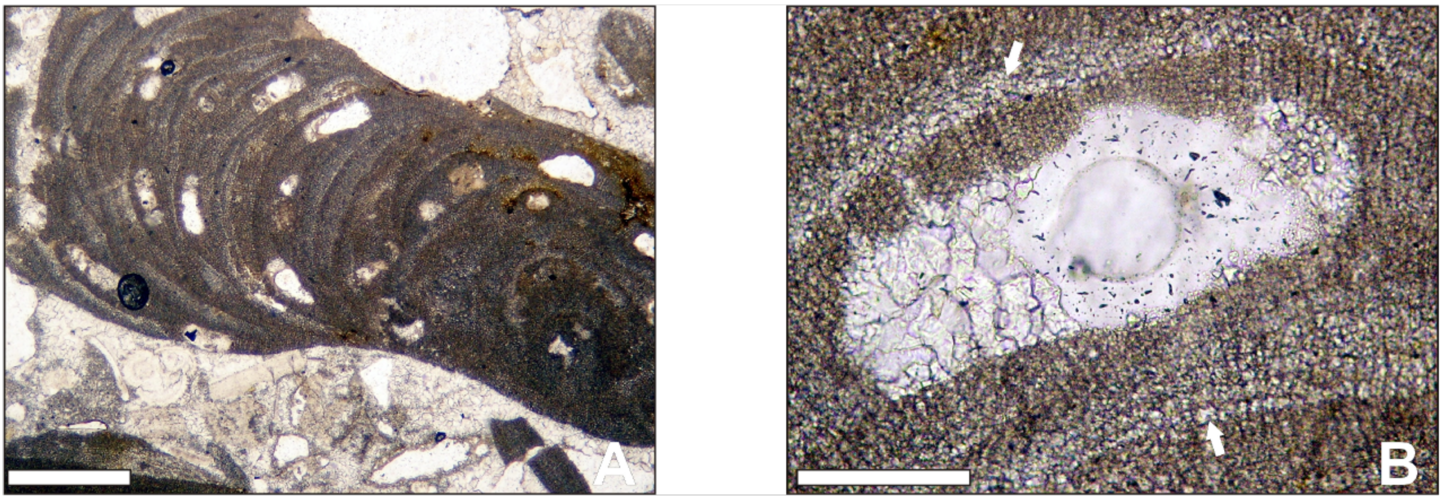

Figure 6.10.2 : figure 8 Hrabovsky et al. 2015 - ?*Lithothamnion* sp 2; Lower Badenian (Early Langhian), Krouzek, Carpathian Foredeep, Czech Republic. A) Section through protuberant portion of thalli with formerly raised conceptacles buried by continuous growth of the protuberance; conceptacles are formed at the tips and at the sides of the protuberance; scale bars=500 µm. B) Detail of multiporate tetra/bisporangial conceptacle with cells of the roof of different dimensions from cells of the rest of the peripheral zone; white arrows=cell fusions in secondary ventral core and peripheral zone; scale bars=100 µm.

6.11 – *Phymatolithon* sp.

Systematic Paleontology

Class Florideophyceae CRONQUIST, 1960

Sub-class Corallinophycidae LE GALL and SAUNDERS, 2007

Order Hapalidiales NELSON et al., 2015

Family Hapalidiaceae GRAY, 1864 (emended HARVEY et al., 2003)

Subfamily Melobesioideae BIZZOZERO, 1885

Genus *Phymatolithon* FOSLIE, 1898

Description

Growth form encrusting to warty-fruticose, protuberances several millimeters wide and several millimeters long (Fig. 6.11.1). The protuberances are formed by various thalli stacked onto each other. Thallus with monomerous organization; only the secondary ventral core interposed between stacked thalli, was observed. Ventral core coaxial to plumose. Peripheral zone remarkably characterized by growth lines created by the alternation of long and shorter cells (Fig. 6.11.1D). Peripheral zone cells are rectangular in section, 5 to 9 µm in diameter and 6 to 17 µm high (Tab. 6.11.1; Fig. 6.11.1D). Cells of adjacent filaments are connected by cell fusions. Epithallial cells were not clearly observed. Trichocytes have not been observed. Multiporate conceptacles slightly raised above the surrounding thallus surface. Conceptacles elliptical in shape and small (110 to 255 µm in diameter and 70 to 115 µm high; Tab. 6.11.1; Fig 6.11.1E-F).

Conceptacle roof approximately 40 µm thick (Tab. 6.11.1; Fig 6.11.1E-F).

Remarks

On the basis of both vegetative and reproductive anatomy the species observed in the Sommières Basin (Fig. 6.11.1) has been identified as a conspecific of *Phymatolithon* sp. of the Lower Langhian of the Parathethys Basin, identified by Hrabovský et al. 2015 (Fig. 6.11.2).

Sporangial thallus		
	Diameter	Height
Peripheral zone (perithallus) cells [µm]	5-9 [7.4 mean; 1 s.d.]	6-17 [10.3 mean; 2 s.d.]
Conceptacles [µm]	110-255 [180 mean; 45 s.d.]	70-115 [95 mean; 15 s.d.]
H/D ratio	0.4-0.65 [0.54 mean; 0.11 s.d]	
Roof thickness [µm]	40	

Table 6.11.1 : biometry of *Phymatolithon* sp.

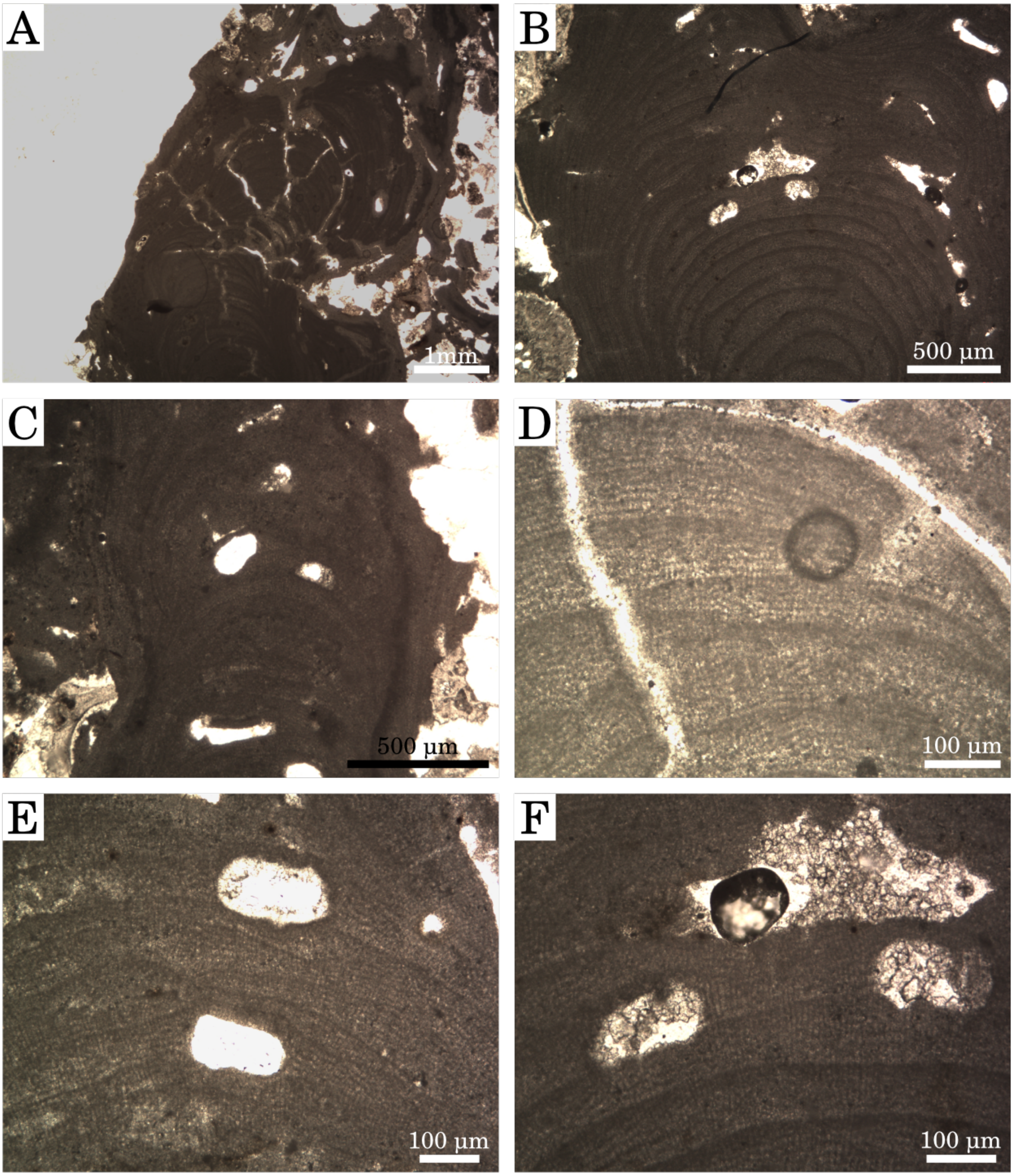

Figure 6.11.1 : *Phymatolithon* sp. A) Sommières Basin, Pondres, Lithozone 4, free-living branch. B) Sommières Basin, Pondres, Lithozone 3, free-living branch. C) Sommières Basin, Pondres, Lithozone 3, detaail of a ramification of a free living branch. D) Sommières Basin, Pondres, Lithozone 4, detail of the zoned perithallus. E) Sommières Basin, Lithozone 3, multiporate conceptacles. F) Sommières Basin, Lithozone 3, multiporate conceptacles.

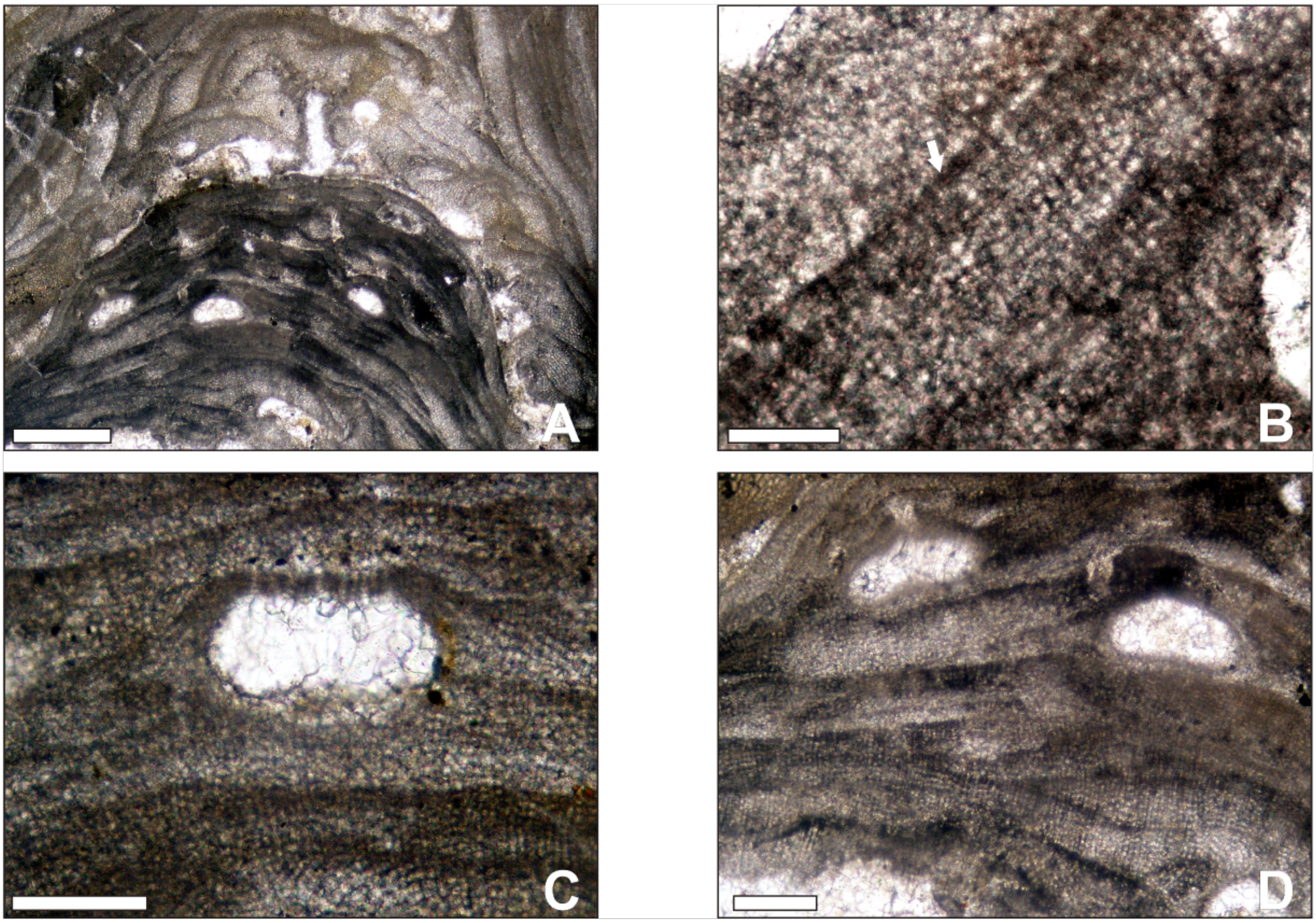

Figure 6.11.2 : figure 13 Hrabovsky et al. 2015 - *Phymatolithon* sp.; Lower Badenian (Early Langhian), Zidlochovice, Carpathian Foredeep, Czech Republic. A) monomerous thalli with non-coaxial VC and zoned PF; gametangial warty protuberant plant is overgrown by tetra/bisporangial plant, and gametangial conceptacles are borne on warty protuberance; scale bar=400 µm. B) layer of epithallial cells above cells of the meristem (arrow) that are as long as or shorter than cells subtending them; scale bar=100 µm. C) multiporate tetra/bisporangial conceptacle with flat to slightly concave roof; partly raised conceptacle; scale bar=100 µm. D) growth zones and gametangial uniporate conceptacles; scale bar=100 µm.

6.12 – *Phymatolithon* sp 1.

Systematic Paleontology

Class Florideophyceae CRONQUIST, 1960

Sub-class Corallinophycidae LE GALL and SAUNDERS, 2007

Order Hapalidiales NELSON et al., 2015

Family Hapalidiaceae GRAY, 1864 (emended HARVEY et al., 2003)

Subfamily Melobesioideae BIZZOZERO, 1885

Genus *Phymatolithon* FOSLIE, 1898

Description

Foliose growth form (Fig. 6.12.1). Single crusts are thin (approximately 100 µm); nearby conceptacles the thallus become thicker (approximately 200-300 µm; Fig 6.12.1C-H). Monomerous organization, plumose ventral core composed of cells with a diameter of 7 to 15 µm and a length of 12 to 35 µm (Tab. 6.12.1; Fig. 6.12.1D-H). The peripheral zone is very thin, with less than 10 layers of cells. Peripheral zone cells are rectangular to square in section, 7-11 µm in diameter and 6-15 µm in height (Tab. 6.12.1). Nearby conceptacles the peripheral zone is thicker and presents growth bands, cells are remarkably longer, they are 7 to 11 µm in diameter and 8 to 23 µm high (Tab. 6.12.1). Cells of adjacent filaments are connected by cell fusions. Epithallial cells are rounded; sub-epithallial initial short as or shorter than their inward derivatives (Fig. 6.12.2A-B). Trichocytes have not been observed.

Multiporate conceptacles remarkably raised above the surrounding thallus surface (Fig. 6.12.2C-H). Conceptacles chambers are elliptical in shape and very large, they measure 370 to 650 µm of diameter and they are 170 to 250 µm high (Tab. 6.12.1; Fig. 6.12.2C-H). Conceptacle roof is 35 to 80 µm micron thick (Tab. 6.12.1; Fig. 6.12.2C-H). Pore canals are cone shaped, they taper toward the roof and they are 15 to 25 µm wide at the base (Tab. 6.12.1; Fig. 6.12.2C-H).

Gamentangial female plants were commonly associated with their asexuate counterparts. The gamentagial thallus has the same vegetative anatomy and growth morphology of the sporangial thallus (Tab 6.12.1; Fig. 6.12.1; Fig. 6.12.2; Fig. 6.12.3). Uniporate conceptacles are very large, 310-660 µm in diameter and 100 to 300 µm in height (Tab. 6.12.1; Fig. 6.12.3E-H). Conceptacle size is very variable testifying different stages of carposporophyte-chamber development. Pore canal is 35 to 70 µm wide at the base and 70 to 130 µm long (Fig. 6.12.3E-H).

Sporangial thallus		
	Diameter	Height
Ventral core cells [µm]	7-15 [10.7 mean; 2.5 s.d.]	12-35 [21.5 mean; 6 s.d.]
Peripheral zone cells [µm]	7-11 [8 mean; 1.1 s.d.]	6-15 [9.6 mean; 2 s.d.]
Peripheral zone (nearby conceptacles) cells [µm]	7-11 [8.6 mean; 1 s.d.]	8-23 [16 mean; 4 s.d.]
Conceptacles [µm]	370-650 [525 mean; 85 s.d.]	170-250 [190 mean; 25 s.d.]
H/D ratio	0.3-0.5 [0.37 mean; 0.06 s.d.]	
Roof thickness [µm]	35-80 [55 mean]	
Gametangial thallus		
Ventral core cells [µm]	6-13 [8.7 mean]	11-32 [17.5 mean]
Peripheral zone cells [µm]	5-10 [7.5 mean]	6-13 [10 mean]
Peripheral zone (nearby conceptacles) cells [µm]	6-11 [8.3 mean; 1.5 s.d.]	10-23 [16 mean; 3 s.d.]
Conceptacles [µm]	310-660 [480 mean; 90 s.d.]	100-300 [210 mean; 90 s.d.]

Table 6.12.1 : biometry of *Phymatolithon* sp 1.

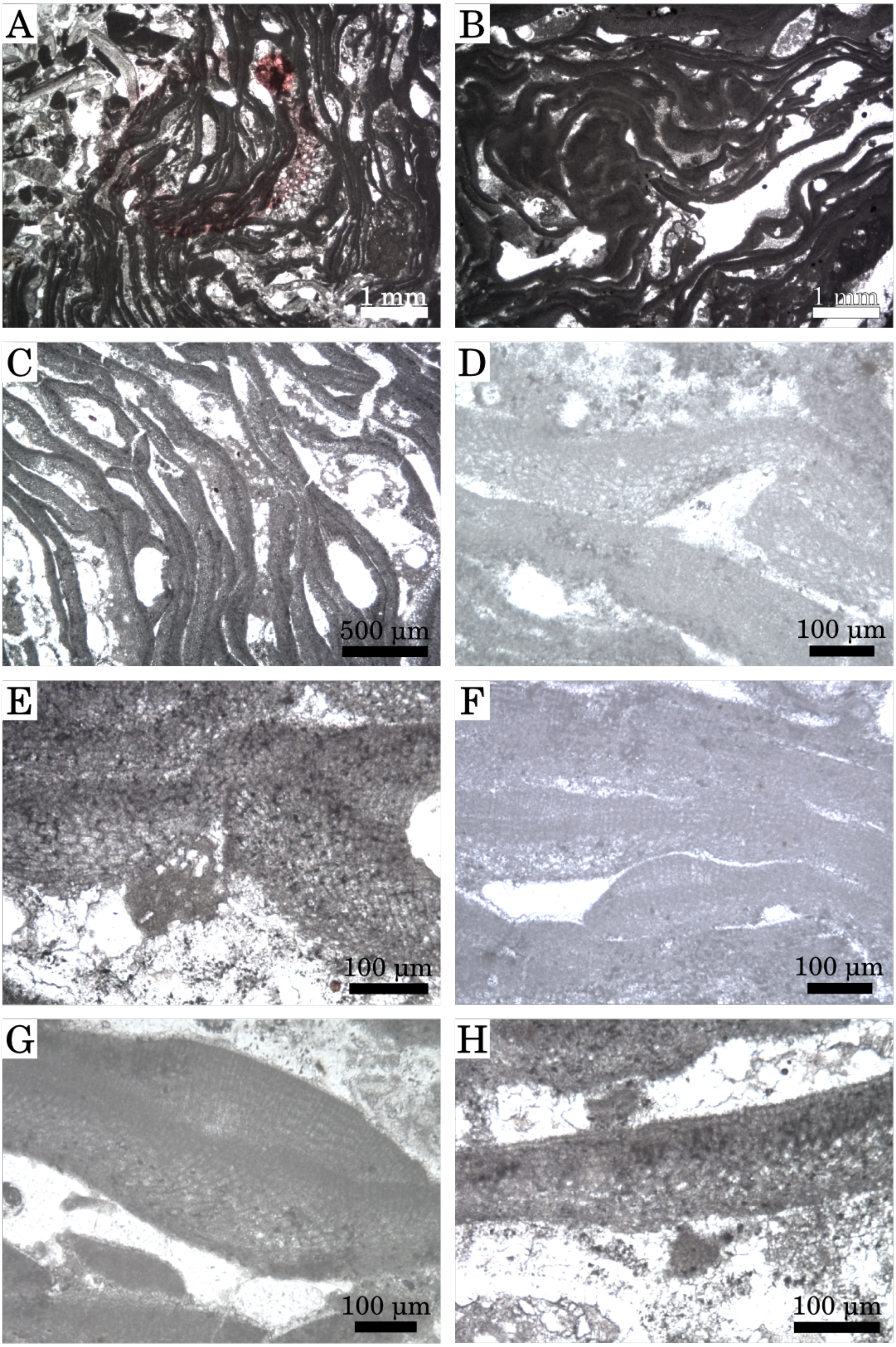

Figure 6.12.1 : Sporangial thallus of *Phymatolithon* sp. 1. A) TPB, Lithozone 4, thallus overiview. B) TPB, Lithozone 4, thallus overview. C) TPB, Lithozone 4, thallus overview. D) TPB, Lithozone 3, ventral core. E) TPB, Lithozone 4, ventral core. F) TPB, Lithozone 4, peripheral region. G) TPB, Lithozone 3, peripheral region nearby a conceptacle. H) TPB, Lithozone 4, normal peripheral region.

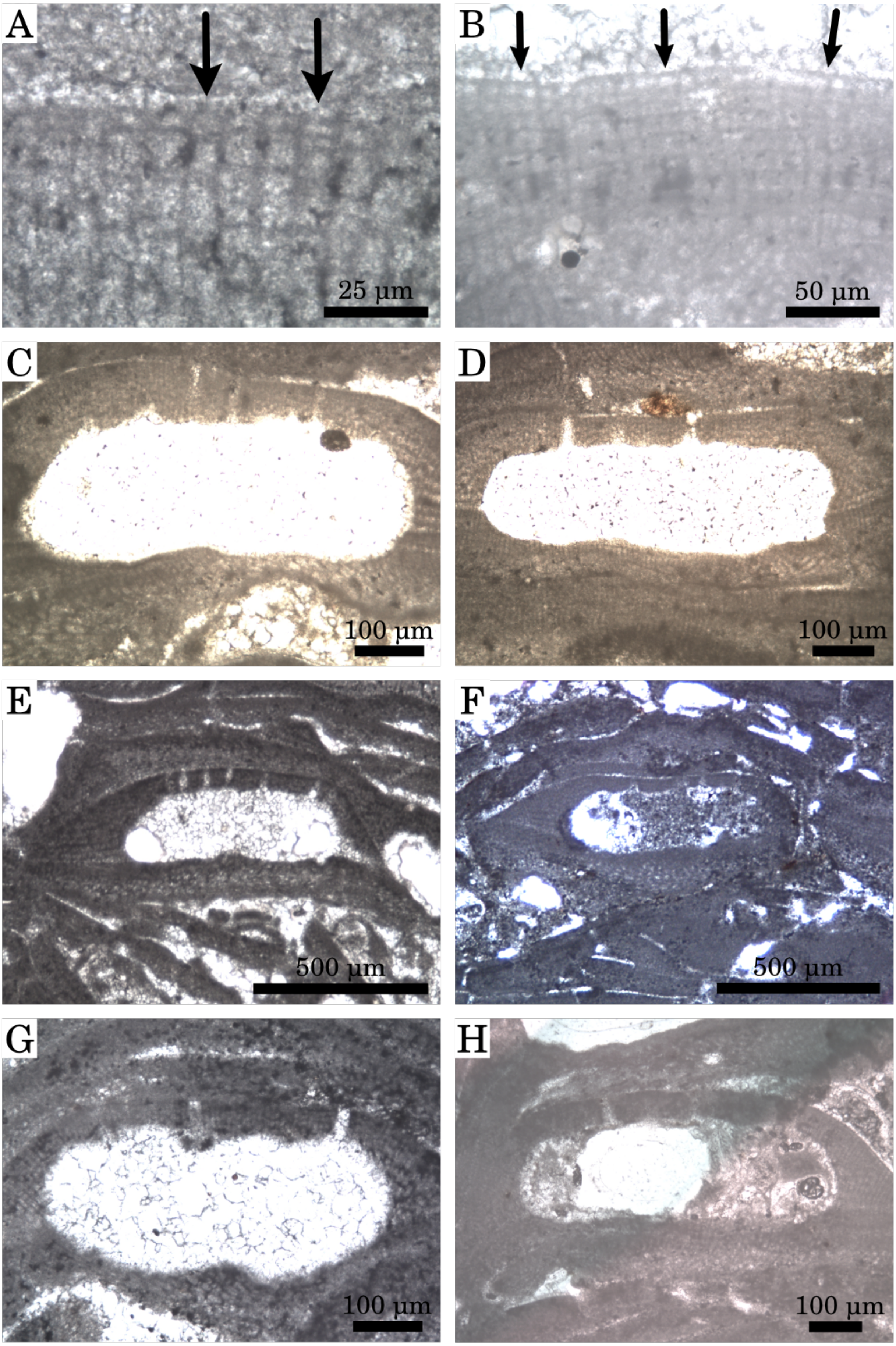

Figure 6.12.2 : Sporangial thallus of Phymatolithon sp. 1. A) TPB, Lithozone 4, detail of epitallial cells; black arrows=sub-epithallial cells as short or shorter than perithallial cells. B) TPB, Lithozone 4, detail of epitallial cells; black arrows=sub-epithallial cells as short or shorter than perithallial cells. C) Sommières, Pondrès , Lithozone 3, multiporate conceptacle. D) Sommières, Pondrès , Lithozone 3, multiporate conceptacle. E) TPB, Lithozone 4, multiporate conceptacle. F) TPB, Lithozone 3, multiporate conceptacle. G) TPB, Lithozone 4, multiporate conceptacle. H) TPB, Lithozone 3, multiporate conceptacle

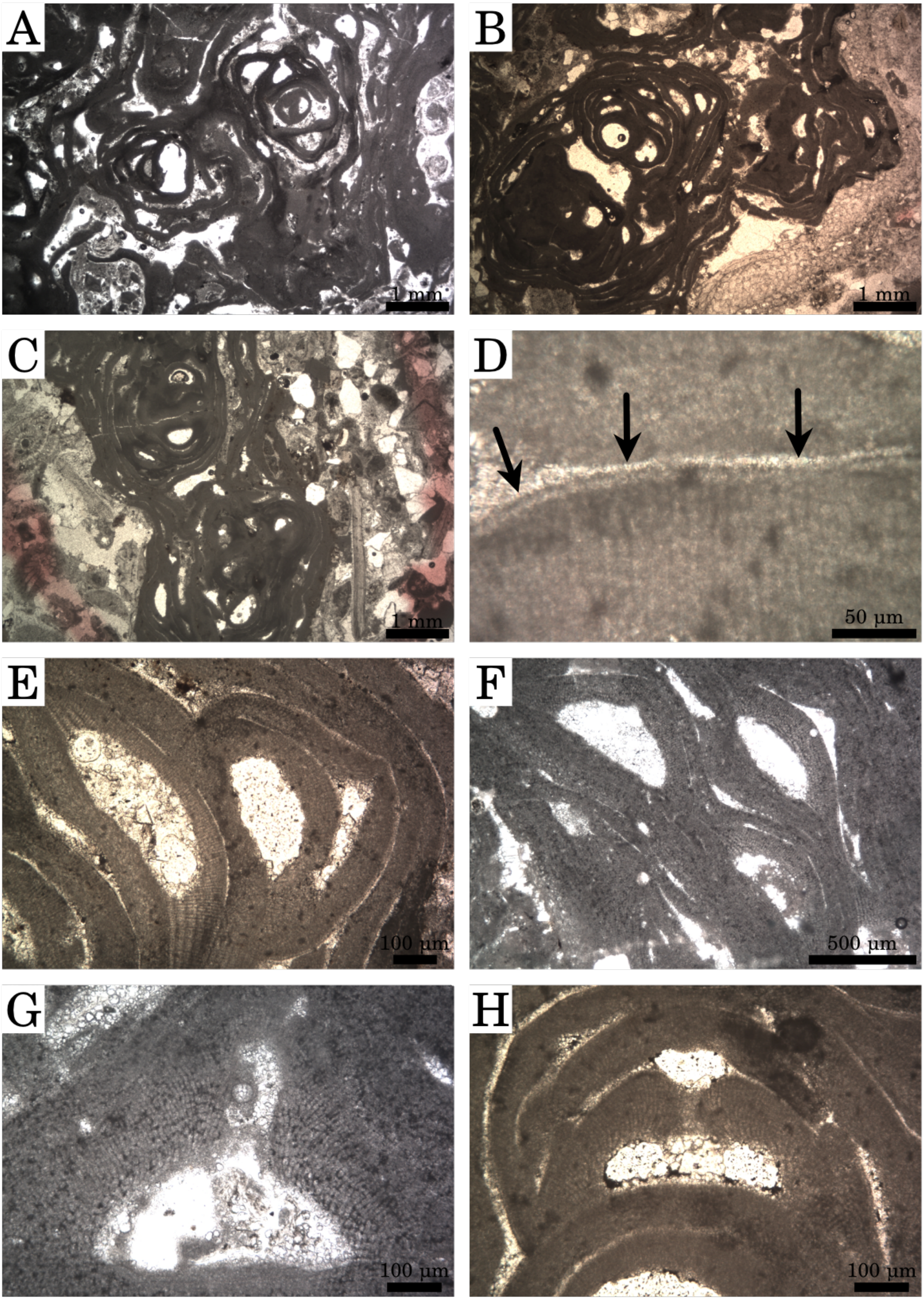

Figure 6.13.3 : Gametangial thallus of *Phymatolithon* sp. 1. A) TPB, overview of the thallus. B) Sommières, Pondres, Lithozone 5, overivew of the thallus. C) Sommières, Pondres, Lithozone 5, overivew of the thallus. D) Sommières, Pondres, Lithozone 5, detail of epithallial cells; black arrows=sub-epithallial cells as short or shorter of perithallial cells. E) Sommières, Pondres, Lithozone 5, reproductive anatomy. F) TPB, Lithozone 4, reproductive anatomy. G) TPB, Lithozone 4, gametangial conceptacle. H) Sommières, Pondres, Lithozone 5, gametangial conceptacle.

7 – Acknowledgments

I would like to deeply thank Grazia Vannucci for her invaluable assistance and precious suggestions on coralline algae identification and on the research world in general. I would like to thank Alfredo Frixa, my PhD supervisor, Akram El Kateb, Silvia Spezzaferri and Sirio Consani, without whose help this work would not have existed in the first place.

I would like to thank Andrea di Capua, Sergio Andò, Giovanni Vezzoli, Chiara Tessarolo, Elisa Malinverno, Agostina Vertino, Erlisiana Anzalone, Laura Borromeo, Fabio Marchese, Valentina Bracchi, Karen Gariboldi, Eduardo Ogliarolo, Alberto Resentini, Aaron Lim, Mara Limonta, Marta Padoan and Francesca Bolognesi for their precious help, suggestions and friendship throughout these years of PhD Scolarship. I also feel obliged to thank Alessandra Savini, Alessandro Cavallo, Cesare Corselli, Eduardo Garzanti, Marco Malusà, Maria Luce Frezzotti, Mauro Negri and Paolo Gentile, they have always been supportive of me and my research.

I am also indebted to Claudio Stalder, Marco Brandano, Luis Pomar, Bruno Granier, John Buckeridge, Dario Sartorio, Juraj Hraboský, Maria Triantaphyllou, Julio Aguirre, Werner Piller, Davide Bassi, Juan Carlos Braga, Yasufumi Iryu, Aki Kato, Amit Gosh, Federica Barillaro, Fulvio Franchi, Michele Piazza, Maria Cristina Bonci, Antonietta Rosso, Marco Taviani, Jean-Yves Reynaud and Ryuji Asami for their help and useful suggestions.

My special thanks also go to Curzio Malinverno and Angela Sanna, whose help has been fundamental, more than once.

I would like to acknowledge the COCARDE – European Research Network and the PhD program of Milano Bicocca University for their economical support, fundamental for the development of this work. I would also like to acknowledge the the University of Genova and the University of Fribourg for their technical and logistical support.
Finally I would like to thank all of my friends and relatives for helping and supporting me throughout these years of work: thank you all very much!

8-References

Abrantes F. (1992) – Paleoproductivity oscillations during the last 130 ka along the Portuguese and NW Africa margins. In Summerhayes C.P., Prell W.L., Emeis K.C. (eds.): Upwelling Systems: Evolution Since the Early Miocene. Geological Society Special Publication, 64, 499-510.

Adams C.G., Benson R.H., Kidd R.B., Ryan W.B.F., Wright R.C. (1977) – The Messinian salinity crisis and evidence of late Miocene eustatic changes in the world ocean. Nature, 269, 383-386.

Adams C.G., Lee D.E., Rosen R.B. (1990) – Conflicting isotopic and biotic evidences for tropical sea-surface temperatures during the Tertiary. Palaeogeography Palaeoclimatology Palaeoecology, 77, 289-313.

Adey W.H., Adey P.J. (1973) – Studies on the biosystematics and ecology of the epilithic crustose Corallinaceae of the British Isles. British Journal of Phycology, 8, 343-408.

Adey W.H., Macintyre I.G. (1973) – Crustose coralline algae: a re-evaluation in the geological sciences. Geological Society of America Bullettin, 84, 883-904

Adey W.H. (1979) – Crustose coralline algae as microenvironmental indicators in the Tertiary. In Gray J., Boucot A.J. (eds) : Historical Biogeography, Plate Tectonics and the changing environment, 459-464

Adey W.H., Townsend R.A., Boykins W.T. (1982) – The crustose coralline algae (Rhodophyta: Corallinaceae) of the Hawaiian Islands. Smithsonian contribution to Marine Sciences, 15, 84 pp.

Adey W.H. (1986) – Coralline algae as indicators of sea-level. In Van de Plassche O. (ed.): Sea-level research: a manual for the collection and evaluation of data. 229-280.

Afonso-Carillo J., Gil-Rodriguez M.C., Wildpret T.W. (1984) – Estudios en las algas Corallinaceae (Rhodophyta) de las Islas Canarias. Aspectos metodologicos. Vieraea, 13, 113-125.

Aguirre J., Riding R., Braga J.C. (2000) – Late Cretaceous incident light reduction: evidence from benthic algae. Lethaia,33, 205-213.

Aguirre J., Riding R., Braga J.C. (2000) – Diversity of coralline red algae: origination and extinction patterns from the Early Cretaceous to the Pleistocene. Paleobiology, 26, 651-667.

Aguirre J., Braga J.C., Reviers B., Woelkerling W.J. (2012) – Reassessment of Lemoine's newly discovered types of fossil corallines (Corallinales, Rhodophyta) preserved at the Muséum national d'histoire naturelle, Paris. Cryptogamie Algologie, 33, 289-326.

Amorosi A. (1995) – Glaucony and sequence stratigraphy: a conceptual framework of distribution in siliciclastic sequences. Journal of Sedimentary Research, 65, 419-425.

Amorosi A. (1997) – Detecting compositional, spatial and temporal attributes of glaucony: a tool for provenance research. Sedimentary Geology, 109, 135-153.

Andrieux-Loyer F., Aminot A. (2001) - Phosphorus Forms Related to Sediment Grain Size and Geochemical Characteristics in French Coastal Areas . Estuarine, Coastal and Shelf Sciences, 52, 617-629.

Allen P., Mange-Rajetzky M., Matter A., Homewood P. (1985) – Dynamic paleogeography of the open Burdigalian seaway. Swiss Molasse Basin. Eclogae Geologicae Helveticae, 78, 351-381.

Bassi D., Carannte G., Murru M., Simone L., Toscano F. (2006) - Rhodalgal/Bryomol assemblage in temperate type carbonate depositional systems: Early Miocene of the Sarcidano area (Sardinia Italy). In Pedley H., Carannante G. (eds.): Cool-Water Carbonate: depositional systems and paleoenvironmental controls. Geological Society of London, Special Publications, 255, 35-52.

Bassi D., Braga J.C., Iryu Y. (2009) – Palaebiogeographic pattern of a persistent monophyletic lineage: Lithophyllum pustulatum species group (Corallinaceae, Corallinales, Rhodophyta). Palæogeography, Palæoclimatology, Palæoecology, 284, 237-245.

Bassi D., Carannante G., Checconi A., Simone L., Vigorito M. (2010) – Sedimentological and paleoecological integrated analysis of Miocene channelized carbonate margin, Matese Mountains, Southern Apennines, Italy. Sedimentary Geology, 230, 105-122.

Basso D. (1991) – Applicazione di un nuovo metodo sperimentale per l'indagine tafonomica in rodoliti attuali: il contributo micropaleontologico. [PhD Seminar,V cycle], 48 pp.

Basso D., Tomaselli V. (1994) – Paleoecological potentiality of rhodoliths: a Mediterranean case history. Bollettino della Società Paleontologica Italiana, Atti del V Simposio di Ecologia e Paleoecologia delle Comunità Bentoniche, Roma 28-30/9/1992, 17-27.

Basso D., Fravega P., Vannucci G. (1996) - Fossil and living corallinaceans related to the Mediterranean endemic species *Lithophyllum racemus* (Lamark) Foslie. Facies, 35, 275-292.

Basso D., Fravega P., Vannucci G. (1997) – The taxonomy of *Lithothamnion ramosissimum* (Gumbel non Reuss) Conti and Lithothamnion operculatum Conti (Rhodophyta, Corallinaceae). Facies, 37, 167-182.

Basso D. (1998) – Deep rhodolith distribution in the Pontinian Islands, Italy, a model for the paleoecology of a temperate sea. Palaeogeography Palaeoclimatology Palaeoecology, 137, 173-187.

Basso D., Fravega P., Piazza M., Vannucci G. (1998) – Biostratigraphic, paleobiogeographic and paleoecological implications in the taxonomic review of Corallinaceae. Rendiconti dell'Accademia dei Lincei, 9, 201-211.

Basso D., Nalin R., Nelson C.S. (2009) – Shallow-water *Sporolithon* rhodoliths from North Island (New Zealand). Palaios, 24, 92-103.

Basso D., Rodondi G., Bressan G. (2011) – A re-description of *Lithothamnion crispatum* and the status of Lithothamnion superpositum (Rhodophyta, Corallinales). Phycologia , 50, 144-155.

Basso D., Quaranta F., Vannucci G., Piazza M. (2012) – Quantification of the coralline carbonate from a Serravallian rhodolith bed of the Tertiary Piedmont Basin (Stazzano, Alessandria, NW Italy). Geodiversitas, 34, 137-149.

Baráth I., Nagy A., Kováč M. (1994) – Sandberské vrstvy – vrchnobádenské marginálne sedimenty východného okraja Viedenskej panvy. Geologické práce Správy, 99, 59-66.

Bartoli G., Sarnthein M., Weinelt M., Erlenkeuser H., Garbe-Schönberg D., Lea D.W. (2005) – Final closure of Panama and the onset of northern hemisphere glaciation . Earth and Planetary Science Letters, 237, 33-44.

Baturin G.N. (2003) – Phosphorous cycle in the ocean. Lithology and Mineralogical Resources, 38, 101-119.

Beavington-Penney S.J., Racey A. (2004) – Ecology of extant nummulitids and other large benthic foraminifera in palaeoenvironmental analysis. Earth Science Reviews, 67, 219-265.

Beavington-Penney S.J., Wright V.P., Racey A. (2005) – Sediment production and dispersal on the foraminifera-dominated Tertiary ramps: the Eocene El Garia Formation, Tunisia. Sedimentology, 52, 537-569.

Beltzer C., Brachert T.C., Nebelsick J. (1997) – The warm temperate carbonate province: a review of the facies, zonations and delimitations. Courier Forschungsinstitut Senkenberg, 201, 83-99.

Berger G.M. (1974) – Carte géologique de la France à 1/50000, Sommières (n°964). BRGM, Orléans.

Besson D., Parize O., Rubino J.L., Aguilar J.P., Aubry M.P., Beaudoin B., Berggren W.A., Clauzon G., Crumeyrolle P., Dexcoté Y., Fiet N., Iaccarino S., Jiménez-Moreno G., Laporte-Galaa C., Michaux J., Salis K., Suc J.P., Reynaud J.Y., Wernli R. (2005) – Un réseau fluviatile d'âge Burdigalien terminal dans le Sud-Est de la France : remplissage, extension, âge, implications. Comptes Rendus Geoscience, 337, 1045-1054.

Bicchi E., Dela Pierre F., Ferrero E. (2002) – Rosignano e Colma: la Pietra da Cantoni. In: D'Atri A., Dela Pierre F., Festa A.R., Gnaccolini M., Piana F., Clari P., Polino R. (eds.) - Tettonica e sedimentazione nel "retroforeland alpino". Società Geologica Italiana, 83-89.

Bicchi E., Dela Pierre F., Ferrero E., Maia F., Negri A., Pirini-Radrizzani C., Radrizzani S., Valleri G.

(2006) – Evolution of the Miocene carbonate shelf of Monferrato (North-western Italy). Bollettino della Società Paleontologica Italiana, 45, 1-24.

Billups K., Scheiderich K. (2010) – A synthesis of Oligocene trough Miocene deep sea temperatures as inferred by Mg/Ca ratios. In: Mutti M., Piller W.E., Betzler C. (eds.) - Carbonate system during the Oligocene-Miocene Climatic Transition. International Association of Sedimentologist, Special Publication, 42, 1-16.

Bittner L., Payri C.E., Maneveldt G.W., Couloux A., Cruaud C., Reviers B., Le Gall L. (2011) – Evolutionary History of the Corallinales (Corallinophycidae, Rhodophyta), inferred from nuclear, plastidial and mitochondrial genomes. Molecula Phylogenetics and Evolution, 61, 697-713.
Bizzozero G. (1885) – Flora veneta crittogamica; Parte II.- Padova, 255 pp.

Blow W.H. (1969) – Late middle Eocene to Recent planktonic foraminifera biostratigraphy. Proceedings of first international conference on planktonic microfossils, Geneve, 1, 199-422.

Bonci C., Clari P.A., Ferrero E., Ghiribaudo G., Pirini C., Ricci B., Valleri G., Violanti D. (1990) – The Diatomites of Marmorito (Westerno Monferrato, Northen Italy). Memorie di Scienze Geologiche dell'Università di Padova, 42, 189-225.

Bodin S., Godet A., Föllmi K.B., Vermeulen J., Arnaud H., Strasser A., Fiet N., Adatte T. (2006) – The late Hauterivian Faraoni oceanic anoxic event in the western Tethys: Evidence from phosphorous burial rates. Palaeogeography, Palaeoclimaology, Palaeoecology, 235, 245-264.

Böhme M. (2003) – The Miocene Climatic Optimum: evidence from ectothermic vertebrates of Central Europe. Palaeogeography, Palaeoclimatology, Palaeoecology, 195, 389-401.

Böhme M., Bruch A., Selmeier A., (2007) – The reconstruction of Early and Middle Miocene climate and vegetation in Southern Germany as determined from the fossil wood flora . Palaeogeography, Palaeoclimatology, Palaeoecology, 253, 91-114.

Borromeo O., Miraglia S., Sartorio D., Bolla E.M., Ortenzi A., Reali S., Castellanos C., Villalobos R. (2011) – The Perla World-class Giant Gas Field, Gulf of Venezuela; Depositional and diagenetic controls on reservoir quality in Early Miocene carbonates. AAPG International Conference and Exibition, Milan, Italy.

Bosellini A., Ginsburg R.N. (1971) – Form and internal structure of recent algal nodules (rhodolites) from Bermuda. Journal of Geology, 79, 669-682.

Bosence D.W.J. (1976) – Ecological studies on two unattached coralline algae from Western Ireland. Palaeontology, 19, 365-395.

Bosence D.W.J. (1983a) - Description and classification of rhodoliths (rodoids, rhodolites). In Peryt T.M. (ed.): Coated Grains. Springer-Verlag, 217-224.

Bosence D.W.J. (1983b) - The occurrence and ecology of recent rhodoliths. In Peryt T.M. (ed.): Coated Grains. Springer-Verlag, 225-242.

Bosence D. (2005) – A genetic classification of carbonate platform based on their basinal and tectonic settings in the Cenozoic. Sedimentary Geology, 175, 49-72.

Boyle E.A. (1992) – Cadmium and $\partial^{13}C$ paleochemical ocean distribution during the stage 2 glacial maximum. Annual Review of Earth and Planetary Sciences, 20, 245-287.

Braga J.C., Bosence D.W.J. & Steneck R.S. (1993) – New anatomical characteristics in fossil coralline algae and their taxonomic implications. Paleontology, 36, 535-547.

Braga J.C., Aguirre J. (1995) – Taxonomy of fossil coralline algal species: Neogene Lithophylloideae (Rhodophyta, Corallinaceae) from southern Spain. Review of Palaeobotany and Palynology 86, 265-285.

Braga J.C., Aguirre J. (2001) – Coralline algal assemblages in Upper Neogene reef and temperate carbonates in Southern Spain. Palaeogeography Palaeoclimatology Palaeoecology, 175, 37-41.

Braga J.C., Vescogni A., Bosellini F.R., Aguirre J. (2009) – Coralline algae (Corallinales, Rhodophyta) in the western and central Mediterranean Messinian reefs. Palaeogeography Palaeoclimatology Palaeoecology, 275, 113-128.

Braga J.C., Bassi D., Piller W. E. (2010) – Paleoenvironmental significance of Oligocene-Miocene coralline red algae – a review. In Mutti M., Piller W.E., Betzler C. (eds.): Carbonate system during the Oligocene-Miocene Climatic Transition. International Association of Sedimentologist, Special Publication 42, 165-182.

Brandano M., Corda L. (2002) – Nutrients, sea level and tectonics: constrains for the facies architecture of a Miocene carbonate ramp in central Italy. Terra Nova, 14, 257–262.

Brandano M., Vannucci G., Pomar L., Obrador A. (2005) – Rhodolith assemblages from the lower Tortonian carbonate ramp of Menorca (Spain): environmental and paleoclimatic implications. Palaeogeography Palaeoclimatology Palaeoecology, 226, 307-323.

Brandano M., Vannucci G., Mateu-Vicens G. (2007) – Le Alghe rosse calcaree come indicatori paleoambientali: l'esempio della rampa carbonatica Laziale-Abruzzese (Burdigaliano, Appennino centrale). Bollettino della Società Geologica Italiana, 126, 55-69.

Brandano M., Frezza V., Tommasetti L., Pedley. M., Matteucci R. (2009) – Facies analysis and paleoenvironmental interpretation of the Late Oligocene Attard Member (Lower Coralline Limestone Formation), Malta. Sedimentology, 56, 1138-1158.

Brandano M., Lipparini L., Campagnoni V., Tomassetti L. (2012) – Downslope-migrating larges dunes in the Chattian carbonate ramp of the Majella Mountains (Central Apennines, Italy). Sedimentary Geology, 255-256, 29-41.

Brandano M., Ronca S. (2014) – Depositional processes of the mixed carbonate-siliciclastic rhodolith beds of the Miocene Saint-Florent Basin, northern Corsica. Facies, 60, 73-90.

Brandano M., Cornacchia I., Raffi I., Tomassetti L. (2016) – The Oligocene–Miocene stratigraphic evolution of the Majella carbonate platform (Central Apennines, Italy) . Sedimentary Geology, 333, 1-14.

Brasier M.D. (1992) – Nutrient enriched waters and the early skeletal fossil record. Journal of the geological society, 149, 621-629.

Brasier M.D. (1995a) – Fossil indicators of nutrient levels 1: eutrophication and climate change. In Bosence D.W.J., Allison P.A. (eds.): Marine Paleoenvironmental Analysis from Fossils. Geological Society Special Pubblication, 83, 113-132.

Brasier M.D. (1995b) – Fossil indicators of nutrient levels 2: evolution and extinction in relation to oligotrophy. In Bosence D.W.J., Allison P.A. (eds.): Marine Paleoenvironmental Analysis from Fossils. Geological Society Special Pubblication, 83, 133-150.

Bressan G. & Babbini L. (2003) – Corallinales del Mar Mediterraneo: Guida alla determinazione. Biologia Marina Mediterranea, 10, 237 pp.

Brett C.E. & Baird G.C. (1986) – Comparative taphonomy: a key to paleoenvironmental interpretations based on fossils preservation. Palaios, 1, 207-227.

Calvert S.E. (1966). Accumulation of diatomaceous silica in sediment of the Gulf of California. Bullettin of the Geological Society of America, 77, 569-596.

Capone D.G., Zehr J.P., Paerl H.W., Bergman B., Carpenter E.J. (1997) – *Trichodesmium* a globally significant marine cyanobacterium. Science 276, 1221-1229.

Carannante G., Esteban M., Milliman J.D., Simone L. (1988) – Carbonate lithofacies as paleolatitude indicators: problems and limitations. Sedimentary Geology, 60, 333-346.

Carannante G., Severini C., Simone, L. (1996) – Off shelf carbonate transport along foramol (temperate-type) open shelf margin: an example from the Miocene of the central and southern Apennines (Italy). Memorie della Società Geologica Francese, 169, 277-288.

Carannante G., Graziano R., Pappone G., Ruberti D., Simone L. (1999) – Depositional System and Response to Sea Level Oscillation of the Senonian Rudist-bearing Carbonate shelves. Examples from Central Mediterranean Area. Facies, 40, 1-24.

Carozzi A.V. (1993) – Sedimentary Petrography. 263 pp.

Cerling T.E., Wang Y., Quade J. (1993) – Expansion of C4 ecosystems as an indicator of global ecological change in the late Miocene. Nature, 361, 344-345.

Civitelli G., Brandano M. (2005) – Atlante delle litofacies e modello deposizionale dei calcari a Briozoi e Litotamni della piattaforma carbonatica Laziale-Abruzzese. Bollettino della Società Geologica Italiana, 124, 611-643.

Checconi A., Bassi D., Carannante G., Monaco P. (2010) – Re-deposited rhodoliths in the Middle Miocene hemipelagic deposits of Vitulano (Southern Appenines, Italy): Coralline assemblage characterization and related trace fossils. Sedimentary Geology, 225, 50-66.

Cherchi A., Murru M. & Simone L. (2000) – Miocene Carbonate Factories in the Sy-rift Sardinia Graben Subbasin (Italy). Facies, 43, 223-240.

Clari P., Dela Pierre F., Novaretti A., Timpanelli M. (1994) – La successione oligo-miocenica del Monferrato occidentale: confronti e relazioni con il Monferrato orientale e la Collina di Torino. Atti Ticinesi Sci. Terra Serie Special, 1, 192-203.

Clari P., Dela Pierre F., Novaretti A., Timpanelli M. (1995) – Late Oligocen-Miocene sedimentary evolution of the critcal Alps-Apennines junction: the Monferrato area, Northwestern Italy. Terra Nova, 7, 144-152.

Clarke K.R., Gorley R.N (2006) - PRIMER v6: User Manual/Tutorial. PRIMER-E. 192 pp.

Corliss B.H. (1985) - Microhabitats of benthic foraminifera within deep-sea nutrients. Nature, 314, 435-438.

Coletti G., Basso D., Frixa A. (2013) – Nutrient “cooling” effect on carbonates: evidence from a Miocene limestone. COCARDE Workshop and field seminar 2013, abstract book.

Coletti G., Basso D., Frixa A. (2016) - Economic importance of coralline carbonates. In Riosmena-Rodriguez R., Nelson W. & Aguirre J. (eds.): Rhodolith/Maerl beds: a Global Perspective. Special volume, Springer-Verlag, Berlin.

Conti S. (1943) – Contributo allo studio delle Corallinaceae del Terziario Italiano: Corallinaceae del Miocene Ligure-Piemontese. Paleontographica Italica, 41, 37-61.

Cronquist A. (1960) – The divisions and classes of plants. The Botanical Review, 26, 425-482.

Cullen J.T., Lane T.W., Morel F.M.M., Sherrell R.M. (1999) – Modulation of cadmium uptake in phytoplankton by seawater CO2 concentration. Nature, 402, 165-167.

Cunningham K.J., Collins L.S. (2002) – Controls on facies and sequence stratigraphy of an upper Miocene carbonate ramp and platform, Melilla basin, NE Morocco. Sedimentary Geology, 146, 285-304.

D'Atri A. (1990) – Facies e sequenze deposizionali nella Formazione di Visone (Miocene inferiore, Bacino Terziario Ligure Piemontese). Memorie della Società Geologica Italiana, 45, 723-729.

D'Atri A., Dela Pierre F., Lanza, R., Ruffini R. (1999) – Distinguishing primary and resedimented vitric volcanoclastic layers in the Burdigalian carbonate shelf deposits in Monferrato (NW Italy). Sedimentary Geology, 129, 143-163.

D'Atri A., Dela Pierre F., Novaretti A., Cosca M.A., Hunziker J.C. (2001) – Miocene plankton biostratigraphy and $^{40}Ar/^{39}Ar$ dating. Eclogae Geolicae Helvetiae, 94, 137-144.

Delaney M.L. (1998) – Phosphorous accumulation in marine sediments and the oceanic phosphorus cycle. Global Biogeochemical Cycles, 12, 563-572.

Delaney M.L., Boyle E.A. (1987) – Cd/Ca in late Miocene benthic foraminifera and changes in global organic carbon budget. Nature, 300, 156-158.

Dela Pierre, F. Mikhailov V., Polino R. (1995) – The tectonosedimentary evolution of the tertiary basin in the western Po plain: Kinematics inferred from subsidence curves. Atti del Convegno "Rapporti tra Alpi e Appennino" Peveragno (CN), Accademia Nazionale delle Scienze, Collana Scritti e Documenti, XIV, 129-146.

Dela Pierre F., Piana F., Fioraso G., Boano P., Bicchi E., Forno M.G., Violanti D., Balestro G., Clari P., D'Atri A., De Luca D., Morelli M., Ruffini R. (2003) - Note illustrative della carta geologica d'Italia alla scala 1:50000; Foglio 157 Trino, Apat e Dipartimento per la Difesa del Suolo, 147 pp.

Demarcq G. (1970) – Etude stratigraphique du Miocène rhodanien. Mémoires du BRGM, 61, 257 pp.

DeMaster D.J. (2002) – The accumulation and cycling of biogenic silica in the Southern Ocean: revisiting the marine silica budget. Deep Sea Research II, 49, 3155-3167.

DePaolo D.J., Finger K.L. (1991) – High-resolution strontium isotope stratigraphy and biostratigraphy of the Miocene Monterey Formation, central California. Geological Society of America Bullettin, 103, 112-124.

Dercourt J., Gaetani M., Vrielynk B., Barrier E., Biju-Duval B., Brunet M.F., Cadet J.P, Crasquin S., Sandulescu M. (eds.) (2000) – Atlas Peri-Tethys, Palaeogeographical maps, 279 pp.

De Santis L., Anderson B.J., Brancolini G., Zayatz I. (1995) – Seismi record of late Oligocene through Miocene Glaciation on the Central and Eastern Continental Shelf of the Ross Sea. In Cooper A.K., Barker F.B., Brancolini G. (eds.): Geology and Seismic Stratigraphy of the Antarctic Margin. Antarctic Research Series, 68, 235-260.

Doláková N., Brzobohatý R., Hladilová Š., Nehyba S. (2008) – The red–algal facies of the Lower Badenian limestones of the Carpathian Foredeep in Moravia (Czech Republic). Geologica Carpathica, 59, 133-146.

Doláková N., Holcová K., Nehyba S., Hladilová Š, Brzobohatý R., Zágoršek K., Hrabovský J., Seko M., Utescher T. (2014) – The Badenian parastratotype at Židlochovice from the perspective of the multiproxy study. Neues Jahrbuch für Geologie und Paläontologie, 271, 169-201.

Duce R.A, Liss P.S., Merrill J.T., Atlas E.L., Buat-Menard P., Hicks B.B., Miller J.M., Prospero J.M., Arimoto R., Church T.M., Ellis W., Galloway J.N., Hansen L., Makuantyson C.P.D.B., Jickelles T.D., Knap A.H., Reinhardt K.H., Schenider B., Soundine A. Tokos J.J., Tsunogai S., Wollast R., Zhou M. (1991) – The atmospheric input of trace species to the world ocean. Global Biogeochemical Cycles, 5, 193-259.

Dugdale R.C., Wilkerson F.P., Minas H.J. (1995) – The role of silicate pump in driving new production. Deep Sea Research I, 42, 697-719.

Dymond J., Suess E., Lyle M. (1992) – Barium in deep-sea sediment: a geochemical proxy for paleoproductivity. Paleoceanography, 7, 163-181.

Erlich R.N., Barrett S.F., Ju G.B (1990) – Seismic and geologic characteristics of drowning events on carbonate platforms. AAPG Bullettin, 74, 1523–1537.

Esteban M. (1996) – An overview of Miocene reefs from Mediterranean areas: general trends and facies models. In Franseen E.K., et al., (eds.) : Models for carbonate stratigraphy from Miocene reef complexes of Mediterranean regions. SEPM (Society for Sedimentary Geology), Concepts in Sedimentology and Paleontology, 5, 3-53.

Falkowsky P.G., Barber R.T., Smetacek V. (1998) – Biogeochemical control and feedbacks on oceans primary production. Science, 281, 200-206.

Falletti P., Gelati R., Rogledi S. (1995) – Oligo-Miocene evolution of Monferrato and Langhe related to deep structures. Atti del Convegno "Rapporti tra Alpi e Appennino" Peveragno (CN), Accademia Nazionale delle Scienze, Collana Scritti e Documenti, XIV, 1-19.

Field J.G., Clarke K.R., Warwick R.M. (1982) – A pratical strategy for analyzing multispecies distribution patterns. Marine Ecology Progresses Series, 8, 37-52.

Filipescu S., Gîrbacea R. (1997) – Lower Badenian Sea-Level Drop on the Western Border of the Transylvanian Basin: Foraminiferal Paleobathymetry and Stratigraphy. Geologica Carpathica, 48, 325-334.

Fiorini F. (2015) – Recent benthic foraminifera from the Caribbean continental slope and shelf off west Colombia. Journal of South America Earth Sciences, 60, 117-128.

Flower B.P., Kennet J.P. (1994) – The middle Miocene climatic transition: East Antarctic ice sheet development, deep ocean circulation and global carbon cycling . Palaeogeography, Palaeoclimatology, Palaeoecology, 108, 537-555.

Flügel E. (2009) – Microfacies of Carbonate Rocks: Analysis Interpretation and Application. 1007 pp.

Föllmi K.B. (1995) – 160 m.y. record of marine sedimentary phosphorous burial: coupling of climate and continental weathering under greenhouse and icehouse conditions. Geology, 23, 859-862.

Föllmi K.B. (1996) – The phosphorous cycle, phosphogenesis and phosphate-rich deposits. Earth-Sciences Review, 40, 55-124.

Foslie M. (1909) – Alogologiske notiser VI. Det Kongelige Norske Videnskaberne Selskabs Skrifter, 2, 1-63

Fournier F., Borgomano J. (2007) – Geological significance of seismic reflections and imaging of the reservoir architecture in the Malampaya gas field (Philippines). AAPG Bullettin, 91, 235–258.

Fravega P., Vannucci G. (1982) – Significato e caratteristiche degli episodi a rhodoliti al top del Serravalliano tipo. Geoloigica Romana, 21, 705-715.

Fravega P., Piazza M., Vannucci G. (1989) – *Archaeolithothamnium* Rothpletz, inidicatore ecologico-stratigrafico?. Simposio di Ecologia e Paleoecologia delle Comunità Bentoniche 1985, Atti, 3, 729-743.

Fravega P., Piazza M., Vannucci G. (1993) – Three new species of coralline algae (genera Lithothamnion and Lithophyllum) from the Tertiary Piedmont Basin. Rivista Italiana di Paleontologia e Stratigrafia, 4, 453-466.

Froelich P.N. (1988) – Kinetic control of dissolved phosphate in natural rivers and estuaries: a primer on the phosphate buffer mechanisms. Limnology and Oceanography, 33, 649-668.

Froelich P.N., Bender M.L., Luedtke N.A., Heath G.R., DeVries T. (1982) – The marine phosphorous cycle. American Journal of Science, 282, 474-511.

Garcia-Castellanos D., Estrada F., Jiménez-Munt I., Gorini C., Fernàndez M., Vergés J., De Vincente R. (2009) – Catastrophic flood of the Mediterranean after the Messinian salinity crisis. Nature, 462, 778-781.

Garcia H.E., Locarini R.A., Boyer T.P., Antonov J.I., Zweng M.M., Baranova O.K., Johnson D.R. (2010) –

In Levitus S.(ed), NOAA Atlas NESDIS 72 : World Oceans Atlas 2009, volume 4: nutrients (phosphate, nitrate and silicate). 398 pp.

Garzanti E. (1993) – Himalayan ironstone, “superplumes”, and the breakup of Gondwana. Geology, 21, 105-108.

Geel T (2000) – Recognition of stratigraphic sequences in carbonate platform and slope deposits: empirical models based on microfacies analysis of Paleogene deposits in southeastern Spain. Palaeogeography Palaeoclimatology Palaeoecology, 155, 211-238.

Goubert E., Nèraudeu D., Rouchy J.M., Lacour D. (2001) – Foraminiferal record of environmental changes: Messinian of the Los Yeos area (Sorbas Basin, SE Spain). Palaeogeography Palaeoclimatology Palaeoecology, 175, 61-78.

Grasso M., Pedley H.M. (1988) – The sedimentology and development of Terravecchia Formation carbonates (Upper Miocene) of North Central Sicily: Possible eustatic influence on facies development. Sedimentary Geology, 57, 131-149.

Gray J.E. (1864) – Handbook of British water-weeds or Algae. R. Hardwicke, London, 123 pp.

Guidry M.W., Mackenzie F.T., Arvidson R.S. (2000) – Role of tectonics in phosphorus distribution and cycling. SEPM special publication, 66, 35-51.

Guidry M.W., Mackenzie F.T. (2003) – Experimental Study of Igneous and Sedimentary Apatite Dissolution: Control of pH, Distance from Equilibrium, and Temperature on Dissolution Rates. Geochimica et Cosmochimica Acta, 67, 2949, 2963.

Haile-Selassie Y. (2001) – Late Miocene hominids from the Middle Awash, Ethiopia. Nature, 12, 178-181.

Hageman S.J., Lukasik J., Mcgowran B., Bone Y. (2003) – Paleoenvironmental Significance of Celleporaria (Bryozoa) from Modern and Tertiary Cool-water Carbonates of Southern Australia. Palaios, 18, 510-527.

Halfar J., Godinez-Orta L., Goodfriend G.A., Mucciarone D.A., Ingle J.C. Jr., Holen P. (2001) –

Holocene-late Pleistocene non-tropical carbonate sediments and tectonic history of the western rift basin margin of the southern Gulf of California. Sedimentary Geology, 144, 149-178.

Halfar J., Godinez-Orta L., Mutti M., Valdez-Holguìn J.E., Borges J.M. (2004) – Nutrient and temperature controls on modern carbonate production: an example from the Gulf of California, Mexico. Geology, 32, 213-216.

Halfar J., Mutti M. (2005) – Global dominance of coralline red-algal facies: a response to Miocene oceanographic events. Geology, 33,481-484.

Halfar J., Strasser M., Riegl B., Gondinez-Orta L. (2006) - Oceanography, sedimentology and acoustic mapping of a bryomol carbonate factory in the northen Gulf of California, Mexico. In Pedley H.M., Carannante G. (eds.): Cool -Water Carbonates : Depositional Systems and Paleoenvironmental Controls. Geological Society, London, Special Publications, 197-215.

Hallock P., Schlager W. (1986) – Nutrient excess and the demise of coral reefs and carbonate platforms. Palaios, 1, 389-398.

Hallock P. (1987) – Fluctuation in the trophic resources continuum: a factor in global diversity cycle. Paleoceanography, 2, 457-471.

Hallock P. (1988a) – The role of nutrient availability in bioerosion: consequences to carbonate buildups. Palaeogeography, Palaeoclimatology, Palaeoecology, 63, 275-291.

Hallock P. (1988b) – Diversification in algal symbiontbearing foraminifera: a response to oligotrophy? Revue de Paleobiologie, Special Volume, 2, 789- 797.

Hallock P., Muller K.F.E., Halas J.C. (1993) – Coral reef decline - anthropogenic nutrients and the degradation of western Atlantic and Caribbean coral reefs. Research and Exploration, 9, 358-378.

Hallock, P. (2001) – Coral reefs in the 21st century: is the past the key to the future? In Greenstein B.J., Carney C.K. (eds.): Proceedings of the 10th Symposium on the Geology of the Bahamas and Other Carbonate Regions (Eds B.J. Greenstein and C.K. Carney). Gerace Research Center, San Salvador, Bahamas, 8-13.

Hallock P. (2005) - Global change and modern reefs: new opportunities to understand shallow-water carbonate depositional processes. Sedimentary Geology, 175, 19-33.

Harrison J.A., Bouwman L., Mayorga E., Seitzinger S. (2010) - Sources of dissolved inorganic phosphorus inputs to surface fresh waters and the coastal zone: a new global model. Global Biogeochemical Cycles 244, doi: 10.1029/ 2009GB003590.

Harvey A.S., Broadwater S.T., Woelkerling W.J., Mitrovski P.J. (2003) – *Choreonema* (Corallinales, Rhodophyta): 18S rDNA phylogeny and resurrection of the Hapalidiaceae for the subfamilies Choreonematoideae, Austrolithoideae, and Melobesioideae. Journal of Phycology, 39, 988-998.

Harzhauser M., Piller W.E. (2007) – Benchmark data of a changing sea: Palaeogeography, Palaeobiogeography and events in the Central Paratethys during the Miocene. Palaeogeography, Palaeoclimaology, Palaeoecology, 253, 8-31.

Haug G.H., Tiedemann R. (1998) – Effect of the formation of the Isthmus of Panama on Atlantic Ocean thermohaline circulation . Nature, 393, 673-676.

Hauck F. (1878) – Beirträge zur Kenntniss der Adriatischen Algen X.- Österreichische Botanische Zeitschrift, 28, 288-295.

Haunold T.G., Baal C. & Piller W.E. (1997) – Benthic foraminiferal associations in the Northern Bay of Safaga, Red Sea, Egypt. Marine Micropaleontology, 29, 185-210.

Heubeck C., Story K., Peng P., Sullivan C., Duff S. (2004) – An integrated reservoir study of the Liuhua 11-1 field using a high-resolution three-dimensional seismic data set. In - Seismic imaging of carbonate reservoirs and systems. AAPG Memorie, 81, 149-168.

Heydrich F. (1897) – Melobesiae. Berichte der deutsche botanischen Gesellschaft, 15, 403-420.

Holburn A., Kuhnt W., Shulz M., Flores J.A., Andersen N. (2007) – Orbitally-paced climate evolution during the middle Miocene “Monterey” carbon-isotope excursion . Earth and Planetary Science Letters, 261, 534-550.

Holcová K., Zágoršek K (2008) – Bryozoa, foraminifera and calcareous nannoplankton as environmental proxies of the "bryozoan event" in the Middle Miocene of Central Paratethys (Czech Republic). Palaeogeography Palaeoclimatology Palaeoecology, 267, 216-234.

Holmes N.J., Harriott V.J., Banks S.A. (1997) – Latitudinal variation in patterns of colonization of cryptic calcareous marine organisms . Marine Ecology Progresses Series, 155, 103-113.

Hottinger L. (1982) – Larger foraminifera, giant cells with a historical background. Naturwissenschaften, 69, 361-371.

Howarth R.W., Jensen H.S., Marino R., Postma H. (1995). Transport to and processing of P in near-shore and oceanic waters. In Tiessen H. (ed.): Phosphorus in the Global Environment – Transfers, Cycles and Management, 323–345.

Howe M.A. (1919) – On some fossil and recent Lithothamnieae of the Panama Canal zone.- United States National Museum Bulletin, 103, 1-13.

Hrabovský J., Fordinál K. (2013) – Paleoecological evaluation of the algal limestones in Stupava-Vrchná Hora locality (Vienna Basin, Slovakia). Mineralia Slovaca, 45, 11-22.

Hrabovský J., Basso D., Doláková N. (2015) - Diagnostic characters in fossil coralline algae (Corallinophycidae: Rodophyta) from the Miocene of southern Moravia (Carpathian Foredeep, Czech Republic). Journal of Systematic Paleontology, DOI: 10.1080/14772019.2015.1071501.

Hsü K.J., Ryan W.B.F., Cita M.B. (1973) – Late Miocene dessication of the Mediterranean. Nature, 242, 240-244.

Iryu Y., Bassi D., Woelkerling W.J. (2009) – Re-Assessment of the type collections of fourteen corallinalean species (Coralline, Rhodophyta) described by W. Ishijima (1942-1960). Paleontology, 52, 401-427.

Jacobs E., Weiss H., Shieds G. (1996) – The Monterey event in the Mediterranean: a record from shelf sediments of Malta . Paleoceanography, 11, 717-728.

James N.P. (1997) - The cool-water carbonate depositional realm. In James N.P., Clarke J.A.D. (eds): Cool-Water Carbonates. SEPM Special Publication, 56, 1-22.

Jessen C., Voolstra C.R., Wild C. (2014) – In situ effects of simulated overfishing and eutrophication on settlement of benthic coral reef invertebrates in the Central Red Sea . PeerJ 2:e339, DOI 10.7717/peerj.339.

Johnson R.G (1962) – Mode of Formation of marine fossil assemblage of the Pleistocene Millerton Formation of California. Geolgical Society of America Bullettin, 73, 113-130.

Johnson M.E., Da Silva C.M., Santos A., Baaril B.G., Cachão M., Mayoral E.J., Rebelo A.C., Ledesma-Vàsquez J. (2011) – Rhodoliths transport and immobilization on a volcanically active rocky shore: Middle Miocene at Cabeço das Laranjas on Ilhéu de Cima (Madeira Archipelago, Portugal). Palaeogeography Paleoclimatology Paleoecology, 300, 113-127.

Johnson J.H. (1962) – The algal genus Lithothamnion and its fossil representatives. Colorado School of Mines Quaterly, 57, 111 pp.

Johnson J.H. (1964) – Eocene Algae from Ishigaki-shima, Ryūkyū-rettō. Geological Survey Professional Paper, 399-C,1-13.

Kamp P.J.J., Harmsen F.J., Nelson C.S., Boyle S.F. (1988) – Barnacle-dominated limestone with giant cross-beds in a non tropical, tide swept, Pliocene forearc seaway, Hawke's Bay, New Zealand. Sedimentary Geology, 60, 173-195.

Kato A., Baba M., Suda S. (2011) – Revision of the Mastophoroideae (Corallinales, Rhodophyta) and Polyphyly in the nongeniculate species widely distributed on pacific coral reefs. Journal of Phycology, 47, 662-672.

Keats D.W., Manevelt G. & Chamberlain Y.M. (2000) – *Lithothamnion superpositum* Foslie: a common crustose red alga (Corallinaceae) in South Africa. Cryptogamie Algologie, 21, 381-400.

Kováč M., Fordinál K., Grigorovich A.S., Halásová E., Hudáčková N., Joniak P., Pipík R., Sabol M., Kováčová M., Sliva Ľ. (2005) – Západokarpatské fosílne ekosystémy a ich vzťah k paleoprostrediu v kontexte neogénneho vývoja eurázijského kontinentu. Geologické práce, Správy, 111, 61-121.

Kraal S.P., Slomp C.P., Reed D.C., Reichart G.J., Poulton S.W. (2012) – Sedimentary phosphorus and iron cycling in and below the oxygen minimum zone of the northern Arabian Sea. Biogeosciences, 9, 2603-2624.

Kramer R., Baumann K.H.,, Henrich R. (2006) – Middle to late Miocene fluctuation in the incipient Benguela Upwelling System by calcareous nannofossil assemblages (ODP site 1085A). Palaeogeography, Palaeoclimaology, Palaeoecology, 230, 319-334.

Krom M.D., Berner R.A. (1981) – The diagenesis of phosphorus in a nearshore marine sediment . Geochimica et Cosmochimica Acta, 45, 207-216.

Kruskal J.B. (1977) – Multidimensional scaling and other methods for discovering structure. In Enslein K., Ralston A., Wilf H.S. (eds.): Statistical methods for digital computers. 296-339.

Kutzing F.T. (1841) – Uber die “Polypieres calciféres” des Lamouroux. In Kutzing F.T. (ed) : Zu der offentlchen Prufung Classen der Realschule zu Nordhausen. p. 3-34.

LagabrielleY., Goddéris Y., Donnadieu Y., Malavieille J., Suarez M. (2009) – The tectonic history of Drake Passage and its possible impacts on global climate. Earth and Planetary Sciences Letters, 279, 197–211.

Lamouroux J.V.F. (1812) – Extrait d'un mémoire sur la classification des Polypiers coralligènes non entièrement pierreux. Noveaux Bullettin des Sciences par la Société Philomathique de Paris, 63, 181-188.

Langer M.R., Hottinger L. (2000) – Biogeography of selected “larger” foraminifera. Micropaleontology, 46, 105-126.

Lee D.E., Scholz J., Gordon D.P. (1997) – Paleoecology of a late Eocene mobile rockground biota from North Otago, New Zealand. Palaios, 12, 568-581.

Le Gall L. & Saunders G.W. (2007) – A nuclear phylogeny of the Florideophyceae (Rhodophyta) inferred from combined EF2, small subunit and large subunit ribosomal DNA: establishing the new red algal subclass Corallinophycidae. Molecular Phylogenetics and Evolution, 43, 1118-1130.

Le Gall L., Payri C., Bittner L., Saunders G.W. (2009) – Multigene polygenetic analyses support recognition of the Sporolithales, ord. nov. Molecular Phylogenetics and Evolution, 54, 302-305.

Lemoine M. (1928) – Un noveau genrse de Mélobésiées: Mesophyllum. Bulletin de la Société Botanique de France. 75, 251-254.

Leszczyński S., Kołodziej B., Bassi D., Malata E., Gasiński M.A. (2012) – Origin and resedimentation of rhodoliths in the Late Paleocene of the Polish Outer Carpathians. Facies, 58, 367-387.

Lewis A.R., Marchant D.R., Ashworth A.C., Hemming S.R., Machlus M.L. (2007) – Major middle Miocene global climate change: evidence from East Antarctica and the Transantarctic Mountains . GSA Bullettin, 119, 1449–1461.

Loeblich A.R., Tappan H. (1987) – Foraminiferal Genera and Their Classification. 1820 pp.

Lund M., Davies P.J., Braga J.C. (2000) – Coralline algal nodules off Fraser Island, Eastern Australia. Facies, 42, 25-34.

Lunt D.J., Valdes P.J., Haywood A., Rutt I.C. (2008) – Closure of the Panama Seaway during the Pliocene: implications for climate and Northern Hemisphere glaciation . Climatic Dynamics, 30, 1-18.

Maffione M., Speranza F., Faccenna C., Cascella A., Vignaroli G., Sagnotti L. (2008) – A syncronous Alpine and Corsica-Sardinia rotation. Journal of Geophysica Research, 113, doi: 10.1029/2007JB005214.

Major J.J. (1998) – Pebble orientation on large, experimental debris-flow deposits. Sedimentary Geology, 117, 151-164.

Martin R.E. (1996) – Secular increase in nutrient levels through the Phanerozoic: implication for productivity, biomass, and diversity of marine biosphere. Palaios, 11, 209-219.

Meybeck M. (1982) - Carbon, nitrogen and phosphorus transport by world rivers. Americal Journal of Science, 282, 401-450.

Minnery G.A., Rezak R., Bright T.J. (1985) – Depth zonation and growth form of crustose coralline algae: Flower Garden Banks, Northwestern Gulf of Mexico . In Toomey D.F., Nitecki M.H. (eds.): Paleoalgology: Contemporary Research and Applications , 237-246.

Molina-Cruz A. (1977). Radiolarian assemblage and their relationship to the oceanography of subtropical Southeastern Pacific. Marine Micropaleontology, 2, 315-352.

Mosbrugger M., Uterscher T., Dilcher D.L. (2005) – Cenozoic continental climatic evolution of Central Europe. Proceedings of the Natural Academy of Sciences U.S.A., 102, 14964-14969.

Mosca P., Polino R., Rogledi S., Rossi M. (2009) – New data from the kinematic interpretation of Alps-Appenines junction (Northwestern Italy). International Journal of Earth Sciences, 99, 833-849.

Murray J. (2006) – Ecology and Applications of Benthic Foraminifera. 426 pp.

Mutti M., Hallock P. (2003) – Carbonate systems along nutrient and temperature gradients: some sedimentological and geochemical constraints. International Journal of Earth-Science, 92, 465-475.

Mutti E., Bernoulli D., Ricci Lucchi F., Tinterri R. (2009) – Turbidite and turbidity currents: from Alpine flysch to the exploration of continental margins. Sedimentology, 56, 267-318.

Nebelsick J.H., Stingl V., Rasser M. (2001) – Autochthonous facies and allochthonous debris flows compared: Early Oligocene Carbonate facies patterns of the lower Inn Valley (Tyrol, Austria). Facies, 44, 31-46.

Neill K.F, Nelson W.A., D'Archino R., Leduc D., Farr T.J. (2015) – Northern New Zealand rhodoliths: assessing faunal and floral diversity in physically contrasting beds. Marine Biodiversity, 45, 63-75.

Negri A., Villa G. (2000) – Calcareous nannofossil biostratigraphy, biochronology and paleoecology at the

Tortonian/Messinian boundary of the Faneromeni section (Crete). Palaeogeography, Palaeoclimatology, Palaeoecology, 156, 195-209.

Nelson W.A., Sutherland J.E., Farr T.J., Hart D.R., Neill K.F., Kim H.J., Yoon H.S. (2015) – Multi-gene phylogenetic analyses of New Zealand coralline algae *Corallinapetra novaezelandiae* gen. et sp. nov. and recognition of the Hapalidiales ord. nov. Journal of Phycology, 51, 454-468.

Neuhaus D., Borgomano J., Jauffred J.C., Mercadier C., Olotu S., Grotsch J. (2004) – Quantitative Seismic Reservoir Characterization of an Oligocene-Miocene Carbonate Buildup: Malampaya Field, Philippines. In Eberli G.B., Masaferro J.L., Sarg J.F. (eds.): Seismic imaging of carbonate reservoirs and systems: AAPG Memoirs, 81, 169-183.

Newman A.W., Ross A. (1976) – Revision of the balanomorph barnacles including a catalog of the species. Memoirs of San Diego Society of Natural History, 9, 1-108.

Nóbrega-Farias J., Riosmena-Rodriguez R., Bouzon Z., Oliveira E.C., Horta P.A. (2010) – *Lithothamnion superpositum* (Corallinales; Rhodophyta): First description for the Western Atlantic or rediscovery of a species?. Phycological Research, 58, 210-216.

Nong G.T., Najjar R.G., Seidov D., Peterso W.H. (2000) – Simulation of ocean temperature change due to the opening of Drake Passage. Geophysical Research Letters, 27, 2689-2692.

Novaretti A., Bicchi E., Condello A., Ferrero E., Maia F., Tonon M., Torta D. (1995) – La successione oligo-miocenica del Monferrato: sintesi dei dati biostratigrafici. Atti del Convegno "Rapporti tra Alpi e Appennino" Peveragno (CN), Accademia Nazionale delle Scienze, Collana Scritti e Documenti, XIV, 39-59.

Odin G.S., Matter A. (1981) – De glauconiarum origine. Sediment, 28, 611-641.

Odin G.S., Fullagar P.D. (1988) – Geological significance of the glaucony facies. In Odin G.S. (ed.): Green Marine Clay, 295-332.

O'Herne L. (1974) – A reconsideration of *Amphistegina lessonii* d'Orbigny, 1826, sensu Brady, 1884 (Foraminifera). Scripta Geologica, 26, 1-53.

Okada H., Honjo S. (1973) – The distribution of oceanic coccolithophorids in the Pacific. Deep-Sea Research, 20, 355-374.

Pagani M., Freeman K.H., Arthur M.A. (1999) – Late Miocene atmospheric CO_2 concentrations and the expansion of C_4 grasses . Science, 285, 876-879.

Parson-Hubbard K.M., Callender W.R., Powell E.N., Brett C.E., Walker S.E., Raymond A.L., Staff G.M. (1999) – Rates of burial and disturbance of experimentally deployed mollusks: Implications for preservation potential. Palaios, 14, 337-351.

Pascelli C., Riul P., Riosmena-Rodriguez R., Scherner F., Nunes M., Hall-Spencer J.M., Oliveira E.C. , Horta P. (2013) – Seasonal and depth-driven changes in rhodolith bed structure and associated macroalgae off Arvoredo Island (Southeastern Brazil). Acquatic Botany, 111, 62-65.

Pattan J.N., Pearce N.J.G., Mislankar P.G. (2001) – Constraints in using Cerium-anomaly of bulk sediments as an indicator of paleo bottom water redox environment: A case study from the central Indian Ocean Basin. Chemical Geology, 221, 260-278.

Paull C.K., Ussler W., Greene H.G., Keaten R., Mitts P., Barry J. (2003) – Caught in the act: the 20 December 2001 gravity flow event in the Monterey Canyon. Geo. Mar. Lett., 22: 227-232.

Pekar S.F., DeCanto R.M. (2006) – High-resolution ice-volume estimates for the early Miocene: evidence for a dynamic ice sheet in Antarctica. Palaeogeography, Palaeoclimatology, Palaeoecology, 231, 101-109.

Perrin C., Bosence D.W.J., Rosen B. (1995) – Quantitative approaches to palaeozonation and palaeobathymetry of corals and coralline algae in Cenozoic reefs. In Bosence D.W.J., Allison P.A. (eds.): Marine Palaeoenvironmental Analysis from Fossils. Geological Society Special Publication, 83, 181-229.

Perrin C., Bosellini F. (2012) – Paleobiogeography of scleractinian reef corals: Changing patterns during the Oligocene–Miocene climatic transition in the Mediterranean. Earth Science Review, 111, 1-24.

Philippi R.A. (1837) – Beweis, dass die Nulliporen Pflanzen sind. Archiv fur Naturgeschichte, 3, 387-393.

Pomar L., Obrador A., Westphal H.. (2002) – Sub-wavebase cross bedded grainstone on adistally steepeend carbonate ramp, Upper Miocene, Menorca, Spain. Sedimentology, 49, 139-169.

Pomar L., Brandano M., Westphal H. (2004) – Environmental factors influencing skeletal grain sediment associations: a critical review of Miocene examples from the western Mediterranean . Sedimentology, 51, 627-651.

Pomar L. & Kendall C.G.St.C. (2007) – Architecture of carbonate platforms: a response to hydrodynamics and evolving ecology. Control on carbonate platform and reef development. SEPM Special Publications, 89, 187-216.

Postgate J.R. (1971) – The fundamentals of nitrogen fixation. 264 pp.

Pufahl P.K. (2010) – Bioelemental sediments In James N.P. & Darlymple R.W. (eds.), Facies Models 4. Geological Association of Canada Special Publications, 6, 477-503.

Puga-Bernabéu A., Martín J.M., Braga J.C., Sánchez-Almazo I.M (2010) – Downslope-migrating sandwaves and platform-margin clinoforms in a current-dominated, distally steepened temperate-carbonate ramp (Guadix Basin, Southern Spain). Sedimentology, 57, 293-311.

Puga-Bernabéu A., Martín J.M., Braga J.C., Aguirre J. (2014) – Offshore remobilization processes and deposits in low-energy temperate-water carbonate-ramp systems: examples from the Neogene bains of the Betic Cordillera (SE Spain). Sedimentary Geology, 304, 11-27.

Quaranta F., Vannucci G., Basso D. (2007) - *Neogoniolithon contii* comb nov based on the taxonomic re-assessment of Mastrorilli's original material from the Oligocene of NW Italy (TPB). Rivista Italiana di Paleontologia e Stratigrafia, 113, 43-55.

Rasser M.W., Piller W.E. (1999) – Application of neontological taxonomic concepts to Late Eocene coralline algae (Rhodophyta) of the Austrian Molasse Zone. Journal of Micropaleontology, 18, 67-80.

Rasser M.W., Piller W.E. (2000) – Designation of *Phymatolithon* (Corallinaceae, Rhodophyta) in fossil material and its paleoclimatological indications. Micropaleontology, 46, 89-95.

Rasser M.W., Nebelsick J.H. (2003) – Provenance analysis of Oligocene autochthonous and allochthonous coralline algae: a quantitative approach towards reconstructing transported assemblages. Palaeogeography Palaeoclimatology Palaeoecology, 201, 89-111.

Raymo M.E., Ruddiman W.F. (1992) – Tectonic forcing of Late Cenozoic climate. Nature, 359, 117-121.

Raymo M.E. (1994) – The Himalayas, organic carbon burial and climate in the Miocene. Paleoceanography, 9, 399-404.

Redfield A.C. (1958) – The biological controls of chemical factors in the environment. American Scientist, 46, 205-221.

Reynaud J.Y., Dalrymple R.W., Vennin E., Parize O., Besson D., Rubino J.P. (2006) – Topographi controls on production and deposition of tidal cool-water carbonates, Uzès Basin, SE France. Journal of Sedimentary Research, 76, 116- 129.

Reynaud J.Y., James N.P. (2012) – The Miocene Sommières basim. SE France: bioclastic carbonates in a tide dominated depositional system. Sedimentary Geology, 282, 360-373.

Rögl F. (1998) – Palaeogeographic considerations for Mediterranean and Paratethys seaways (Oligocene to Miocene). Annales des Naturhistorischen Museums in Wien, 99, 279-310.

Rögl F. (1999) – Mediterranean and Paratethys facts and hypotheses of an Oligocene to Miocene paleogeography (short overview). Geologica Carpathica, 50. 339-349.

Rossi M., Mosca P., Polino R., Rogledi S., Biffi U. (2009) – New outcrop and subsurface data in the Tertiary Piedmont Basin: unconformity-bounded stratigraphic units and their relationships with basin-modification phases. Rivista Italiana di Paleonotologia e Stratigrafia, 115, 305-335.

Rubino J.L., Lesueur J.L., Guy L., Clauzon G. (1990) – Le Miocène inférieur et moyen du bassin rhodanien, stratigraphie séquentielle et sédimentologie. Unpublished ASF field-trip guide.

Ruffini R. (1995) – Evidenze di attività vulcanica terziaria nelle Alpi occidentali: problemi ed ipotesi. [PhD thesis]. 160 pp.

Ruttenberg K.C. (1992) – Development of a sequential extraction method for different form of phosphorous in marine sediments. Limnology and Oceanography, 37, 1460-1482.

Ruttenberg K.C., Berner R.A. (1993) – Authigenic apatite formation and burial in sediments from non-upwelling, continental margin environments . Geochimica et Cosmochimica Acta, 57, 991-1007.

Ruttenberg K.C. (2004) - The global phosphorus cycle. In Holland H.D. Turekian K.K. (eds.): Treatise on Geochemistry, 585–643.

Ruttenberg K.C., Ogawa N.O., Tamburini F., Briggs R.A., Colasacco N.D., Joyce E. (2009) – Improved, high throughput approach for phosphorus speciation in natural sediments via the SEDEX sequential extraction method. Limnology and Oceanography: Methods, 7, 319-333.

Saint Martin J.P., Merle D., Cornée J.J., Filipescu S., Saint Martin S., Bucur, I.I. (2007) – Les constructions coralliennes du Badénien (Miocène moyen) de la bordure occidentale de la depression Transylvanie (Roumanie). Paléontologie générale (Paléoécologie), 6, 37-46.

Sanford E., Menge B.A. (2001) – Spatial and temporal variation in barnacle growth in coastal upwelling system. Marine Ecology Progresses Series, 209, 143-157.

Sarnthein M., Winn K., Duplessy J.C., Fontugne M.R. (1988) – Global variations of surface oceans productivity in low and mid latitudes: influence on CO2 reservoirs of the deep oceans and atmosphere during the last 21000 years. Paleoceanography, 3, 361-399.

Sattler U., Zampetti V., Schlager W., Immenhauser A. (2004) – Late leaching under deep burial conditions: a case study from the Miocene Zhujiang Carbonate Reservoir, South China Sea. Marine Petroleum Geology, 21, 977–992.

Schlager W. (2003) – Benthic carbonate factories of the Phanerozoic. Internation Journal of Earth Sciences, 92, 445-464.

Schlanger S.O., Johnson C.J. (1969) – Algal banks near La Paz, Baja California – Modern Analogues of source areas of transported shallow water fossils in Pre-Alpine flysch depostis. Palaeogeography Palaeoclimatology Palaeoecology, 6, 141-157.

Schneider B., Schmittner A. (2006) – Simulating the impact of the Panamanian seaway closure on ocean circulation, marine productivity and nutrient cycling. Earth and Planetary Science Letters, 246, 367-380.

Schüttenhelm R.T.E. (1976) – History and modes of Miocene carbonate deposition in the interior of the Piedmont Basin, NW Italy. [PhD thesis]. Utrecth Micropaleontological Bull, 4, 207 pp.

Séranne M., Camus H., Lucazeau F., Barbarand J., Quinif, Y. (2002) – Surrection et érosion polyphasées de la Bordure cévenole: un exemple de morphogenèse lente. Bulletin de la Societe Geologique de France, 173, 97-112.

Setchell W.A. (1943) – *Mastophora* and the Mastophoreae: genus and subfamily of Corallinaceae. Proceedings of the National Academy of Science of the United States of America. 29, 127-135.

Shevenell A.E., Kennet J.P., Lea D.W. (2004) – Middle Miocene Southern Ocean cooling and antarctic cryosphere expansion . Science, 35, 1766-1770.

Shields G., Stille P. (2001) - Diagenetic constraints on the use of cerium anomalies as palaeoseawater redox proxies: an isotopic and REE study of Cambrian phosphorites. Chemical Geology, 175, 29-48.

Silva P.C., Basson P.W., Moe R.L. (1996) – Catalogue of the benthic marine algae of the Indian Ocean. University of California Press, Berkeley, 1129 pp.

Silva P., Johansen H.W. (1986) – A reappraisal of the order Corallinales (Rhodophyceae). European Journal of Phycology, 21, 245-254.

Slomp C.P., Epping E.H.G., Helder W., Van Rapist W. (1996) – A key role for iron-bound phosphorus in authigenic apatite formation in North Atlantic continental platform sediments. Journal of Marine Research, 54, 1179-1205.

Slomp C.P., Thomson J., DeLange G.J. (2002) - Enhanced regeneration of phosphorus during formation of the most recent eastern Mediterranean sapropel (S1). Geochimica and Cosmochimica Acta, 66, 1171-1184.

Slomp C.P. (2011) – Phosphorous cycling in the estuarine and coastal zones: sources, sinks and transformations. In Wolanski E., Mclusky D. (eds.): Treatise in Estuarine and Coastal Sciences, 201-229.

Smith S.V., Swaney D.P., Talaue-McManus L., Bartley J.D., Sandhei P.T., McLaughlin C., Dupra V.C., Crossland C.J., Buddemeier R.W., Maxwell B.A., Wulff F. (2003) - Humans, hydrology, and the distribution of inorganic nutrient loading to the ocean. Bioscience, 53, 235–245.

Sneed E.D., Folk R.L. (1958) – Pebbles in the Colorado River, Texas, a study of particle morphogenesis. Journal of Geology, 66, 114-150.

Staff G.M., Stanton R.J. Jr., Powell E.N., Cummins H. (1986) – Time-averaging, taphonomy and their impact on paleocommunity reconstruction: death assemblages in Texas bays. Geological Society of America Bulletin, 97, 428-443.

Steneck R.S. (1986) – The ecology of Coralline Algal Crusts: Convergent Patterns and Adaptive Strategies. Annual Review of Ecology, 17, 273-303.

Stickley C.E., Brinkhuis H., Schellenberg S.A., Sluijs A., Rohl, U., Fuller M., Grauert M., Huber M., Warnaar J., Williams G.L. (2004) – Timing and nature of the deepening of the Tasmanian Gateway. Paleoceanography, 19, doi:10.1029/2004PA001022.

Stock W.A., Siegfried J.J. (2013) – One Essay on Dissertation Formats in Economics. The American Economic Review: Papers and Proceedings, 103, 648-653.

Takahashi K. (1986) – Seasonal fluxes of pelagic diatoms in the subartic Pacific. Deep-Sea Research, 33, 1225-1251.

Thiede J., Jönger B. (1992) – Faunal and floral indicators of ocean coastal upwelling (NW African and Peruvian Continental margins). In Summerhayes C.P., Prell W.L., Emeis K.C. (eds.): Upwelling Systems: Evolution Since the Early Miocene. Geological Society Special Publication, 64, 47-76.

Tiedmann R., Sarnthein M., Stein R. (1989) – Climatic changes in the western Sahara: aeolo-marine record for the last 8 M.y. (ODP sites 657-661). In Ruddiman W., Sarnthein M., Baldaue J. et al. (eds.): Proceedings of the Ocean Drilling Program, 108.

Tyrrel T. (1999) – The relavtive influence of nitrogen and phosphorous on ocean primary production. Nature, 400, 525-531.

Tyson R.V., Pearson T.H. (1991) – Modern and ancient continental shelf anoxia: an overview. In Tyson R.V., Pearson T.H. (eds.): Modern and Ancient Continental Shelf Anoxia. Geological Society of London, Special Publication, 58, 1-26.

Vahrenkamp V.C., David F., Duijndam P., Newall M., Crevello P. (2004) – Growth architecture, faulting, and karstification of a middle Miocene carbonate platform, Luconia Province, offshore Sarawak, Malaysia. AAPG Memoirs, 81, 329-350.

Van Andel Tj.H. (1964) – Recent marine sediments of Gulf of California. In Van Andel Tj.H., (ed): Marine Geology of the Gulf of California. AAPG Memoirs, 3, 216-310.

Vannucci G., Piazza M., Fravega C., Abate C. (1996) – Litostratigrafia e paleoecologia di successioni a rodoliti della Pietra da Cantoni (Monferrato Orientale, Italia Nord-Occidentale). Atti Società Toscana di Scienze Naturali, Memorie, Serie A, 103, 69-86.

Vannucci G., Quaranta F., Piazza M., Fravega P. (2003) - The Oligocene reefal facies of Bric San Bernardino (Millesimo, NW Italy). Le facies recifali oligoceniche di Bric San Bernardino (Millesimo, Italia nord-occidentale). Atti Ticinesi di Scienze della Terra, 44, 35-44.

Vannucci G., Quaranta F., Basso D. (2008) – Revision and redocumentation of M. Airoldi species of *Lithophyllum* from the Tertiary Piedmont Basin. Rivista Italiana di Paleontologia e Stratigrafia, 114, 515-528.

Verheij E. (1993) – The genus Sporolithon (Sporolithaceae fam. nov., Corallinales, Rhodophyta) from thc Spermonde Archipelago, Indonesia. Phycologia, 32, 184-196.

Vigorito M., Murru M., Simone L. (2005) – Anatomy of a submarine channel system and related fan in a foramol/rhodalgal carbonate sedimentary setting: a case history from the Miocene syn-rift Sardinia Basin (Italy). Sedimentary Geology, 174, 1-30.

Vigorito M., Murru M., Simone L. (2006) – Architectural patterns in a multistorey mixed carbonate-siliciclastic submarine channel, Porto Torres Basin, Miocene, Sardinia, Italy. Sedimentary Geology, 186, 213-236.

Von Breymann M.T., Emesiss K.C., Suess E. (1992) – Water depth and diagenesis constraints on the use of barium as a paleoproductivity indicator. In Summerhayes C.P., Prell W.L., Emeiss K.C. (eds.): Upwelling Systems: Evolution Since the Early Miocene. Geological society of London, Special Publication, 64, 273-284.

Wade B.S., Pearson P.N., Berggren W.A., Pälike H. (2011) – Review and revision of Cenozoic tropical planktonic foraminiferal biostratigraphy and calibration to the geomagnetic polarity and astronomical time scale. Earth-Science Review, 104, 111-142.

Wilks K.M., Woelkerling W.J. (1995) – An account of Southern Australian species of Lithothamnion (Corallinaceae, Rhodophyta). Australian Systematic Botany, 8, 549-583.

Williams H.D., Burgress P.M., Wright V.P., Della Porta G., Granjeon D. (2011) – Investigating carbonate platform types: multiple controls and a continuum geometries. Journal of Sedimentary Research, 81, 18-37.

Williams J.D.H., Jaquet J.M., Thomas R.L. (1976) – Form of phosphorous in the surficial sediments of Lake Erie. Journal of the Fisheries Research Board of Canada, 33, 413-429.

Wilson M.V.H. (1988) – Taphonomic processes: information loss and information gain. Geosciences Canada, 15, 131-148.

Wilson M.E.J., Vecsei A. (2005) – The apparent paradox of abundant foramol facies in low latitudes: their environmental significance and effect on platform development . Earth-Science Reviews, 69, 133-168.

White N.M., Pringle M., Garzanti E., Bickle M., Najman Y., Chapman H., Friend P., (2002) – Constraints on the exhumation and erosion of the High Himalayan Slab, NW India, from foreland basin deposits . Earth and Planetary Science Letters, 195, 29-44.

Wood R. (1993) – Nutrients, Predation and the History of Reef-Building. Palaios 8, 526-543.

Woelkerling W.J. (1988) – The coralline red algae: an analysis of the genera and subfamilies of nongeniculate Corallinaceae. 268 pp.

Woelkerling W.J., Irvine L.M., Harvey A.S. (1993) – Growth-forms in non-geniculate coralline red algae (Corallinales, Rhodophyta). Australian Systematic Botany, 6, 277-293.

Woelkerling W.J., Granier B., Dias-Brito D. (2014) – *Heydrichia* (?) *poignantii*, sp. nov. (Sporolithaceae, Sporolithales, Rhodophyta), a 100 million year old fossil coralline red alga from north-eastern Brazil, and a new Hauterivian record of *Sporolithon* from Switzerland. Carnets de Géologie, 14, 139-158.

Zachos J., Pagani M., Sloan L., Thomas E., Billups K. (2001) – Trends, Rhythms, and Aberrations in Global Climate 65 Ma to Present . Science, 292, 686-693.

Zingg T. (1935) – "Beitrag zur Schotteranalyse". Schweizerische Mineralogische und Petrographische Mitteilungen, 15, 39–140.